GENETIC INFLUENCES ON SOCIAL COGNITION, EXECUTIVE FUNCTION, AND ASSOCIATED NEURAL NETWORKS

By

Reid Blanchett

A DISSERTATION

Submitted to
Michigan State University
in partial fulfillment of the requirements
for the degree of

Genetics—Doctor of Philosophy

2022

ABSTRACT

GENETIC INFLUENCES ON SOCIAL COGNITION, EXECUTIVE FUNCTION, AND ASSOCIATED NEURAL NETWORKS

By

Reid Blanchett

Fundamental cognitive domains include executive function and social cognition. Both social cognition and executive functioning can be studied using neuroimaging techniques that allow direct observations to be made about brain structure and function. These techniques can also be applied to the study of brain development, revealing how circuits involved in executive function and social cognition change during important developmental periods such as infancy. Along with providing a window into brain maturation, neuroimaging can be used to study cases where cognitive domains are disrupted and make comparisons to learn about typical brain development and function. For my dissertation, I have explored these cognitive domains and associated neural circuits both in typically developing individuals and in individuals with Turner syndrome, a condition caused by the full or partial absence of the second sex chromosome. **First**, I used a classic twin design and demonstrated relatively low narrow-sense heritability estimates for neonatal resting-state functional connectivity phenotypes. I studied both between- and within- network connectivity in neonates and demonstrated that only 6 out of 36 phenotypes had heritability estimates greater than 0.10; no estimates were statistically significant. These within- and between-network phenotypes included networks heavily recruited for social cognition and executive functioning. I also showed statistically significant associations between neonate resting-state functional connectivity phenotypes and specific demographic and medical history variables. **Second,** I compared

structural and functional connectivity between typically developing male and female infants and infants with Turner syndrome. I saw no differences between the three groups in integrity of the superior longitudinal fasciculus or reduced connectivity between the right precentral gyrus and brain regions in the occipital and parietal regions involved with social cognition, visuospatial reasoning, and executive function. Fronto-parietal connectivity and integrity of the superior longitudinal fasciculus are disrupted in older individuals with Turner syndrome and these results suggested that these changes emerge after the first year of life. I conducted a further exploratory analysis of 54 fiber tracts and showed significant group differences that primarily reflected masculinization of white matter microstructure in TS. Other differences may have arisen due to hemizygosity of the pseudoautosomal region. **Finally,** I developed a browser-based online testing platform targeting domains such as executive functioning and social cognition, which are often disrupted in Turner syndrome. I then validated the battery via administration to neurotypical males and females and to adult women with Turner syndrome, who performed more poorly on tests of executive function and visuospatial reasoning. Taken together, the results presented in this dissertation contribute greatly to our understanding of the role of genetics in social cognition, executive function, and their related neural networks. These results can be further utilized in longitudinal studies of brain development and in future cognitive testing research.

ACKNOWLEDGEMENTS

I would first like to thank my mentor, Dr. Rebecca Knickmeyer, for her unwavering support, constant encouragement, and dedication to helping me achieve my goals and dreams. I could never have even conceived of doing something this big without her on my team. I would like to acknowledge the members of the Knickmeyer lab as well who were there with me every step of the way, especially Dr. Ann Alex with whom I will always share a special bond. Additionally, I want to thank the Genetics and Genome Sciences Program for being so flexible and for its commitment to its students. My committee has also been a source of great support, and I would like to thank Drs. Alex Burt, Arjun Krishnan, Brian Schutte, and David Zhu for their time and investment in my future. Finally, I would like to thank the family that I have made along the way during my time in higher education. Jasmine Charter-Harris, Billie-Heard, my friends at MSU, and most especially the Santelli family who were there for every triumph and every tear on my adventure.

TABLE OF CONTENTS

LIST OF TABLES

LIST OF FIGURES

KEY TO ABBREVIATIONS

SC: Social cognition

EF: Executive function

rs-fMRI: Resting-state functional magnetic resonance imaging

DTI: Diffusion tensor imaging

BOLD: Blood oxygen level dependent

FP: Frontoparietal

VA: Ventral Attention

DA: Dorsal Attention

Lim: Limbic

SS: Somatosensory

SC: Subcortical

Vis: Visual

DM: Default mode

ADHD: Attention deficit hyperactivity disorder

ASD: Autism spectrum disorder

PFC: Prefrontal cortex

FPN: Frontoparietal network

SLF: Superior longitudinal fasciculus

FA: Fractional anisotropy

RD: Radial diffusivity

MD: Mean diffusivity

AD: Axial Diffusivity

RDoC: Research domain criteria

ToM: Theory of mind

DMN: Default mode network

ILF: Inferior longitudinal fasciculus

TS: Turner syndrome

GLM: General linear model

MZ: Monozygotic

DZ: Dizygotic

EBDS: Early brain development study

VR: Visual reasoning

MRI: Magnetic resonance imaging

TD: Typically developing

UNC: University of North Carolina

TR: Repetition time

TE: Echo time

QC: Quality control

FADTTS: Functional analysis of diffustion tensor tract statistics

PAR: Pseudoautosomal region

IFOF: Inferior fronto-occipital fasciculus

CHD: Congenital heart disease

CPT: Continuous performance task

SRT: Simple response time

ASQ: Autism spectrum quotient

CTSA: Clinical translational science award

FDR: False discover rate

Chapter 1

Introduction

The objective of the presented dissertation is to better understand genetic influences on social cognition (SC), executive function (EF), and associated neural circuits. This objective was achieved via 3 specific aims: (1) identify genetic and environmental factors influencing neonatal resting-state functional connectivity including connectivity within and between the frontoparietal and default mode networks, which play critical roles in EF and SC respectively. (2) identify anatomical and functional connectivity differences in the brains of infants with Turner syndrome when compared to typically developing children, and (3) creating an online cognitive battery targeting cognitive domains that are often disrupted in Turner syndrome including SC and EF. The first two aims were carried out via neuroimaging techniques. Thus, the introduction to the dissertation begins by describing the two neuroimaging modalities utilized in this work: resting-state functional magnetic resonance imaging (rs-fMRI) and diffusion tensor imaging (DTI). Sections 2 and 3 will describe EF and SC and their relevance to psychiatry along with what is currently known about their underlying neurobiology, roles in development, their genetic architecture, and potential sex differences. Aims 2 and 3 focus on individuals with Turner syndrome, a developmental disorder that is caused by the complete or partial absence of the second sex chromosome and is often accompanied by deficits in both SC and EF. Thus, Section 4 of the introduction explains why Turner syndrome is a powerful model for understanding genetic influences on EF and SC. Finally, different developmental periods are presented with the challenges and advantages associated with each in terms of studying cognition and its coupling with neuroimaging.

Neuroimaging Modalities Used in this Dissertation

Resting state functional MRI

In Aims 1 and 2 of this dissertation I used resting state functional MRI (rs-fMRI) to better understand genetic influences on brain networks involved in SC and EF.

The basis of fMRI is the observation of blood oxygen level dependent response (BOLD). The principle behind BOLD is that when a neuron is activated, there is increased blood flow with increased oxygen to that area of the brain as the glucose needed by the neuron is aerobically metabolized[1] through cellular respiration. fMRI[2] signals can be collected in either a task-based fMRI, or a resting-state fMRI but both are based in the principle of BOLD responses. Task-based fMRI has primarily been used to identify brain regions functionally involved in different cognitive processes, while rsfMRI explores the intrinsic functional segregation of brain networks by looking at the temporally correlated hemodynamic responses of the brain at rest[3]. rsfMRI is especially suitable for the study of infants as it requires no task to be performed by the participant. A sleeping infant is perfectly appropriate for rsfMRI and yields results that add to the growing body of literature concerning network development.

rsfMRI data can be analyzed in multiple ways. In Aim 1 of this dissertation, I focus on eight intrinsic functional networks that were originally identified in adults. They include the frontoparietal (FP), ventral attention (VA), dorsal attention (DA), limbic (Lim), somatosensory (SS), subcortical (SC), visual (Vis), and default mode (DM) networks. To calculate functional connectivity within and between these networks, a neonate specific AAL atlas is used to define 90 regions covering the neonatal cerebral cortex. The average

BOLD time course is extracted from each region for each subject to construct a 90 x 90 correlation matrix. The correlation matrix is Fisher-Z transformed to be the functional connectivity matrix for each subject. The 90 regions are assigned to the eight networks as shown in Table 1.1. Subsequently, within- and between-network connectivity is calculated by averaging the FC values of the within-/between- networks for each subject. This method was most appropriate for testing my central hypothesis that measures of within network and between-network connectivity would be heritable, with the strongest genetic effect evident for early maturing networks involved in perception and movement and the weakest genetic effects evident in later maturing networks involved in EF and SC. I took a slightly different approach in Aim 2. Once again, a neonate specific AAL atlas is used to define 90 regions covering the neonatal cerebral cortex, but instead of creating a 90 x 90 correlation matrix, I focused on functional connectivity between the right precentral gyrus and five specific anatomical brain regions: right and left calcarine cortex, right and left lingual cortex, and right supramarginal cortex This greatly reduced the number of multiple corrections needed and hones in on the main hypotheses of the study.

Table 1.1 The eight adult canonical resting-state networks and their subcomponents.

Canonical network	Subcomponents	Function
Somatosensory	Precentral gyrus	A network of structures in the brain that interpret pain, body position, touch, and temperature.
	Rolandic operculum	
	Supplementary motor area	
	Postcentral gyrus	
	Paracentral lobule	
	Heschl gyrus	
	Superior temporal gyrus	
Default Mode	Superior frontal gyrus	The default mode network[4] is associated with the neural correlates of the everyday mind at rest, being anticorrelated with task performances[5]. However, the DM network has shown activation in SC tasks[6,7].
	Orbitofrontal cortex	
	Anterior cingulate gyrus	
	Posterior cingulate gyrus	
	Angular gyrus	
	Precuneus	
	Middle temporal gyrus	
Limbic	Orbitofrontal cortex	A network involved in sense of smell, socioemotional functioning[8], and hedonic processing[9].
	Olfactory	
	Rectus gyrus	
	Parahippocampal gyrus	
	Temporal pole	
Frontoparietal	Middle frontal gyrus	Heavily involved in EF, the FP network processes goal-directed behavior and is involved in higher-order cognitive processing[10]
	Orbitofrontal cortex	
	Inferior frontal gyrus	
	Inferior parietal lobule	
Ventral Attention	Insula	Recruited for stimulus-driven attention control[11]
	Middle cingulate gyrus	
	Supramarginal gyrus	
Subcortical	Hippocampus	A network involved in emotional control, memory storage, planning, reward processing.
	Amygdala	
	Caudate	
	Putamen	
	Pallidum	
	Thalamus	

Table 1.1 (cont'd)

Dorsal Attention	Superior parietal gyrus	Voluntary orientation of attention[11]
	Inferior temporal gyrus	
Visual	Calcarine cortex	Involved in spatial awareness, object recognition, and processing of visual information.
	Cuneus	
	Lingual gyrus	
	Superior occipital gyrus	
	Middle occipital gyrus	
	Inferior occipital gyrus	
	Fusiform gyrus	

Diffusion Tensor Imaging

In Aim 2, in addition to assessing functional connectivity, I also used diffusion tensor imaging (DTI)[12] to assess the integrity of white matter tracts involved in EF and SC. White matter tracts, or fasciculi, are bundles of axons connecting anatomically distinct regions of the brain. They can be visualized and characterized in either two or three dimensions. Using the principles of Brownian motion, which is based on the random movement of water molecules in this specific case, one can analyze diffusion of water molecules present in a voxel. A voxel, similar to a pixel but in three dimensions, is a unit of volume that can be measured by MRI. The distribution and displacement of the water molecules within this voxel conveys structural information about the brain as tissues may not share similar qualities in all directions, resulting in different and detectable patterns of motion. When the diffusion of water molecules is directional this is referred to as anisotropic diffusion. In contrast, isotropic diffusion is the same in all directions. In the case of white matter, diffusion in the direction of the fibers is faster than the perpendicular direction where it is restricted by cell membranes, the myelin sheath, and microfilament. It can then be assumed that the direction of the fastest diffusion would point to the overall

direction and orientation of the fibers. Consequently, one can use diffusion to reconstruct and visualize major fiber tracts within the brain including projection fibers, which connect the cortex to the lower parts of the brain and brainstem, association fibers, which connect different cortical regions in the same hemisphere, and commissural fibers, which are interhemispheric connections. Major white matter tracts in the brain are listed in Table 1,2 along with the brain regions they connect and the functions they support.

Simplified, the diffusion of water within a voxel can be imagined as an ellipsoid. Axial diffusivity represents diffusivity along the principal axis while the minor axes represent radial diffusivity. Axial diffusivity has been related to axonal integrity and radial diffusivity to degree of myelination of the axons[13]. From axial and radial diffusivity, fractional anisotropy, which reflects the preferred orientation of water diffusion, and mean diffusivity, representing the mean amount of water diffusion, can be calculated. Structural disintegration has been associated with increases in mean and radial diffusivity while higher fractional anisotropy and axial diffusivity are related to preserved fiber integrity[14]. Quantitative analysis of these diffusivity indices along reconstructed fiber tracts is known as quantitative tractography.

Table 1.2 Major white matter tracts in the brain organized by fiber type.

	Tract/Fasciculus	Connections	Function
Association	Arcuate	Temporal and parietal lobe to frontal lobe	Language processing[15], executive control[16], attention
	Inferior fronto-occipital	Occipital lobe to frontal lobe	Visuospatial processing, planning, facial recognition[17]
	Superior longitudinal	Occipital and parietal cortices to frontal cortices	EF including set shifting and working memory[18], visuospatial processing, attention[19]
	Inferior longitudinal	Occipital areas to anterior temporal regions	Integration of visuo-behavioral processes, facial recognition, object recogntion[20]
	Cingulum	Frontal and parietal, as well as subcortical structures to the cingulate gyrus	Episodic memory (hippocampal portion), attention, processing speed[21]
	Uncinate	Orbitofrontal cortex to temporal lobe	Response inhibition, reward processing
	Fornix	Hippocampus to mammillary bodies of the hypothalamus, preoptic nuclei, ventral striatum, orbital cortex and anterior cingulate cortex	Episodic memory, specifically recall[22]
Commissural	Corpus callosum	Cortices of left and right hemispheres	Transferring sensory, motor, and cognitive information from both cerebral hemispheres to each other[23]
	Optic tract	Retina to visual cortex in occipital lobes	Vision

Table 1.2 (cont'd)

	Optic radiation	Geniculate nucleus of thalamus to primary visual cortex	Vision
Projection	Corticospinal	Motor and somatosensory cortices to brain stem	Voluntary motor function[24]
	Corticofugal	Cerebral cortex to brainstem and spinal cord	Modulation of sensory information[25]
	Corticoreticular	Primary motor cortex to pontomedullary junction	Gait function and postural control[26]
	Corticothalamic	Cerebral cortex to thalamus	Sends sensory information for relay into other portions of brain

Executive Functions (EF)

Definition of EF and Component Processes

EFs are a group of top-down cognitive processes supporting goal-directed behavior. These processes include flexible thinking, working memory, and inhibitory control[27,28]. Flexibility refers to the ability of switching between tasks and changing behavior based on inputs from the environment. Common tasks meant to test this process are flanker-type tasks[29] and Stroop[30] tasks. The inhibitory aspect of EF also plays a role in flexibility, as inhibitory control allows individuals to ignore goal-irrelevant stimuli. In contrast to long-term memory, working memory consists of the small amount of information that can be held by the mind for cognitive functioning, which is required for both flexibility and inhibitory control. Working memory can be probed with tasks such as Corsi block[31] or digit span[32]. When used together these functions go on to support higher

order executive functions such as planning, reasoning, and problem solving. Working memory and inhibitory control can be broken up into multiple subdomains. Working memory includes active maintenance (maintaining information over a delay), flexible updating (updating or replacing information), and interference control (selective attention to stimuli). Inhibitory control can be divided into goal selection (suppression of stimuli inappropriate for accomplishing a given goal) and response selection (choosing an appropriate behavior or movement and inhibiting those when inappropriate as a response)[33].

Relevance of EF to Psychiatry

Atypical EF is a common thread uniting many psychiatric disorders. Attention deficit hyperactivity disorder[34–36] (ADHD), depression[37,38], schizophrenia[39–41], and the autism spectrum disorders[42–44] (ASDs) all show deficits in some or all aspects of EF. Deficits in EF play a central role in ADHD, a condition characterized by inattentiveness, hyperactivity, and impulsivity with a prevalence of 9.4% in children between the ages of 2-17[45]. The core diagnostic criteria for ADHD involves deficits in attention, working memory (particularly response selection), and flexible thinking, all important aspects of EF[46]. These individuals typically are known to struggle in shifting focus between tasks, selecting an appropriate behavioral response, and accessing their working memory[47]. As research into ADHD continues to develop, there has been a shift in conceptualizing the disorder as merely a behavioral problem to a condition of EF deficits that result in the observed phenotype.

Neurobiology of EF

The prefrontal cortex (PFC) plays a critical role in EF. A meta-analysis performed by Yuan and Raz[48] found that larger and thicker prefrontal cortex volumes were associated with better EF performance. The PFC is integral for spatial attention[49] and mediates both top-down and bottom-up cognition[50]. The PFC is also considered the "circuit breaker"[50] for response inhibition, turning on to suppress a response or partially activating to pause a response[51]. The parietal lobe additionally plays an instrumental role in EF[52], coupling with the PFC to form the frontoparietal network (FPN) which is heavily involved in working memory[50]. The temporoparietal junction, a component of the FPN, is key for reorientation of attention when presented with a stimulus[53,54]. Volumetric reductions in the parietal lobe additionally can help cause reduced response inhibition. When coupled with a volumetric reduction in the frontal cortex, and working memory overall is decreased[55,56]. The inferior and posterior portion of the parietal cortex additionally support the function of the PFC through their involvement in working memory[57–60] and cognitive control[61–63], respectively.

The coupled frontal and parietal cortices essential for EF compose the FPN, one of the most highly globally connected networks in the brain[64,65]. EF has a strong and well-studied association with rs-functional networks, with the FPN at the forefront of investigation. Reineberg et al.[66] demonstrated that individual differences in an overall and general EF measure correlated with variation in the frontoparietal network in its connection to other resting-state networks. The FPN is associated with flexible thinking[67]. Interestingly, the DMN shows an inverse level of activity during activation of the FPN. The DMN is characterized by low activity during focused attention and high activity when the

mind is not involved in behavioral tasks[4,50,68]. Disruption to this deactivation is a proposed basis for mental health disorders. Schizophrenia, for example, has been shown to have hyperconnectivity of the DMN with the FPN due to a lack of deactivation of the DMN, leading to deficits in EF[68–73].

Frontal and parietal regions involved in EF are anatomically connected by axonal bundles such as the superior longitudinal fasciculus (SLF) which is a key white matter tract involved in EF cognitive processes[19,74,75]. Inhibition has been shown to be inversely correlated with mean diffusivity in the SLF. Increased fractional anisotropy in the SLF is associated with increased skill level in set shifting, a key component of EF where the brain is able to unconsciously switch between tasks[19]. Working memory is also heavily influenced by SLF integrity, with increased FA associated with better working memory skills[18,76,77]. This pattern of altered diffusivity in the SLF is seen in schizophrenia[78] and ASD[79], and is supported by lesion studies[80,81].

Development of EF and Associated Neural Circuits

Development of the prefrontal cortex is protracted in comparison to other brain regions, continuing into the third decade of life[82]. The brain develops in a “back-to-front” manner reflecting phylogeny, with the highly specialized frontal cortex developing last[83] and the more primitive portions developing first[84]. The frontal cortex itself also develops in a “back-to-front” manner. The PFC can grow and differentiate independently from other areas and in mice it has been shown that specific fetal growth factors regulate the regionalization[85,86] even before innervation from afferent axons is made[85]. The PFC delineates into distinct regions including the medial, lateral, and orbitofrontal aspects[87]

beginning the third month prenatally[88]. In infancy, specifically between birth and two years of age, the prefrontal cortex develops rapidly.

The development of EF abilities coincides with the development of the prefrontal cortex, with an extended development allowing for vulnerability to perturbation and environmental influences. Executive attention, or the ability to block interfering information from current attention, develops around four months of age[89]. Other aspects of EF such as flexibility and set shifting emerge between five and eight months of age[90], with appreciable working memory developing just before the sixth month[91]. Though there is a detectible temporal pattern in emerging aspects of EF, this time period is especially sensitive to disturbances that have long lasting impacts. Preterm birth[92,93], influences from parenting[90], maternal depression and anxiety[94], and prenatal maternal stress[95] can all be factors in determination of long-term EF outcomes. It his hypothesized that because the infant brain changes so dynamically during this early developmental changes, integration of aberrations can all have long-lasting, permanent effects.

During childhood, the brain reaches its final adult volume at approximately 6 years of age[96]. The grey matter volume increases in the frontal lobe peaks at around 12 years of age, or just ahead of puberty, and is followed by a decline in adulthood[97]. The grey matter development and subsequent pruning follows an “inverted-u shaped” trajectory[98]. This second surge of neuronal growth is one of the most dynamic periods of development only after infancy. The brain undergoes a rewiring until approximately 24 years old with drastic changes made to the prefrontal cortex in terms of synaptic pruning and myelination[82].

The FPN is detectable prenatally but is the last of the canonical networks to show adult-like integration between itself and other networks. While adult brains rely on far-reaching connectivity functioning between networks, the connectivity of the brains of infants are mostly based on anatomical connections, or regions physically near each other[99]. Through time, segregation, or a general decrease in correlation strength in anatomically near regions, and integration, an increase in correlation between regions not necessarily anatomically connected, occurs[99,100]. This increase in between-network connections allow for a more efficient brain in terms of processing. Regions of higher order cognitive function, such as the FPN, maintain their own spatial and developmental independence moving through development[101] and lag behind those more fundamental functions again defined by phylogeny.

The SLF is a key connector that the brain heavily relies on for EF. It as well has protracted growth, not easily identifiable in its full form even after birth[102,103]. It is still noticeably small in the developmental period of 3 to 12 months[104] with lower FA up to 13-24 months[105]. Elongation of major white matter tracts, such as the SLF, are generally not completed until around nine months, while the myelination process continues into late childhood and adolescence[101,106].

Genetic architecture of EF and associated neural circuits

The heritability of EF has been estimated at 86%-100%[107–109]. A common, latent EF variable determined by Friedman and colleagues[107] was estimated at 99%, with the subdomains of updating and set shifting having an estimated heritability of 56% and 42%, respectively. Working memory specifically has had reported heritability between 42% and 46%[110] and inhibition is estimated at 60%[111]. Polygenic risk scores have established

relationships between EF domains and psychiatric disorders. Schizophrenia shows association with poor cognitive flexibility, ADHD and depression for inhibitory control, and bipolar disorder with working memory[112]. Genetic factors are also the main source for phenotypic correlations between flexible thinking, working memory, and schizophrenia[113–115]. These genetic factors driving the disorders manifest in neuroimaging endophenotypes that may allow for earlier diagnosis of psychiatric disease. These studies have primarily been conducted in adults. In the second chapter of this dissertation, we extend the current literature by estimating the heritability of resting-state networks involved in EF during early infancy.

Sex Differences in EF

In early childhood males perform more poorly than females in attention, working memory, and inhibitory control[116–118]. In a meta-analysis of sex-differences in adults in EF, heterogeneity in results was a major finding and was attributed to heterogeneity in the administration of the cognitive tests[119]. However, it was demonstrated consistently that males scored higher than females in working memory tasks and females performed better in response inhibition[119].

The prevalence of ADHD in the population is estimated anywhere from 4-15%[120–123] in grade school children with the ratio of males to females observed at 3:1[124,125]. Different symptomology is associated with each sex, with females showing more inattentiveness and males having higher rates of impulsivity[126–128]. Females are also more likely to be diagnosed with anxiety and depression prior to being diagnosed with ADHD with females being 5.4 times more likely to be diagnosed with major depression before their ADHD diagnosis[127,129,130]. Females are also more likely to have comorbid psychiatric

disorders and less externalizing problems than males[127,129,131,132]. The mechanisms contributing to sex differences in EF and EF-related disorders are an area of ongoing debate. Chapters 3 and 4 of this dissertation will help address this question by (1) determining how the loss of a second sex chromosome influences white matter tracts and brain networks involved in EF in infancy, and (2) creating an online platform for testing EF in adult women with X monosomy.

Social Cognition (SC)

Definition of SC and Component Processes

SC, or the "knowing of people"[133], is the set of psychological processes that allow individuals to engage and take advantage of being part of a social group[134]. The Research Domain Criteria (RDoC)[33] breaks SC into multiple subdomains. These include attachment, perception and understanding of others, perception and understanding of self, and social communication which is further broken down into reception and production of facial and non-facial communication[135]. According to the RDoC, attachment is selective engagement in positive social interactions with other individuals which develops a social bond. Attachment involves the processing of social cues as well as social learning and memory that are associated with the forming and maintenance of relationships[33]. Facial and non-facial communications involve one's ability to both convey and perceive an emotional state of another nonverbally via facial expressions, or non-verbal gesture, affect, and body language[33]. Theory of Mind (ToM) is the understanding that others have beliefs, desires, and intentions that differ from an individual's own and is also a key component of SC[136]. Measures of SC can include tests such as Reading the Mind in the

Eyes, a task that requires an individual to look at a set of eyes and select which emotion they believe the eyes are conveying[137]. This probes both ToM and facial communications. Additional testing measures include other emotion recognition tasks, such as the Penn Emotion Recognition Task[138] and the Bell Lysaker Emotion Recognition Task[139] which both have been evaluated to have useful psychometric properties. Tests for SC outside of the emotion recognition tasks include the Edinburgh Social Cognition Test[140], which addresses ToM and an understanding of social norms, and The Awareness of Social Interference Test[141].

Relevance of SC to Psychiatry

Social cognitive disturbances arise in numerous psychiatric disorders and sometimes form the foundation of the diagnostic criteria. This is the case for autism spectrum disorders (ASDs)[142]. Characterized by profound impairments in interpersonal interaction and communication, levels of SC are directly related to levels of social functioning[143]. Though there are many changes in the degree of severity in certain symptoms of ASD over life, social difficulties tend to remain the most stable[144]. Schizophrenia-spectrum disorders[145,146] are also characterized by social cognitive deficits. While ASD is characterized by "insufficient" inferences, schizophrenia can be classified by its "excessive" mental attributions, leading to the hypothesis that the two are diametrically related disorders of SC[147,148]. In schizophrenia, levels of cognition and overall functioning are mediated by SC[145,149], which has been reported as the greatest unmet treatment need in the disorder[150]. ADHD also has a component of social cognitive deficiency in childhood and adolescence, showing poorer abilities in recognizing emotion facially in others[151–153]. Like in schizophrenia, individuals with ADHD show increased functional impairments as

social cognitive abilities decrease[154] taking the pattern of a loop in which improvement in one is needed to improve the other[155].

Neurobiology of SC

In SC, ToM has been shown to be associated with the left medial prefrontal cortex[156–158] and the amygdala, part of the limbic system, in facial expression recognition[159–161]. The orbitofrontal cortex is implicated in understanding and displaying appropriate social behaviours[162–164]. The temporoparietal junction is an additional area with strong support for its role in SC[165] and is thought to control representation of the self or another individual[166 153].

ASD with its social cognitive deficits show volumetric abnormalities, specifically in the parietal lobe. Children with ASD show localized reduction in grey matter in the parietal networks[167] which are implicated in various aspects of SC[168]. Specifically, research has shown a role for the inferior parietal lobule in SC[169] in ASD, displaying a negative correlation between grey matter volumes and social cognitive scales.

The DMN is a major component of the “social brain” and is involved in empathy, morality, ToM, and perceiving and interpreting other’s emotional states[170]. Three main components of the DMN are the temporoparietal junction, the posterior cingulate cortex, and the medial prefrontal cortex. Within-network connectivity of the DMN shows an inverse correlation with the severity of autistic traits[163171]. Aberrant within-network functional connectivity is additionally observed in ADHD in the DMN[172]. Both ASD and ADHD are characterized by their unique social behaviors, and the DMN appears to have a key role in this system. The temporoparietal junction is also implicated in SC including

theory of mind[173], empathy[174], and moral judgements[175 176], and is a necessary component for mentalizing based on lesion studies[173]. Depression and schizophrenia, which both involve disruptions in higher-level social functioning, show lower connectivity between the temporoparietal junction and the posterior cingulate cortex and overall show reduced resting-state functional connectivity between the temporoparietal junction and other key regions of social processing[177]. Aberrant functional connectivity was additionally found between the temporoparietal junction and key areas that control behavior and SC in a study comparing individuals with major depressive disorder to controls[178].

The integrity of specific white matter pathways is also important to the function of the "social brain". The inferior longitudinal fasciculus, the inferior fronto-occipital fasciculus, and the superior longitudinal fasciculus are all linked to facial recognition and processing[179]. ASD is often accompanied by disrupted white matter microstructure[180–182], and lower fractional anisotropy of the superior longitudinal fasciculus has shown to be positively correlated with social interaction scores in ASD[183–185] The inferior longitudinal fasciculus (ILF) is also implicated in SC as it is heavily involved with emotional facial recognition[20], with lower FA being reported in disorders of SC[183,186]. The ILF is directly connected to the amygdala whose relation to SC has been previously touched upon. The arcuate fasciculus, which connect the temporoparietal junction to the frontal cortex, showed reduced white matter integrity in a study of high-functioning autism that simultaneously showed weaker functional connectivity between the temporoparietal junction and frontal areas[187].

Development of SC

Like in EF, the prefrontal cortex is integral for the development of SC. The parietal networks, inferior parietal lobule, and temporoparietal junction all play a role in SC as well. The prefrontal cortex has been discussed in terms of prenatal development above. The parietal lobe can be defined visually between gestational weeks 14 and 26, with the formation of the parieto-occipital sulcus[188,189]. In infancy at approximately 2 months of age the inferior parietal areas are used in facial recognition[190]. In the second year of life, the inferior parietal cortices show the fastest rate of surface area expansion compared to other regions[191]. The grey matter of the parietal lobe increases in childhood and peaks at 10.2 years for females and 11.8 years for males, declining in adolescence[97]. This pattern is similar to what occurs in the frontal lobe, but the decline is more substantial in the parietal lobe[97].

Aspects of SC are measurable even from the early stages of infancy. Between two and three months infants are able to distinguish between two facial expressions[192]. This finding should be interpreted with caution though because although a discrimination is able to be made, understanding of the emotional meaning of the facial expression has not developed. Theory of Mind, or at least its precursors, are evident in infancy during the 12-18 month period[193]as evidenced by “mind reading”, or the ability to predict the goals of others[194]. Over development, understanding of disgust and anger in facial expressions increases drastically, whereas recognition of fear and happiness show stability from early childhood[195]. Between the ages of three and six, considered the preschool years, understanding of Theory of Mind exhibits conceptual changes such as understanding of false-beliefs and the beliefs of others[196–198].

Key white matter tracts that influence SC include the inferior longitudinal fasciculus, the inferior fronto-occipital fasciculus, and the superior longitudinal fasciculus. Fetal development of white matter tracts occur in four phases, with the superior and inferior longitudinal fasciculi developing in the second wave (approximately 14 weeks gestation) and the inferior-occipital fasciculus in the fourth wave (approximately 20 weeks gestation)[103]. These association fibers can be identified with tractography in neonates but lack sufficient development to be detected by tractography at 20 weeks gestation[199,200]. During infancy the number of discernable tracts, their length and volume, and fractional anisotropy increase with age, with a plateau between ages 3 and 5[201].

The default mode network is a primary focus in the study of functional networks involved in SC. Functional networks can be observed *in utero* as early as the second trimester[202–204]. In a study *in utero* examining functional connectivity in the fetal brain, statistically significant overlap was found between adult and prenatal default mode network modules (average age 33.5 weeks gestation)[202]. Over gestation, these modules gain more long-range connections and the default mode network becomes more specialized[205,206], with the posterior cingulate cortex acting as a hub of the network[207]. In full-term babies, a “proto-default network” has been described, with only a portion of the adult resting-state connections observed in these infants[208]. At approximately two years of age, the network gains more adult-like topology, integrating the anatomical portions missing from the network in neonates[209]. However, research in early school age children still show only sparse functional connectivity, though over development integration with other networks occurs[210].

Genetic architecture of SC

Vasopressin and oxytocin receptor genes playing a part in SC is a recently growing area of research, with specific relevance to schizophrenia as well as ASD[211–213]. For example, genetic variants in the oxytocin repressor gene show deficits in global social functioning as well as in social affect recognition[213,214]. The genetic underpinnings of SC have been studied widely, with multiple association studies revealing SNPs related to social functioning[215–217]. A study by St. Pourcain and colleagues[218] estimated the heritability of social communication at 18% which was replicated by an additional study by the group[215] but shown to vary with age[219]. Studies focusing on the broad general concept of SC have reported heritability of 68%[220], with attention to specific subdomains such as emotion identification being estimated at 36%[221]. Emotion identification specifically has been shown to associate with polygenic risk for schizophrenia[222], a disorder that has been previously discussed for its great influence on SC. Studies involving neuroimaging endophenotypes as markers for these genetic factors have primarily been conducted in adults. Chapter 2 of this dissertation will extend the current literature by estimating the heritability of resting-state networks involved in SC during early infancy.

Sex differences in SC

Sex-differences in social cognitive testing are very dependent on the test administered[223]. However, typically developing females have been shown to have a greater general ability to decipher facial expressions than in typically developing males[224–226], have better nonverbal communication[227,228], and are better at expressing emotional

experiences[229]. Women also tend to score higher than men on empathy ratings and emotional regulation[230].

The autism spectrum disorders additionally show a sex-bias. The ratio of diagnosis in males to females is estimated at 3:1[231,232] to 4:1[233,234] with prevalence in the population observed at approximately one percent[234–236]. Females are typically diagnosed later than males[237] and have more pronounced difficulties with social communication and interaction[238,239] at a young age compared to the male ASD population. However, girls with ASD that lack cognitive impairment are consistently better at camouflaging, or using compensatory behaviors, to mask ASD's associated social challenges[240–242]. Another area of observed differences in clinical presentation of ASD between the sexes is in cases of intellectual impairment. With intellectual disability, the symptomology of ASD in girls is more severe[243] and the sex ratio becomes closer to 2:1 M:F whereas the ratio climbs to approximately 11:1 M:F in individuals without intellectual impairment[244,245]. The mechanisms contributing to sex differences in SC and SC-related disorders are an area of ongoing debate and that Chapters 3 and 4 of this dissertation will help address this question by (1) determining how the loss of a second sex chromosome influences white matter tracts and brain networks involved in SC in infancy, and (2) by creating an online platform for testing SC function in adult women with X monosomy.

Turner syndrome as a model for understanding sex chromosome effects on EF and SC

Described by Henry Turner in 1938[246], Turner syndrome (TS) or X monosomy occurs in approximately 1 in 2000 live female births and results from a complete or partial absence of the second sex chromosome[247]. Mosaicisms may occur, in which different

cells in the body contain different chromosomal arrangements. Common phenotypes of TS include congenital heart defects, renal abnormalities, liver disorders, and gonadal dysgenesis[248,249]. Girls and women with TS often exhibit a unique cognitive profile with normal or above average intelligence and deficits in three specific cognitive domains. These include EF, SC, and visuospatial processing. These skills are essential for everyday functioning and influence short-term memory recall, social interactions, and an understanding of space and measurement.

These neurocognitive domains affected in TS shows great relevancy to both ASD and ADHD as they share similar deficits[250,251]. TS can also be comorbid with ASD and ADHD. TS individuals are more likely to be diagnosed with these disorders than XX females. In one early study, Turner syndrome girls had a risk of developing ASD 300 times higher than typically developing girls[252]. As a note, the study had a very small sample size and worked under the assumption that the population prevalence of ASD in females was 1:10,000, the accepted prevalence at the time. A more updated study put the estimation at four times more likely and used a registry system, yielding a much larger sample size[253]. In a separate study, an 18-fold increase in the prevalence of ADHD in TS girls compared with girls in the general population was found, equating to a prevalence of approximately 25% in TS girls[254]. The ADHD presentation is also more similar to males with ADHD than females, with higher hyperactivity scores being reported for females with TS[255]. However, the aforementioned registry study did not find any association between TS and ADHD, though this could be due to its retrospective design and the underdiagnosis of ADHD in TS[253]. Elevated risk for male-based neurodevelopmental conditions in phenotypically female individuals with TS may have a genetic explanation.

Females with TS are more similar to typically developing males in the sense that 1) both are hemizygous for genes that escape X inactivation (approximately 15%[256]), and 2) there is only the presence of one X chromosome, uncovering X chromosome mutations.

Differences in neuroanatomy and brain connectivity have also been observed in TS and align with the known neurocognitive challenges. For example decreased grey matter volumes are consistently reported in the parieto-occipital cortex [257–261], which plays a key role in visuospatial processing. Consistently, reduction in volume of the parietal lobe and increase in volume of the amygdala and orbitofrontal cortex has been reported[257,259,262,263]. White matter volume increases have also been consistently observed in the temporal lobe in TS which is implicated in language and SC[257–259].. TS has a very distinct structural connectivity profile as well which is supported by the literature. Multiple studies have reported reduced FA in the superior longitudinal fasciculus (SLF) with others reporting more global reductions[258,264,265]. As discussed previously, the SLF is a part of brain networks that process working memory, language, visuospatial attention, and numerical tasks[76,266,267]. Functional connectivity studies have also contributed to our understanding of the neurocognitive profile of X monosomy. Numerous lines of investigation have demonstrated altered functional connectivity in TS,[268] which have implications to the symptomology of the disorder, including the neurocognitive domains[269–271]**.** Although the work was done using task-based fMRI, Bray and colleagues[271] were the first to demonstrate abnormalities in the parieto-occipital and parieto-temporal pathways, which implies a root to the deficits in visuospatial processing. A recent study of infants with TS indicates that volume differences are already present at

one year of age[272], but no studies have looked at the DTI or resting-state MRI phenotypes in TS infants. This dissertation will address this gap in Chapter 3.

There is significant heterogeneity within TS in terms of the cognitive phenotype, which remains unexplained. Thorough cognitive testing is needed to understand qualitatively and quantitatively the unique domains affected in TS. This ability is currently limited by both access to resources such as clinical testing centers and licensed software as well as geographical constraints based on location of the testing facility. A browser-based online platform is needed to facilitate large-scale studies of how genetic and clinical factors influence EF and SC variation within TS. A solution to this challenge is approached in Chapter 4 of this dissertation.

The importance of studying EF and SC circuits during infancy

To date, the vast majority of imaging genetics has been performed on adults and adolescents, missing a critical window in which vulnerability to psychiatric disorders is established in early life. A high-familial risk study by Auerbach and colleagues[273], with groups defined by severity of paternal presence of ADHD, shows ADHD may also begin to emerge in infancy as developmental pathways are enacted[274,275]. ASD is another disorder that's descent into clinical presentation is focused on infancy and early childhood[276,277], but evidence of abnormal developmental changes are discernable prenatally as well. ASD has recently been considered prenatally derived due to the exponential proliferation of cortical neurons between ten and twenty weeks of gestation that result in the hallmarked overgrowth of the cerebral cortex later in life[278]. Additionally, most ASD risk genes are expressed prenatally in higher levels than postnatal development[278,279]. Altered prenatal gene expression for ADHD has also been reported,

with differentially methylated genes also playing a role[280,281]. Overall, the fetal and infant brain are growing at an exceptionally high rate, making it potentially vulnerable to both genetic and environmental disruptions. Prenatal stress, which includes physical stress, nutrition, hormonal, substance use, infection, and psychological stress, can have long lasting effects on the brain, specifically in cognition and susceptibility to the future development of psychiatric disorders. Famine and maternal malnutrition during pregnancy has been shown to result in higher levels of schizophrenia in offspring[282–284]. Maternal psychiatric stress has also been shown to increase the probability of the presentation of anxiety and depression in offspring later in adolescence and adulthood[285–287].

In addition, there are specific challenges in using an adult population to study the genetic influences on brain anatomy and function. Adults carry with them years of behavioral-environmental interactions and, in the individuals with chronic psychiatric illnesses, the added complication of prolonged use of psychotropic medication. For example, the use of lithium in bipolar disorder is characterized by increases in grey matter volumes as part of the treatment response[288]. Conversely, the use of antipsychotics is linked to decreased grey matter volumes in individuals taking these medications[289]. Examining the influence of genetic risk for bipolar disorder on brain development in presymptomatic individuals, beginning in infancy, may provide clearer insights into etiology. TS, as previously mentioned, is characterized by short stature and gonadal dysgenesis, among other defining features. As a result, most girls go through some type of hormone therapy to ameliorate the repercussions of the illness[290]. Individuals may also take medications for heart problems, renal problems, or take psychotropics[291].

Medications, including hormone therapy, could cause changes in brain structure and function in these individuals that are not directly related to X chromosome loss.

Infant neuroimaging could also facilitate the development and implementation of early interventions, which would increase quality of life for affected individuals. In the work of Emerson et al.[292], the group was able to use functional connectivity measures from six-month-old infants as a predictor for the diagnosis of autism spectrum disorder with a positive predictive value of 100%. This demonstrates that at-risk individuals can be identified based on their infant neuroimaging phenotypes. The outcomes of autism spectrum disorder are heavily reliant on early detection and intervention[292]. Dawson and colleagues[293] demonstrated that specialized early intervention significantly improved IQ and adaptive behavior over a two-year period beginning in early childhood in comparison to children receiving only standardized care from a physician.

Rationale for the dissertation

The overarching goal of this dissertation is to determine how genetic variation influences neural circuits and cognitive domains relevant to psychiatric illness with a particular focus on EF and SC. In this introduction, I have demonstrated that EF and SC are heritable, disrupted in multiple psychiatric disorders, differ between males and females, and linked to brain regions and neural circuits with protracted developmental trajectories that can be studied via neuroimaging. I have also identified specific research gaps that will be addressed by my dissertation studies. Specifically, in Aim 1 I will identify genetic and environmental factors influencing the FPN, DMN, and other resting-state networks in infancy, a period that has been relatively understudied. In Aim 2, I will determine if differences in functional connectivity and white matter integrity, identified in

adults and adolescents with TS and linked to EF and SC deficits, are also present in infancy. Finally, in Aim 3 I will develop a browser-based online cognitive testing platform targeting EF, SC, and other areas of challenge in TS. This will facilitate large-scale studies of how genetic variation influences SC and EF in TS. In the following paragraphs, I will explain each aim in greater detail. Together, the successful completion of the three aims provides novel information about genetic influences on EF, SC, and connectivity in associated neural circuits. Ultimately, understanding the genetic basis for variation in EF and SC could open up new opportunities for identifying at-risk individuals in early life and lead to the identification of treatment targets.

In my first aim I sought to identify genetic and environmental factors influencing neonatal resting-state functional connectivity including connectivity within and between the frontoparietal and default mode networks, which play critical roles in EF and SC respectively. I hypothesized that measures of within-network and between-network connectivity would be heritable, with the earliest maturing networks having the strongest genetic effect. Conversely, I hypothesized that the later maturing networks, FP and DM for example, would be under the least amount of genetic control in this developmental period. Additionally, I hypothesized that maternal psychiatric history would be associated with within- and between-network functional connectivity in the limbic network, which also plays a role in SC. Accomplishment of this aim defines an incredibly early timepoint in the determination of genetic control over the brain's connectivity profile. This timepoint links prenatal findings with those in older infants, helping to create a more complete map of the genetic architecture of the developing human brain.

In the second aim, I compared the anatomical and functional connectivity differences in infants with TS to typically developing children of the same age. I hypothesized that infants with TS would have aberrant diffusivity in the SLF as well as reduced functional connectivity between the precentral gyrus and regions involved in basic visual processing (calcarine cortex), SC (supramarginal gyrus and lingual cortex), and EF (supramarginal gyrus). Successful completion of this aim will have a positive impact on the field by having the potential to show whether differences in structural and functional connectivity observed in older children and adults with TS are present in infancy, versus emerging at a later developmental stage. This has implications for early intervention strategies and therapies for TS that could help ameliorate neurocognitive deficits in the disorder.

In my final aim, I created an online browser-based cognitive battery targeting domains that are often disrupted in TS including EF and SC. I validated the battery by comparing females with TS, XX females, and XY males. I hypothesized that, overall, the TS group would perform significantly worse on the tests in all domains, with longer response times and lower accuracy on the tests. At the completion of this aim, I will have a validated set of tasks that can be used to measure cognition in TS on an online platform that can be done from anywhere with an internet connection and circumvents the need for in person testing. In person testing limits the geographical area a researcher can pull from; thus, this objective allows for an expansion of women with TS that can be reached. My work provides the foundation for a future large-scale study of genetic influences on cognition in TS.

Chapter 2

Genetic and Environmental Factors Influencing Neonatal Resting-State Functional Connectivity

Abstract

Functional magnetic resonance imaging has been used to identify complex brain networks by examining the correlation of blood-oxygen-level-dependent signals between brain regions during the resting state. Many of the brain networks identified in adults are detectable at birth, but genetic and environmental influences governing connectivity within and between these networks in early infancy has yet to be explored. We investigated the genetic influences on neonatal resting-state connectivity phenotypes by generating intraclass correlations and performing mixed effects modeling to estimate narrow-sense heritability on measures of within network and between-network connectivity in a large cohort of neonate twins. We also used backwards elimination regression and mixed linear modeling to identify specific demographic and medical history variables influencing within and between network connectivity in a large cohort of typically developing twins and singletons. Of the 36 connectivity phenotypes examined, only 6 showed narrow-sense heritability estimates greater than 0.10, with none being statistically significant. Demographic and obstetric history variables contributed to between- and within-network connectivity. Our results suggest that in early infancy genetic factors minimally influence brain connectivity. However, specific demographic and medical history variables such as gestational age at birth and maternal psychiatric history may influence resting-state connectivity measures.

Introduction

Historically, functional magnetic resonance imaging (fMRI) studies of the brain have focused on localizing functions to specific cortical and subcortical areas without addressing the functional integration of different brain areas, which is essential for complex behavior. More recently, resting-state functional connectivity studies have provided new insights into large-scale brain organization by examining the temporal correlation of blood-oxygen-level-dependent (BOLD) signals between brain regions that are not necessarily anatomically connected [294]. Regions with strongly correlated BOLD activity are thought to represent functional networks. Around ten major canonical networks have been identified in adults [295], including the default mode, somatosensory, frontoparietal, visual, dorsal attention, ventral attention, limbic, and subcortical networks. Understanding individual differences in resting-state connectivity is of interest because these networks play critical roles in perception [296–299] and high-level cognition [67,300,301], encompassing social cognition [302–304], executive functioning [66,305], and attention [306,307]. Furthermore, abnormalities in these resting-state connectivity networks are associated with the development of psychiatric diseases. Schizophrenia [308–310], obsessive compulsive disorder [311], and autism spectrum disorders [312] all show distinct patterns of within- and between-network connectivity when compared to typically developing individuals.

The prenatal and early postnatal period represents a critical epoch in the establishment of resting state networks. *In utero*, the intrinsic connectivity of the entire human brain increases over time, with the greatest period of change observed between 26- and 29-weeks gestation. This period of rapidly increasing connectivity occurs first in

occipital cortex, and then in temporal, frontal, and parietal cortex [313]. Modularity is present in the fetal human brain, but in contrast to canonical brain networks measured in adulthood, which often include spatially distant brain areas, these fetal modules are spatially restricted. Modularity is defined in the context of networks as separate clusters of function within the brain as a whole that interact more with themselves than in the network community. Some of these modules may represent very early versions of adult canonical networks including the sensorimotor network and the default mode network. Interestingly, modularity decreases during the third trimester, suggesting more integration between different brain regions [205]. Neuroimaging of neonates reveals that many resting-state networks are detectable shortly after birth [101,208,209,314–317]. Some of these networks already demonstrate an adult-like topology, including the sensorimotor network, the auditory/language network, and primary visual networks. Others, involving high-order association cortices show a less mature topology. This includes the default mode network, the lateral visual/parietal network, the salience network, and frontoparietal networks involved in executive function [318]. The maturation of canonical networks during the first two years of life follows a specific temporal sequence, beginning with primary sensorimotor/auditory networks, proceeding to visual networks, then to salience and default-mode networks, and finally to executive control networks. During this same period, and later in childhood, within-network connectivity strengthens while between-network connectivity wanes [319].

Individual differences in the development of resting-state connectivity could be due to both genetic and environmental factors. In adults, resting state connectivity metrics are under modest-to-moderate genetic control [320,321], with stronger heritability observed in

within- as opposed to between-network connectivity [322]. The default mode network, for example, has been reported to have a heritability of 0.424 for functional connectivity measures [320], with an average heritability of connection strengths in adults for a BOLD time course at 15-18% [321]. In adolescents, longitudinal age-related changes in both between- and within-network connectivity are pervasive, with up to 53% of the variation attributable to heritability [323]. Studies on genetic contributions to resting-state connectivity in infancy are extremely limited. In a 2014 paper, Gao and colleagues [324] used voxel-wise general linear model (GLM) regression analysis to test the effect of genetic relatedness on voxel-wise functional connectivity patterns in neonates, one-year-old infants, and two-year-old infants. In neonates, genetic effects were observed in the posterior cingulate cortex, cuneus, fusiform gyrus, and bilateral middle and inferior frontal gyri. In one-year-olds, genetic effects were observed in the paracentral lobule, posterior cingulate cortex, bilateral lingual gyrus, right middle occipital gyrus, right angular gyrus/parietal-temporal-occipital junction, bilateral middle and inferior frontal gyri, and ventromedial prefrontal cortex. In two-year-olds, genetic effects were observed in the left middle temporal gyrus and left supramarginal gyrus. The authors also reported modest genetic effects on within-network connectivity that varied with age but did not examine between network connectivity.

Because infancy is a critical period in the establishment of functional brain networks, the pre- and perinatal environment could also be important factors in explaining inter-individual variation in brain connectivity. Two of the most studied factors to date include maternal depression and prenatal drug exposure. Regarding maternal depression, high prenatal maternal depressive symptoms are associated with greater

functional connectivity between the amygdala and an array of brain regions involved in emotional regulation including the left insula and bilateral anterior cingulate, medial orbitofrontal and ventromedial prefrontal cortices [325]. Interestingly, similar patterns of altered connectivity have been observed in adults and adolescents with major depressive disorder [326–328]. Brain networks involved in emotional regulation also appear to be particularly sensitive to prenatal drug exposures including cocaine and marijuana [329–332]. Further, prenatal cocaine exposure is associated with hyperconnectivity between the thalamus and the frontal regions of the brain [333], while multiple drugs are associated with a hypo-connectivity between the thalamus and motor-related regions. Many other aspects of the pre- and perinatal environment, which are known to have major effects on neonatal brain structure [334], have yet to be examined in relation to functional connectivity.

The main objectives of the current study are to (1) investigate genetic influences on neonatal resting-state connectivity phenotypes using twin data and (2) understand how major demographic and medical history variables affect neonatal resting-state connectivity phenotypes using a large, prospective cohort of singletons and twins. We address the first objective by generating intraclass correlations and performing mixed effects modeling on measures of within network and between-network connectivity. We address the second objective via linear mixed modeling. Based on the literature reviewed above, we hypothesized that measures of within network and between-network connectivity would be heritable, with the strongest genetic effect evident for early maturing networks involved in perception and movement. As discussed above, maternal depression has been linked to changes in limbic connectivity in offspring, therefore we further hypothesized that maternal psychiatric history would be associated with functional

connectivity within the limbic network and between the limbic network and other networks. Additionally, we hypothesized that gestational age at birth would be associated with connectivity within the somatosensory network and between the somatosensory network and other networks. We based this hypothesis on studies showing that disrupted development of the somatosensory network in preterm infants is associated with downstream cognitive deficits [335,336].

Materials and Methods

Participants

Participants were 268 neonates (average gestational age of 261 days), both male and female, including singleton, unpaired, monozygotic (MZ) and dizygotic (DZ) twins. The current sample represents a subset of 1329 infants enrolled in the Early Brain Development Study (EBDS) [337–339] at the University of North Carolina at Chapel Hill that were imaged via MRI around 1 month post-birth and had usable resting state fMRI scans. Exclusion criteria for the parent study were set at enrollment and included the presence of abnormalities on fetal ultrasound or major medical illness in the mother. Additional exclusion criteria for the current analysis included gestational age at birth 32 weeks or fewer and missing medical/demographic information. Opposite-sex twin pairs were also excluded. Demographic variables including maternal and paternal age, education, and ethnicity, household income, maternal smoking during pregnancy, and paternal psychiatric history were collected via maternal report. Income was factorized by dividing it into three categories, each defined as falling into either at or below 200%, between 200% and 400%, and above 400% of the federal poverty level. The infant's date of birth

was used to identify the federal poverty level for each specific case while also taking into account family size. Maternal psychiatric history was assigned based upon both maternal report and review of medical records. Maternal and paternal psychiatric history were considered binary variables. A positive psychiatric history included a diagnosis in any of the following DSM-V categories: autism spectrum disorders, Tourette's syndrome, attention-deficit hyperactivity disorders, obsessive-compulsive and related disorders, anxiety disorders, mood disorders, or schizophrenia spectrum and other psychotic disorders. Medical history variables (gestational age at birth, birthweight, APGAR scores, gestation number, delivery method, and stay in neonatal intensive care unit over 24 h) were collected from maternity and pediatric medical records [337].

MRI Acquisition and Processing

A detailed description of image acquisition and processing can be found in [340]. Briefly, functional MRI data was acquired using a T2*-weighted EPI sequence: TR=2 s, TE = 32 ms, 33 slices, and 4mm isotropic resolution, with 150 volumes acquired over 5 min. Similar scan durations have been used in prior infant imaging studies and minimize data loss due to infants waking up during the scan (Gao, Gilmore et al. 2013, Alcauter, Lin et al. 2014, Gao, Alcauter et al. 2015, Gao, Lin et al. 2017). Structural images were acquired using a 3D MPRAGE sequence: TR = 1820 ms, TE = 4.38 ms, and 1 mm isotropic resolution. Two different scanners were used: a 3T head-only Siemens Allegra during the early years of the project, and a 3T Siemens TIM Trio (Siemens Medical Supplies, Erlangen, Germany) during later years. There were 42 infants imaged on the TIM Trio and 226 on the Siemens Allegra. All infants were in a natural sleep state during the imaging session.

Functional data were preprocessed using the FMRIB (for Functional MRI of the Brain) Software Library (FSL; version 6.0; [341]) and Analysis of Functional NeuroImages (AFNI; [342]). Steps included discarding the first 3 volumes (6s), slice-timing correction, rigid-body motion correction, bandpass filtering (0.01–0.08 Hz), and removing the nuisance signals including the signals of white matter, CSF, the 6 motion parameters and their derivative, quadratic terms. The 6 motion parameters were estimated using rigid body registration for each volume with the first volume as the reference image. The nuisance signals were band-pass filtered before regression to match the frequency of the blood oxygen level-dependent signal. Data scrubbing was implemented with scrubbing criteria at global signal changes >0.5% or framewise displacement >0.3mm [343–345] with continuous data points no less than 3. This approach is commonly used in infant resting state fMRI studies in the field [346] and has been shown to minimize motion artifacts. Participants with less than three minutes (90 data points) of functional data after scrubbing were excluded and all infants' functional data were truncated into 90 volumes to ensure consistency across subjects. We chose the three-minute threshold to balance sample size and duration of available time series after scrubbing. This threshold is widely

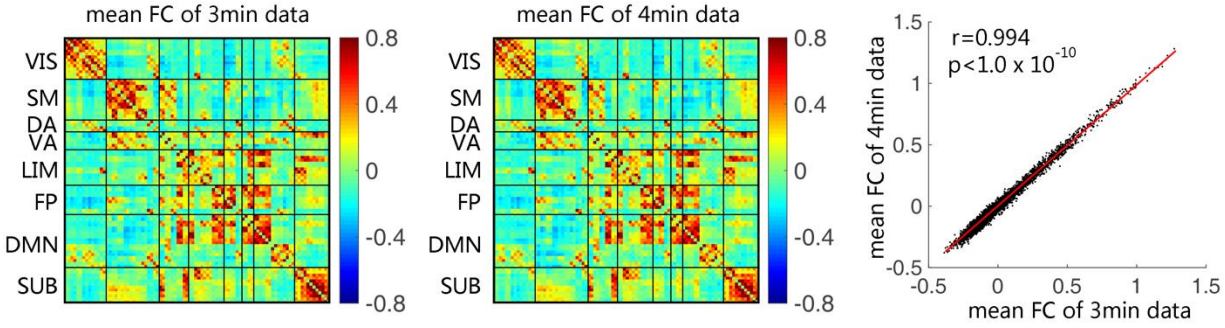

Figure 2.1 Comparison of the functional connectivity values from three-minute and four-minute data from a subsample of 58 subjects. The left panel is the mean functional connectivity (FC) of the 58 subjects with truncated 3-minute (3min) data, the middle panel is the mean FC of the same 58 subjects with their 4-minute (4min) data; the

Figure 2.1 (cont'd)

right panel is the scatter plot of the mean FC between 3min data and 4min data, as well as their correlation.

used in the field [318,346–348], and previous test-retest studies confirm a three-minute duration provides reasonable test-retest reliability[349–351]. Further, when we compare a functional connectivity matrix generated using the three-minute threshold to one created using a four-minute threshold in a subset of 58 infants, we find they are almost identical (Figure 2.1), supporting the validity of a three-minute threshold.

After scrubbing, a single global signal regression step was performed to remove the global signal re-introduced by scrubbing. A template-based skull-stripping method was used the extract the brain from T1 image. After performing a rigid-body registration between the functional data and T1-weighted structural images of the same subject, a nonlinear registration (fNIRT in FSL) was done between individual T1-weighted images and the neonatal template images [352]. The combined transformation field was used to warp the preprocessed rs-fMRI functional images to the neonate template [353]. Finally, the images were spatially smoothed with Gaussian kernel (full width at half maximum = 6mm).

As outlined in Gao et al. [101], a neonate specific AAL atlas was used to define 90 regions covering the neonatal cerebral cortex, as defined by Tzourio-Mazoyer et al and Shi et al. [353,354] for infants. The average BOLD time course was extracted from each region for each subject to construct a 90 by 90 correlation matrix. The correlation matrix was Fisher-Z transformed to be the functional connectivity matrix for each subject.

The 90 regions from neonate specific AAL atlas were assigned to eight intrinsic functional networks [355] based on spatial overlapping (i.e., winner-take-all approach to

assign each region to the network with the highest level of overlap in volume) to group all connections as either within one (both nodes within one network) or between two networks (each node belonging to a different network) (Table A.1). Subsequently, within- and between-network connectivity was calculated by averaging the FC values of the within-/between- networks for each subject. The following networks were examined: default mode, sensorimotor, frontoparietal, visual, dorsal attention, ventral attention, limbic, and subcortical network. Each network was given a number and an abbreviation as shown in Table 2.1.

Table 2.1 Assigned networks numbers, network name, and network abbreviation for the eight assigned resting-state connectivity networks.

	Network	**Abbreviation**
1	Visual	Vis
2	Somatosensory	SS
3	Dorsal Attention	DA
4	Ventral Attention	VA
5	Limbic	Lim
6	Frontoparietal	FP
7	Default Mode	DM
8	Subcortical	SC

Statistical Analyses

To investigate genetic and environmental influences on neonatal resting-state connectivity phenotypes, we calculated intra-class correlations in both MZ and DZ twin pairs with correction for residual framewise displacement, which indicates subject motion. Analyses were performed with R statistical software 4.0.1 [356] using the 'irr' package [357] (version 0.84.1).

To estimate narrow sense heritabilities we fitted mixed-effects models to data from MZ and DZ twins jointly using the nlme R-package. The model was as follows: $y_{ij} = \mu +$

$x_{ij}\beta_i + \epsilon_{ij}$ where y_{ij} is an imaging phenotype (pre-adjusted by the effect of the scanner, motion correction, and sex) for the *j*th twin of the *i*th twin-pair, μ is an intercept, x_{ij} took value 1 for MZ twins and $\sqrt{0.5}$ for DZ twins, β_i is a raondom effect common to a twin pair, assumed to be normally distributed with mean 0 and variance σ_β^2,and ϵ_{ij} is an error term, assumed to be normally distributed, independent across subjects, with mean zero and a variance that varied by zygosity $Var(\epsilon_{ij}) = \sigma_{\epsilon_{MZ}}^2$ and $Var(\epsilon_{ij}) = \sigma_{\epsilon_{DZ}}^2$ for MZ and DZ twins, respectively. Note that with this setting the covariance between twins is $Cov(x_{ij}\beta_i, x_{ij'}\beta_i) = x_{ij}x_{ij'}\sigma_\beta^2$ which is equal to σ_β^2 for MZ twins and equal to $0.5\sigma_\beta^2$ for DZ twins. Therefore, σ_β^2 represents the additive genetic variance for the trait. For MZ twins the error variance represent the variance of non-genetic effects (on the other hand, for DZ twins the error variance also includes the variance due to mendelian sampling). Thus, the heritability of the trait was estimated using $\frac{\sigma_\beta^2}{\sigma_\beta^2+\sigma_{\epsilon_{MZ}}^2}$. This method was also used to estimate the heritability of the motion variable. Confidence intervals were calculating using Bootstrap, and a permutation analysis was performed to generate p-values.

To understand how major demographic and medical history variables affect neonatal resting-state connectivity phenotypes, we performed AIC based backward-elimination regression of the demographic and medical history variables described in the "Participants" section. We then ran mixed effects models including the selected variables for effect size estimation and significance testing and to estimate r^2 values. A Bonferroni correction for the number of mixed effect models run was applied (0.05/36 = .00139). To account for familial relatedness within MZ and DZ twins, we incorporated a standard ACE model as described in Xia et al. [358]. In brief, the twin-based ACE model heritability of each

connectivity measure was estimated by fitting a regression model $y_i = \mu + x_i\beta + a_i + c_i + e_i$, where y_i is the connectivity value of individual i (i =1, …, n), μ is the overall mean, x_i are covariates, and a_i, c_i, and e_i denote the (random) additive genetic, shared environmental, and residual effects. This is done under the assumption that the three random terms are mutually independent and normally distributed with mean 0 and variances σ_a^2, σ_c^2, and σ_e^2.

A power analysis was performed in R by creating a function to fit a mixed-effects additive model using restricted maximum likelihood and then applying it to simulated data. The simulation included narrow-sense heritabilities of 0.1, 0.15, 0.25, and 0.5 with a simulated number of twin pairs, assuming an equal number of MZ and DZ pairs, of 25, 50, 75, 100, and 150. Because this is an additive model of inheritance, dizygotic twins were given a coefficient of relatedness of 0.5 and monozygotic twins a coefficient of 1.0.

Results

Participants for Objective 1

Descriptive statistics for the demographic and medical history variables can be found in Table 2.2. These statistics only include MZ and DZ twins and apply to the first aim of the current study: determination of intraclass correlations and estimation of heritability for each neuroimaging phenotype. Of the 126 participants, 64 are DZ and 62 are MZ, representing a total of 63 twin pairs. Twin pairs were scanned using the same scanner type. Delivery method, household income, and maternal age were significantly different between the cohorts used on the separate scanners (Table A.2).

Intraclass correlations

Figure 2.1 shows the calculated intra-class correlations. Seven of the between-network pairs are located in quadrant one (Figure 2.a), indicating positive correlations between both MZ and DZ twins. None of the within network connectivity measures were located in quadrant one (Figure 2.2b). Quadrant two indicates that the ICC coefficient was

Table 2.2 Demographic and medical history variables for objective 1 participants.

Continuous Variables		Average	SD	Min	Max
Birth weight (g)		2475	441	1470	3650
Gestational age at birth (days)		254	12	224	273
Gestational age at MRI (days)		292	14	248	348
5 min APGAR score		8	0.75	4	10
Maternal education (years)		15	3.	6	24
Paternal education (years)		15	3	6	24
Maternal age (years)		29	5	16	42
Paternal age (years)		32	6	20	49
Residual framewise displacement		0.11	0.02	0.07	0.17
Categorical variables		*N*		%	
Sex	Male	60		47%	
	Female	66		52%	
Delivery Method	Vaginal	40		31%	
	C-section	86		68%	
Household income	High	46		36%	
	Mid	26		20%	
	Low	54		42%	
Maternal ethnicity	White	96		76%	
	Black	28		22%	
	Asian	4		3%	
	Native American	0		0%	
Paternal Ethnicity	White	82		65%	
	Black	38		30%	
	Asian	6		4%	
	Native American	0		0%	
Maternal psychiatric history	No	98		73%	
	Yes	28		26%	
Paternal psychiatric history	No	120		95%	
	Yes	6		4%	
Scanner	Allegra	100		79%	
	TIM Trio	26		20%	
Maternal smoking	No	122		96%	
	Yes	4		3%	
NICU Stay	No	124		98%	
	Yes	2		1%	

negative in MZ twins, but positive in DZ twins. Phenotypes falling in this quadrant include the FP, DA, DM, and Lim networks, and the DM-DA, Lim-DA, SC-VA, DA-Vis, VA-Vis, and FP-VA network pairs. Quadrant three displays coefficients that are negative both in the MZ and DZ twins for that phenotype. This includes the Vis and SC networks and SC-DA, DM-Lim, VA-SS, and VA-DA network pairs. Finally, quadrant four displays MZ coefficients that are positive while the DZ twins' coefficients are negative. The networks and network pairs included in quadrant four are the SS and VA networks and Lim-VA, SC-Lim, DA-SS, FA-DA, DM-Vis, DM-SS, FP-Lim, DM-FP, SC-SS, SC-Vis, FP-Vis between-network pairs. We used the correlations as an exploratory analysis and chose to use mixed effects modeling for the heritability estimation because it is a more powerful model and allows

estimation of heritability using all data from MZ and DZ twins together.

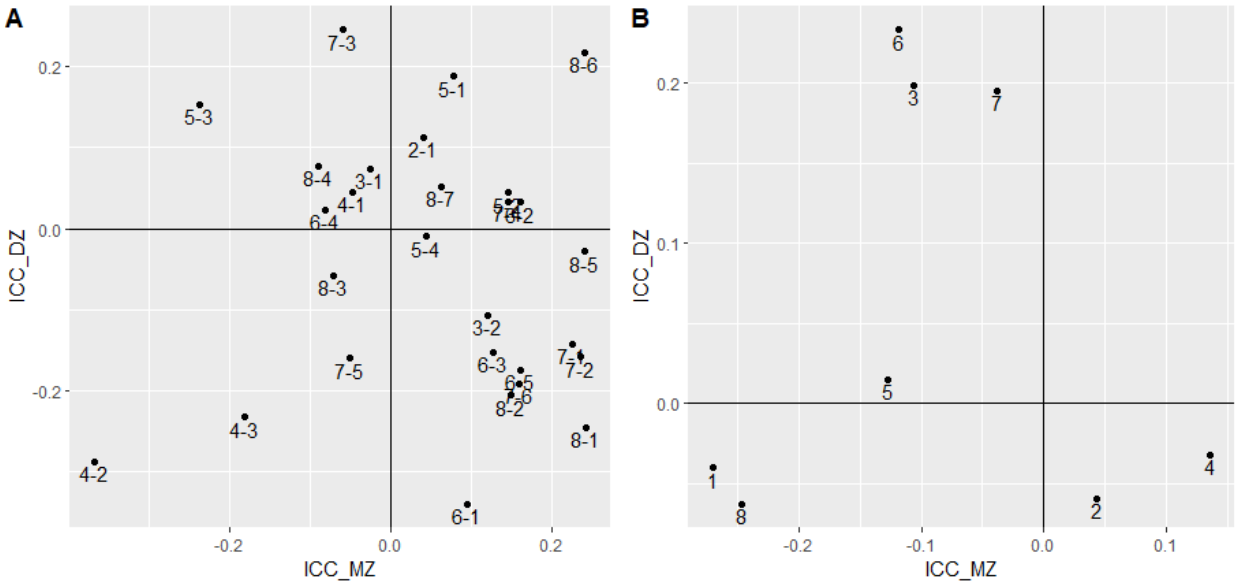

Figure 2.2 Twin-twin correlations of connectivity. A) Between-network functional connectivity measures. B) Within network connectivity measures. Network numbers are as follows: 1: Vis, 2: SS, 3: DA, 4:VA, 5: Lim, 6: FP, 7:DM, 8: SC.

Additive mixed-effects modeling

None of the phenotypes examined showed an h^2 greater than 0.25. Six between-network pairs (SC-FP, SC-Vis) showed an h^2 greater than 0.1 (Table A.3, Figures 2 and 3). The narrow-sense heritability estimation of motion as a heritable trait yielded a value of 0.208 (CI = (0,0.05); p-value = 0.076).

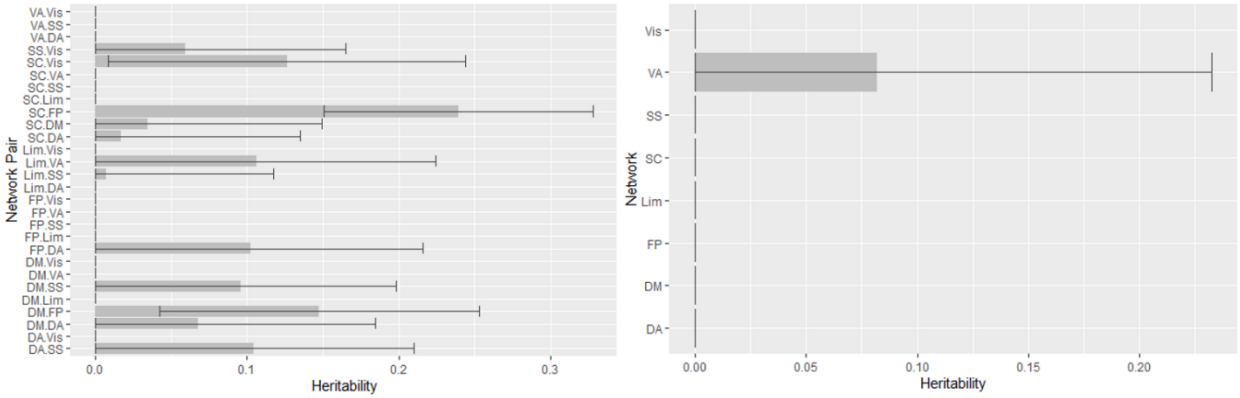

Figure 2.3 Narrow-sense heritability values for all networks and network pairs. Between network pairs (left) and networks (right) display the narrow sense heritability with the 95% confidence interval included.

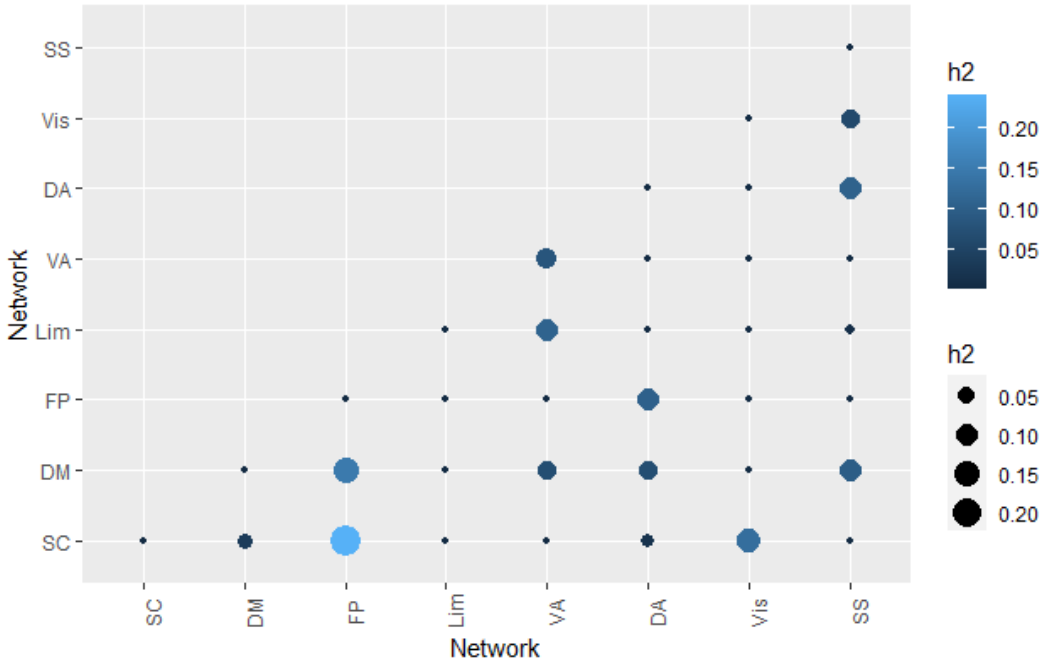

Figure 2.4 Between- and within-network narrow-sense heritability estimates for resting-state phenotypes. The narrow-sense heritability estimates are represented both by the size of the dot and the gradient of the color.

Participants for Objective 2

The demographic and medical history statistical values can be found in Table 2.4. These statistics include MZ and DZ twins, singletons and unpaired twins and apply to the second aim of the current study: determination of demographic and medical history variables that may contribute to the observed phenotypes. Maternal and paternal age, household income, gestation number, and smoking status were all significantly different between scanner type (Table A.1). Correlations above 0.7 between the continuous predictor variables were seen in birth weight and gestational age, maternal and paternal education, and age, and then a correlation between education and age (Figure A.1).

Table 2.3 Demographics and medical history of participants for objective 2.

Continuous Variables		Average	SD	Min	Max
Birth weight (g)		2797	649	840	4820
Gestational age at birth (days)		261	17	210	295
Gestational age at MRI (days)		295	14	248	348
5 min APGAR score		9	0.809	4	10
Maternal education (years)		15	3	6	24
Paternal education (years)		15	3	6	24
Maternal age (years)		30	6	16	44
Paternal age (years)		32	7	18	64
Duration in NICU (days)		1	6	0	60
Residual framewise displacement		0.113	0.023	0.061	0.192
Categorical variables		*N*		%	
Sex	Male	134		50%	
	Female	134		50%	
Delivery Method	Vaginal	120		44%	
	C-section	148		55%	
Household income	High	84		31%	
	Mid	71		26%	
	Low	113		42%	
Maternal ethnicity	White	207		77%	
	Black	55		20%	
	Asian	3		1%	
	Native American	3		1%	
Paternal Ethnicity	White	184		68%	
	Black	74		27%	
	Asian	9		3%	
	Native American	1		0%	
Maternal psychiatric history	No	189		70%	
	Yes	79		29%	
Paternal psychiatric history	No	230		85%	
	Yes	38		14%	
Scanner	Allegra	226		84%	
	TIM Trio	42		15%	
Maternal smoking	No	244		91%	
	Yes	24		8%	
Gestation Number	Twin	125		46%	
	Singleton	143		53%	
NICU Stay	No	244		91%	
	Yes	24		8%	

Backwards elimination regression

The covariates selected in the backwards elimination of each phenotype are shown in Table A.3. Overall, technical variables (type of scanner, motion), gestation number, gender, gestational age at birth, birth weight, gestational age at MRI, and presence of maternal psychiatric history were selected for 25% or more of the phenotypes examined.

Mixed Linear Modeling

The phenotypes for the between-network pairs included five statistically significant associations that passed Bonferroni correction (Table A.4). Gestational age at MRI was found to positively affect the SS-Vis network-pair ($p = 0.0004$; explains 5.20% of the variance) and gestational age at birth was an important negative predictor for both VA-DA ($p = 0.0009$, explains 10.40% of variance) and DM-FP ($p = 0.0004$, explains 4.90% of the variance) connectivity (Figure 2.4). Presence of a maternal psychiatric history was positively and significantly associated with FP-VA ($p = 0.0012$, explains 3.66% of the variance) connectivity. Finally, the scanner type used to collect the MRI data was found to be significantly and positively associated with the VA-Vis network pair ($p = 0.0009$, explains 3.46% of the variance).

For the within-network phenotypes, two variables passed Bonferroni correction to yield statistically significant associations with connectivity in the DA network. Gestational number was positively associated ($p = 0.00016$) with and paternal education at enrollment was negatively associated ($p = 0.00049$) (Figure 2.5) with the DA network (Table A.4), explaining 8.47% and 10.80% of the variance respectively.

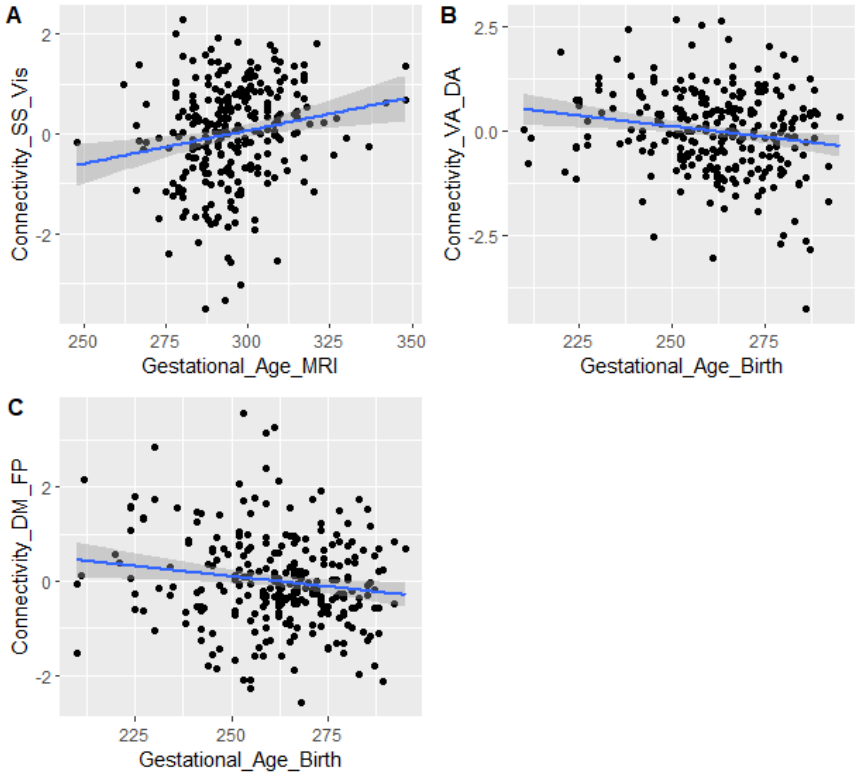

Figure 2.5 Scatterplots of each continuous variable with statistical significance in the mixed modeling. A) Gestational age at MRI plotted against the Z-score of the connectivity for the SS-Vis between-network pair. B) Gestational age at birth plotted against the Z-score of the connectivity for the VA-DA between-network pair. C) Gestational age at birth plotted against the Z-score of the connectivity for the DM-FP between-network pair. The plots are fitted with a regression line with a 95% confidence interval.

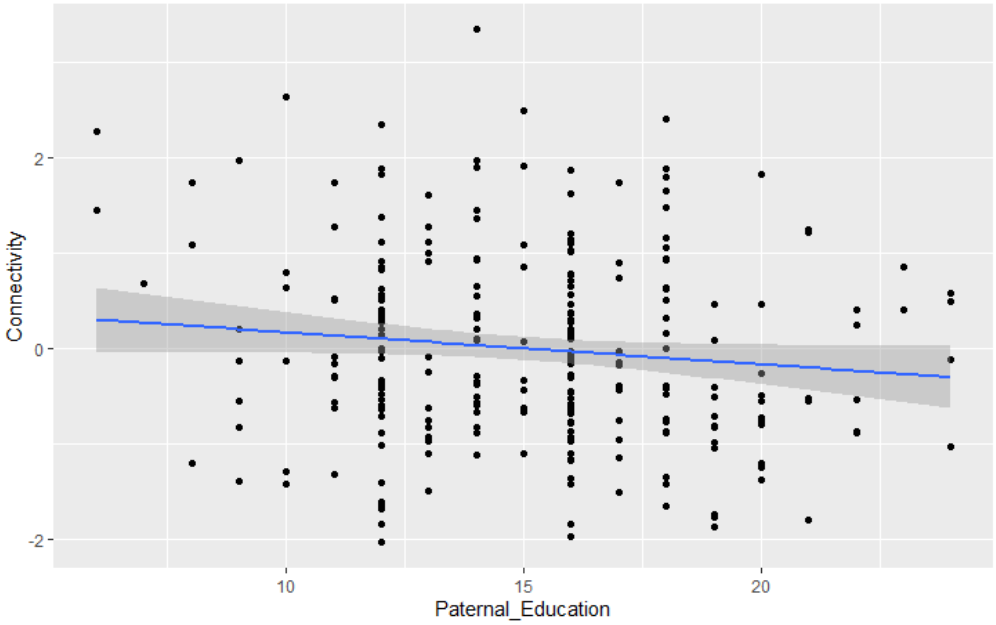

Figure 2.6 Scatterplot of paternal education against the Z-score of the connectivity values in the dorsal attention network. The regression line is plotted along with a 95% confidence interval.

Power analysis

The results of the power analysis indicate that this study is well powered (80%) to detect heritabilities of 0.5 and greater using our current number of twin pairs (Figure 2.6). We have moderate power to detect heritabilities between 0.25 and 0.45 and low power to detect heritabilities less than 0.25.

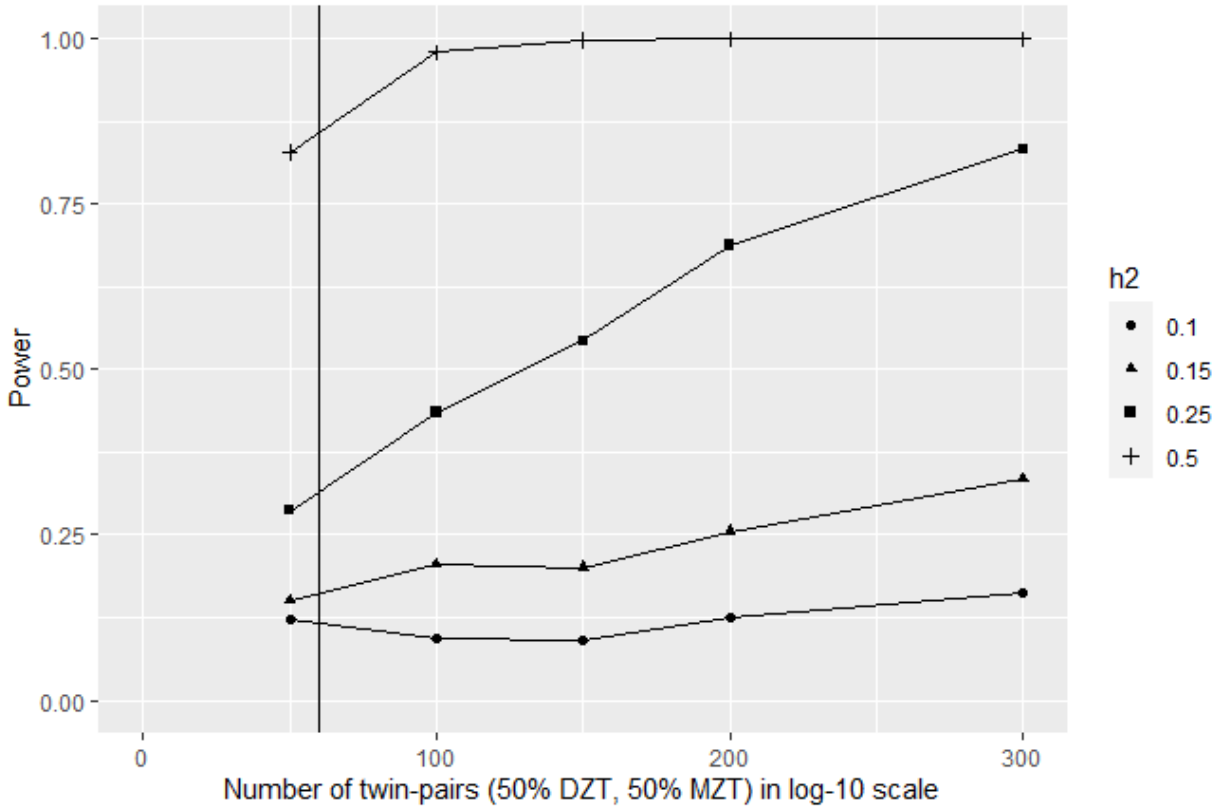

Figure 2.7 Power analysis using simulated data. The vertical line indicates the number of twin pairs contained in the current study.

Discussion

To our knowledge, this study is the first to examine both genetic and environmental influences acting upon resting-state functional connectivity in a large sample of typically developing neonates. Overall, our twin study suggests that genetic factors have relatively little influence on within and between network connectivity in early infancy, while our backward elimination regression and mixed-modelling analyses identified specific demographic and medical history variables that may influence infant functional connectivity measures, including gestational age at birth and maternal psychiatric history.

Our original hypothesis that measures of within-network and between-network connectivity would be heritable, with the strongest genetic effect evident for early maturing networks involved in perception and movement, was not well supported. Of the 36 connectivity phenotypes examined, only six showed narrow-sense heritability estimates greater than 0.10, though none were statistically significant. In contrast, heritability estimates in children for between-networks of the Lim-FP and SC-FP can exceed heritability of 0.50 and 0.60, respectively [359]. To demonstrate significance of a heritability estimate in this range, over 2000 twin pairs would be needed based on our power analysis. Our conclusion that genetic factors play a relatively minor role in explaining individual variation in neonatal measures of within and between network connectivity is supported by results from the intraclass correlations. Our results suggest that the genetic architecture of within and between network connectivity is quite different at different life stages. One possible explanation for the observed patterns is the potential role of experience-dependent learning in shaping inter-individual differences in infancy. For example, the development of the frontal cortex is heavily dependent on early-life experiences, with socioeconomic stressors playing a large role in the progression of structure and function in the first year of life [360]. Though our study may not provide strong evidence that resting-state connectivity phenotypes are heritable in early infancy, we can't rule out that significant heritability could be detected in a larger study.

Interestingly, our intraclass correlation analyses revealed many phenotypes which showed negative correlations between DZ twins. A few phenotypes showed negative correlations between MZ twins as well. Low or negative correlations between DZ twins have been observed for some other phenotypes, especially parent ratings of

temperament [361]. In that particular case, low DZ resemblance is thought to arise from parents exaggerating the differences between DZ twins, a phenomenon known as the contrast effect. The current study did not involve parent ratings, but direct measures of physiology. However, it is possible that parents might treat members of a DZ pair differently in such a way that the development of functional connectivity is affected. Furthermore, both MZ and DZ twins may compete for restricted resources such as prenatal nutrition, postnatal nutrition, or parental attention, that may offset genetic factors.

Through our backward elimination and mixed modeling approach, we were able to identify multiple demographic and obstetric history variables that contribute to between- and within-network connectivity phenotypes including gestational age at birth, gestational age at MRI, and presence of maternal psychiatric history. As regards gestational age at birth, our initial hypothesis that the somatosensory network would be impacted by gestational age at birth was partially supported. While gestational age at birth was not selected for within network connectivity of the somatosensory network, it was selected for 4 between network pairs involving somatosensory cortex including SS-Vis, DA-SS, DM-SS, and FP-SS. Gestational age at birth was also selected for eight other between network pairs and was especially strongly associated with connectivity between the default mode network and the frontoparietal, and ventral attention and dorsal attention networks, explaining about 10.40% and 4.90% of the individual variability, respectively. Interestingly, in most cases gestational age at birth was associated with decreased between-network connectivity. This was unexpected as the final trimester of pregnancy is generally characterized by greater integration between distant brain regions [205]. Our finding is in contrast to a small-scale machine learning study of gestational age effects on

resting state connectivity which demonstrated that connections both within and between networks are typically reduced in preterm infants [362]. However, research exploring brain volumes in neonates has reported increased brain volumes in earlier born children [337], indicating perhaps that these children undergo accelerated brain growth due to factors such as experiencing a richer sensory environment outside the womb, or as a protective adaptation resulting in faster brain growth to compensate for the physical delays in pre-term and early birth.

Gestational age at MRI was selected as an important variable for 8 between-network pairs (SS-Vis, VA-Vis, Lim-VA, Lim-SS, FP-SS, DM-Lim, DM-FP, SC-SS) and for functional connectivity within the visual network. Functional connectivity within the visual network increased with age. Some between network pairs showed decreasing connectivity over age, while other showed increasing connectivity. The strongest relationship we observed with age was connectivity between the visual and somatosensory cortex, which increased over development. Age explained approximately 5.20% of the variance in this particular phenotype. These are both early maturing networks and clearly play important roles in how the very young infant interacts with and learns about the world. We note that the proportion of variance explained by age in our functional connectivity phenotypes is substantially less than we have observed for structural MRI phenotypes in this same age-range. For example, age explains 51% of the variation in intracranial volume during early infancy, 55% of the variation in surface area, and 18% of the variation in cortical thickness [337].

As regards maternal psychiatric history, we originally hypothesized that it would preferentially affect connectivity phenotypes involving the limbic system. Our data did not

support this hypothesis, but maternal psychiatric history was selected as a potentially important predictor for 8 between-network phenotypes (DA-Vis, Lim-SS, Lim-VA, FP-Vis, FP-SS, FP-VA, DM-SS, SC-FP) and 1 within network phenotype (FP). Of these the FP-VA and FP-Vis network pairs were significantly associated with maternal psychiatric history in our mixed modeling analysis. The frontoparietal network and its resting-state connectivity are heavily associated with executive functioning later in life. Reineberg et al. [66] demonstrated that individual differences in an overall and general executive functioning measure are based on variation in the frontoparietal network. Individual variation in set-shifting, a subcomponent of executive function, was significantly associated with the ventral attention network. The ventral attention network was additionally shown to have great influence on set-shifting in a later work by Reineberg et al. [305].

We note that most of the women with a positive psychiatric history in our study had been diagnosed with a mood and/or anxiety disorder. Consequently, our results are relevant to a growing body of literature addressing potential relationships between maternal depression and anxiety and offspring executive function. Interestingly, multiple epidemiological studies have observed associations between maternal depression and offspring risk for ADHD [363–368]. These relationships could arise due to shared genetic vulnerabilities for depression and ADHD, but could also reflect the impact of in utero exposure to physiological features associated with depression (high levels of glucocorticoids, pro-inflammatory cytokines, and altered function of serotonin systems). The current study suggests that functional connectivity between the frontoparietal and

other networks may play a role in the mechanistic pathways that link maternal depression to attention problems in offspring.

Focusing specifically on the within-network resting-state connectivity phenotypes, paternal education at enrollment was selected as a statistically significant contributor to the dorsal attention network in our second objective. Interestingly, the relationship is negative, suggesting that higher paternal education is associated with delayed development of the dorsal attention network. This may seem surprising given previous studies showing that higher parental education is associated with better cognitive function [369–371] and reduced risk for ADHD [372]. No study has specifically examined whether a faster or slower maturational rate of this network in infancy is associated with later cognitive outcomes or risk for attention problems, although a study by [373] demonstrated that increased connectivity between specific components of the dorsal network correlates with sustained attention in females between 4 and 7 years of age. We note that prior research conducted by our group found a negative association between paternal education and cortical thickness in the frontal lobe during early infancy [334]. This may be relevant to the current findings, as the dorsal attention network incorporates frontal regions [374].

Gestation number was also selected for this network. It has been documented that a majority of multiples are born with low birth weight, which is a major predictor of hyperactivity and attention problems in later years, including the development of attention deficit hyperactivity disorder [375–378]. However, in our backward selection analysis, gestation number was selected as an important predictor of within network connectivity in the dorsal attention network, while birthweight itself was not. This suggests that the

association between gestation number and connectivity within this network is not simply a function of low birthweight. Alternative explanations include obstetric complications and nutrition competition between twins. Intrauterine competition is present in the gestation of multiples. Examples include unequal placental sharing, chorionic circulatory imbalance, and the physiological challenges of providing resources to nurture more than one fetus [379,380].

Technical variables such as scanner type and subject motion were also frequently selected in our backwards elimination regression analyses, although the only relationship meeting our criteria for significance in the mixed models was between scanner type and connectivity between the ventral attention and visual networks. Independent groups have demonstrated the impact of motion artifacts on fMRI [344,381,382]. We addressed this known challenge in several ways including: (1) regressing out 6 motion parameters during preprocessing, (2) implementing the widely accepted data scrubbing approach with scrubbing criteria at 0.5% signal change and 0.5mm framewise displacement, and (3) including a measure of subject motion in our analyses. We note that motion shows a strong genetic component in both children and adults [383,384]. In adults, three measures of head motion during the fMRI (mean translation, maximum translation, and mean rotation) have heritabilities ranging from 37 to 51% [383]. Our work adds to that literature by showing that motion during neonatal scans has low-to-moderate heritability.

The current study had many strengths including the use of a prospective cohort design, state-of-the-art methods for the acquisition and analysis of infant imaging data, and collection of rich metadata. One potential limitation is the use of sleeping subjects. Functional connectivity in sleeping infants more closely resembles adult slow wave sleep

rather than the patterns of awake adults [385], and connectivity measures can be influenced by stage of the sleep cycle [386]. We were not able to track when in the sleep cycle our infant subjects were scanned, and this could have introduced noise and reduced the power of our analyses. This may be one reason we did not see strong positive correlations between our MZ and DZ twins. However, use of sleeping subjects is widely accepted for infant imaging studies as it minimizes subject motion, as compared to awake scanning [208,385,387–389], and does not require anesthesia, which at such a young age causes aberrant brain development [390].

In addition, some of the variables examined in Objective 2 should not be conceptualized as exclusively environmental. For example, gestational age at birth is influenced by both fetal and maternal genetic factors in addition to environmental factors [391]. In a study by Wu and colleagues, the broad-sense heritability for gestational age at birth was estimated at 24.45%, with 60.33% attributed to environmental influences such as maternal stress, exposure to tobacco, and possible infections [392]. Birthweight is also a heritable trait heavily influenced by the environment. Heritability of weight increases during the second and third trimesters, culminating in a heritability estimate of 26% for singletons and 29% for twins at birth [393]. Furthermore, one must consider the distinction between objective and effective environments. Objective environments refer to environments as measured by the researcher, while effective environments are defined by the outcomes they produce. It is possible for an objectively shared event (e.g. gestational age at birth) to have effectively non-shared, or child-specific, effects (e.g. one child in a pair might remain in the NICU longer after being born early or suffer more severe neurodevelopmental effects) [394]. Finally, we acknowledge that classic twin studies rely on

certain fundamental assumptions including (1) findings from twins are generalizable to the rest of the population, (2) in utero environment is identical with no chorion or amnion differences, (3) environment affects MZ and DZ twins equally, and (4) there are no gene by environmental correlations or interactions.

An alternative approach that could be used would be to define functional networks based on neonatal data as opposed to the adult map. Argument for either method is depended on the question one seeks to answer. The present study aimed to examine how canonical functional networks are impacted by genetic and environmental factors so adult-defined networks were used to facilitate interpretation of the findings. Our utilization of the adult networks allows us to directly compare to adult resting-state networks and make comparisons to the literature.

In conclusion, our twin study suggests that genetic factors do not play a major role in explaining individual variation in resting-state connectivity measures in early infancy, though the low power of the study does not let us directly conclude a failure to reject the null hypothesis. Future studies will be needed with larger participant numbers to corroborate our findings. However, specific demographic and medical history variables were identified that may influence functional connectivity measures. Future research could map the development of heritability in a longitudinal study, observing the maturation of the connections into adolescence where connectivity has been demonstrated to be mostly under genetic control.

Chapter 3

Anatomical and functional connectivity differences in the brains of infants with TS when compared to TD children

Abstract

Turner syndrome (TS), a condition caused by complete or partial loss of an X-chromosome, is often accompanied by deficits in specific cognitive domains. Magnetic resonance imaging studies of adults and children with TS suggest these deficits may reflect differences in anatomical and functional connectivity. However, no imaging studies have explored connectivity in infants with TS. Consequently, it is unclear at what point in development connectivity differences emerge. To address this, we compared functional and structural connectivity of one-year-old infants with TS to typically developing one-year-old boys and girls. We examined functional connectivity between the right precentral gyrus and five regions that show reduced volume in 1-year old infants with TS compared to either male or female controls and found no differences. To assess anatomical connectivity, we examined diffusivity indices along the superior longitudinal fasciculus (SLF). An exploratory analysis of 54 additional white matter tracts was also performed. TS and control groups did not differ along the SLF. However, exploratory analyses revealed significant group differences in nine tracts. The results suggest the first year of life is a window in which interventions might prevent connectivity differences observed at later ages, and by extension, some of the cognitive challenges associated with TS.

Introduction

Described by Henry Turner in 1938 [246], Turner syndrome (TS) is caused by the partial or complete loss of an X-chromosome. The condition occurs in approximately 1 in 2000 live female births [247], making it one of the most common aneuploidies. TS represents a unique population for studying X chromosome effects on human development [268,269,395], because females with TS are hemizygous for many genes in the pseudoautosomal regions (PAR) of the X chromosome, when compared to both XX females and XY males [396]. For the 15% of genes outside the PAR that escape X-inactivation [397], females with TS have reduced gene dosage compared to XX females, but are similar to XY males. The loss of the second sex chromosome produces multi-systemic effects. TS is often accompanied by gonadal dysgenesis, congenital heart defects, renal abnormalities, and liver disorders [398], as well as a unique neurocognitive profile. Deficits in social cognition (SC) [399–401], executive functioning (EF) [270,402,403], and visuospatial reasoning (VR) [404,405] are often present. Furthermore, individuals with TS appear to be at increased risk for male-biased neurodevelopmental disorders including Autism Spectrum Disorders (ASDs) [252,253] and Attention Deficit Hyperactivity Disorder (ADHD) [268].

Structural magnetic resonance imaging (MRI) has been used to identify neuroanatomical features of TS that may explain the unique cognitive profile and increased risk for male-biased neurodevelopmental disorders. To date, most neuroimaging studies of TS have been performed on adults and adolescents, who show structural changes consistent with the observed cognitive challenges: for example, decreased grey matter volume in parieto-occipital regions implicated in visuospatial reasoning [257–261]. Consistently, white matter volume increases in TS have been observed

in the temporal lobe, which is implicated in language and social cognition [257–259]. The first quantitative neuroimaging study of infants with TS observed many structural features consistent with those present in adolescents and adults with TS, suggesting that many of the neuroanatomical phenotypes in TS are established early and persist into adulthood [272].

High-level cognitive processes disrupted in TS, such as executive function and social cognition, require coordination between structurally segregated brain regions. Thus, studies of anatomical and functional brain connectivity, using diffusion tensor imaging (DTI) and resting-state functional magnetic resonance imaging, provide additional insights into the neurological basis of the TS cognitive profile. While DTI allows researchers to examine the integrity of axonal pathways connecting different brain regions, functional connectivity analyses of rs-fMRI imaging data provide insight into the organization of large-scale brain networks supporting these processes.

In older children, adolescents, and adults, TS has a distinct structural connectivity profile which is well supported by the literature. Multiple studies have reported reduced fractional anisotropy (FA) in the superior longitudinal fasciculus (SLF) with others reporting more global reductions [258,264,265]. The SLF facilitates working memory, language, visuospatial attention, and numerical tasks [76,266,267], all domains affected in TS individuals. The age at which these differences in white matter integrity emerge is currently unknown.

Reduced functional connectivity at rest has been reported in the frontoparietal and dorsal attention networks in girls with TS, which may explain the increased prevalence of ADHD in the TS population [268]. Whole-brain reduction in functional connectivity strength

was identified in the postcentral gyrus/intraparietal sulcus, angular gyrus, and cuneus and the right cerebellum in girls with TS [269]. This study also showed a relationship between these connectivity deficits and cognitive domains such as working memory and visuospatial reasoning. Using task-based fMRI, Bray and colleagues [271] were the first to demonstrate abnormal connectivity in the parieto-occipital and parieto-temporal pathways, which could explain deficits in visuospatial processing.

As previously stated, most neuroimaging studies of TS have been performed on adults and adolescents, leaving the question of when in development these observed differences in structural and functional connectivity arise unanswered. Consequently, it is unclear whether observed differences are a direct consequence of hemizygosity of X-chromosome genes during the prenatal and early postnatal period, when axonal pathways and functional networks are first established, or occur later. If these difference do arise later in childhood, they could reflect common postnatal clinical experiences such as treatment with growth hormone and estrogen replacement therapy, which are commonly used to increase adult height and initiate puberty, respectively [290,406]. Individuals with TS may also take medications for the heart and renal problems previously mentioned, undergo surgery with general anesthesia, or take psychotropics [291] with potential consequences for brain development. Finally, postnatal deficiency in gonadal steroid hormones could also be involved [407–409].

The current study focuses on one-year-old infants that have not yet been exposed to growth hormone and estrogen replacement therapy. Our main objective was to determine whether anatomical and functional connections between frontal and parietal/occipital cortices are altered in one-year-old infants with TS. We focus on brain

regions that showed volume differences in a prior study of the same cohort [272]. We addressed this objective through a cross-sectional case-control study of TS and typically developing (TD) infants with DTI and rs-fMRI scanning data. Based on the literature summarized above, we hypothesized that infants with TS would have aberrant diffusivity in the superior longitudinal fasciculus (SLF) and reduced functional connectivity between the precentral gyrus and regions involved in basic visual processing (calcarine cortex), social cognition (supramarginal gyrus and lingual cortex), and executive function (supramarginal gyrus). To our knowledge, this study is the first of its kind to utilize rs-fMRI and DTI together in TS to answer questions of brain structure and function at this developmental stage. Our results have the potential to show whether differences in structural and functional connectivity observed in older children and adults with TS are present in infancy, versus emerging at a later developmental stage. This has implications for early intervention strategies and therapies for TS that could help ameliorate neurocognitive deficits in the disorder.

Methods

Participants

Imaging data from 26 females with X monosomy (6 mosaic, and 20 with complete X monosomy), 39 typically developing males, and 47 typically developing females were used in this study. All participants were approximately one year of age and had resting-state connectivity data. Usable DTI scans were available for 24 females with X monosomy, 31 TD males, and 36 TD females. TS participants were recruited through the University of North Carolina's (UNC) Pediatric Endocrinology Department, UNC's Turner Syndrome Clinic, national support groups, and heath care providers from across the

United States. Typically developing subjects represent a subset of the Early Brain Development Study (EBDS) cohort at the University of North Carolina at Chapel Hill [337–339]. Exclusion criteria for both groups included substance abuse or major health problems in the mother during pregnancy, major psychiatric illness in either parent, extreme prematurity of the child, and any congenital abnormality in the subject not associated with TS.

rs-fMRI and DTI Acquisition and Processing

Imaging data were acquired over a ten-year period on either a Siemens Allegra head-only or a Siemens Tim Trio scanner (Siemens Medical System, Inc., Erlangen, Germany) which replaced the Allegra part way through the study. There were 32 infants imaged on the TIM Trio and 81 on the Siemens Allegra. All infants were in a natural sleep state during imaging.

Functional imaging was performed using a T2-weighted EPI sequence: TR=2 s, TE = 32 ms, 33 slices, and 4mm isotropic resolution, while structural images were acquired using three-dimensional magnetization-prepared rapid acquisition with gradient echo (MPRAGE) sequence, which is a T1-weighted imaging technique. The sequence is as follows: TR = 1820 ms, TE 4.38 ms, and 1 mm isotropic resolution. These methods are described in [353].

A 6-direction protocol with the following parameters was used to collect DTI data on the Allegra during the initial years of the study (81 infants total): Repetition Time (TR)/ Echo Time (TE) = 5,200/73 ms, slice thickness = 2 mm, and in-plane resolution = 2 × 2 mm^2, with a total of 45 slices in 6 unique directions using *b* value of 1,000 s/mm^2 and 1 baseline image (*b* value = 0) per sequence. In total, 35 DWIs were generated per subject

by repeating the sequence five times to improve the signal-to-noise ratio. Later imaging on the Allegra used 42 directions of diffusion sensitization with a *b* value of 1,000 s/mm^2 in addition to seven baseline images, which generated a total of 49 DWIs. The parameters for the 42-direction data were as follows: TR/TE/Flip angle = 7,680/82/90°, slice thickness = 2 mm, and in-plane resolution = 2 × 2 mm^2, with a total of 60–72 slices. The remainder of subjects were scanned on the Tim Trio following the same parameters as the 42-direction Allegra protocol. These methods are described in [410].

Image analysis (rs-fMRI)

Functional data were preprocessed using the FMRIB (for Functional MRI of the Brain) Software Library (FSL; version 6.0; [341]) and Analysis of Functional NeuroImages (AFNI; [342]). Steps included discarding the first 3 volumes (6s), slice-timing correction, rigid-body motion correction, bandpass filtering (0.01–0.08 Hz), and regression of white matter, CSF, the 6 motion parameters and their derivative, quadratic terms. The nuisance signals were band-pass filtered before regression to match the frequency of the blood oxygen level-dependent signal. A single global signal regression step was performed after the scrubbing to eliminate global signal re-introduced by scrubbing. Data scrubbing was implemented with scrubbing criteria at global signal changes >0.5% and framewise displacement >0.3mm [343] with continuous datapoints no less than 3. Participants with less than three minutes (90 datapoints) of functional data after scrubbing were excluded. Then, to make the same length of data, all infants' functional data were truncated into 90 volumes. Finally, the images were spatially smoothed with Gaussian kernel (full width at half maximum = 6mm).

After performing a rigid-body registration between the functional data and T1-weighted structural images of the same subject, a nonlinear registration (fNIRT in FLS) was done between individual T1-weighted images and infant age specific AAL template images [352]. The combined transformation field was used to warp the preprocessed rs-fMRI functional images to the neonate template [353]. The structural image skull-stripping was done using a template-based method. After performing a rigid-body registration between the functional data and T1-weighted structural images of the same subject, a nonlinear registration (fNIRT in FLS) was done between individual T1-weighted images and an infant-specific AAL template [352] which includes 90 regions of interest. The combined transformation field was used to warp the preprocessed rs-fMRI functional images to the group template [353].

For the current analysis, we extracted the average BOLD time course from the right precentral gyrus, right and left calcarine cortex, right and left lingual cortex, and right supramarginal cortex (regions which showed reduced volumes in infants with TS). Correlations between the right precentral gyrus and the other five regions were then calculated for each subject. The correlations were then Fisher-*Z* transformed for statistical analysis.

Statistical Analyses (rs-fMRI)

All statistical analyses were performed using R statistical software 4.0.5 [411] using base functions.

Two-sided Fisher's exact tests were used to evaluate group differences in categorical variables. A two-sided Kruskal-Wallis H-test was run on each of the continuous variables with a Dunn test used for post hoc comparisons.

A one-way ANCOVA was used to test differences in functional connectivity between the three groups (TS females, XX females, XY males) with post-hoc FDR-corrected pairwise comparisons. Five outcome variables were examined: (1) connectivity between right precentral gyrus and right calcarine cortex, (2) connectivity between right precentral gyrus and left calcarine cortex, (3) connectivity between right precentral gyrus and right lingual cortex, (4) connectivity between right precentral gyrus and left lingual cortex, and (5) connectivity between right precentral gyrus and right supramarginal cortex. To reduce the variance, covariates were chosen that are variables previously associated with imaging outcomes. In this case we used the scanner type, birth weight, maternal and paternal education, and gestational age at MRI.

Image Analysis (DTI)

All image analysis steps for DTI are described in Girault et al. [410] and represent a neonate-specific pipeline adapted from the general UNC-Utah NA-MIC DTI pipeline [412]. Quality control (QC) is an automated protocol using DTIPrep [413]. DTIPrep detects slice-wise and gradient-wise intensities and corrects for motion artifacts and eddy current effects [413]. Images with large motion artifacts and aberrant gradients are excluded. Weighted least squares fitting was used to estimate the diffusion tensors. Additional expert-guided QC was performed using 3D Slicer. Skull stripping was performed as specified in Verde et al. [412]. A DTI atlas derived from one-year-olds was used to map the images. Successful registration was confirmed by visually comparing the warped DTI

images and the atlas. Atlas fibers were then mapped onto the individual subject space, and DTIAtlasFiberAnalyzer was used to extract the fractional anisotropy (FA), mean diffusivity (MD), radial diffusivity (RD) and axial diffusivity (AD) profiles. A correlation analysis was then made for all individuals of the plot of the atlas against the four metrics. Profiles with a correlation value above 0.7 were considered well mapped to the atlas space; profiles that did not meet this criterion were excluded.

Statistical Analyses (DTI)

As described in Jha et al. [414], FADTTS, or functional analysis of diffusion tensor tract statistics [415], was used to test group differences in FA, AD, and RD along the SLF white matter tract. Mean diffusivity (MD) was not included as it is an overall, general measure of diffusivity as a whole and based on AD and RD. FADTTS gives a global test statistic, and local test statistics along the white matter fiber tracts. We included DTI protocol, gender, ICV, postnatal age at MRI, gestational age at birth, and two motion measures as covariates. The first motion measure was calculated by taking the sum of the slices and volumes excluded due to artifacts along with the number of excluded volumes due to residual motion. The second measurement is the number of volumes exceeding the threshold of the rotational angle (angle > 1 degree) and translational volume (translation > 2mm). Within each tract, local p-values are corrected for multiple comparisons with FDR. The local p-values are then merged with the test statistics onto the corresponding fiber locations for visualization.

Exploratory Analyses (DTI)

The processes for DTI image and statistical analyses are the same as those described for the SLF. A total of 54 tracts were generated which include, bilaterally, the arcuate fasciculus (frontoparietal, frontotemporal, and temporoparietal segments), anterior portion of the cingulum, posterior cingulum adjoining the hippocampus, corpus callosum (body, genu, motor, parietal, premotor, rostrum, splenium, and tapetum segments), corticofugal (motor, parietal, prefrontal, premotor segments), corticoreticular, corticospinal, corticothalamic (motor, parietal, prefrontal, premotor, superior segments), fornix, fronto-occipital fasciculus, inferior longitudinal fasciculus, optic tract, optic radiation, superior longitudinal fasciculus, and uncinate fasciculus. However, only 46 tracts passed quality control and had an *n* greater than or equal to 20 for each group (Table B.1). Tracts excluded from the statistical analyses include: the right temporoparietal portion of the arcuate fasciculus, left corticospinal, left optic tract, right superior longitudinal fasciculus, right premotor and prefrontal corticofugal tracts, and left premotor and prefrontal corticofugal tracts.

Results

Participants

Descriptive statistics for the demographic and medical history variables of the participants in this study are in Table 3.1. Significant differences were found between the three groups in gestational age at birth, birthweight, scanner type, and maternal ethnicity. On average, children with TS were born earlier than control participants and had the

lowest birthweight. The children with TS were more likely to be scanned on the Tim Trio than the Allegra and were more likely to be White.

Connectivity Measures

No statistically significant relationships were found after FDR correction (Table 3.2). However, the following connectivity pairs had uncorrected p values below 0.05 and FDR correct p-values below 0.10: right precentral gyrus to right calcarine cortex and right precentral gyrus to right lingual cortex. We proceeded with pairwise comparisons for these two phenotypes, and found significant differences in the XX-X0 group for both the right calcarine cortex (p=0.029) after FDR correction and right lingual cortex (p=0.0187) (Table 3.3).

Table 3.1 Demographics and medical history for one-year-old infants with Turner syndrome and their typically developing male and female counterparts.

Variable	TS		Female control		Male Control		*p*
	N	**Mean (SD) range**	***N***	**Mean (SD) range**	***N***	**Mean (SD) range**	
Gestational age at birth (days)	26	268 (11) 246-286	47	277 (9) 259-295	39	274 (10) 241-289	0.006
Birth weight (grams)	26	2803 (421) 2155-3925	47	3380 (428) 2340-4414	39	3386 (469) 2375-4562	<.0001
Age at MRI (days)	26	389 (16) 359-419	47	382 (22) 339-439	39	382 (18) 343-422	0.357
Maternal age (years)	25	29 (6) 21-42	47	30 (5) 20-40	39	30 (4) 20-41	0.531
Paternal age (years)	25	32 (7) 23-50	47	32 (6) 21-50	37	32 (4) 22-39	0.842
Maternal education (years)	25	15 (3) 6-20	47	16 (3) 9-23	39	16 (3) 10-22	0.235
Paternal education (years)	24	14 (3) 3-23	46	16 (3) 8-22	39	16 (3) 9-22	0.093
Total household income (dollars)	24	76094.5 (69420) 0-330000	45	68280 (46264) 0-205000	37	73562 (47217) 0-195000	0.913
	N	Percent	N	Percent	N	Percent	
<u>Maternal ethnicity</u>							0.0181
White	23	92.0%	32	68.1%	35	89.7%	
Black	2	8.0%	13	27.7%	2	5.1%	
Asian	0	0.0%	2	4.3%	2	5.1%	
<u>Paternal ethnicity</u>							0.056
White	23	92.0%	32	68.1%	33	86.8%	
Black	2	8.0%	13	27.7%	3	7.9%	
Asian	0	0.0%	2	4.3%	2	5.3%	

Table 3.1 (cont'd)

Smoking							0.843
Yes	1	3.8%	3	6.4%	1	2.6%	
No	25	96.2%	44	93.6%	38	97.4%	
Scanner							0.0185
Trio	13	50.0%	11	23.4%	7	17.9%	
Allegra	13	50.0%	36	76.6%	32	82.1%	
Allegra directionality							
A06	5	45%	9	35%	9	35%	0.834
A42	6	55%	17	65%	17	65%	

Table 3.2 Pairwise comparison of the resting-state functional connectivity between the right precentral gyrus and the five listed regions.

Region	LS (SE) TS	LS (SE) Female	LS (SE) Male	Uncorrected p-value	FDR Corrected p-value
Right calcarine cortex	-0.358 (0.170)	-0.018 (0.15)	-0.151 (0.153)	0.0397	0.099
Left calcarine cortex	-0.312 (0.170)	0.003 (0.15)	-0.123 (0.153)	0.59	0.59
Right lingual cortex	-0.3920 (0.152)	-0.067 (0.134)	-0.184 (0.137)	0.025	0.099
Left lingual cortex	-0.268 (0.150)	-0.019 (0.132)	-0.133 (0.135)	0.099	0.165
Right supramarginal gyrus	0.25 (0.188)	0.095 (0.166)	0.033 (0.169)	0.299	0.37

Table 3.3 Pairwise comparison of the resting-state functional connectivity between the right precentral gyrus and the right calcarine and lingual cortices.

Region	Comparison	Estimate	SE	p-value
Right calcarine cortex				
	XX-XY	0.133	0.105	0.421
	XX-X0	0.340	0.131	0.029
	XY-X0	0.208	0.126	0.231
Right lingual cortex				
	XX-XY	0.0118	0.094	0.425
	XX-X0	0.325	0.117	0.0187
	XY-X0	0.207	0.112	0.0163

DTI Measures

In our primary analysis, which focused on the superior longitudinal fasciculus, we did not observe statistically significant differences between individuals with TS and male or female controls (Table 3.4). The right superior longitudinal fasciculus was left out of the results due to the previously described cutoff for subject numbers after quality control.

Table 3.4 Paired comparisons between the three groups for structural connectivity of the left superior longitudinal fasciculus. Axial diffusivity (AD), radial diffusivity (RD), and fractional anisotropy (FA) are represented in the post hoc analysis and show no statistical significance.

Superior Longitudinal Fasciculus, Left		**Uncorrected global p-value**	**FDR-corrected global p-value**	**FDR-corrected p-values**		
				AD	RD	FA
	Female control, Male control	0.099	0.171	0.068	0.31	0.654
	Female control, Turner syndrome	0.585	0.621	0.427	0.515	0.296
	Male control, Turner syndrome	0.092	0.165	0.212	0.077	0.205

Exploratory Analyses

Of the white matter tracts examined, we found significant differences between TS participants and controls in nine white matter tracts (Table 3.5): the frontotemporal segment of the right arcuate fasciculus, the right posterior cingulum adjoining the hippocampus, the motor and tapetum segments of the corpus collosum, the left motor segment of the corticofugal tract, the premotor segment of the right corticothalamic tract, the left inferior fronto-occipital fasciculus, the left inferior longitudinal fasciculus, and the right optic tract.

AD was statistically significant in the right frontotemporal segment of the arcuate fasciculus (p=0.009 female control and Turner syndrome), the right posterior cingulum

adjoining the hippocampus (p=0.004 female control and male control, p=0.001 female control and Turner syndrome), the motor segment of the corpus callosum (p=0.024, female control and Turner syndrome), the tapetum segment of the corpus callosum (p=0.042, female control and Turner syndrome), and the left motor segment of the corticofugal tract (p=<0.0001 in both female control and male control, and female control and Turner syndrome, p=0.004 for male control and TS). Additionally, the premotor portion of the right corticothalamic tract (p<0.0001 female control and male control, and p=0.005 for female control and Turner syndrome), the left inferior fronto-occipital fasciculus (p=0.003 male control and Turner syndrome) all present with statistically significant FDR-corrected p values.

RD showed statistical significance in the right posterior cingulum adjoining the hippocampus (p=0.002 female control and Turner syndrome, and p<0.0001 female and male controls), the left motor section of the corticofugal tract (p=0.024 female and male control; p<0.0001 female control and Turner syndrome), and the left inferior longitudinal fasciculus (p=0.044 female control and Turner syndrome).

Finally, FA was statistically significant in the tapetum of the corpus collosum (p=0.011, female control and Turner syndrome), the left motor segment of the corticofugal tract (p=0.021, female control and Turner syndrome; p<0.0001, male control and Turner syndrome), the left inferior fronto-occipital fasciculus (p=0.046, female control and Turner syndrome; 0.012 male control and Turner syndrome), the left inferior longitudinal fasciculus (p=0.039, female control and Turner syndrome), and the right optic tract (p=0.007, male control and Turner syndrome).

Table 3.5 Fasciculi with statistically significant FDR-corrected global p-values and post hoc FDR-correct p-values for individual diffusivity metrics. AD indicates axial diffusivity, RD indicates radial diffusivity, and FA indicates fractional anisotropy.

				Post hoc FDR-corrected p-values		
		Global p-value	Global FDR-corrected p-value	AD	RD	FA
Arcuate fasciculus, right, frontotemporal						
	Female control, Male control	0.026	0.076	0.062	0.013	0.255
	Female control, Turner syndrome	0.007	0.033	0.009	0.224	0.078
	Male control, Turner syndrome	0.387	0.455	0.329	0.725	0.319
Cingulum adjoining the hippocampus, right						
	Female control, Male control	<0.0001	<0.00092	0.004	<0.0001	0.526
	Female control, Turner syndrome	<0.0001	<0.00092	0.001	0.002	0.197
	Male control, Turner syndrome	0.466	0.522	0.608	0.87	0.899
Corpus callosum, motor						
	Female control, Male control	0.013	0.054	0.099	0.863	0.641
	Female control, Turner syndrome	0.007	0.033	0.027	0.426	0.261
	Male control, Turner syndrome	0.607	0.644	0.419	0.584	0.477
Corpus callosum, tapetum						
	Female control, Male control	0.312	0.403	0.84	0.941	0.104
	Female control, Turner syndrome	0.004	0.022	0.042	0.241	0.011
	Male control, Turner syndrome	0.051	0.1104	0.178	0.505	0.09

Table 3.5 (cont'd)

Corticofugal, left, motor						
	Female control, Male control	<0.0001	<0.00092	<0.0001	<0.0001	0.654
	Female control, Turner syndrome	<0.0001	<0.00092	<0.0001	<0.0001	0.021
		<0.0001	<0.00092	0.004	0.087	
	Male control, Turner syndrome					<0.0001
Corticothalamic, right, premotor						
	Female control, Male control	<0.0001	<0.00092	<0.0001	0.338	0.008
	Female control, Turner syndrome	0.003	0.018	0.005	0.311	0.129
	Male control, Turner syndrome	0.452	0.515	0.319	0.574	0.626
Inferior fronto-occipital fasciculus, left						
	Female control, Male control	0.029	0.080	0.075	0.378	0.077
	Female control, Turner syndrome	0.032	0.083	0.088	0.14	0.046
	Male control, Turner syndrome	0.001	0.007	0.003	0.066	0.012
Inferior longitudinal fasciculus, left						
	Female control, Male control	0.017	0.065	0.045	0.801	0.313
	Female control, Turner syndrome	0.001	0.007	0.201	0.044	0.039
	Male control, Turner syndrome	0.028	0.078	0.339	0.247	0.073
Optic tract, right						
	Female control, Male control	0.024	0.073	0.098	0.084	0.018
	Female control, Turner syndrome	0.035	0.087	0.406	0.211	0.388
	Male control, Turner syndrome	0.008	0.035	0.145	0.06	0.007

We classified group differences into six categories based on both global and local test statistics: XX>X0=XY, X0=XY>XX, X0>XY=XX, XX=XY>X0, X0=XX>XY, and XY>X0=XX. We refer to both XX>X0=XY and X0=XY>XX as “masculinization” patterns because the TS females are similar to TD males but differ from TD females. We refer to both X0>XY=XX and XX=XY>X0 as “PAR” patterns because the suggest a role for gene in the pseudoautosomal regions of the sex chromosomes. Finally, we refer to both X0=XX>XY and XY>X0=X as “sex difference” patterns because phenotypic females (TS and TD) differ from TD males. The primary pattern for each diffusivity measure and each tract that showed significant group difference in post-hoc analyses is shown in Table 3.6. Figure 3.1 illustrates how these three different patterns manifest in the right premotor portion of the corticothalamic tract, the left inferior longitudinal fasciculus, and the left inferior fronto-occipital fasciculus. All other fasciculi can be seen in Figures B.1-B.12.

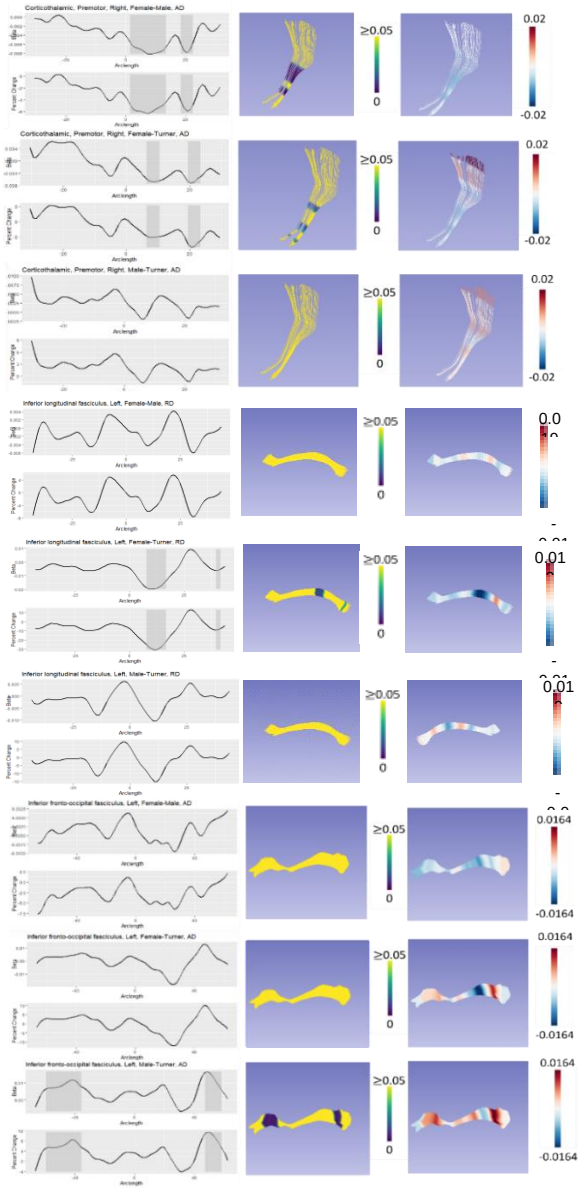

Figure 3.1 Models of DTI results for the right premotor portion of the corticothalamic tract (top), the left inferior longitudinal fasciculus (middle), and left inferior fronto-occipital fasciculus (bottom). In each panel, the leftmost graph shows the beta value over the arclength of the fasciculus, with areas of local statistical significance highlighted in grey. Below that is the percent change in the beta value over time for that tract in the specified comparison for the specific diffusivity measure. The middlemost image in each panel shows an overlay of the p-values on the fasciculus, with regions of statistical significance showing a color other than yellow. Finally, the rightmost panel shows the beta values from the specific comparison with the model of the tract. Here, the corticothalamic tract is an example of a masculinization, the inferior longitudinal fasciculus an example of the effects from the PAR, and the anterior portion of the inferior fronto-occipital fasciculus an example of a sex difference.

Table 3.6 Chromosomal hierarchies for each statistically significant tract shown for axial diffusivity, radial diffusivity, and fractional anisotropy. XX indicates typically developing female, X0 indicates TS female, and XY indicates typically developing male. Classifications in this table represent the dominant pattern we observed. However, examination of local tract statistics often revealed regional complexities, which we describe in more detail in the discussion section.

Fasciculus	Axial Diffusivity	Radial Diffusivity	Fractional Anisotropy
Arcuate, right, frontotemporal	XX> X0 = XY		
Cingulum adjoining hippocampus, right	XX > X0 = XY	XX > X0 = XY	
Corpus callosum, motor	X0 = XY > XX		
Corpus callosum, tapetum	XX = XY > X0		XX = XY > X0
Corticofugal, left, motor	XX > X0 = XY	XX > X0 = XY	X0 > XY = XX
Corticothalamic, right, premotor	XX > X0 = XY		
Inferior fronto-occipital fasciculus, left	XX= X0 > XY		X0 = XX > XY
Inferior longitudinal fasciculus, left		XX = XY > X0	X0 > XX = XY
Optic tract, right			X0 = XY > XX

Discussion

The current work is, to our knowledge, the first to use rs-fMRI and DTI data to explore brain connectivity in Turner syndrome in infancy. Overall, our study suggests a unique developmental pattern in Turner syndrome in which structural and functional connectivity differences arise at varying times in the life span. Our primary analyses indicate that diffusivity differences in the SLF are not present at one year of age and presumably emerge during early childhood, as they have been reported in older children and adults. Similarly, differences in functional connectivity between frontal and parietal/occipital regions were not detected in the current study but are evident later in

life. Our exploratory DTI analyses revealed nine fasciculi that differed between TD and TS infants.

Our original hypothesis that infants with TS would have reduced functional connectivity between the precentral gyrus and our five selected regions came from previous work showing volumetric differences in the brains of the same cohort of individuals [272]. The five selected regions also contribute to cognitive functions that are often disrupted in TS, supporting visual processing (left and right calcarine cortex) executive functioning (supramarginal gyrus) and social cognition (left and right lingual cortex). It is intriguing that there are such pronounced volumetric differences in this cohort of infants, but no differences were observed in functional connectivity, especially as disrupted connectivity between frontal and parietal regions has been reported in older individuals with TS[74,416–418] .

For structural connectivity we hypothesized there would be diffusivity differences between TS infants and TD infants in the SLF, a tract that connects frontal and parietal brain regions and is involved in executive functioning, attention, and working memory [74,416–419]. This hypothesis was based on the extant literature in adults [258,264,265] and prepubescent girls with TS [265]. However, we did not observe significant differences between groups in the current study. Integrating our results with the existing literature suggests the SLF develops normally in TS until at least 1 year of age but deviates during the toddler and preschool years.

Null findings for fronto-parietal connectivity, assessed with both DTI and rs-fMRI, parallel findings on early cognitive development in TS. Infants with TS show a relatively normal cognitive profile at 12 months of age with a potentially slower rate of progression

in visual reception and fine motor skills from 12 to 24 months[420]. If differences in fronto-parietal connectivity arise after 12 months of age, there may be an opportunity to prevent those changes through early intervention, thereby preventing or ameliorating some of the cognitive impairments observed in school-aged children with TS. Historically, diagnosis of TS was made when a female failed to go through puberty or fell two or more standard deviations below the mean height for their age group, resulting in relatively late diagnosis and reduced intervention opportunities [421,422]. However, characteristics such as lymphedema in infancy, presence of cardiac abnormalities which occur in approximately 50% of the TS population [421,423,424], and the advancement of prenatal diagnostics such as genetic amniocentesis, sonograms, and circulating cell-free DNA have contributed to earlier diagnoses. The most recent clinical practice guidelines for TS encourage annual developmental and behavioral screenings for TS and recommend academic adjustments to accommodate learning and performance issues [398]. They also suggest that evidence-based interventions for cognitive or psychosocial problems in other populations be adapted to meet the needs of girls/women with TS. The possible benefits of administering early interventions in a proactive manner, before cognitive deficits emerge, is not addressed. Early interventions clearly improve cognitive and psychosocial outcomes for individuals with ADHD [425–427] and ASDs [428,429], conditions that share key characteristics with TS. Especially relevant to the current study, it has been shown that white matter diffusivity measurements improve with therapy in toddlers and preschoolers with ASD [430], and both functional and structural connectivity have been proposed as potential biomarkers for monitoring early interventions [431].

This leads directly into our exploratory DTI analysis, which revealed that some white matter tracts already display statistically significant differences at one year of age between the three groups. The majority of these exploratory findings followed a pattern in which TS infants differed from XX females but were similar to XY males. In other words, they suggest masculinized development of these tracts in TS. In tract-wide comparisons, this pattern was observed for specific diffusivity metrics in the right arcuate fasciculus (AD), right posterior cingulum (AD & RD), the motor segment of the corpus callosum (AD), the left corticofugal motor tract (AD, RD), and the right premotor corticothalamic tract (AD). Examination of local statistics revealed that this pattern was also present in portions of the left corticofugal motor tract (FA), left IFOF (AD & FA), left ILF (RD), and right optic tract (FA). Two possible explanations exist for this pattern, one being the relative lack of postnatal estrogen exposure in TD males and TS females. Another possibility is that these tracts are influenced by genes that lie outside the pseudoautosomal region but escape X-inactivation. Like TD males, TS girls are expected to be hemizygous for these genes. Interestingly, this pattern was generally observed in relation to AD and AD was generally lower in TS females and XY males. AD is known to decrease sharply across the first year of life [432]. Thus, one could interpret high AD as delayed maturation and low AD as accelerated maturation. Alternatively, lower AD in infants with TS may reflect axonal damage (Winklewski et al. 2018), but this seems an unlikely explanation for the lower AD observed in XY males as compared to XX females.

The second most common pattern we observed was one in which TS infants differed from both XX females and XY males, who were similar to each other. In tract-wide comparisons, this pattern was observed for the tapetum (AD & FA), left ILF (RD,

FA)), left corticofugal motor tract (FA), and left IFOF (FA). Examination of local statistics revealed that this pattern was also present for AD in a posterior area of the left IFOF. This pattern suggests a role for dosage sensitive genes in pseudoautosomal regions of the sex chromosomes, as TD males and females have two copies and TS females have one. However, this pattern could also reflect the influence of clinical characteristics that are more common in infants with TS such as congenital heart disease (CHD) and exposure to general anesthesia during surgeries to correct CHD, kidney abnormalities, or frequent ear infections. Interestingly, this pattern was seen most frequently for FA with TS females having higher FA than TD males or females. FA increases over development such that high FA can be interpreted as faster maturation and low FA as slower maturation. FA does not capture a single biological process, but reflects increasing myelination and axonal integrity [433].

The least frequently observed pattern was one in which TS infants were similar to XX females and both differed from XX males. We refer to this as the “sex difference” pattern and it was observed in several regions of the left IFOF (FA) and the right optic tract (FA). This could indicate a role for testosterone in the development of these tracts. Testosterone is significantly higher in XY males as compared to XX females during mid gestation and in the first 6 months of postnatal life[434–439]. Testosterone levels in TS are expected to be similar to XX females during gestation and even lower than XX females postnatally. It could also indicate a role for Y chromosome material in the development of these tracts. The relative lack of sex differences is in keeping with prior literature on the development of white matter integrity in infancy[440]. In subsequent paragraphs we discuss

the pattern of results for each tract in more detail and discuss the potential functional and clinical implications of the patterns we observed.

The right frontotemporal segment of the arcuate fasciculus connects the middle and inferior temporal gyri with the precentral gyrus and posterior portion of the inferior and middle frontal gyri in the right hemisphere. This tract is involved in visuospatial processing and some aspects of language processing, especially prosody. Damage or underdevelopment of the right arcuate fasciculus is also associated with poorer ability in facial expression-based Theory of Mind (Nakajima et al. 2018), a subdomain of social cognition in which girls and women with TS are often deficient. We observed a pattern in which XX females had greater AD than females with TS, who were similar to XY males, which suggests that both TS females and XY males have more mature tracts than XX females. This seems slightly paradoxical given that this tract is involved in cognitive functions that are often disrupted in TS. Perhaps the development of this tract slows after one year of age in TS females or it may asymptote at a lower level than XX females.

The right cingulum originates in the orbital frontal cortices, travels along the dorsal surface of the corpus callosum, then down the temporal lobe to the entorhinal cortex. In addition to linking frontal, parietal, and medial temporal sites, it also connects subcortical nuclei to the cingulate gyrus. We observed masculinization of both AD and RD in the posterior portion of the cingulum adjoining the hippocampus. Like AD, RD decreases over development. While changes in AD are thought to reflect increased numbers of fibers and/or axonal caliber, increased RD is thought to reflect myelination [14]. As with the right frontotemporal segment of the arcuate fasciculus, our results suggest more rapid development of this tract in both XY males and TS females.

The right cingulum is known to be involved in general cognition and has been linked to a myriad of psychiatric disorders including ASD and ADHD, with lower FA than the TD population being observed [441,442]. The cingulum as a whole is one of the last fasciculi to develop fully, with changes seen in the tract until nearly the third decade of life [443,444]. Because the developmental period is so long, this allows for more susceptibility to damage or altered growth as there are more opportunities for disruption in development. Based on the ROIs of the atlas presented in Tamnes et al., the statistical significance we found is localized to the parahippocampal segment of the cingulum adjoining the hippocampus [443]. It does not appear that the right cingulum adjoining the hippocampus has been studied specifically in development, and this study, to our knowledge, is the first to look in TS in comparison to a normative sample. The parahippocampal segment of the cingulum stems from the temporal lobe and fans out into the occipital lobe [445] and is involved in recognition memory [446]. The parahippocampal subdivision also includes projections from the amygdala, a structure typically enlarged in TS [262,447]. Specifically, the left amygdala was observed to be larger in TS. The left amygdala functions in fear recognition in facial expressions, which is an area of deficit in TS [448].

The motor portion of the corpus callosum, connecting the primary motor cortices in both hemispheres, also presents a masculinizing effect (X0 = XY > XX) at the global level, but in this case, AD is greater in TD males and TS females than in TD females, leading us to the opposite conclusion; there is more mature growth of this fasciculus in TD females than TS females or TD males. Examination of local statistics shows that the overall masculinizing pattern largely reflects difference near the center of the tract. There is also a small region near the left hemisphere periphery that follows a PAR pattern.

Individuals with TS have documented difficulties with motor functions in terms of speed and number of motions required for a task [449,450]. The greater the spatial processing on these tasks, the poorer performance observed in motor control [451]. However, the deficits in motor function do not appear to be linked to the cognitive profile observed in TS [452].

The tapetum is a segment of the corpus callosum that extends laterally on either side into the temporal lobe [453]. The tapetum has been reported in the literature for TS as having aberrant diffusivity [265,454]. This aligns with the cognitive profile of TS as the tapetum is an important contributor to visuospatial functioning [455], and social and communicative functioning [456]. In general, our results for FA are in keeping with the existing literature with TD females having greater overall fiber integrity than TS females at multiple locations along the tract. In the literature, lower FA has been associated with TS in the tapetum [264,265]. However, there were two locations, one in the far left periphery of the tract and one in the far right periphery of the tract, where TS females had higher FA than the control groups. For AD, examination of local statistics revealed two regions where females with TS differed significantly from XX females. In one region AD was higher in TS females, suggesting delayed development; in the other AD was lower in TS females, suggesting faster development. Although not statistically significant, similar differences were observed when comparing TS females to XY males, suggesting PAR-mediated effects on both FA and RD in this tract.

Corticofugal tracts include corticoefferent and corticopetal fiber groups that interconnect the cerebral cortex, corona radiata, internal capsule, cerebral peduncles, pontine nuclei and/or the brainstem. For AD and RD, the left motor corticofugal tract follows the same pattern we see in the right cingulum adjoining the hippocampus, with

TD females showing slower maturation than TD males and females with TS. Significant group differences were also observed for FA. However, the primary pattern of differences for FA is more in keeping with a PAR effect than a masculinization effect with TS females having higher FA than both TD males and TD females. Existing literature does not report aberrant DTI measures for the corticofugal tracts in TS, suggesting these differences do not persist. The corticofugal tracts also travel through the internal capsule, which shows lower FA in TS girls than TD girls [258,265]. Into middle age, the internal capsule shows higher FA in males than females, demonstrating that the patterns continue to differentiate through time [457]. The relationship we observed in the left motor corticofugal tract could also be a contributor to the motor phenotype observed in TS.

Corticothalamic fiber tracts are white matter pathways that radiate from the thalamus to the cerebral cortex, via the internal capsule and corona radiata. They are also known as thalamic radiations. Beginning in the thalamus, the premotor corticothalamic tract travels to the premotor regions of the frontal cortex which function in the planning and organization of movements.

Again, showing an indication of earlier maturation, the masculinization of the right premotor corticothalamic tract (XX > X0 = XY; AD) follows the previously mentioned patterns. As previously discussed for the corticofugal tract, lower FA in the internal capsule was observed in young girls with TS than TD girls [258,265].

The left inferior fronto-occipital fasciculus (IFOF) connects orbitofrontal cortex and the inferior frontal gyrus to the occipital lobe. We observed substantial regional heterogeneity in how group membership affected diffusivity in the IFOF. For AD, we observed a potential sex difference in the anterior IFOF with TS females having

significantly lower AD than XY males, but similar AD to females, suggesting faster development of this area in XY males. In the posterior IFOF, we identified a region where AD was increased in TS compared to both XX females and XY males, indicating a PAR effect. For FA, we observed potential sex differences in the anterior frontal lobe and midsection where females (both XX and XO) had greater tract integrity than XY males. There was also a section in the posterior frontal lobe that followed a PAR pattern with TS showing more integrity than both TD males and females. Finally, we observed a possible masculinization effect on a section of the posterior IFOF where TS females had greater tract integrity compared to XX females, but were similar to XY males. The IFOF is involved in attentional control and may contribute to attentional difficulties in ADHD [458], so the fact that we observed delayed maturation of AD in this fasciculus in TS could partially explain the increased vulnerability of girls with TS to ADHD.

The left inferior longitudinal fasciculus connects the temporal and occipital lobes. Group differences in this tract for both FA and RD seemed to reflect hemizygosity in the PAR with TS individuals exhibiting greater myelination and higher tract integrity compared to both males and females. Typically in ASD a reduced FA in the ILF [459–461] and visual processing deficits are observed, which is the opposite of what we have found for TS. In a study in girls with TS from ages 7-14, a reduction in FA was observed in the ILF [264]. The ILF is also implicated in visuospatial working memory [462] which would suggest a reduction in FA in our TS group, but it could be that our participants with TS undergo a stagnation in the development of the fasciculus after infancy that then becomes apparent with age.

Finally, the right optic tract transports visual information from the optic chiasm to the right lateral geniculate body as a part of the visual pathway. Global test statistics

suggest that group differences in primarily reflect a sex difference in FA with both TS females and XX females differing significantly from XY males, but not differing from each other. Examination of local test statistics reveals additional complexity. FA differences in the anterior part of this tract are challenging to classify into one of the three patterns with significant differences between TS females and XY males (X0 > XY), but small and non-significant differences between TS and XX females and between XX females and XY males. The posterior part of this tract shows a pattern of masculinized FA (X0 = XY > XX). To our knowledge this tract has not been examined in adolescence or adulthood in TS. Nor are we aware of any studies reporting a sex difference in this tract.

The current study has many strengths including the use of advanced image acquisition and analysis techniques optimized for studies of the infant brain. The inclusion of both male and female control groups provides unique insights into possible underlying mechanisms. The developmental period we have chosen also alleviates the issue of the treatment of TS with hormone therapy used to induce puberty which has been demonstrated to cause changes in connectivity [463] . A possible limitation to the study is our moderate sample size which may cause us to be underpowered to detect subtle differences in anatomical and functional connectivity.

In conclusion, this study provides novel information about anatomical and functional connectivity in infants with TS. By comparing our results to the existing literature in older children, adolescents, and adults with TS, we have begun to construct a developmental model of this condition. Our results indicate that disrupted connectivity between frontal cortex and parieto-occipital cortex, as indexed by diffusivity measures in the SLF and resting-state connectivity between the right precentral gyrus and right and

left calcarine cortex, right and left lingual cortex, and right supramarginal cortex, is not present in late infancy. Early intervention could potentially prevent these brain phenotypes from emerging and lessen the cognitive impact of this genetic disorder in later stages of development. However, our exploratory studies revealed diffusivity differences in other white matter tracts during infancy. Some of these differences appear to persist into adulthood, while others appear to be specific to this developmental period. It is suggested that future studies look longitudinally at structural and functional connectivity in girls with TS in order to better understand brain development in this group, identify biomarkers for later cognitive challenges, and identify critical periods for intervention.

Chapter 4

An online platform for testing the disrupted cognitive domains of women with Turner syndrome

Abstract

Turner syndrome is a relatively rare genetic disorder resulting from the partial or complete loss of the second X chromosome in phenotypically female individuals. Turner syndrome is accompanied by a wide array of multisystemic challenges that include a unique cognitive profile. This profile includes disruptions in executive functioning, visuospatial reasoning, and social cognition. Though the disorder is one of the most common chromosomal aneuploidies, girls and women with Turner syndrome are spread sparsely across the country. Current research to understand cognitive challenges in Turner syndrome requires in-person participation in a clinical setting that thus puts geographic and resource constraints on scientists trying to understand the disorder. To counter this problem, we have developed an online browser-based cognitive testing battery that circumvents the geographical challenges and requirement of trained clinicians for test administration. The online battery targets the three neurocognitive domains that are consistently disrupted in TS through the use of seven videogame-like tests and two traditional surveys. We administered the battery to a cohort of women with TS, with neurotypical men and women as controls. Our results showed discrimination between the three groups on all but one task in the battery, validating the battery for use in other studies.

Introduction

X monosomy, or Turner syndrome (TS), is one of the most common chromosomal aneuploidies, occurring in approximately 1 in 2000 live female births[247]. The disorder is caused by the partial or complete loss of the X-chromosome, making TS a uniquely powerful model for studying X-chromosome effects on human development[268,269,395,464]. TS is characterized by multisystemic challenges such as gonadal dysgenesis, renal abnormalities, congenital heart defects, and liver disorders[398]. TS is often characterized by a unique cognitive profile, with high-level processes such as executive functioning (EF)[270,402,403] and social cognition (SC)[399–401] being affected, along with visuospatial reasoning (VR)[404,405]. These domains affect skills essential for everyday functioning and influence cognitive flexibility, social interactions, and an understanding of space and measurement.

This cognitive profile also includes a higher risk for autism spectrum disorders (ASD) and attention-deficit/hyperactivity disorder (ADHD) which share deficits in these neurocognitive domains[250,251]. These comorbid disorders are male-biased in the general population[464], with a higher prevalence seen in males than females. However, ASD and ADHD have an even higher prevalence in the TS population than the male population. Though a small sample size was used, Turner syndrome girls had a risk of developing ASD 300 times higher than typically developing girls[252]. In a separate study, an 18-fold increase in the prevalence of ADHD was found in TS girls compared with girls in the general population, equating to a prevalence of approximately 25% in TS girls[254].

The genetics of TS are what make it a compelling model to explore these sex-biased disorders. Females with TS are hemizygous for genes in the pseudoautosomal regions of the sex-chromosomes which makes them different from both typically developing XX females and XY males[396]. However, X0 females can also be conceptualized as partially masculinized at the genetic level as they are expected to be hemizygous for the 15% of genes outside the pseudoautosomal region that escape X-inactivation[397], when compared to XX females, but would have similar gene dosage to XY males.

The ability to qualitatively and quantitatively investigate the unique domains affected in TS involve a wide array of tests, tasks, and surveys. To explore the cognitive profile of TS, typically a geographically centered cohort is needed, and testing involves an in-person visit to a research facility and the utilization of generally proprietary software. This makes it very difficult to reach a large geographic sample for a relatively rare disorder. Additionally, it would be impossible to conduct this important research without a team of trained specialists with access to subscriptions to the proprietary software, excluding many researchers from exploring questions about cognition in TS due to resource restraints.

The current research seeks to ameliorate this large barrier in TS research capabilities by creating an online browser-based cognitive battery that can be taken on a computer anywhere in the United States. This would allow for larger cohorts of TS women to be included in studies without the geographical and resource constraints. In this study we utilize women with TS, and XX females and XY males as controls from across the United States. The objective of this study was to validate the battery as a usable metric

for collecting cognitive testing data. We utilize seven tasks and two traditional surveys in the battery, selected for their sensitivity in each cognitive domain.

To investigate EF, we used a continuous performance test (CPT), a flanker task, a Corsi block test, and a digit span test. The CPT test requires the participant to push the space bar when the stimulus “X” is present and to ignore all other stimulus letters. Omission errors are then interpreted a measure of sustained attention and errors of commission are viewed as a measure of impulsivity. For the CPT we hypothesized that women with TS would make more errors of commission and omission and have longer reaction times and less accuracy than the controls[465].

The flanker task requires participants to indicate which direction a stimulus arrow is pointed while surrounded by congruent or incongruent errors. This test is conceptualized as a measure of both selective attention and inhibitory control. TS participants are expected to have longer response times and lower accuracy than the controls in the flanker task, with this pattern being more pronounced in the incongruent tests[466].

The Corsi block tasks requires a pattern to be memorized and repeated back by selecting blocks on the screen in the order they were presented. It measures visuospatial working memory. In comparison to the normative sample, participants with TS are expected to have a shorter length in pattern recall in the Corsi block test due to documented deficits in both working memory and visuospatial skills[467].

The final measure of EF, the digit span test, requires the participant to repeat a set of numbers shown briefly to them in a specific order. It is a non-visuospatial test of working

memory. We hypothesized that the lengths repeated by the TS group would be significantly less than the control groups[468,469].

A mental rotation task was used to explore VR in the TS population The mental rotation task takes a three-dimensional polygon and the participant is asked to select the polygon in an array that is the stimulus polygon, but rotated. We hypothesized that TS participants would have poorer accuracy and longer response times than controls.

Reading the Mind in the Eyes, a test of facial emotion recognition developed by Simon Baron-Cohen, was used to evaluate social cognition. It involves being presented with a set of eyes and being asked to choose which of four emotions you believe the eyes to be conveying. For Reading the Mind in the Eyes the working hypothesis is that TS participants will have lower accuracy than controls[465,468].

The final video-game like task was a simple response time (SRT) test designed to measure processing speed. It asks the participant to react when an “X” appears on the screen. We hypothesized that women with TS would exhibit more anticipations on the simple response time task and a longer response time due to an average slower processing time than controls and higher levels of impulsivity[470].

The two traditional surveys used in the battery include the ADHD self-report scale and the Autism Spectrum Quotient (ASQ). We hypothesized that for the ASQ, scores would be higher for women with TS than the normative sample. We expected more TS women to score above threshold on the ADHD report scale than controls due to the higher prevalence of ADHD in TS than the general population[254]. Further, the presence of ADHD

based on the report scale will have a significant relationship with higher errors and response time and lower accuracy on the CPT.

Methods

Participants

Women with Turner syndrome (TS) over the age of 18 were contacted via emails provided through the Turner Syndrome Society of the United States (TSSUS) that were solicited after an IRB approved message was sent to members across the country asking for participation. Thirty women that responded to the call for participants also finished the cognitive battery in its entirety (Table 4.1). The control group consisted of 34 men and 61 women without TS between the ages of 18-60 and without any health issues or medication usage as reported to the ResearchMatch database, which was used to gather participants for the control portion of the study (Table 4.2). ResearchMatch is a national health volunteer registry that was created by several academic institutions and is supported by the U.S. National Institutes of Health as part of the Clinical Translational Science Award (CTSA) program. ResearchMatch has a large population of volunteers who have consented to be contacted by researchers about health studies for which they may be eligible. Review and approval for this study and all procedures was obtained from Michigan State University's Institutional Review Board.

Table 4.1 Demographic and medical history variables for Turner Syndrome participants.

Diagnosed condition	*N*	%	Variable	*N*	%	Mean (SD) range
X0 karyotype of those that reported	7	58%	Ethnicity			
Aortic dissection	1	3%	Asian	1	3%	
Aortic enlargement	2	7%	White	25	83%	
Arthritis	4	13%	Native American	1	3%	
Chronic ear infections	11	37%	Age of diagnosis			
Chronic kidney disease	0	0%	Prenatal	1	3%	
Coronary artery disease	0	0%	Less than 1	8	27%	
Craniofacial abnormality	1	3%	Childhood	20	67%	10.6 (5.1) 1-18
Curvature of spine	4	13%	Greater than 20	1	3%	
Diabetes	3	10%	Treated with estrogen replacement therapy	22	73%	
Gastrointestinal problems	3	10%	Age of estrogen replacement therapy			14.6 (2) 10-18
Glucose intolerance	2	7%	Currently receiving estrogen replacement therapy	18	60%	
Hearing impairment	16	53%	Treated with growth hormone therapy	14	47%	
Heart abnormality	7	23%				
High blood pressure	9	30%				
High cholesterol	11	37%				
Kidney abnormality	7	23%				
Learning disorder	4	13%				
Liver disease	3	10%				
Osteoporosis	7	23%				
Ovarian failure	20	67%				
Seizures	0	0%				
Stroke	1	3%				
Thyroid disease	10	33%				
Visual impairment	12	40%				

Table 4.1 (cont'd)

Vitamin D deficiency	9	30%

Table 4.2 Demographic variables for control participants.

Variable	**Female**			**Male**		
	N	%	Mean (SD) range	*N*	%	Mean (SD) range
Age	61		40 (15) 18-60	34		41 (13) 22-60
Race						
White	48	79%		24	71%	
Black	4	7%		4	12%	
Asian	4	7%		2	6%	
Mulit-racial	1	2%		0	0%	
Other	4	7%		1	3%	
Ethnicity						
Hispanic	3	5%		4	12%	
Not Hispanic	58	95%		30	88%	

Cognitive Battery

The cognitive battery was designed and hosted on RedCap[471,472], a browser-based software for creating surveys and managing databases. Designed in collaboration with the Michigan State University Biomedical Research Informatics Core (BRIC), the battery consisted of two traditional surveys and seven interactive game-like tests. The metrics included in the full battery are as follows: mental rotation task, flanker task, Reading the Mind in the Eyes, continuous performance task, Corsi block task, digit span task, simple response time task, the autism spectrum quotient, and the ADHD report scale.

Mental rotation task

Three dimensional polygons were used as the stimuli for the mental rotation task and were acquired from a validated dataset in a previously published work that created

the stimulus set[473]. The stimulus three-dimensional polygon was shown at the top of the screen, followed by five three-dimensional polygons beneath which were the stimulus polygon but rotated 50, 100, and 150 degrees in an order set by a random number generator. Only one of the five polygons was the stimulus polygon merely rotated, as opposed to mirrored, or mirrored and rotated. There were 36 different sets of polygons given to the participant. Participants had unlimited time to respond. Reaction time in milliseconds and accuracy were recorded.

Flanker task

The participant is given a set of five arrows. The middle arrow is randomly pointed left or right, and the four flanking arrows (two on each side of the middle arrow) are randomly facing left or right as well. Sometimes the middle arrow is congruent with the flanking arrows, and sometimes it is incongruent. There were 96 trials given. We measured accuracy and response time stratified by congruent and incongruent stimuli,

Reading the Mind in the Eyes

This test assesses the participant's ability to use non-verbal cues to determine an emotion. Individuals are shown a pair of eyes and are then asked to pick from four choices which emotion they think best fits the stimulus. A definition was provided with each emotion. This test was developed in 1997[474], with an updated version published in 2001[137]. Outcome was the number of stimuli identified correctly.

Continuous performance task

Continuous performance tasks are designed to measure both sustained attention and inhibitory control[475]. Our continuous performance task (CPT) is exactly 14 minutes in

length. The goal of the task is to press the space bar on a computer's keyboard when a letter other than "X" appears on the screen. There are 360 trials with 36 X's randomly appearing within 324 non-X stimuli. Randomly, there are 1, 2, or 4 seconds between presentation of the letters. Outcome measures included the number of commissions (pressing the space bar when "X" is shown on the screen), number of omissions (not pressing the space bar when a letter other than "X" is on the screen), reaction time for each trial, and overall accuracy.

Corsi block task

Nine identical and spatially separated blocks are shown on the screen which light up in a specific order. Participants were then asked to repeat this order back by clicking on the boxes in the sequence originally presented. Longest length of pattern and reaction time, defined as the amount of time a participant took to repeat back the sequence, were measured. The pattern sequence increases by an additional block each turn and the task ended when an incorrect response was returned.

Digit span task

A list of numbers is given one by one which had to be repeated back by the participant in the same order it was given by typing the numbers into the program. Participants were allowed three errors total throughout the task. The number pattern increased by one each trial until the participant returned an incorrect input three times. The length of numbers repeated back was the outcome measure. An ANOVA was performed between the three groups to identify differences in working memory capacity.

Simple response time task

The simple response time task (SRT) is a reaction time task in which a single stimulus (an 'X') appears at a specifiable delay 1-3 seconds from the previous response. Two hundred trials were performed. Anticipations, or the number of times the spacebar is pushed before the stimulus appears on the screen, were measured along with response time which was defined as the time between when the stimulus was shown and when the spacebar was pressed.

Autism spectrum quotient

The autism spectrum quotient (ASQ) is a self-assessment tool for screening autism spectrum disorders (ASD). Each question gets one point if answered disagree/agree or strongly disagree/strongly agree. There are 50 questions total with 25 eliciting "disagree" responses and 25 meant to elicit "agree" responses. A cutoff of 32+ distinguishes well between individual with ASD and controls[476].

ADHD report scale

A self-assessment tool for screening ADHD. The first six questions were used for scoring. A point was given if sometimes/often/very often was chosen for the first three questions, and an additional point is given for an often/very often selection on the three questions following. A score of four or more is indicative of possible ADHD.

Statistical Analysis

All group comparisons were done with an ANOVA. Post hoc analysis was performed using a Benjamini-Hochberg for multiple corrections. All analyses were run both with and

without outliers, which were defined as data points more than two standard deviations above and below the mean for the combined groups.

Results

Mental rotation task

Looking at overall differences in reaction time, the data were heavily skewed to the right (Figure C.1). Thus, a log transformation was performed on the data (Figure C.2). The ANOVA between the three groups showed statistical significance ($p<2x10^{-16}$; Figure 4.1a; Table 4.3). After outlier removal the relationship remained significant ($p<2x10^{-16}$; Figure 4.1b). The post hoc test revealed statistical significance between X0 and XY, and X0 and XX ($p<2x10^{-16}$; $p<2x10^{-16}$) in which the X0 group had longer response times, but no difference between control groups (Table 4.4).

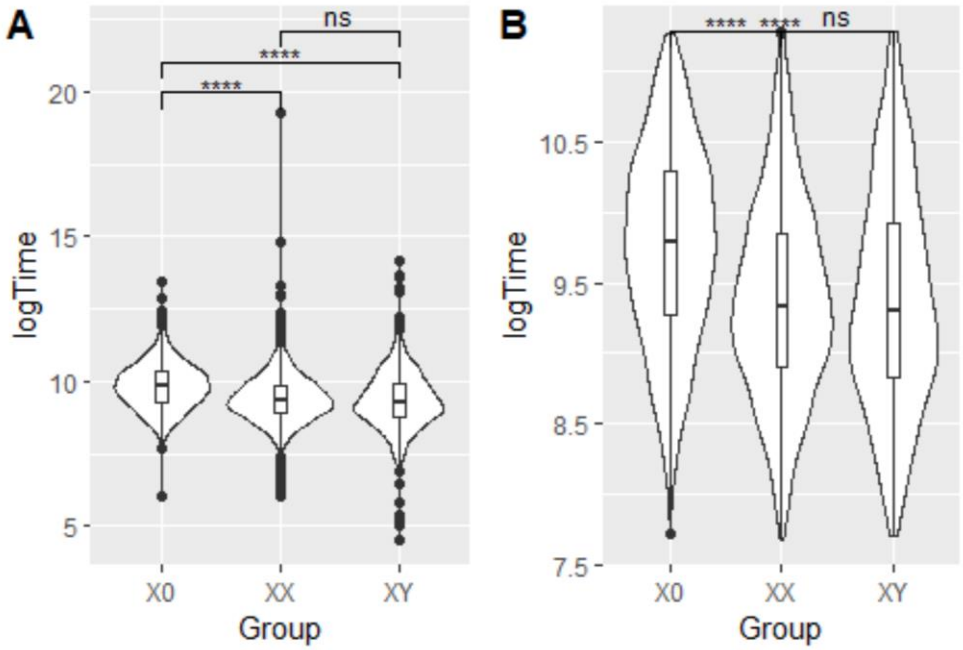

Figure 4.1 Overall differences in reaction times between groups. A) Differences in reaction times before outlier removal. Based on the ANOVA, $p<2x10^{-16}$. B) Differences in reaction time after outlier removal at two times the standard deviation above and below the mean. Based on the ANOVA, $p<2x10^{-16}$.

Table 4.3 ANOVA results for general rection time between the three groups on the Mental Rotation Task. A) Log transformed differences in reaction times before outlier removal. B) Log transformed differences in reaction time after outlier removal.

	Sum Sq	Mean Sq	F	p-value
(A) Group	79.7	39.83	55.24	$<2x10^{-16}$
(B) Group	66.3	33.13	54.16	$<2x10^{-16}$

Table 4.4 Post hoc comparison of general reaction times over all rotational groups after outlier removal and log transformation on the Mental Rotation Task.

	Comparison	**Adjusted p-value**
General reaction time		
	X0-XX	$<2x10^{-16}$
	X0-XY	$<2x10^{-16}$
	XX-XY	0.76

The data for general accuracy showed a normal distribution (Figure C.3), so an ANOVA was run. When general accuracy between the three groups was queried a statistically significant relationship was found ($p=2.8x10^{-7}$; Figure 2a; Table 4.5) before but not after outlier removal (p=0.143 ; Figure 4.2b; Table 4.5). Post hoc comparisons again showed the pattern of significance between X0 and controls, but not between the controls themselves with X0 showing the lowest scores (Table 4.6).

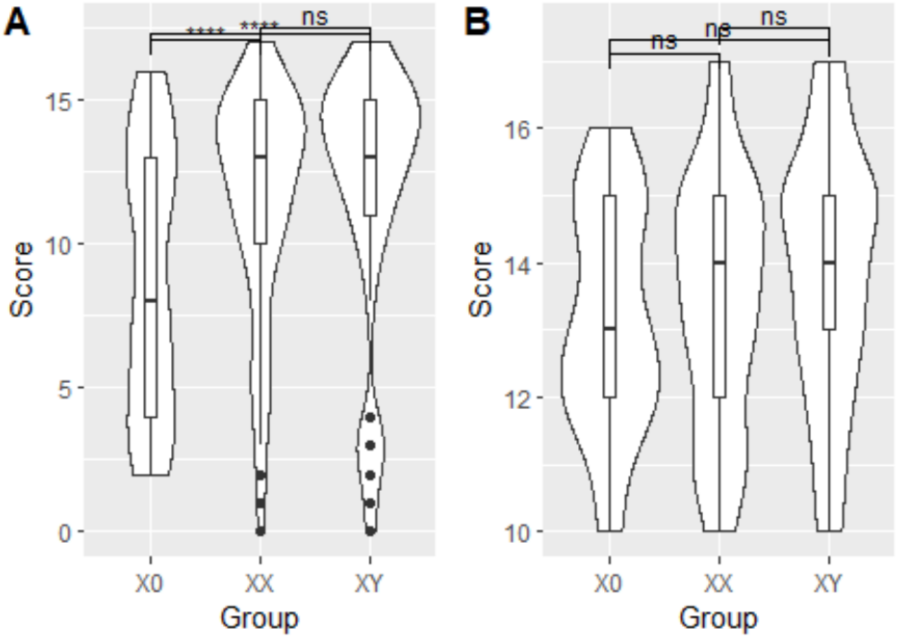

Figure 4.2 Overall differences in accuracy between groups on the Mental Rotation Task. A) Differences in reaction times before outlier removal. Based on the ANOVA, $p=2.8x10^{-7}$. B) Differences in reaction time after outlier removal at two times the standard deviation above and below the mean. Based on the ANOVA, p=0.143.

Table 4.5 ANOVA results for general accuracy between the three groups on the Mental Rotation Task. A) Before outlier removal. B) After outlier removal.

	Sum Sq	Mean Sq	F	p-value
(A) Group	571	25.67	15.72	$2.8x10^{-7}$
(B) Group	13.4	6.72	1.96	0.143

Table 4.6 Post hoc comparison of general accuracy over all rotational groups before outlier removal.

	Comparison	Adjusted p-value
General accuracy		
	X0-XX	$1.5x10^{-6}$
	X0-XY	$1.5x10^{-6}$
	XX-XY	0.58

Flanker task

The reaction time data were distributed in a skewed manner thus, a log transformation was performed on the data (Figures C.2 and C.3). A comparison between the three groups in an ANOVA yielded a statistically significant relationship for response time on congruent patterns of the flanker both before and after removal of outliers ($p<2x10^{-16}$; $p<2x10^{-16}$; Figure 4.3; Table 4.7) with each pairwise comparison also showing statistical significance both before and after outlier removal (Table4. 9). X0 had the longest response time followed by XY and XX.

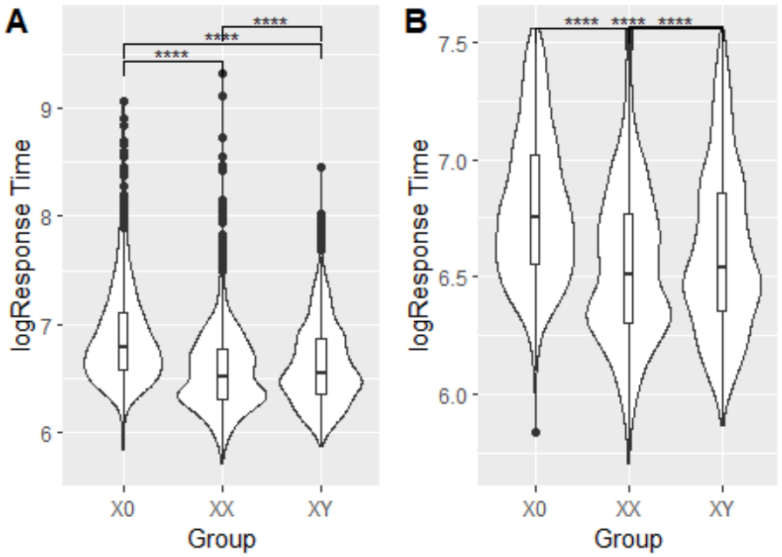

Figure 4.3 Differences in log transformed response times on congruent stimuli on the Flanker task. A) Differences in response times after log transformation but before outlier removal. Based on the ANOVA, $p<2x10^{-16}$ B) Differences in response time after

Figure 4.3 (cont'd)

log transformation and outlier removal at two times the standard deviation above and below the mean. Based on the ANOVA, $p<2x10^{-16}$.

Table 4.7 ANOVA results for log transformed reaction time on congruent stimuli for the Flanker task. A) Before outlier removal. B) After outlier removal.

	Sum Sq	Mean Sq	F	p-value
(A) Group	57	28.5	340.9	$<2x10^{-16}$
(B) Group	103.3	51.66	261.2	$<2x10^{-16}$

Although a relationship in the response time exists between the three groups, there was no statistical significance between TS and controls on accuracy for congruent markers (p=0.18).

For incongruent trials, the reaction time data did not have a normal distribution so a log transformation was performed (Figure C.5 and C.6). The same pattern was observed for questions on the Flanker task with incongruent arrows; significant group differences were found in response time ($p<1x10^{-15}$; Figure 4.4), but not accuracy (p=0.25).

The pairwise comparison of the three groups on incongruent response time showed significant differences between all three groups both pre- and post-outlier removal (Table 4.9). Like the congruent questions, response time was greatest in X0, followed by XY and XX.

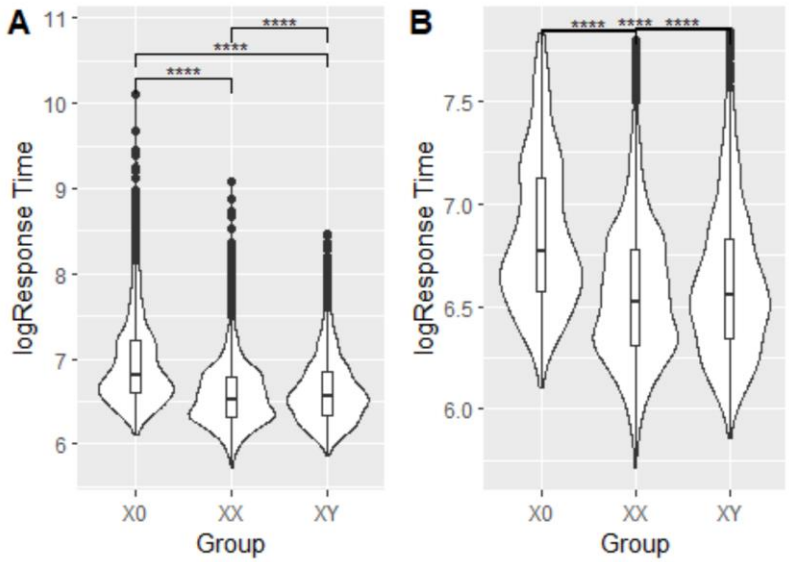

Figure 4.4 Differences in response times on incongruent stimuli on the Flanker task. A) Differences in response times before outlier removal. Based on the ANOVA, $p<1x10^{-15}$. B) Differences in response time after outlier removal at two times the standard deviation above and below the mean. Based on the ANOVA, $p<1x10^{-15}$.

Table 4.8 ANOVA results for log transformed reaction time on incongruent stimuli for the Flanker task. A) Before outlier removal. B) After outlier removal.

	Sum Sq	Mean Sq	F	p-value
(A) Group	155.2	77.6	420.8	$<2x10^{-16}$
(B) Group	74.8	37.9	295.4	$<2x10^{-16}$

Table 4.9 Post hoc comparisons for log transformed reaction time, congruent and incongruent trials, on the Flanker task both before and after outlier removal.

Congruency	**Comparison**	**Adjusted p-value**
Congruent pattern		
	X0-XX	$<2x10^{-16}$
	X0-XY	$<2x10^{-16}$
	XX-XY	$6.1x10^{-9}$
Congruent pattern (outliers removed)		
	X0-XX	$<2x10^{-16}$
	X0-XY	$<2x10^{-16}$
	XX-XY	$3.1x10^{-10}$
Incongruent pattern		
	X0-XX	$<2x10^{-16}$
	X0-XY	$<2x10^{-16}$
	XX-XY	$6.7x10^{-6}$

Table 4.9 (cont'd)

Incongruent pattern (outliers removed)		
	X0-XX	$<2x10^{-16}$
	X0-XY	$<2x10^{-16}$
	XX-XY	$2x10^{-7}$

Reading the mind in the eyes

The data in the Reading the Mind in the Eyes had a normal distribution for all three chromosomal arrangements (Figure C.7). Based on the ANOVA, no statistical significance was found between the three groups in their accuracy on the 36-question test (p = 0.068; Figure 4.5; Table 4.10). The comparison between X0 and XX had a p-value of 0.062 and is noted in Figure 4.5.

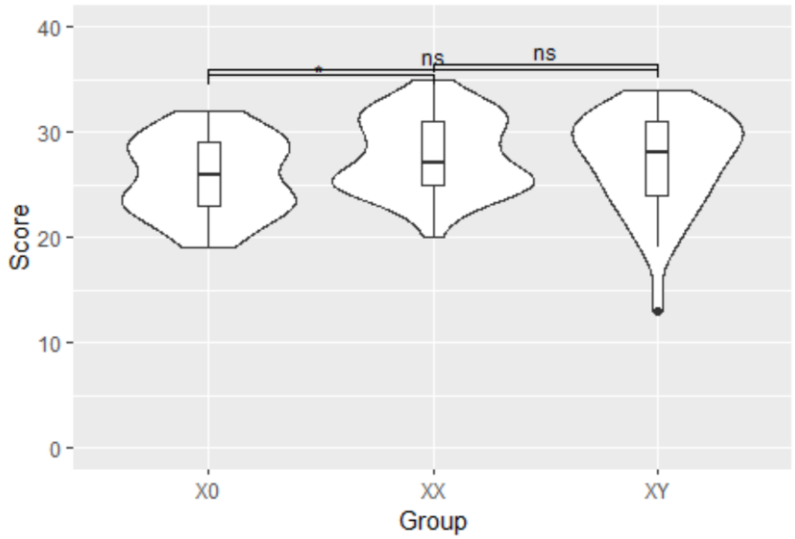

Figure 4.5 Differences in the score on the Reading the Mind in the Eyes task between the three groups. The ANOVA was not significant.

Table 4.10 ANOVA results between the three groups for Reading the Mind in the Eyes.

	Sum Sq	Mean Sq	F	p-value
Group	83.5	41.77	2.757	0.068

Continuous performance task

All data were deemed normally distributed after outlier removal, with the exception of errors of omission, which was skewed slightly to the right (Figures C.8-C.15) No difference was found between the groups on reaction time both before and after outlier removal (p=0.38; p=0.31). Based on the ANOVAs, the three groups did not show statistically significant differences in the number of correct responses both before and after outlier removal (p=0.8; p=0.42). No differences were found between groups on errors of commission before and after outlier removal (p=0.8; p=0.5), nor on errors of omission (p=0.797; p=0.855).

Corsi block task

The data were normally distributed both before and after outlier removal (Figures C.17 and C.18). Length of pattern repeated was measured, and an ANOVA calculated between the XX, XY, and X0 groups. The ANOVA showed a statistically significant relationship ($p=1.37x10^{-5}$; Figure 4.6a; Table 4.11). Post hoc comparisons showed the difference being driven by significant differences between X0 and XX, and XY and X0, but not XX and XY (Table 4.2). After outlier removal, the ANOVA was still significant ($p=4.8x10^{-5}$; Figure4.6b; Table 4.11) and post hoc group differences were similar (Table 4.12).

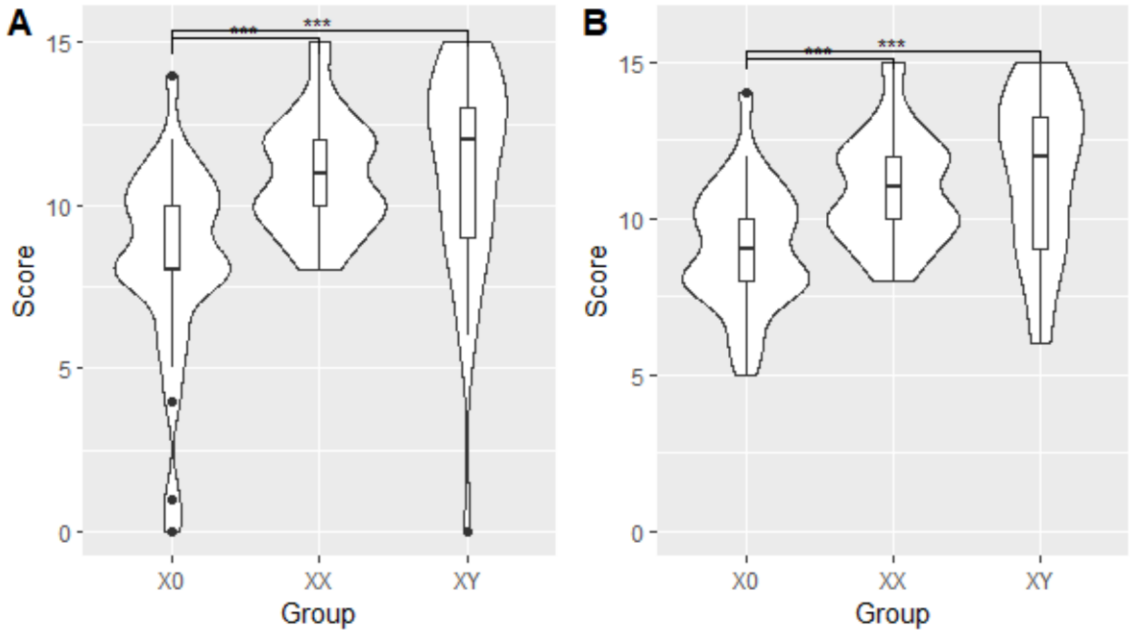

Figure 4.6 Differences in the length of blocks repeated on the Corsi Block Test. A) Before outlier removal. The ANOVA is significant at $p = 1.37 \times 10^{-5}$. B) After outlier removal. The ANOVA is significant at $p = 4.8 \times 10^{-5}$.

Table 4.11 ANOVA results between the three groups for the Corsi Block Task for length of blocks repeated. A) ANOVA results before the removal of outliers. B) ANOVA results after the removal of outliers.

	Sum Sq	Mean Sq	F	p-value
(A) Group	1600.6	80.29	12.32	$1.37x10^{-5}$
(B) Group	13.91	6.95	4.62	$4.8x10^{-5}$

Table 4.12 Post hoc comparisons for maximum blocks repeated on the Corsi Block Task before and after outlier removal.

	Comparison	**Adjusted p-value**
Max blocks		
	X0-XX	$4.6x10^{-5}$
	X0-XY	$4.6x10^{-5}$
	XX-XY	0.71
Max blocks (outliers removed)		
	X0-XX	0.0003
	X0-XY	$6.5x10^{-5}$
	XX-XY	0.22

Digit span task

The data were deemed normally distributed (Figure C.19). ANOVA indicated significant differences between the three groups when the entire sample was evaluated (p=0.041; Figure 4.7a) and when outliers were removed (p=0.011; Figure 4.7b) While post-hoc pairwise comparisons were not significant in the full sample, when outliers were removed post- hoc analysis revealed that XX women and XY men could recall longer numbers strings than women with TS (Table 4.14).

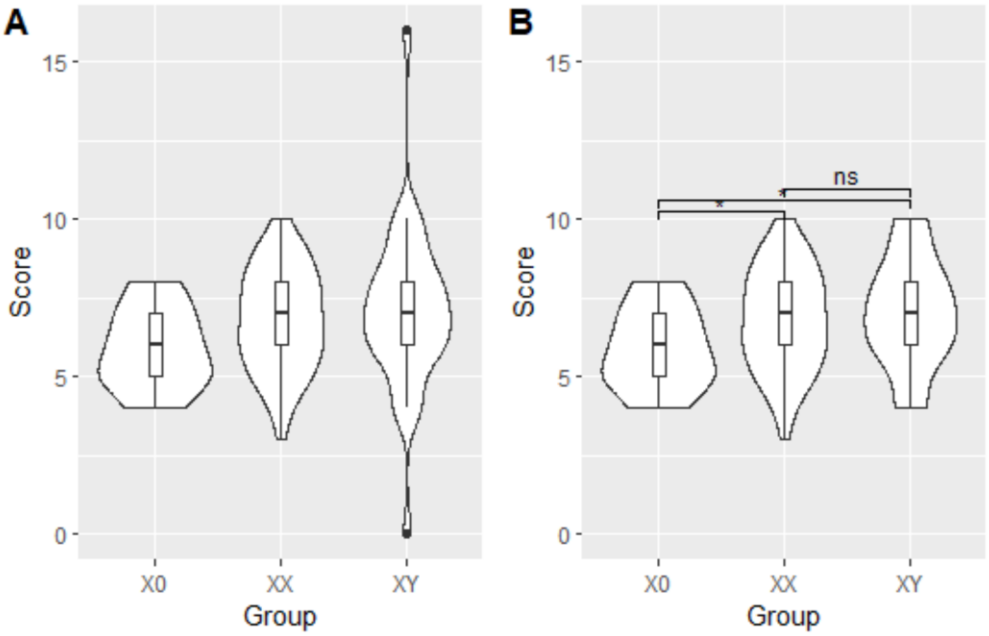

Figure 4.7 Differences in the length of numbers repeated on the Digit Span Task. A) Before outlier removal. The ANOVA is significant at p =0.041. B) After outlier removal. The ANOVA is significant at p=0.011.

Table 4.13 ANOVA results between the three groups for the Digit Span task for length of numbers repeated. A) ANOVA results before the removal of outliers. B) ANOVA results after the removal of outliers.

	Sum Sq	Mean Sq	F	p-value
(A) Group	36.4	18.179	3.293	0.041
(B) Group	23.14	11.569	4.68	0.011

Table 4.14 Post hoc comparisons for maximum number of repeated numbers on the Digit Span Task after outlier removal.

	Comparison	**Adjusted p-value**
Max number repeated (outliers removed)		
	X0-XX	0.013
	X0-XY	0.013
	XX-XY	0.56

Simple response time task

The response time data were heavily skewed to the right, and thus log transformed (Figures C.20 and C..21). Based on the ANOVA, there is a statistically significant difference between the three groups on the SRT ($p=<2x10^{-16}$; Figure 4.8a; Table 4.14), which became stronger after removal of outliers ($p<<2x10^{-16}$; Figure 4.8b; Table 4.15). Table 4.16 displays the post hoc relationships, which show that X0 participants had a longer reaction time than XY participants, and XY had longer reaction times than XX.

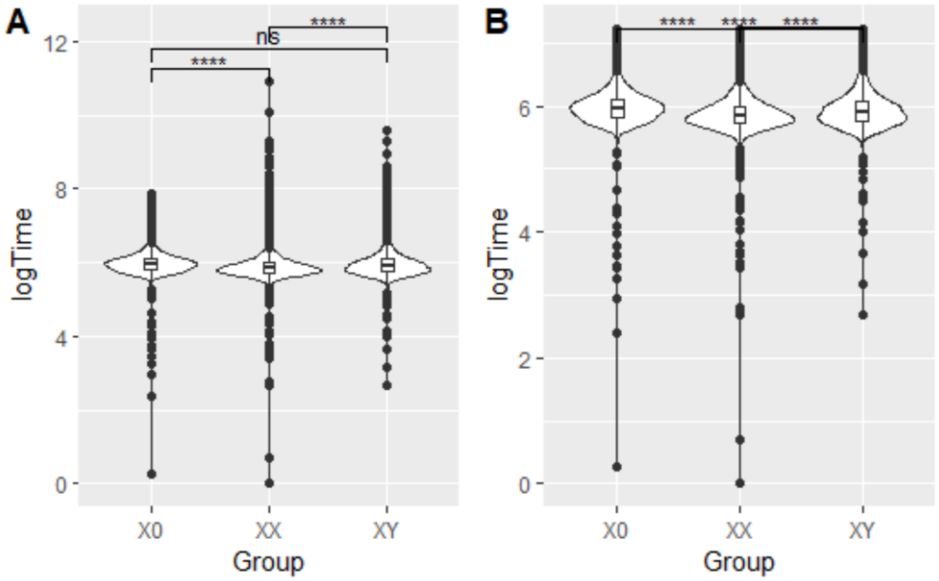

Figure 4.8 Reaction time between the three groups on the Simple Response Time Task. A) Before outlier removal. The ANOVA is significant at $p <2x10^{-16}$. B) After outlier removal. The ANOVA is significant at $p<2x10^{-16}$.

Table 4.15 ANOVA results between the three groups for the Simple Response Time Task for reaction time. A) ANOVA results before the removal of outliers. B) ANOVA results after the removal of outliers.

	Sum Sq	Mean Sq	F	p-value
(A) Group	42.9	21.4	193	$<2x10^{-16}$
(B) Group	42.2	21.1	269.6	$<2x10^{-16}$

Table 4.16 Post hoc comparisons for reaction time on the Simple Response Time Task before and after outlier removal.

	Comparison	Adjusted p-value
Reaction time		
	X0-XX	$<2x10^{-16}$
	X0-XY	0.17
	XX-XY	$<2x10^{-16}$
Reaction time (outliers removed)		
	X0-XX	$<2x10^{-16}$
	X0-XY	$1.7x10^{-12}$
	XX-XY	$<2x10^{-16}$

Autism spectrum quotient

The data were normally distributed (Figure C.22). The ANOVA between the three groups did not yield a statistically significant relationship (p=0.285; Figure 9) when total score was measured. A score of thirty-two or above is indicative of the presence of some autistic traits.

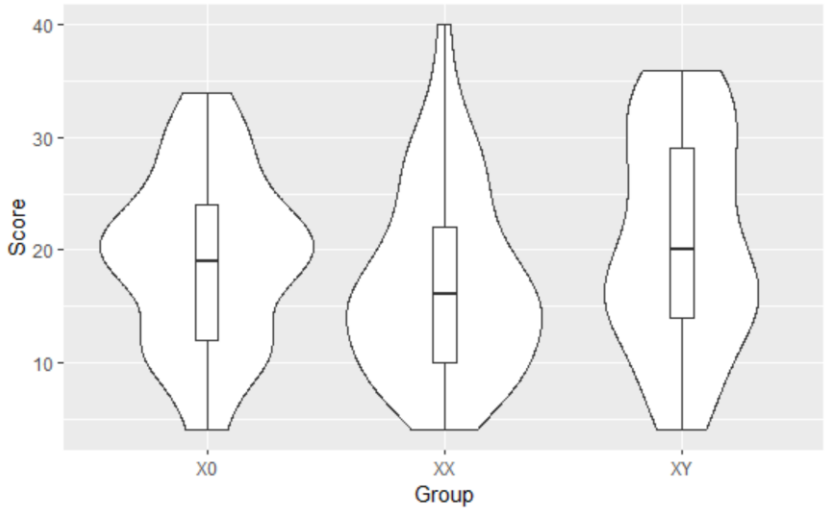

Figure 4.9 Score on the Autism Spectrum Quotient between the three groups. The ANOVA was not significant.

ADHD report scale

The data were deemed to be normally distributed after outlier removal (Figures C.23 and C.24). No statistical significance was found between the three groups on the ADHD report scale in terms of total score (p=0.137; Figure 4.10a) both before and after outlier removal (p=0.98; Figure 4.10b).

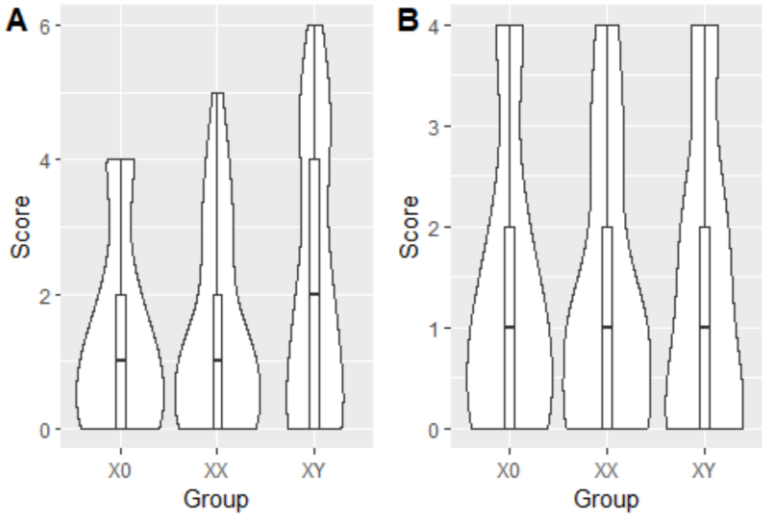

Figure 4.10 Score on the ADHD Report Scale between the three groups. A) The ANOVA was not significant for the relationship before outlier removal. B) The ANOVA was not significant for the relationship after outlier removal.

Discussion

To our knowledge, we are the first group to have created and validated a browser-based online cognitive testing platform that is able to show differences between women with TS and male and female controls across all three cognitive domains affected in TS. Overall, all but the two surveys, Reading the Mind in the Eyes, and the CPT in the battery showed separation between X0 and controls in some aspect, indicating the effectiveness and sensitivity of the battery.

Regarding the tests of EF, we did not see differences in accuracy on the flanker task. This is not unexpected, as accuracy on flanker tests is typically very high and in our own data, most individuals performed at/near ceiling. Reaction time data revealed that women with TS responded significantly more slowly than both control females and control males on both congruent and incongruent trials. Slower reaction time for congruent trials could represent an impairment in sustained attention in women with TS, while slower reaction time on incongruent trials could reflect deficits in selective attention and inhibitory control [398], which rely on activation of the fronto-parietal network[477], specifically the anterior cingulate cortex (ACC)[478,479]. Studies of sustained attention have shown conflicting results in TS. In contrast, studies of inhibitory control have been more consistent in showing impairments in TS. Conditional accuracy functions, which show how accuracy varies as a function of reaction time, can also be estimated on the flanker task. The conditional accuracy functions demonstrate that accuracy for congruent and incongruent responses approach the same level when more time is taken for incongruent responses[480]. Individual differences in conditional accuracy are a marker of inhibitory control and selective attention with the flankers being processed first, followed by the middle arrow[481]. It could reasonably be assumed that in the case of TS participants, who have a deficit in response inhibition and selective attention[403], would have lower conditional accuracy than controls.

We saw no statistical significance on any of the four aspects of the CPT (score, reaction time, commissions and omissions). This could be due to the test's length (14 minutes) and the fact that the test was not taken in a clinical setting void of most distractions. However, it has been shown previously that there is no statistically significant

difference between at-home and in-clinic testing when using a cognitive battery, though the CPT was not part of this cited battery[482]. Typically, brain networks implemented when taking the CPT include the default mode network[483] which is involved in activities of sustained attention[484,485]. The previously mentioned ACC[486] is also involved in sustained attention which is the goal measurement of the CPT.

The simple response time task showed statistical significance between the three groups. The SRT is a measure of processing speed[487] and the observed pattern of X0 having the longest reaction times followed by XY aligns with our hypotheses. Because the SRT is a measure of processing speed, these results should be taken into consideration in the context of the rest of our findings on the battery that rely on measurements of reaction time. The processing speed is an underlying factor that influences any and all of the reaction time measurements taken in this battery. General processing speed has been shown to recruit the frontal, parietal, and temporal cortices, which are connected via the superior and inferior longitudinal fasciculi[19,488]. The superior longitudinal fasciculus plays a large role in cognition, specifically EF.

The Corsi block and digit span tasks compose our exploration into the EF subdomain of working memory. We were able to reject the null hypothesis in both cases as both tasks showed statistical significance in distinguishing the three groups based on length of blocks or numbers repeated. The Corsi block test has been shown in the literature to be an effective tool in discriminating between TS and TD individuals in children[489]. The same situation is found for the digit span, in which the literature shows a statistically significant difference between TS and TD children[490] . These results validate our battery's ability to function as a method to test working memory in these two cases,

and situate it in a successful position to test measurements of EF. In terms of the visuospatial component of the Corsi block task, forming the spatial map required to repeat the sequence recruits the temporo-parietal junction for maintenance of this map[491]. Both the occipital and parietal lobe are recruited for this task[491,492].

Visuospatial reasoning was tested via the mental rotation task. The 1980 paper by Rovet and Netly[493] concerning the mental rotation task in women with TS demonstrated poorer accuracy and poorer reaction time in the TS group which has been shown across the literature[399,494]. We are now able to add to this rich literature base with our own results that are able to reject the null hypothesis in terms of seeing both a difference in accuracy and in reaction time. This validates an additional cognitive domain disrupted in TS in our battery. Previous work has shown the degree of activation in the superior parietal cortex is proportional to the degree in which the object is rotated[495].

We were unable to reject the null hypothesis in our measure of social cognition. Reading the Mind in the Eyes showed no differences between the groups. It has been shown that typically developing females generally have an advantage on the Mind in the Eyes test[496] over TD males.. It has been previously demonstrated that fronto-temporoparietal connectivity[497] is a key circuit involved in the processing required for this task. Specifically, the temporoparietal junction[498] is a main structural neural substrate that may be required for this task. Levels of activation in the orbitofrontal cortex have also been associated with performance on the task[499].

Though both Likert-style surveys did not display any statistical significance when comparing the three groups, the pattern observed for both the ASQ and ADHD report scale match what we would have expected to see; control males have higher scores of

symptomologies for both ASD and ADHD than control females before outlier removal. TS participants showed greater scores of symptomologies than female participants, which aligns with the observed higher prevalence of ADHD and ASD in the TS population, however, control males scored higher than the TS participants which we hypothesized would have been greater or equal to the control males. This may be due to lack of sufficient sample size, but could also be a function of selection bias. The control participants chosen for the study were selected using filters that removed any medical conditions and medication use, which reduces the potential for ASD and ADHD diagnoses to come through. Additionally, the participants who completed the study, both TS and controls, were able to finish an hour-long battery, a feat that possibly would be unattainable with a more severe presentation of ADHD or ASD traits.

Limitations to this study include a relatively small sample size and possible factors introduced by not performing the battery in a clinical environment such as interruptions, multitasking, and the possible presence of other persons. Though fewer than thirty participants from the controls and TS groups were involved in the study, we were still able to show high levels of statistical significance across all but the CPT, Reading the Mind in the Eyes, and the two surveys. As previously noted, it has been shown that there is no statistically significant difference between a cognitive battery given at home, or in a clinic. The fact that the battery is able to be applied with merely the need for an internet connection and does not require travel to a clinical setting or staffing professionals in the clinic makes it an incredibly useful tool that has the potential to have more far-reaching applications than a traditional battery. Uninhibited by geographical location, the presented battery could potentially be used across the country.

In future iterations of the presented cognitive battery the CPT should be removed. No statistically significant differences were found between the three groups. Additionally, zeroes were scored which indicates that either the instructions were not clear, or that the test was not taken with the individual's fullest attention and effort. The CPT is a very long test at 14 minutes, and may be entirely too long to have on the battery when discrimination between the groups is based on data that show the test was not taken properly.

In conclusion, the presented study has shown validity in our testing method, paving the way for the battery to be expanded to encompass larger populations of women with TS and including more items. The creation of this cognitive battery gives researches to opportunity to expand research in TS to explore associations with brain structure, brain function, and perhaps the genetic underpinnings that drive neurodysgenesis.

Chapter 5

Conclusions and future directions

Summary

The research presented in this dissertation broadens our understanding of the genetic underpinnings of executive function, social cognition, and associated neural networks. In **Aim 1 (Chapter 2),** I used a classic twin design to investigate genetic and environmental factors influencing neonatal resting-state functional connectivity including connectivity within and between networks involved in executive function and social cognition. In **Aim 2 (Chapter 3),** I compared functional and structural connectivity between typically developing male and female infants and infants with Turner syndrome. In **Aim 3 (Chapter 4),** I developed an online testing platform targeting cognitive domains that are often disrupted in TS, including executive function and social cognition, and validated the online testing platform by administering it to neurotypical males and females and to adult women with Turner syndrome. In the following paragraphs I summarize the key findings for each aim and discuss their statistical and biological significance.

In Aim 1, I demonstrated that narrow-sense heritability estimates for resting-state phenotypes were relatively low with only 6 of the 36 phenotypes examined showing narrow-sense heritability estimates greater than 0.10, indicating a small effect size. This suggests that environmental factors play a greater role than genetic factors in shaping individual differences during this critical period in the establishment of brain circuitry. In addition, statistically significant associations between neonate resting-state functional connectivity phenotypes and specific demographic and medical history variables were observed. One key finding is that maternal psychiatric history was positively associated with a between-network pair that included the frontoparietal network ($p=0.0012$; explains 3.66% of variance). This network is involved in higher order levels of cognitive processing.

This result is highly significant biologically speaking as it implies a possible root to executive functioning development in the offspring. Overall, I concluded that the study was well powered to detect heritability of 0.5 or greater at 80% power, but had low power to detect heritability less than 0.25. A larger sample size has the potential to show that the low heritability estimates observed are significant, but at present I determined that these specific resting-state connectivity phenotypes are not highly heritable at this stage in development. A similar study in a larger sample size is suggested for future works along with the possibility of a study focusing specifically on the environmental determinants of these phenotypes in which I did find statistical significance. A more extensive discussion of future research directions can be found later in this chapter.

For Aim 2, my initial hypotheses that infants with TS would show altered integrity of the superior longitudinal fasciculus and reduced connectivity between the right precentral gyrus and occipital and parietal regions involved in executive function, social cognition, and visuospatial processing was not supported. The FDR adjusted p-values ranged from 0.1 to 0.59 with effect sizes as calculated by eta squared of 0.07 (medium; right calcarine cortex), 0.08 (medium; left calcarine cortex), 0.081 (medium; right lingual cortex), 0.063 (medium; left lingual cortex), and low at 0.033 for the right supramarginal gyrus. This null result is important as it suggests that altered fronto-parietal connectivity in TS emerges after one year of age and could potentially be prevented by early intervention. For the right calcarine and lingual cortices a statistically significant value was found before FDR correction. In conjunction with the medium effect sizes, the statistical significance may suggest a biologically important effect. Additionally, an exploratory analysis revealed several fasciculi that differed between the groups. Some of these

fasciculi are involved in cognitive domains disrupted in TS, such as the inferior fronto-occipital fasciculus (XY-X0; corrected p = 0.007). I also observed unexpected results such as differences in the optic tract (XY-X0; corrected p = 0.035), which is a difference never before reported. In terms of the effect size of the findings, each tract is unique. The effect sizes of the statistically significant exploratory tracts, represented in percent change are as follows: corpus callosum tapetum FA and AD (0.01%, 8%), left inferior longitudinal fasciculus RD, FA (30%, 0.02%), left IFOF AD, FA (12%, 0.15%), corpus callosum motor AD (15%), left motor corticofugal tract FA, AD and RD (0.03%, 300%, 150%), left corticothalamic tract AD (6%), right cingulum adjoining the hippocampus AD, RD (7%, 15%), right arcuate fasciculus frontotemporal region AD (6%), and the right optic tract FA (0.08%). Though all were statistically significant, those percent changes lower than one percent may not be of clinical relevance whereas the left motor corticofugal tracts change of 300% and 150% may show biological significance. Those percent changes falling in the middle (12%-30%) may be of biological significance and a larger sample size would be able to hone in on a more accurate estimation. Overall, the key findings from my exploratory analysis are that X0 and XY individuals show greater maturity for several white matter tracts compared to XX females as indexed by AD. A logical next step would be to determine how long these differences persist by conducting a longitudinal study. Additional future directions are discussed further in this chapter.

For Aim 3, Women with TS performed more poorly on tests measuring visuospatial reasoning and executive functioning with adjusted p-values ranging from $2x10^{-16}$ at the smallest to 0.013 as the largest. Using Cohen's D to calculate effect sizes on the battery items that showed a statistically significant difference, reaction time on the mental

rotation task showed a medium effect size for the X0-XX comparison (0.6) and X0-XY comparison (0.58). A small to medium effect size of 0.49 was observed for the Flanker task on congruent questions for response time for the X0-XY comparison while the X0-XX comparison had a medium effect size of 0.62. As previously discussed TS can be thought of as having a masculinizing effect. This may be why the observed effect size is greater between XX and X0 females. This pattern also holds true for the response time on incongruent stimuli in the Flanker, though the effect sizes are much larger (X0-XY = 0.71; X0-XX = 0.92). This is most likely due to the increased difficulty in choosing a target when the flanker and center arrow are not in the same direction, creating a larger gap in scores. Cohen's D was positive in the last three examples because the reaction time was greater in the X0 group than the controls. The following two examples have negative Cohen's D scores because the controls scored larger on repeating both blocks and number strings in the Corsi Block test and Digit Span test. For the Corsi blocks, as mentioned, the TS group scored lower in repeated block patterns than the neurotypical controls with large effect sizes (X0-XY = -0.97; X0-XX = -0.94). The Digit Span additionally showed lower scoring in the repetition of numbers in TS than in the control groups though this effect was only medium to high or medium (X0-XY = -0.77; X0-XX = -0.63). Further in this chapter future directions are discussed more fully for Chapter 4, but overall the online platform successfully revealed robust differences between the three groups and a continuation of the research would be to investigate if factors contributing to individual differences in TS women can be distinguished.

Rigor and reproducibility

Currently, science is plagued with a crisis of reproducibility[500,501]. Scientists are unable to replicate the studies of others, or even their own studies. Contributing factors to this crisis include inappropriate correction for multiple testing and lack of methodological details in published studies. To uphold scientific rigor and construct this manuscript in a way that is reproducible, this dissertation applied false discovery rate corrections to all applicable situations, making sure that the statistical significance was not artificially inflated due to improper accounting of multiple testing. This dissertation additionally includes the packages and versions of each R package utilized along with the version of R it was built under. All methods are detailed for ease in reproducing and active contact information is available for researchers to engage with if questions arise. Ultimately, all data from Chapter 4 will be deposited in the Turner Syndrome Research Registry for future use by scientists.

Future work

Longitudinal imaging of infants

As previously discussed, the heritability of resting-state functional connectivity is under mild to moderate influence in adults and adolescents. At the two-week postnatal timepoint, we do not observe this established heritability. A continuation of our work in Aim 1 would be to look longitudinally at a cohort of DZ and MZ twins and watch the development of the resting-state networks over time. This has the potential to show where exactly genetics begins to play a larger role in the brain's functional connectivity and helps to define a critical period in development where the environment may play a larger role in

the shaping of networks. A larger cohort of infant twin-pairs would need to be used as well to overcome the barrier of insufficient power.

In a study by Gao and colleagues[324] intersubject variability in the brain's functional connectivity was shown across the age span of infancy at timepoints of 1 month, 1 year, and 2 years. The study demonstrated an overall decrease in variability over time in the connectivity in a back to front manner, with higher-order cognitive networks demonstrating the highest variability at the end of the age range. This study combined with the results from my Aim 1 speak to the process of canalization and now gives evidence to canalization of resting-state functional connectivity. As age increases intersubject variability decreases, as previously stated, and I hypothesize that with this decrease, heritability increases in the same back to front pattern that is consistently observed throughout the literature, i.e., higher order cognitive processes will be the last networks to achieve a heritability value consistent with adult and adolescent levels.

Utilization of sample-derived networks in the imaging of neonates

A potential path for future analysis for Aim 1 includes not using an adult-defined atlas to map the neonates' networks onto, but instead defining the networks based on the neonatal data. An examination of heritability and environmental effects would then follow. This would be considered an exploratory study but has the potential to be more infant-specific and perhaps give different heritabilities than by using the adult atlas. For Aim 1 I chose to use the adult-defined atlas because we aimed to examine how canonical networks that are commonly identified in adults are impacted by genetic and environmental factors. Thus, adult-defined networks were used to facilitate interpretations of our findings. This chosen approach has the limitation that neonates do not have these

fully developed networks during this period, and the adult atlas is an estimation. An alternative approach to address this limitation is the use of independent component analysis (ICA) which is data-driven and model free, allowing for an exploratory analysis. This approach was not chosen for the current study as there were specific hypotheses made and an overall research question. However, it would be an interesting direction for future research.

The temporal relationships between volume, tract integrity, and resting state connectivity in TS

Aim 2's objectives and hypotheses were largely based on previous work showing differences in brain volumes in the same cohort, as explained in Chapter 3. We did not see connectivity between these regions at this age which indicates that these characteristic markers of TS develop later in life. Pinpointing the developmental time in which the SLF loses white matter integrity as evidenced by a reduction in FA sets a period in which interventions could be given to help ameliorate the difficulties that occur later in life. This same idea holds true for the connectivity between the frontal and visual cortices. Finding the intersection between volumetric and anatomical or functional changes could also have implications for other neurodevelopmental disorders in which connectivity could still be developing even though a volume difference is observed. The reverse may also be true and would require a longitudinal study of the one-year-old infants into childhood and adolescence to look at if the strengthening of connectivity in the SLF and frontal-visual connectivity via therapeutic intervention reduces the volumetric differences seen between the three cohorts. This would help to establish a stronger connection between brain volumes and its implications for brain connectivity. Research investigating the

coupling of structural and functional connectivity have shown regional patterns in age, sex, and cognitive phenotypes[502,503], with wide ranging patterns. The strength of these couplings has additionally been shown to follow the back to front development pattern of other brain characteristics, with the regions involved in higher order cognitive processes such as executive functioning growing in strength with age[503].

Implementation of the cognitive battery on a sample of TS women with sequenced exomes

As discussed in previous chapters, TS is characterized by deficits in the visuospatial, executive function, and social cognitive domains. Chapter 4 in this dissertation successfully established a cognitive battery designed specifically for use in TS to measure and assess these cognitive domains. This battery would be very simple to utilize in other studies related to probing cognition in TS. Currently, there exists a cohort of 188 TS women that also have had their exomes sequenced[504]. This cohort previously participated in an exome sequencing study involving investigation of the genetics of aortopathy in TS. By utilizing this cohort and having them take our validated battery, we have the potential to be the first to show genes and pathways that influence these cognitive domains in TS with implementation of an exome-wide association study. As previously stated, this cohort of women were involved in an aortopathy exome sequencing study. The result of that study yielded identification of a genetic variant associated with the specific aortopathy, indicating that the statistical methods used were powerful enough and had high enough sensitivity to discern variants, despite a sample size smaller than what is traditionally used for association studies. A recent trend in TS research is to not consider the disorder as a single disease, but as a condition that causes a predisposition

to a wide range of diseases caused by the loss of the sex chromosome genes sensitizing the genetic background[505,506]. This sensitization for developing other diseases is a contributing factor as to why a small sample size is sufficient in these types of studies. As laid out in previous chapters, TS has a larger prevalence of ASD and ADHD than the XX female population, looking more like the XY male population. These developmental disorders share similar deficits in cognition as observed in TS. The exome-wide association study then has the potential to uncover genetic variants that also play a role in these male-biased disorders.

Selection of appropriate data analysis approach for Aim 1

Throughout the course of the research process, changes were made to the data analysis plan in Chapter 2 in order to provide the best statistical analysis possible relating to the estimation of heritability. Originally, a DeFries-Fulker regression analysis was run on the neonatal resting-state connectivity data using a Rogers-Kohler method that involved double entering, and then bootstrapping was used to estimate confidence intervals that we then used to gauge statistical significance in broad-sense heritability estimations. This method was abandoned in favor of the mixed effects modeling approach outlined in Chapter 2 that concentrates on narrow-sense heritability. We did this for multiple reasons, the first being that the DeFries-Fulker method produced negative heritability estimates with confidence intervals having both negative values that did not include zero. With the mixed modeling approach, the lower threshold was zero, which not only made more sense biologically but also simplified the results. Second, the mixed modeling approach allowed us to estimate p-values via permutation testing, not just the confidence intervals. This became important because multiple narrow-sense heritability

estimates produced confidence intervals that did not contain zero but the p-value was not statistically significant. Switching the methods from a broad-sense to narrow-sense heritability estimation has limitations in the sense that narrow-sense heritability considers only additive genetic effect and does not account for factors such as epistasis, dominance, and gene x environment interactions. Future studies in larger sample sizes are needed to probe these potential effects.

Conclusion

Taken together, the results presented in this dissertation add to the growing body of literature that explores cognition in both normal and pathological populations. Genetics play a large role in shaping brain connectivity which directly influences cognition. Though resting-state connectivity may not be under a substantial amount of additive genetic effect in neonates, connectivity and cognition are shaped by the presence or absence of an X chromosome. This dissertation provides groundwork for new avenues of discovery building off of the results that have been presented which provide new perspectives on the brain.

APPENDICES

APPENDIX A:

Supplemental data for Chapter 2

Table A.1 The 90 regions from the neonate specific AAL atlas assigned to the eight intrinsic functional networks.

NO.	Region/Node		Hemisphere	Abbreviation	Network
1	Precentral gyrus		left	PreCG-L	Somatosensory
2	Precentral gyrus		right	PreCG-R	Somatosensory
3	Superior frontal gyrus	(dorsal)	left	SFGdor-L	Default Mode
4	Superior frontal gyrus	(dorsal)	right	SFGdor-R	Default Mode
5	Orbitofrontal cortex	(superior)	left	ORBsup-L	Limbic
6	Orbitofrontal cortex	(superior)	right	ORBsup-R	Limbic
7	Middle frontal gyrus		left	MFG-L	Frontoparietal
8	Middle frontal gyrus		right	MFG-R	Frontoparietal
9	Orbitofrontal cortex	(middle)	left	ORBmid-L	Frontoparietal
10	Orbitofrontal cortex	(middle)	right	ORBmid-R	Frontoparietal
11	Inferior frontal gyrus	(opercular)	left	IFGoperc-L	Frontoparietal
12	Inferior frontal gyrus	(opercular)	right	IFGoperc-R	Frontoparietal
13	Inferior frontal gyrus	(triangular)	left	IFGtriang-L	Frontoparietal
14	Inferior frontal gyrus	(triangular)	right	IFGtriang-R	Frontoparietal
15	Orbitofrontal cortex	(inferior)	left	ORBinf-L	Default Mode
16	Orbitofrontal cortex	(inferior)	right	ORBinf-R	Default Mode
17	Rolandic operculum		left	ROL-L	Somatosensory
18	Rolandic operculum		right	ROL-R	Somatosensory
19	Supplementary motor area		left	SMA-L	Somatosensory
20	Supplementary motor area		right	SMA-R	Somatosensory
21	Olfactory		left	OLF-L	Limbic
22	Olfactory		right	OLF-R	Limbic
23	Superior frontal gyrus	(medial)	left	SFGmed-L	Default Mode
24	Superior frontal gyrus	(medial)	right	SFGmed-R	Default Mode
25	Orbitofrontal cortex	(medial)	left	ORBmed-L	Default Mode
26	Orbitofrontal cortex	(medial)	right	ORBmed-R	Default Mode
27	Rectus gyrus		left	REC-L	Limbic

Table A.1 (cont'd)

28	Rectus gyrus	right	REC-R	Limbic
29	Insula	left	INS-L	Ventral Attention
30	Insula	right	INS-R	Ventral Attention
31	Anterior cingulate gyrus	left	ACG-L	Default Mode
32	Anterior cingulate gyrus	right	ACG-R	Default Mode
33	Middle cingulate gyrus	left	MCG-L	Ventral Attention
34	Middle cingulate gyrus	right	MCG-R	Ventral Attention
35	Posterior cingulate gyrus	left	PCG-L	Default Mode
36	Posterior cingulate gyrus	right	PCG-R	Default Mode
37	Hippocampus	left	HIP-L	Subcortical
38	Hippocampus	right	HIP-R	Subcortical
39	ParaHippocampal gyrus	left	PHG-L	Limbic
40	ParaHippocampal gyrus	right	PHG-R	Limbic
41	Am ygdal a	left	AMYG-L	Subcortical
42	Am ygdal a	right	AMYG-R	Subcortical
43	Calcarine cortex	left	CAL-L	Visual
44	Calcarine cortex	right	CAL-R	Visual
45	Cuneus	left	CUN-L	Visual
46	Cuneus	right	CUN-R	Visual
47	Lingual gyrus	left	LING-L	Visual
48	Lingual gyrus	right	LING-R	Visual
49	Superior occipital gyrus	left	SOG-L	Visual
50	Superior occipital gyrus	right	SOG-R	Visual
51	Middle occipital gyrus	left	MOG-L	Visual
52	Middle occipital gyrus	right	MOG-R	Visual
53	Inferior occipital gyrus	left	IOG-L	Visual
54	Inferior occipital gyrus	right	IOG-R	Visual
55	Fusiform gyrus	left	FFG-L	Visual

Table A.1 (cont'd)

56	Fusiform gyrus		right	FFG-R	Visual
57	Postcentral gyrus		left	PoCG-L	Somatosensory
58	Postcentral gyrus		right	PoCG-R	Somatosensory
59	Superior parietal gyrus		left	SPG-L	Dorsal Attention
60	Superior parieta lgyrus		right	SPG-R	Dorsal Attention
61	Inferior parietal lobule		left	IPL-L	Frontoparietal
62	Inferior parietal lobule		right	IPL-R	Frontoparietal
63	Supramarginal gyrus		left	SMG-L	Ventral Attention
64	Supramarginal gyrus		right	SMG-R	Ventral Attention
65	Angular gyrus		left	ANG-L	Default Mode
66	Angular gyrus		right	ANG-R	Default Mode
67	Precuneus		left	PCUN-L	Default Mode
68	Precuneus		right	PCUN-R	Default Mode
69	Paracentral lobule		left	PCL-L	Somatosensory
70	Paracentral lobule		right	PCL-R	Somatosensory
71	Caudate		left	CAU-L	Subcortical
72	Caudate		right	CAU-R	Subcortical
73	Putamen		left	PUT-L	Subcortical
74	Putamen		right	PUT-R	Subcortical
75	Pallidum		left	PAL-L	Subcortical
76	Pallidum		right	PAL-R	Subcortical
77	Thalamus		left	THA-L	Subcortical
78	Thalamus		right	THA-R	Subcortical
79	Heschl gyrus		left	HES-L	Somatosensory
80	Heschl gyrus		right	HES-R	Somatosensory
81	Superior temporal gyrus		left	STG-L	Somatosensory
82	Superior temporal gyrus		right	STG-R	Somatosensory
83	Temporal pole	(superior)	left	TPOsup-L	Limbic
84	Temporal pole	(superior)	right	TPOsup-R	Limbic

Table A.1 (cont'd)

85	Middle temporal gyrus		left	MTG-L	Default Mode
86	Middle temporal gyrus		right	MTG-R	Default Mode
87	Temporal pole	(middle)	left	TPOmid-L	Limbic
88	Temporal pole	(middle)	right	TPOmid-R	Limbic
89	Inferior temporal gyrus		left	ITG-L	Dorsal Attention
90	Inferior temporal gyrus		right	ITG-R	Dorsal Attention

Table A.2 Differences in demographics and medical history variables between the two cohorts scanned on either the Allegra or Trio MRI for Objective 1.

Allegra					Trio					***p***
Continuous Variables	Average	SD	Min	Max	**Continuous Variables**	Average	SD	Min	Max	
Birth weight (g)	2443026	443	1470	3263	Birth weight (g)	2597.92	430.62	1930	3650	0.29
Gestational age at birth (days)	253.2	12.8	224	273	Gestational age at birth (days)	257.88	7.91	242	268	0.11
Gestational age at MRI (days)	293.88	16.31	248	348	Gestational age at MRI (days)	289.53	7.82	278	308	0.18
5 min APGAR score	8.63	0.78	4	10	5 min APGAR score	8.84	0.612	7	10	0.211
Maternal education (years)	15.56	3.6	6	24	Maternal education (years)	15.3	3.18	9	21	0.86
Paternal education (years)	15.28	3.78	6	24	Paternal education (years)	15.92	3.26	12	21	0.29
Maternal age (years)	29.04	5.36	16	42	Maternal age (years)	33.15	3.93	25	39	0.000221
Paternal age (years)	32.28	6.67	20	49	Paternal age (years)	32.69	6	22	42	0.538
Residual framewise displacement	0.112	0.023	0.068	0.169	Residual framewise displacement	0.116	0.02	0.083	0.154	0.402
Categorical variables	*N*		%		**Categorical variables**	*N*		%		

Table A.2 (cont'd)

Sex	Male	48	48.00%	Sex	Male	12	46.15%	1
	Female	52	52.00%		Female	14	53.85%	
Delivery Method	Vaginal	26	26.00%	Delivery Method	Vaginal	14	53.85%	0.009
	C-section	74	74.00%		C-section	12	46.15%	
Household income	High	30	30.00%	Household income	High	16	61.54%	0.013
	Mid	22	22.00%		Mid	4	15.38%	
	Low	48	48.00%		Low	6	23.08%	
Maternal ethnicity	White	76	76.00%	Maternal ethnicity	White	20	76.92%	1
	Black	22	22.00%		Black	6	23.08%	
	Asian	2	2.00%		Asian	0	0.00%	
	Native	0	0.00%		Native	0	0.00%	

Table A.2 (cont'd)

	American				American			
Paternal Ethnicity	White	68	68.00%	Paternal Ethnicity	White	14	53.85%	1
	Black	30	30.00%		Black	8	30.77%	
	Asian	2	2.00%		Asian	4	15.38%	
	Native American	0	0.00%		Native American	0	0.00%	
Maternal psychiatric history	No	80	80.00%	Maternal psychiatric history	No	18	69.23%	0.29
	Yes	20	20.00%		Yes	8	30.77%	
Paternal psychiatric history	No	94	94.00%	Paternal psychiatric history	No	26	100.00%	0.34
	Yes	6	6.00%		Yes	0	0.00%	
Maternal smoking	No	96	96.00%	Maternal smoking	No	26	100.00%	0.34

Table A.2 (cont'd)

	Yes	4	4.00 %		Yes	0	0.00 %	
NICU Stay	No	98	98.0 0%	NICU Stay	No	26	100.0 0%	1
	Yes	2	2.00 %		Yes	0	0.00 %	

Table A.3 Differences in demographics and medical history variables between the two cohorts scanned on either the Allegra or Trio MRI for Objective 2.

Allegra						Trio					***p***
Continuous Variables		Average	SD	Min	Max	**Continuous Variables**		Average	SD	Min	Max	
Birth weight (g)		2803.6	650.9	1289	4820	Birth weight (g)		2761.93	656.54	840	4234	0.668
Gestational age at birth (days)		261.8	17.9	210	295	Gestational age at birth (days)		259.66	13.09	227	285	0.243
Gestational age at MRI (days)		295.56	14.49	248	348	Gestational age at MRI (days)		291.93	10.16	276	320	0.047
5 min APGAR score		8.66	384	4	10	5 min APGAR score		8.8	0.59	7	10	0.414
Maternal education (years)		15.42	3.47	6	24	Maternal education (years)		15.95	3.36	9	22	0.283
Paternal education (years)		14.93	3.47	6	24	Paternal education (years)		16.38	3.22	12	22	0.007
Maternal age (years)		28.94	5.72	16	42	Maternal age (years)		32.9	4.59	21	44	1.73E-05
Paternal age (years)		32.08	6.94	18	64	Paternal age (years)		33.38	5.63	22	45	0.09
Duration in NICU (days)		0.093	0.29	0	1	Duration in NICU (days)		0.1	0.3	0	1	0.962
Residual framewise displacement		0.11	0.02	0.06	0.17	Residual framewise displacement		0.12	0.02	0.06	0.19	0.216
Categorical variables		*N*		%		**Categorical variables**		*N*		%		
Sex	Male	114		50.44 %		Sex	Male	20		47.62%		0.866
	Female	112		49.56 %			Female	22		52.38%		
Delivery Method	Vaginal	101		44.69 %		Delivery Method	Vaginal	19		45.24%		1

Table A.3 (cont'd)

	C-section	125	55.31%		C-section	23	54.76%	
Household income	High	60	26.55%	Household income	High	8	19.05%	0.00026
	Mid	61	26.99%		Mid	10	23.81%	
	Low	105	46.46%		Low	24	57.14%	
Maternal ethnicity	White	174	76.99%	Maternal ethnicity	White	33	78.57%	0.7524
	Black	47	20.80%		Black	8	19.05%	
	Asian	2	0.88%		Asian	1	2.38%	
	Native American	3	1.33%		Native American	0	0.00%	
Paternal Ethnicity	White	157	69.47%	Paternal Ethnicity	White	27	64.29%	0.1293
	Black	63	27.88%		Black	11	26.19%	
	Asian	5	2.21%		Asian	0	0.00%	
	Native American	1	0.44%		Native American	4	9.52%	
Maternal psychiatric history	No	158	69.91%	Maternal psychiatric history	No	31	73.81%	0.713
	Yes	68	30.09%		Yes	11	26.19%	

Table A.3 (cont'd)

Paternal psychiatric history	No	192	84.96 %	Paternal psychiatric history	No	38	90.48%	0.713
	Yes	34	15.04 %		Yes	4	9.52%	
Maternal smoking	No	202	89.38 %	Maternal smoking	No	42	100.00 %	0.019
	Yes	24	10.62 %		Yes	0	0.00%	
Gestation Number	Twin	100	44.25 %	Gestation Number	Twin	26	61.90%	0.011
	Singleton	126	55.75 %		Singleton	16	38.10%	
NICU Stay	No	205	90.71 %	NICU Stay	No	38	90.48%	1
	Yes	21	9.29%		Yes	4	9.52%	

Table A.4 Narrow-sense heritability estimates for between-network connectivity phenotypes.

Network Pair	h2	SE	CI	p-value
SS.Vis	0.059315	0.105614	0, 0.165	0.343
DA.Vis	1.50E-08	0.144986	0, 0	0.611
DA.SS	0.104354	0.105552	0, 0.21	0.263
VA.Vis	1.41E-08	0.099494	0, 0	0.627
VA.SS	6.17E-09	0.140848	0, 0	0.776
VA.DA	9.35E-09	0.098091	0, 0	0.689
Lim.Vis	1.79E-08	0.105051	0, 0	0.625
Lim.SS	0.00713	0.110165	0, 0.117	0.467
Lim.DA	2.59E-07	0.110272	0, 0	0.494
Lim.VA	0.106135	0.118269	0, 0.224	0.26
FP.Vis	1.69E-09	0.084142	0, 0	0.994
FP.SS	1.09E-08	0.072328	0, 0	0.67
FP.DA	0.102387	0.113716	0, 0.216	0.241
FP.VA	4.15E-09	0.092033	0, 0	0.847
FP.Lim	7.55E-09	0.102465	0, 0	0.728
DM.Vis	2.53E-09	0.090047	0, 0	0.951
DM.SS	0.095551	0.102864	0, 0.198	0.23
DM.DA	0.06769	0.116867	0, 0.184	0.3
DM.VA	5.81E-07	0.126204	0, 0	0.461
DM.Lim	4.75E-09	0.118395	0, 0	0.833
DM.FP	0.147621	0.105236	0.042, 0.252	0.162
SC.Vis	0.126146	0.117892	0.008, 0.244	0.188
SC.SS	1.71E-08	0.09408	0, 0	0.604
SC.DA	0.016909	0.117945	0, 0.134	0.445
SC.VA	7.21E-08	0.117867	0, 0	0.484

Table A.5. Narrow-sense heritability estimates for within-network connectivity phenotypes.

Network	h2	SE	CI	p-value
Vis	2.73E-09	0.107542	0, 0	0.94
SS	2.06E-08	0.129447	0, 0	0.566
DA	1.81E-08	0.11841	0, 0	0.565
VA	0.081704	0.150855	0, 0.232	0.265
Lim	4.18E-09	0.135226	0, 0	0.867
FP	9.19E-09	0.138587	0, 0	0.678
DM	9.96E-09	0.134392	0, 0	0.675
SC	1.73E-09	0.106999	0, 0	0.994

Table A.6 Mixed linear modeling results after backwards elimination for between-network phenotypes.

Between-network pair	R-squared	Predictor	*p-value*	Beta	r^2
Somatosensory-Visual	0.075	Income	0.1230		
		Income (Middle)		0.00846	6.53E-04
		Income (High)		0.041322	1.72E-02
		Gestational Number	0.1320	0.03515	1.41E-02
		Gestational Age at Birth	0.0647	-0.00158	3.47E-02
		Birthweight	0.0358	4.75E-05	4.46E-02
		Gestational Age at MRI	0.0004	0.00239	5.20E-02
Dorsal Attention - Visual	0.063	Scanner	0.0372	0.0456179	1.54E-02
		Gender	0.0470	0.032319	1.46E-02
		Gestational Age at Birth	0.0021	0.001449	3.47E-02
		Maternal Psychiatric History	0.1300	-0.026034	8.20E-03
Dorsal Attention-Somatosensory	0.049	Method of Delivery	0.0847	-0.02859	1.19E-02
		Gestational Age at Birth	0.0106	-0.00195	6.63E-02
		Birthweight	0.0834	3.41E-05	2.89E-02
		Maternal Education at Enrollment	0.0245	-0.007836	4.31E-02
		Paternal Education at Enrollment	0.0493	0.006866	3.33E-02
Ventral Attention-Visual	0.083	Scanner	0.0009	0.067067	3.46E-02
		Gender	0.0292	-0.03257	1.54E-02
		Gestational Age at Birth	0.0026	-0.002236	8.60E-02
		Birthweight	0.0528	3.60E-05	3.18E-02

Table A.6 (cont'd)

		Gestational Age at MRI	0.0156	0.00137	2.12E-02
Ventral Attention - Somatosensory	0.011	Scanner	0.0818	0.6579	1.08E-02
Ventral Attention - Dorsal Attention	0.066	Gender	0.0607	-0.02818	1.24E-02
		Gestational Age at Birth	0.0009	-0.002366	1.04E-01
		Birthweight	0.1000	3.03E-05	2.42E-02
		Residual Framewise Displacement	0.0368	0.64719	1.48E-02
Limbic - Visual	0.045	Paternal Ethnicity	0.3030		
		Paternal Ethnicity (Black)		0.0283	1.00E-02
		Paternal Ethnicity (Native American)		0.12467	3.59E-03
		Paternal Ethnicity (Asian)		0.040412	3.29E-03
		Maternal Education at Enrollment	0.1030	0.005592	2.31E-02
		Paternal Education at Enrollment	0.1670	-0.0046566	1.61E-02
		Paternal Psychiatric History	0.0520	0.04249	1.39E-02
		Residual Framewise Displacement	0.0498	-0.63119	1.40E-02
Limbic - Somatosensory	0.04	Gestational Age at MRI	0.0083	-0.00147	2.66E-02
		Maternal Psychiatric History	0.0272	0.03674	1.84E-02
Limbic - Dorsal Attention	0.052	Gestational Age at Birth	0.0026	-0.00204	8.57E-02

Table A.6 (cont'd)

		Birthweight	0.1190	2.79E-05	2.29E-02
		Paternal Ethnicity	0.1690		
		Paternal Ethnicity (Black)		0.0358	1.78E-02
		Paternal Ethnicity (Native American)		0.0003167	2.59E-08
		Paternal Ethnicity (Asian)		0.02645	1.58E-03
Limbic - Ventral Attention	0.048	Scanner	0.1040	-0.03387	9.90E-03
		Gender	0.0112	-0.03866	2.44E-02
		Gestational Age at MRI	0.1320	-0.0008229	8.53E-03
		Maternal Psychiatric History	0.0665	0.02956	1.24E-02
Frontoparietal - Visual	0.043	Income	0.1820		
		Income (Middle)		0.0005633	3.46E-06
		Income (High)		-0.02727	8.96E-03
		Maternal Psychiatric History	0.0059	-0.0441	2.36E-02
		Residual Framewise Displacement	0.0428	-0.6435	1.31E-02
Frontoparietal - Somatosensory	0.067	Gender	0.0816	0.02694	9.64E-03
		Gestational Age at Birth	0.0389	0.001597	4.01E-02
		Birthweight	0.0700	-3.56E-05	2.83E-02
		Gestational Age at MRI	0.0131	-0.001519	2.38E-02
		Maternal Psychiatric History	0.0018	0.05302	3.23E-02

Table A.6 (cont'd)

Frontoparietal - Dorsal Attention	0.04	Scanner	0.1080	-0.03138	9.04E-03
		Gestational Age at Birth	0.0874	-0.00124	3.18E-02
		Birthweight	0.0785	3.12E-05	2.85E-02
		Stay in NICU	0.1250	0.044723	1.18E-02
		Paternal Psychiatric History	0.1480	-0.0308	8.19E-03
Frontoparietal - Ventral Attention	0.059	Scanner	0.0151	-0.04911	1.80E-02
		Maternal Ethnicity	0.4590		
		Maternal Ethnicity (Black)		0.028	7.25E-03
		Maternal Ethnicity (Native American)		0.0505	1.60E-03
		Maternal Ethnicity (Asian)		0.01755	1.92E-04
		Paternal Education at Enrollment	0.0409	0.0004675	1.48E-02
		Maternal Psychiatric History	0.0012	0.0547388	3.66E-02
Frontoparietal - Limbic	0.051	Income	0.0778		
		Income (Middle)		0.01653	2.56E-03
		Income (High)		0.04373	1.98E-02
		Scanner	0.0337	-0.0455	1.32E-02
		Gender	0.0028	-0.04787	2.76E-02
Default Mode - Visual	0.037	Maternal Ethnicity	0.1290		
		Maternal Ethnicity (Black)		0.030902	1.69E-02

Table A.6 (cont'd)

		Maternal Ethnicity (Native American)		0.03547	1.51E-03
		Maternal Ethnicity (Asian)		-0.003501	1.47E-05
		Paternal Age at Enrollment	0.0421	0.00164	1.33E-02
		Paternal Psychiatric History	0.1170	-0.0249	8.40E-03
Default Mode - Somatosensory	0.02	Method of Delivery	0.5770	0.007276	1.19E-03
		Maternal Psychiatric History	0.0279	0.03033	1.80E-02
Default Mode - Dorsal Attention	0.056	Stay in NICU	0.0016	0.062188	3.86E-02
		Maternal Age at Enrollment	0.0177	0.002989	3.46E-02
		Paternal Age at Enrollment	0.0520	-0.0020569	2.27E-02
		Paternal Psychiatric History	0.1600	-0.0224075	7.37E-03
Default Mode - Ventral Attention	0.014	Method of Delivery	0.1160	-0.0187952	1.01E-02
		Gestational Age at Birth	0.1070	-0.00054467	1.02E-02
Default Mode - Limbic	0.04	Gestational Number	0.2710	0.01468	4.64E-03
		Scanner	0.0240	-0.03949	1.82E-02
		APGAR 5-minute	0.0875	0.01449	1.22E-02
		Stay in NICU	0.1680	0.032023	7.67E-03
		Maternal Ethnicty	0.4440		
		Maternal Ethnicity (Black)		0.00904	1.18E-03
		Maternal Ethnicity		0.03367	1.11E-03

Table A.6 (cont'd)

		(Native American)			
		Maternal Ethnicity (Asian)		-0.09862	9.52E-03
		Paternal Ethnicity	0.7810		
		Paternal Ethnicity (Black)		-0.01655	4.85E-03
		Paternal Ethnicity (Native American)		0.001295	5.52E-07
		Paternal Ethnicity (Asian)		0.0253288	1.84 e-3
		Gestational Age at MRI	1.0000	-2.19E-07	8.22E-10
Default Mode - Frontoparietal	0.109	Scanner	0.2510	-0.0195	4.28E-02
		Gestational Age at Birth	0.0004	-0.001395	4.90E-02
		Maternal Ethnicity	0.0063		
		Maternal Ethnicity (Black)		-0.032082	1.43E-02
		Maternal Ethnicity (Native American)		-0.20876	4.10E-02
		Maternal Ethnicity (Asian)		-0.060884	3.49E-03
		Paternal Ethnicity	0.3710		
		Paternal Ethnicity (Black)		0.0148856	3.77E-03
		Paternal Ethnicity (Native American)		0.13739	5.97E-03

Table A.6 (cont'd)

		Paternal Ethnicity (Asian)		0.04255	5.00E-03
		Gestational Age at MRI	0.0062	0.001324	2.89E-02
Subcortical - Visual		None Selected	-	-	-
Subcortical - Somatosensory	0.114	Smoking	0.1430	-0.04617	7.81E-03
		Gestational Number	0.0313	-0.03891	1.65E-02
		APGAR 5-minute	0.0096	-0.029024	2.48E-02
		Stay in NICU	0.0539	-0.06275	1.50E-02
		Maternal Age at Enrollment	0.0585	0.00389	2.23E-02
		Paternal Age at Enrollment	0.0161	-0.00385	3.04E-02
		Paternal Education at Enrollment	0.1130	-0.004077	8.95E-03
		Gestational Age at MRI	0.0015	-0.0019	3.15E-02
		Paternal Psychiatric History	0.0296	0.054333	1.65E-02
		Residual Framewise Displacement	0.0774	-0.6194	9.75E-03
Subcortical - Dorsal Attention	0.0354	Stay in NICU	0.0978	0.0451012	9.95E-03
		Maternal Education at Enrollment	0.0776	-0.006418	2.84E-02
		Paternal Education at Enrollment	0.0716	0.0065465	2.97E-02
		Motion Correction	0.1380	0.49936	8.15E-03
Subcortical - Ventral Attention	0.038	Scanner	0.0281	-0.05022	1.41E-02
		Gender	0.7280	-0.00621	4.07E-04
		Gestational Age at Birth	0.4710	0.00037198	1.73E-03

Table A.6 (cont'd)

		Paternal Psychiatric History	0.0820	0.045381	1.08E-02
		Residual Framewise Displacement	0.1130	-0.597	8.15E-03
Subcortical - Limbic	0.036	Gestational Number	0.0259	-0.05495	2.96E-02
		Gender	0.0874	-0.03218	1.04E-02
		Birthweight	0.0512	-3.65E-05	2.28E-02
		Paternal Age at Enrollment	0.3970	0.0011855	2.58E-03
		Residual Framewise Displacement	0.2190	0.48468	5.36E-03
Subcortical - Frontoparietal	0.027	Income	0.3290		
		Income (Middle)		0.004623	1.68E-04
		Income (High)		0.034023	1.00E-02
		Gestational Number	0.1340	-0.031004	9.43E-03
		Maternal Psychiatric History	0.1490	0.03095	8.37E-03
Subcortical - Default Mode	0.09	Income	0.1800		
		Income (Middle)		0.02719	9.73E-03
		Income (High)		0.026916	1.05E-02
		Smoking	0.0263	-2.84E-05	1.76E-02
		Scanner	0.0048	-0.05677	2.88E-02
		Gender	0.0889	-0.02424	9.93E-03
		Birthweight	0.0120	-2.84E-05	2.29E-02
		APGAR 5-minute	0.0528	0.01749	1.26E-02

Table A.6 (cont'd)

Paternal Psychiatric History	0.0833	0.03503	1.03E-02

Table A.7 Mixed linear modeling results after backwards elimination for between-network phenotype.

Network	R-squared	Predictor	*p-value*	Beta	r^2
Visual	0.078	Gestational Number	7.09E-03	0.05935	2.69E-02
		Scanner	8.93E-02	-0.0443	8.12E-03
		Method of Delivery	1.21E-01	-0.0312	7.54E-03
		NICU Stay	1.02E-02	0.09195	2.24E-02
		Gestational Age at MRI	4.14E-02	0.00144	1.27E-02
		Residual Framewise Displacement	2.44E-03	1.312	3.05E-02
Somatosensory	0.052	Smoking	6.14E-02	0.0765	1.26E-02
		Paternal Age at Enrollment	3.39E-02	0.003609	1.57E-02
		Paternal Ethnicity	2.75E-01		
		Paternal Ethnicity (Black)		0.05033	1.34E-02
		Paternal Ethnicity (Native American)		0.00533	2.80E-06
		Paternal Ethnicity (Asian)		0.0361	1.12E-03
		Paternal Psychiatric History	2.21E-02	0.0756	1.88E-02
Dorsal Attention	0.1	Gestational Number	1.59E-04	0.118	8.47E-02
		Gestational Age at Birth	1.96E-02	0.00204	3.10E-02
		Maternal Education at Enrollment	2.01E-02	0.0123	4.56E-02
		Paternal Education at Enrollment	4.92E-04	-0.0188	1.08E-01

Table A.7 (cont'd)

		Residual Framewise Displacement	1.33E-02	1.22	2.13E-02
Ventral Attention	0.052	Scanner	1.44E-01	0.0426	7.73E-03
		Gender	1.11E-02	0.0341	9.37E-01
		Method of Delivery	1.19E-02	-0.0537	2.30E-02
		Paternal Ethnicity	2.98E-01		
		Paternal Ethnicity (Black)		0.0279	5.04E-03
		Paternal Ethnicity (Native American)		0.0287	9.88E-05
		Paternal Ethnicity (Asian)		0.0977	1.00E-02
Limbic	0.056	Gender	7.10E-02	-0.0364	1.22E-02
		Maternal Ethnicity	1.44E-01		
		Maternal Ethnicity (Black)		-0.0394	9.36E-03
		Maternal Ethnicity (Native American)		-0.0029	3.51E-06
		Maternal Ethnicity (Asian)		-0.0167	1.14E-02
		Paternal Age at Enrollment	8.06E-03	-0.00399	2.67E-02
Frontoparietal	0.017	Gestational Number	2.80E-01	-0.02859	7.09E-03
		Gender	6.34E-02	-0.0398	1.41E-02
		Gestational Age at Birth	2.82E-01	-0.000826	7.20E-03
Default Mode	0.008	Scanner	1.31E-01	0.025	8.20E-03
Subcortical	0.028	Gestational Number	1.33E-02	-0.0766	3.74E-02
		Gender	1.89E-01	0.03075	6.18E-03
		Birthweight	9.96E-02	-3.91	1.69E-02

APPENDIX B:

Supplemental data for Chapter 3

Table B.1 The 46 tracts that passed quality control with global FDR p-values given, along with local p-values in the estimation of axial diffusivity (AD), radial diffusivity (RD), and fractional anisotropy (FA).

		Global_Omnibus	Global_FDR	AD	RD	FA
Arcuate, left, frontoparietal						
	Female control, Male control	0.086	0.16483	0.163	0.23	0.064
	Female control, Turner syndrome	0.489	0.5442097	0.751	0.475	0.129
	Male control, Turner syndrome	0.138	0.226714	0.238	0.229	0.192
Arcuate, left, frontotemporal						
	Female control, Male control	0.004	0.02208	0	0.557	0.505
	Female control, Turner syndrome	0.536	0.5870476	0.39	0.499	0.939
	Male control, Turner syndrome	0.328	0.4066726	0.398	0.363	0.169
Arcuate, left, temporoparietal						
	Female control, Male control	0.0001	0.00092	0.098	0	0.051
	Female control, Turner syndrome	0.02	0.069	0.25	0.113	0.056
	Male control, Turner syndrome	0.046	0.1075932	0.015	0.15	0.3
Arcuate, right, fronotparietal						
	Female control, Male control	0.076	0.1518	0.137	0.029	0.358

Table B.1 (cont'd)

	Female control, Turner syndrome	0.057	0.1191818	0.103	0.418	0.145
	Male control, Turner syndrome	0.123	0.2139	0.03	0.063	0.056
Arcuate right, frontotemporal						
	Female control, Male control	0.026	0.0763404	0.062	0.013	0.255
	Female control, Turner syndrome	0.007	0.0333103	0.009	0.224	0.078
	Male control, Turner syndrome	0.387	0.4557479	0.329	0.725	0.319
Cingulate gyrus, left						
	Female control, Male control	0.137	0.2267143	0.103	0.193	0.51
	Female control, Turner syndrome	0.39	0.4557479	0.287	0.513	0.715
	Male control, Turner syndrome	0.387	0.4557479	0.78	0.441	0.569
Cingulate gyrus, right						
	Female control, Male control	0.023	0.0721364	0.031	0.046	0.332
	Female control, Turner syndrome	0.047	0.1081	0.052	0.25	0.539
	Male control, Turner syndrome	0.708	0.7291343	0.501	0.879	0.977
Cingulum adjoining hippocampus, left						
	Female control, Male control	0.002	0.0131429	0.154	0.007	0.078
	Female control, Turner syndrome	0.018	0.0671351	0.24	0.009	0.035

Table B.1 (cont'd)

	Male control, Turner syndrome	0.22	0.31625	0.43	0.399	0.058
Cingulum adjoining hippocampus, right						
	Female control, Male control	0.0001	0.00092	0.004	0	0.526
	Female control, Turner syndrome	0.0001	0.00092	0.001	0.002	0.197
	Male control, Turner syndrome	0.466	0.5228293	0.608	0.87	0.899
Corpus callosum, body						
	Female control, Male control	0.001	0.0072632	0.004	0.144	0.495
	Female control, Turner syndrome	0.159	0.2493409	0.217	0.631	0.466
	Male control, Turner syndrome	0.386	0.4557479	0.168	0.91	0.723
Corpus callosum, genu						
	Female control, Male control	0.005	0.0265385	0.004	0.106	0.074
	Female control, Turner syndrome	0.188	0.2882667	0.627	0.378	0.249
	Male control, Turner syndrome	0.333	0.4066726	0.318	0.639	0.893
Corpus callosum, motor						
	Female control, Male control	0.013	0.0543636	0.099	0.863	0.641
	Female control, Turner syndrome	0.007	0.0333103	0.027	0.426	0.261

Table B.1 (cont'd)

	Male control, Turner syndrome	0.607	0.6443538	0.419	0.584	0.477
Corpus callosum, parietal						
	Female control, Male control	0.0001	0.00092	0	0.007	0.112
	Female control, Turner syndrome	0.052	0.1104	0.173	0.088	0.06
	Male control, Turner syndrome	0.656	0.6858182	0.59	0.381	0.145
Corpus callosum, premotor						
	Female control, Male control	0.148	0.2402824	0.334	0.384	0.176
	Female control, Turner syndrome	0.199	0.2952903	0.067	0.861	0.361
	Male control, Turner syndrome	0.157	0.2490345	0.074	0.83	0.614
Corpus callosum, rostrum						
	Female control, Male control	0.023	0.0721364	0.148	0.386	0.023
	Female control, Turner syndrome	0.108	0.1910769	0.08	0.33	0.121
	Male control, Turner syndrome	0.445	0.51175	0.037	0.685	0.339
Corpus callosum, splenium						
	Female control, Male control	0.009	0.0388125	0.033	0.042	0.087
	Female control, Turner syndrome	0.021	0.0706829	0.016	0.013	0.022

Table B.1 (cont'd)

	Male control, Turner syndrome	0.328	0.4066726	0.766	0.367	0.107
Corpus callosum, tapetum						
	Female control, Male control	0.312	0.4038716	0.84	0.941	0.104
	Female control, Turner syndrome	0.004	0.02208	0.042	0.241	0.011
	Male control, Turner syndrome	0.051	0.1104	0.178	0.505	0.09
Corticofugal, left, motor						
	Female control, Male control	0.0001	0.00092	0.0001	0.0001	0.654
	Female control, Turner syndrome	0.0001	0.00092	0.0001	0.0001	0.021
	Male control, Turner syndrome	0.0001	0.00092	0.004	0.087	0.0001
Corticofugal, left, parietal						
	Female control, Male control	0.007	0.0333103	0.055	0.012	0.233
	Female control, Turner syndrome	0.099	0.1774286	0.128	0.383	0.105
	Male control, Turner syndrome	0.002	0.0131429	0.097	0.029	0.02
Corticofugal, right, motor						
	Female control, Male control	0.033	0.0843333	0.015	0.231	0.517
	Female control, Turner syndrome	0.045	0.107069	0.089	0.811	0.176

Table B.1 (cont'd)

	Male control, Turner syndrome	0.008	0.0356129	0.013	0.35	0.002
Corticofugal, right, parietal						
	Female control, Male control	0.023	0.0721364	0.048	0.058	0.472
	Female control, Turner syndrome	0.263	0.3537087	0.205	0.42	0.833
	Male control, Turner syndrome	0.02	0.069	0.103	0.861	0.034
Corticoreticular, left						
	Female control, Male control	0.0001	0.00092	0.001	0	0.351
	Female control, Turner syndrome	0.062	0.1277015	0.374	0.086	0.016
	Male control, Turner syndrome	0.463	0.5228293	0.188	0.946	0.285
Corticoreticular, right						
	Female control, Male control	0.052	0.1104	0.059	0.057	0.352
	Female control, Turner syndrome	0.051	0.1104	0.072	0.164	0.19
	Male control, Turner syndrome	0.314	0.4038716	0.432	0.509	0.132
Corticospinal, right						
	Female control, Male control	0.003	0.018	0.03	0.054	0.094
	Female control, Turner syndrome	0.352	0.4261053	0.163	0.849	0.567
	Male control, Turner syndrome	0.019	0.069	0.006	0.212	0.387

Table B.1 (cont'd)

Corticothalamic, left, motor						
	Female control, Male control	0.319	0.4038716	0.29	0.241	0.204
	Female control, Turner syndrome	0.319	0.4038716	0.29	0.241	0.204
	Male control, Turner syndrome	0.853	0.8592263	0.892	0.962	0.882
Corticothalamic, left, parietal						
	Female control, Male control	0.0001	0.00092	0.009	0.005	0.192
	Female control, Turner syndrome	0.688	0.7138647	0.506	0.745	0.367
	Male control, Turner syndrome	0.218	0.31625	0.308	0.774	0.141
Corticothalamic, left, prefrontal						
	Female control, Male control	0.042	0.1016842	0.097	0.133	0.16
	Female control, Turner syndrome	0.083	0.1613239	0.067	0.137	0.1
	Male control, Turner syndrome	0.241	0.3359394	0.056	0.211	0.506
Corticothalamic, left, premotor						
	Female control, Male control	0.0001	0.00092	0	0.07	0.227
	Female control, Turner syndrome	0.036	0.0887143	0.081	0.047	0.037
	Male control, Turner syndrome	0.638	0.6720916	0.325	0.971	0.761

Table B.1 (cont'd)

Corticothalamic, left, superior						
	Female control, Male control	0.0001	0.00092	0	0.019	0.206
	Female control, Turner syndrome	0.193	0.2926813	0.599	0.196	0.133
	Male control, Turner syndrome	0.845	0.8574265	0.539	0.8	0.901
Corticothalamic, right, motor						
	Female control, Male control	0.027	0.077625	0.01	0.619	0.039
	Female control, Turner syndrome	0.031	0.0822692	0.008	0.405	0.167
	Male control, Turner syndrome	0.871	0.871	0.892	0.865	0.911
Corticothalamic, right, parietal						
	Female control, Male control	0.0001	0.00092	0.003	0.001	0.176
	Female control, Turner syndrome	0.393	0.4557479	0.343	0.224	0.592
	Male control, Turner syndrome	0.136	0.2267143	0.102	0.275	0.054
Corticothalamic, right, prefrontal						
	Female control, Male control	0.241	0.3359394	0.263	0.497	0.594
	Female control, Turner syndrome	0.281	0.3728654	0.131	0.618	0.7
	Male control, Turner syndrome	0.29	0.3811429	0.454	0.255	0.963

Table B.1 (cont'd)

Corticothalamic, right, premotor						
	Female control, Male control	0.0001	0.00092	0	0.338	0.008
	Female control, Turner syndrome	0.003	0.018	0.005	0.311	0.129
	Male control, Turner syndrome	0.452	0.5155041	0.319	0.574	0.626
Corticothalamic, right, superior						
	Female control, Male control	0.0001	0.00092	0.001	0.507	0.042
	Female control, Turner syndrome	0.025	0.075	0.019	0.435	0.251
	Male control, Turner syndrome	0.507	0.559728	0.318	0.573	0.957
Fornix, left						
	Female control, Male control	0.015	0.0591429	0.101	0.037	0.011
	Female control, Turner syndrome	0.014	0.0568235	0.055	0.054	0.064
	Male control, Turner syndrome	0.229	0.3257938	0.161	0.13	0.363
Fornix, right						
	Female control, Male control	0.172	0.2666966	0.435	0.17	0.252
	Female control, Turner syndrome	0.57	0.6145313	0.403	0.767	0.941
	Male control, Turner syndrome	0.554	0.6019843	0.588	0.637	0.726
Inferior fronto-occiptal fasciculus, left						

Table B.1 (cont'd)

	Female control, Male control	0.029	0.08004	0.075	0.378	0.077
	Female control, Turner syndrome	0.032	0.0833208	0.088	0.14	0.046
	Male control, Turner syndrome	0.001	0.0072632	0.003	0.066	0.012
Inferior fronto-occipital fasciculus, right						
	Female control, Male control	0.089	0.1682466	0.127	0.11	0.126
	Female control, Turner syndrome	0.153	0.2455116	0.184	0.772	0.275
	Male control, Turner syndrome	0.264	0.3537087	0.181	0.229	0.251
Inferior longitudinal fasciculus, left						
	Female control, Male control	0.017	0.0651667	0.045	0.801	0.313
	Female control, Turner syndrome	0.001	0.0072632	0.201	0.044	0.039
	Male control, Turner syndrome	0.028	0.0788571	0.339	0.247	0.073
Inferior longitudinal fasciculus, right						
	Female control, Male control	0.031	0.0822692	0.106	0.031	0.139
	Female control, Turner syndrome	0.05	0.1104	0.279	0.132	0.072
	Male control, Turner syndrome	0.124	0.2139	0.589	0.118	0.273
Optic tract, right						

Table B.1 (cont'd)

	Female control, Male control	0.024	0.0736	0.098	0.084	0.018
	Female control, Turner syndrome	0.035	0.0878182	0.406	0.211	0.388
	Male control, Turner syndrome	0.008	0.0356129	0.145	0.06	0.007
Optic radiation, left						
	Female control, Male control	0.001	0.0072632	0.1	0	0.001
	Female control, Turner syndrome	0.095	0.1748	0.935	0.033	0.031
	Male control, Turner syndrome	0.246	0.33948	0.502	0.169	0.352
Optic radiation, right						
	Female control, Male control	0.0001	0.00092	0.001	0.005	0.048
	Female control, Turner syndrome	0.072	0.1461176	0.065	0.013	0.188
	Male control, Turner syndrome	0.806	0.8239111	0.55	0.928	0.528
Superior longitudinal fasciculus, left						
	Female control, Male control	0.099	0.1774286	0.068	0.31	0.654
	Female control, Turner syndrome	0.585	0.625814	0.427	0.515	0.296
	Male control, Turner syndrome	0.092	0.1715676	0.212	0.077	0.205
Uncinate, left						
	Female control, Male control	0.197	0.2952903	0.14	0.45	0.136

Table B.1 (cont'd)

	Female control, Turner syndrome	0.25	0.3415842	0.177	0.763	0.154
	Male control, Turner syndrome	0.077	0.1518	0.057	0.067	0.182
Uncinate, right						
	Female control, Male control	0.13	0.2214815	0.027	0.669	0.039
	Female control, Turner syndrome	0.21	0.3082979	0.094	0.471	0.202
	Male control, Turner syndrome	0.332	0.4066726	0.231	0.443	0.467

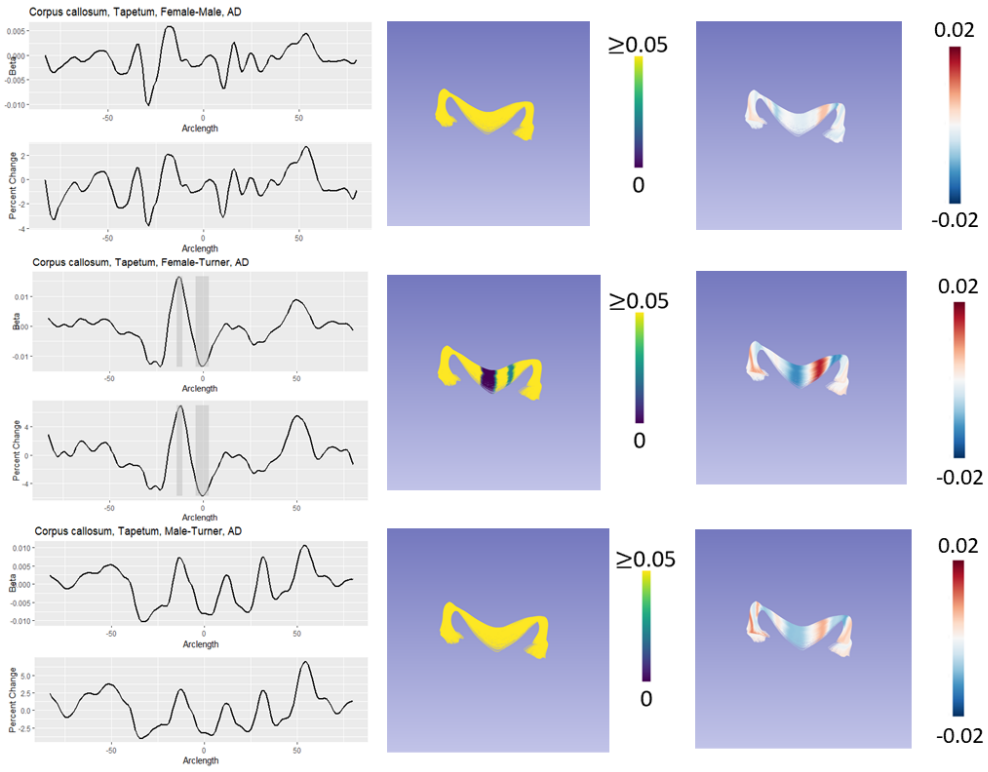

Figure B.1 Model of DTI results for the tapetum portion of the corpus callosum for measures of axial diffusivity. In each panel, the leftmost graph shows the beta value over the arclength of the fasciculus, with areas of local statistical significance highlighted in grey. Below that is the percent change in the beta value over time for that tract in the specified comparison for the specific diffusivity measure. The middlemost image in each panel shows an overlay of the p-values on the fasciculus, with regions of statistical significance showing a color other than yellow. Finally, the rightmost panel shows the beta values from the specific comparison with the model of the tract.

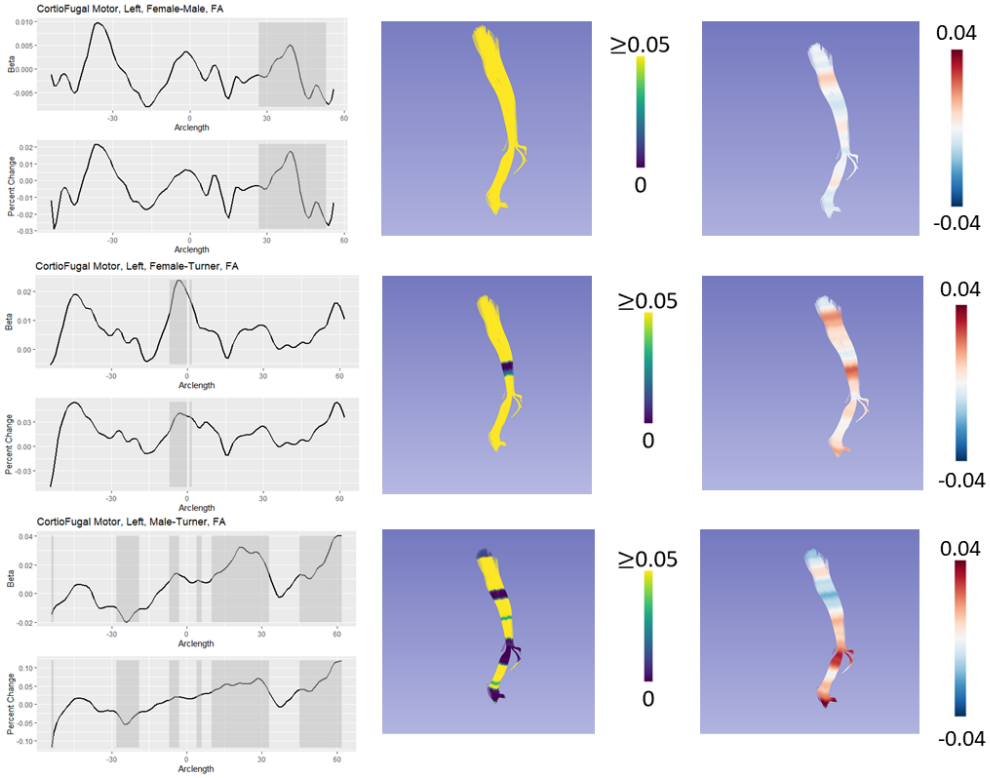

Figure B.2 Model of DTI results for the left corticofugal tract for measures of fractional anisotropy. In each panel, the leftmost graph shows the beta value over the arclength of the fasciculus, with areas of local statistical significance highlighted in grey. Below that is the percent change in the beta value over time for that tract in the specified comparison for the specific diffusivity measure. The middlemost image in each panel shows an overlay of the p-values on the fasciculus, with regions of statistical significance showing a color other than yellow. Finally, the rightmost panel shows the beta values from the specific comparison with the model of the tract.

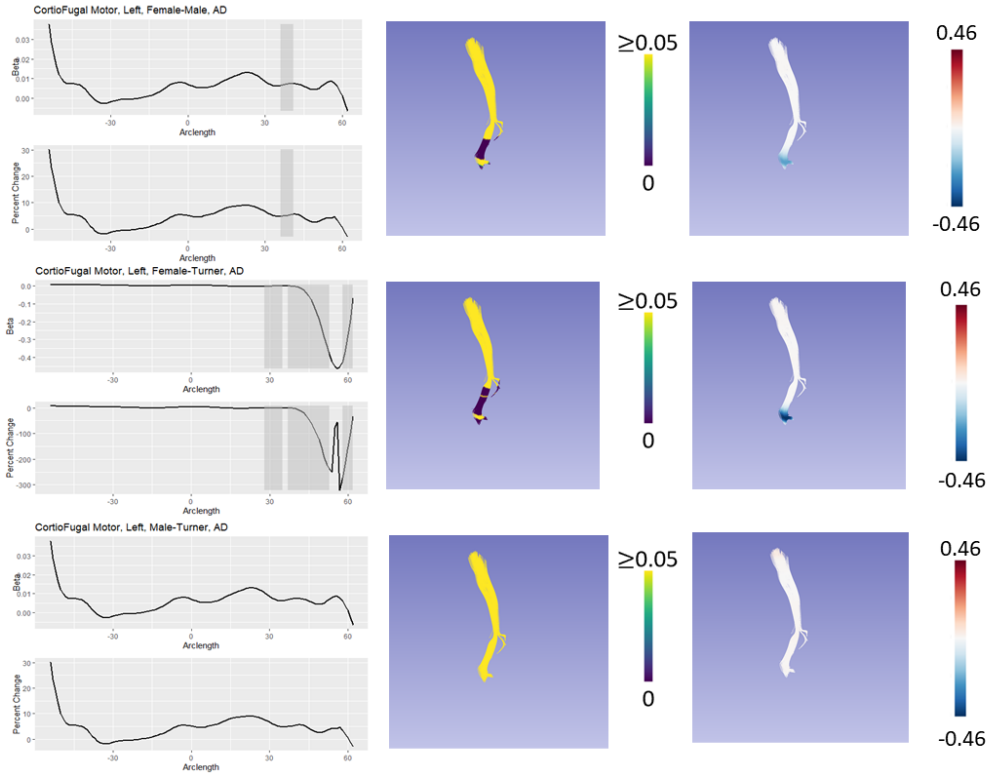

Figure B.3 Model of DTI results for the left motor corticofugal tract for measures of axial diffusivity. In each panel, the leftmost graph shows the beta value over the arclength of the fasciculus, with areas of local statistical significance highlighted in grey. Below that is the percent change in the beta value over time for that tract in the specified comparison for the specific diffusivity measure. The middlemost image in each panel shows an overlay of the p-values on the fasciculus, with regions of statistical significance showing a color other than yellow. Finally, the rightmost panel shows the beta values from the specific comparison with the model of the tract.

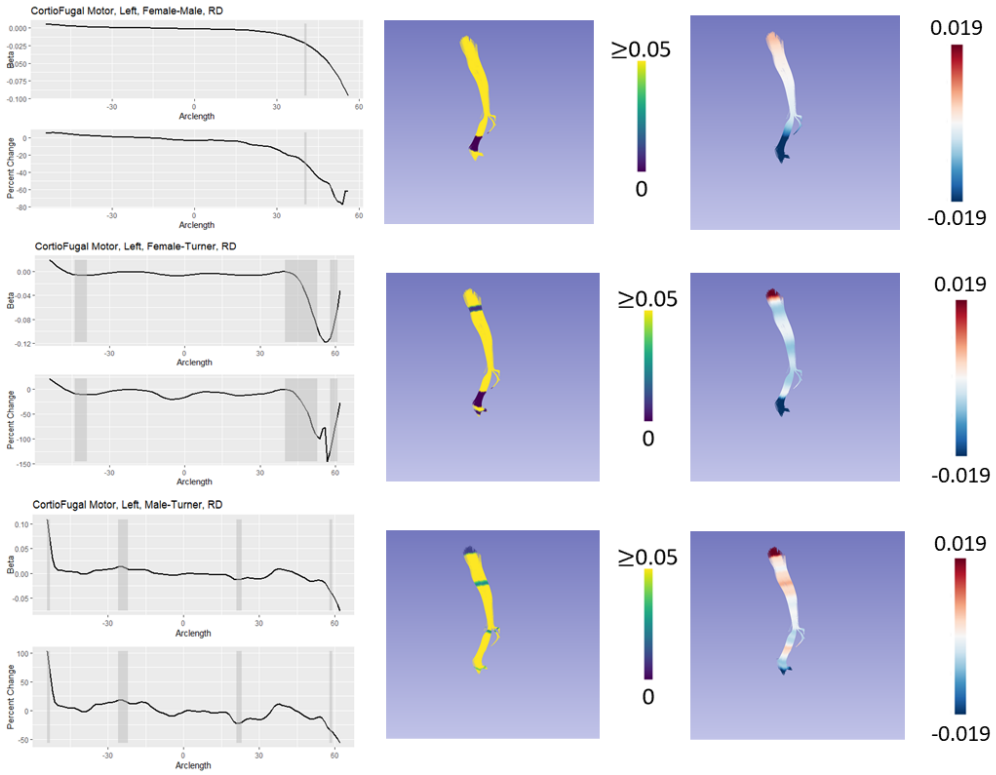

Figure B.4 Model of DTI results for the left motor corticofugal tract for measures of radial diffusivity. In each panel, the leftmost graph shows the beta value over the arclength of the fasciculus, with areas of local statistical significance highlighted in grey. Below that is the percent change in the beta value over time for that tract in the specified comparison for the specific diffusivity measure. The middlemost image in each panel shows an overlay of the p-values on the fasciculus, with regions of statistical significance showing a color other than yellow. Finally, the rightmost panel shows the beta values from the specific comparison with the model of the tract.

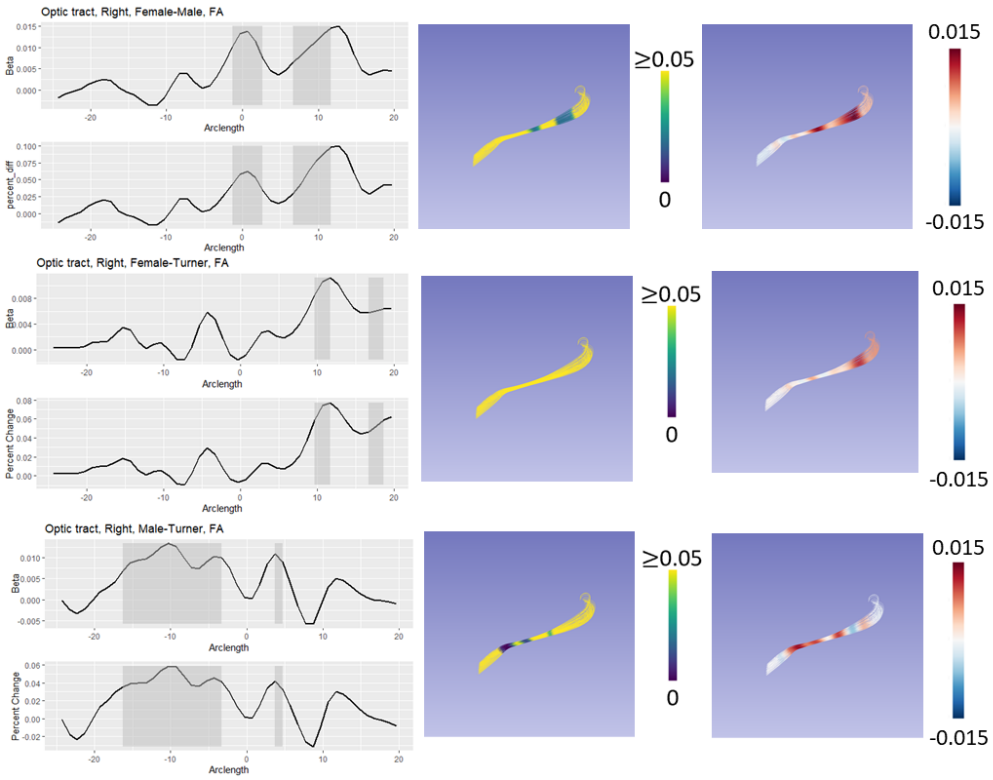

Figure B.5 Model of DTI results for the right optic tract for measures of fractional anisotropy. In each panel, the leftmost graph shows the beta value over the arclength of the fasciculus, with areas of local statistical significance highlighted in grey. Below that is the percent change in the beta value over time for that tract in the specified comparison for the specific diffusivity measure. The middlemost image in each panel shows an overlay of the p-values on the fasciculus, with regions of statistical significance showing a color other than yellow. Finally, the rightmost panel shows the beta values from the specific comparison with the model of the tract.

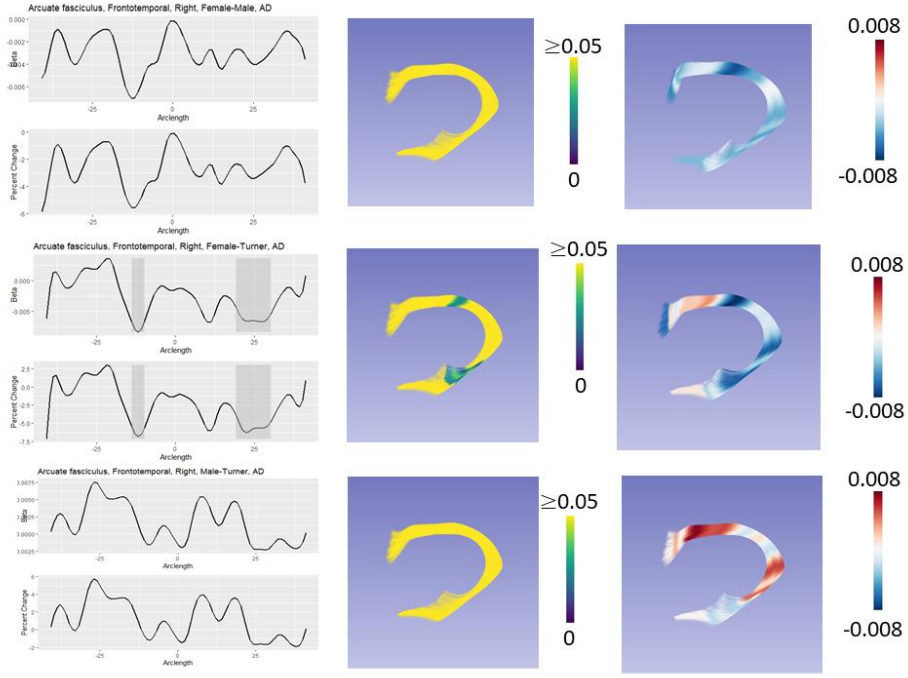

Figure B.6 Model of DTI results for right frontotemporal region of the arcuate fasciculus for measures of axial diffusivity. In each panel, the leftmost graph shows the beta value over the arclength of the fasciculus, with areas of local statistical significance highlighted in grey. Below that is the percent change in the beta value over time for that tract in the specified comparison for the specific diffusivity measure. The middlemost image in each panel shows an overlay of the p-values on the fasciculus, with regions of statistical significance showing a color other than yellow. Finally, the rightmost panel shows the beta values from the specific comparison with the model of the tract.

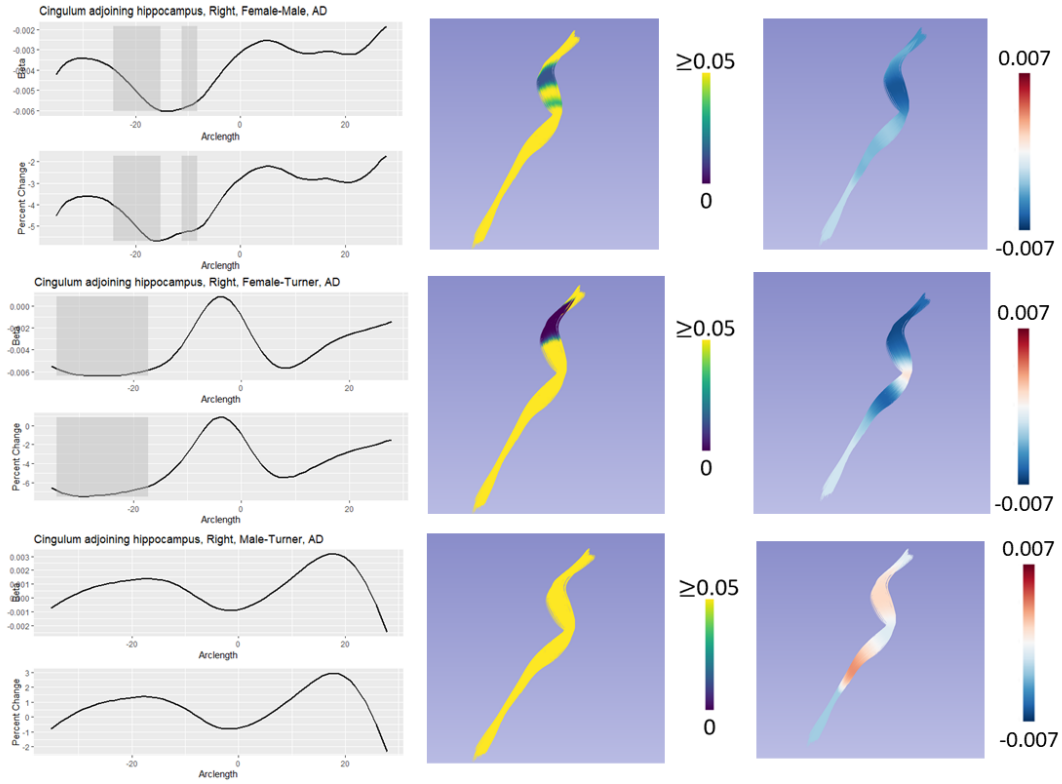

Figure B.7 Model of DTI results for the cingulum adjoining the hippocampus for measures of axial diffusivity. In each panel, the leftmost graph shows the beta value over the arclength of the fasciculus, with areas of local statistical significance highlighted in grey. Below that is the percent change in the beta value over time for that tract in the specified comparison for the specific diffusivity measure. The middlemost image in each panel shows an overlay of the p-values on the fasciculus, with regions of statistical significance showing a color other than yellow. Finally, the rightmost panel shows the beta values from the specific comparison with the model of the tract.

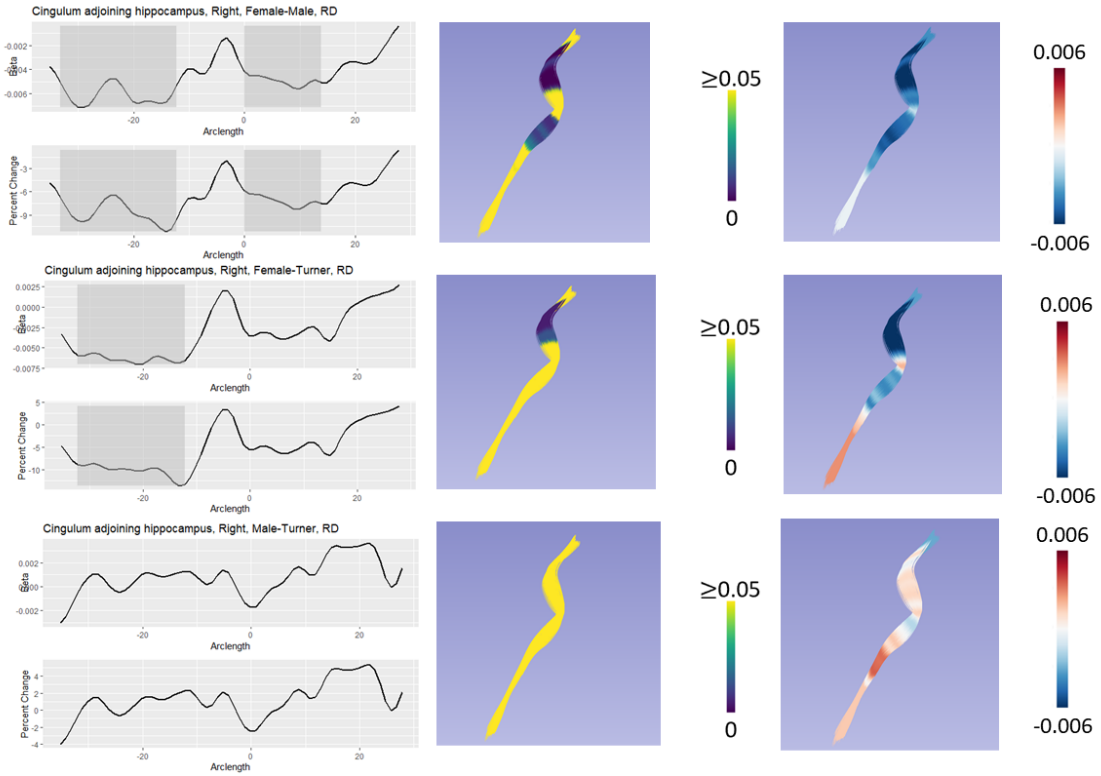

Figure B.8 Model of DTI results for the cingulum adjoining the hippocampus for measures of radial diffusivity. In each panel, the leftmost graph shows the beta value over the arclength of the fasciculus, with areas of local statistical significance highlighted in grey. Below that is the percent change in the beta value over time for that tract in the specified comparison for the specific diffusivity measure. The middlemost image in each panel shows an overlay of the p-values on the fasciculus, with regions of statistical significance showing a color other than yellow. Finally, the rightmost panel shows the beta values from the specific comparison with the model of the tract.

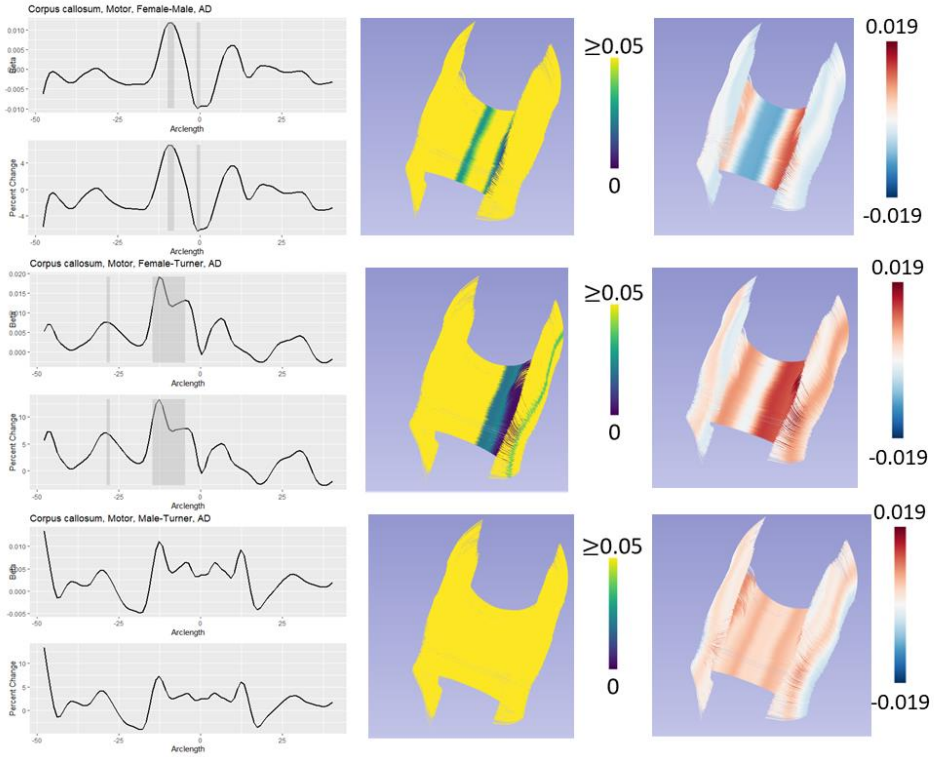

Figure B.9 Model of DTI results for the motor bundle of the corpus callosum for measures of axial diffusivity. In each panel, the leftmost graph shows the beta value over the arclength of the fasciculus, with areas of local statistical significance highlighted in grey. Below that is the percent change in the beta value over time for that tract in the specified comparison for the specific diffusivity measure. The middlemost image in each panel shows an overlay of the p-values on the fasciculus, with regions of statistical significance showing a color other than yellow. Finally, the rightmost panel shows the beta values from the specific comparison with the model of the tract.

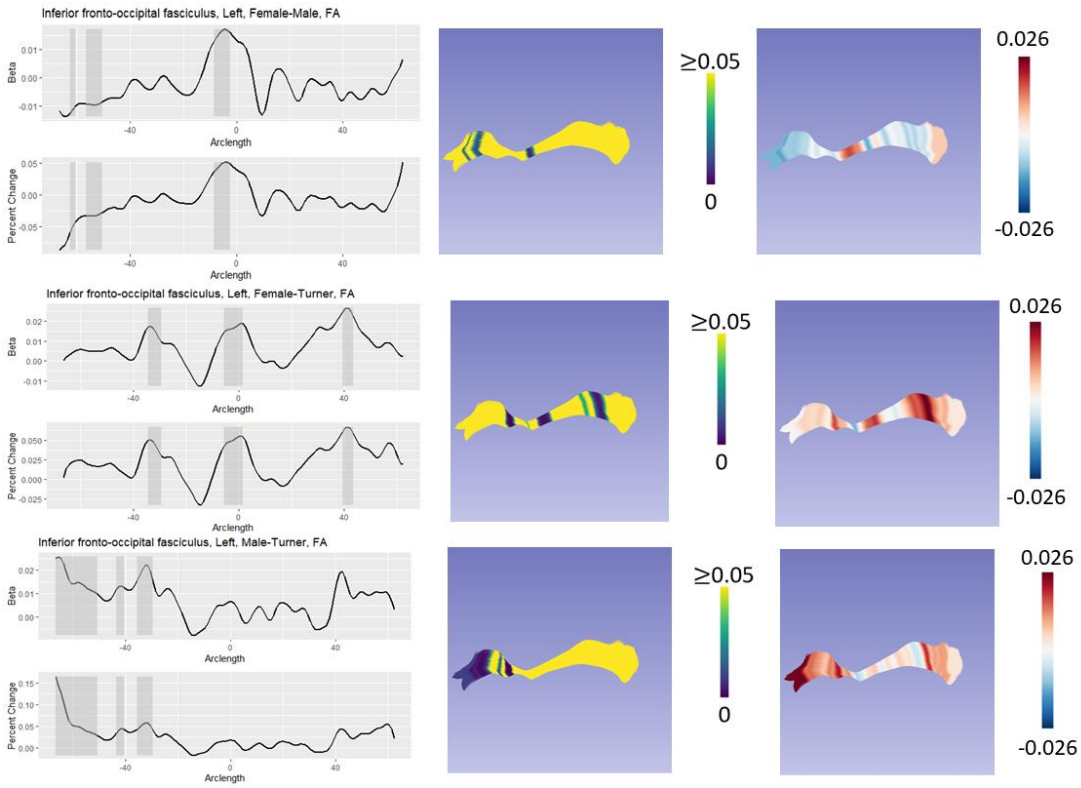

Figure B.10 Model of DTI results for the left inferior fronto-occipital fasciculus for measures of fractional anisotropy. In each panel, the leftmost graph shows the beta value over the arclength of the fasciculus, with areas of local statistical significance highlighted in grey. Below that is the percent change in the beta value over time for that tract in the specified comparison for the specific diffusivity measure. The middlemost image in each panel shows an overlay of the p-values on the fasciculus, with regions of statistical significance showing a color other than yellow. Finally, the rightmost panel shows the beta values from the specific comparison with the model of the tract.

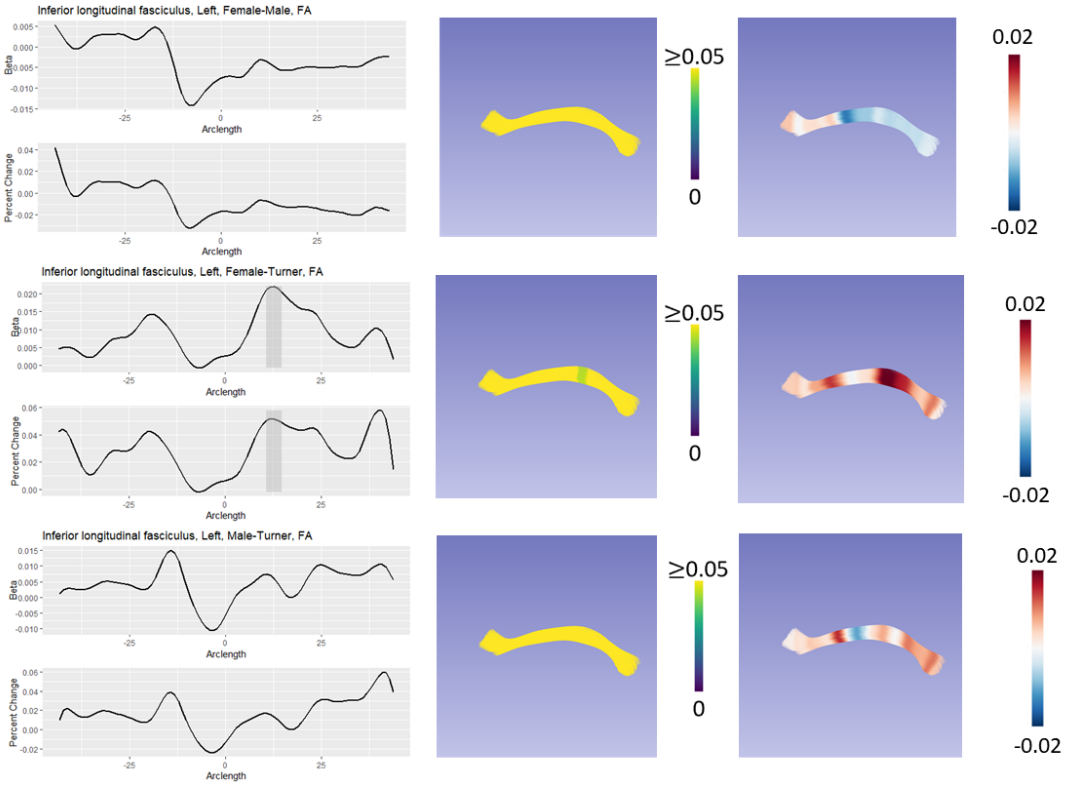

Figure B.11 Model of DTI results for the inferior longitudinal fasciculus for measures of fractional anisotropy. In each panel, the leftmost graph shows the beta value over the arclength of the fasciculus, with areas of local statistical significance highlighted in grey. Below that is the percent change in the beta value over time for that tract in the specified comparison for the specific diffusivity measure. The middlemost image in each panel shows an overlay of the p-values on the fasciculus, with regions of statistical significance showing a color other than yellow. Finally, the rightmost panel shows the beta values from the specific comparison with the model of the tract.

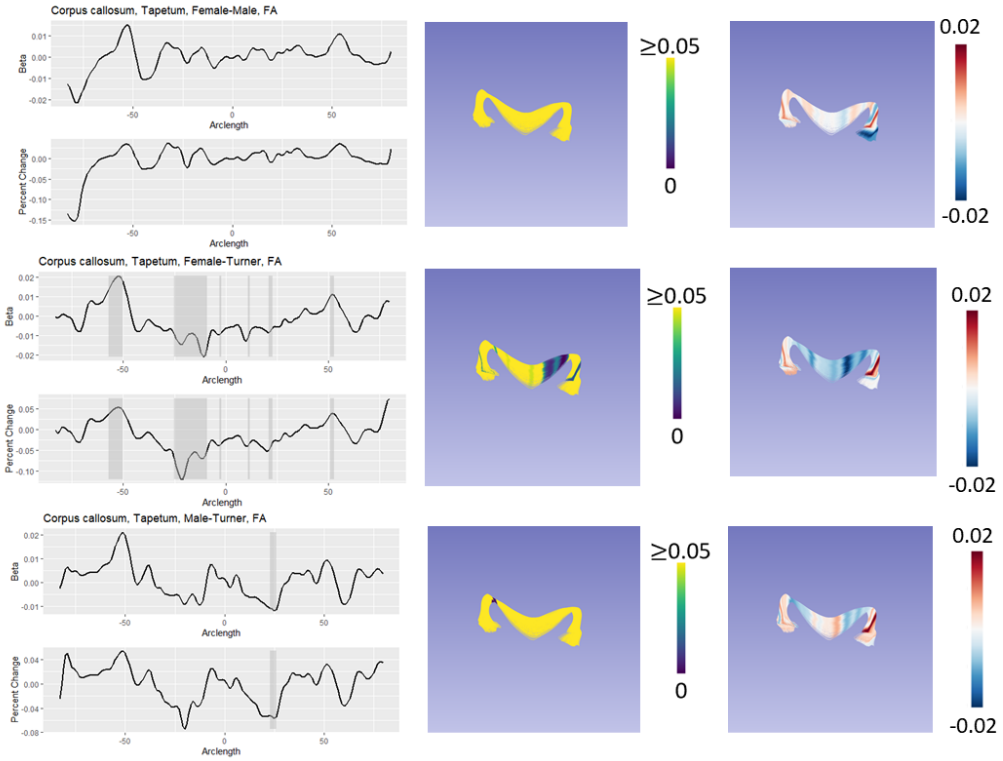

Figure B.12 Model of DTI results for the tapetum region of the corpus callosum for measures of fractional anisotropy. In each panel, the leftmost graph shows the beta value over the arclength of the fasciculus, with areas of local statistical significance highlighted in grey. Below that is the percent change in the beta value over time for that tract in the specified comparison for the specific diffusivity measure. The middlemost image in each panel shows an overlay of the p-values on the fasciculus, with regions of statistical significance showing a color other than yellow. Finally, the rightmost panel shows the beta values from the specific comparison with the model of the tract.

APPENDIX C:

Supplemental data for Chapter 4

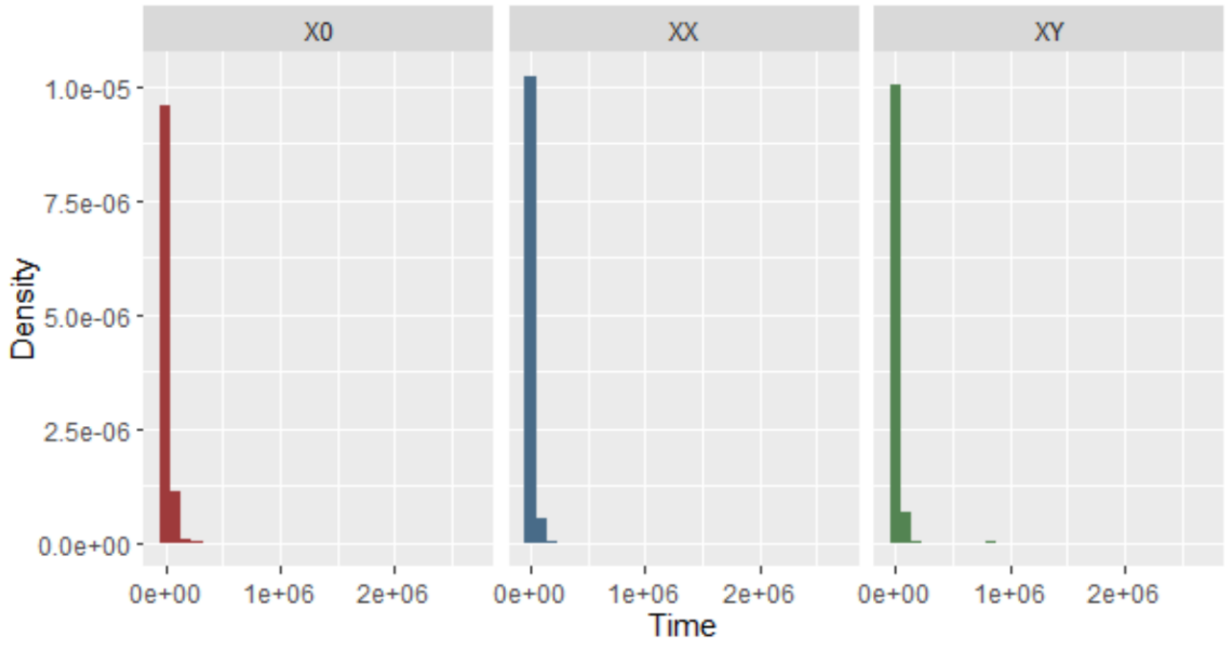

Figure C.1 Density plot of reaction time in milliseconds for the Mental Rotation Task between the three groups.

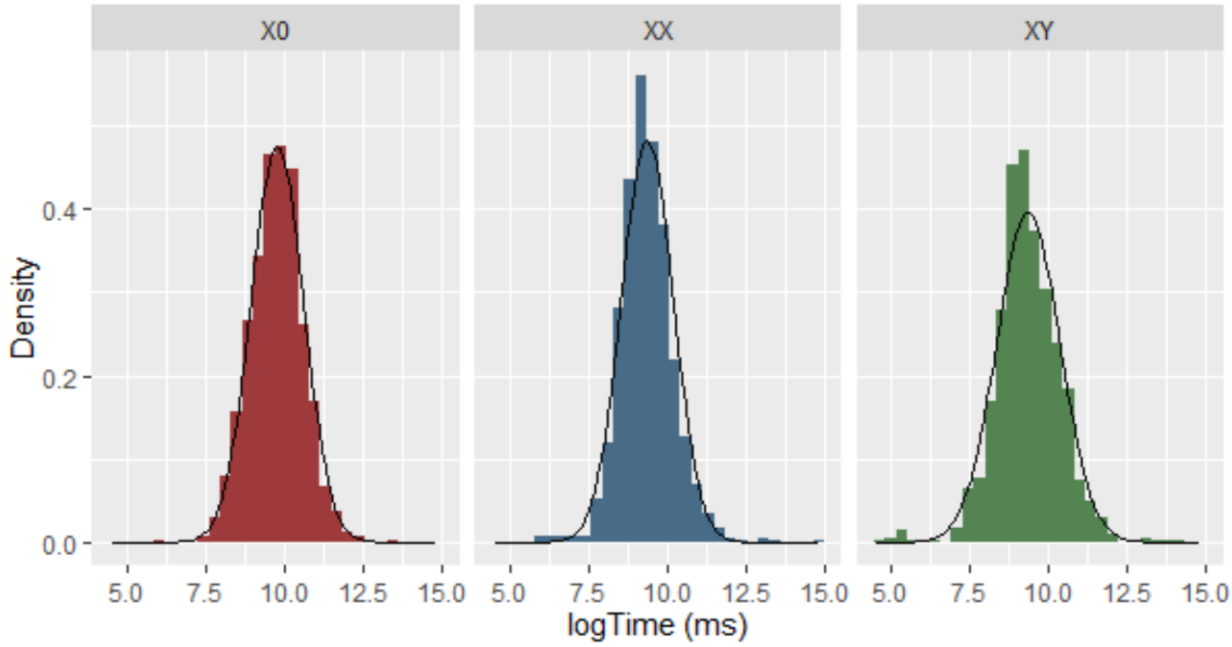

Figure C.2 Density plot of reaction time in milliseconds after log transformation for the Mental Rotation Task between the three groups.

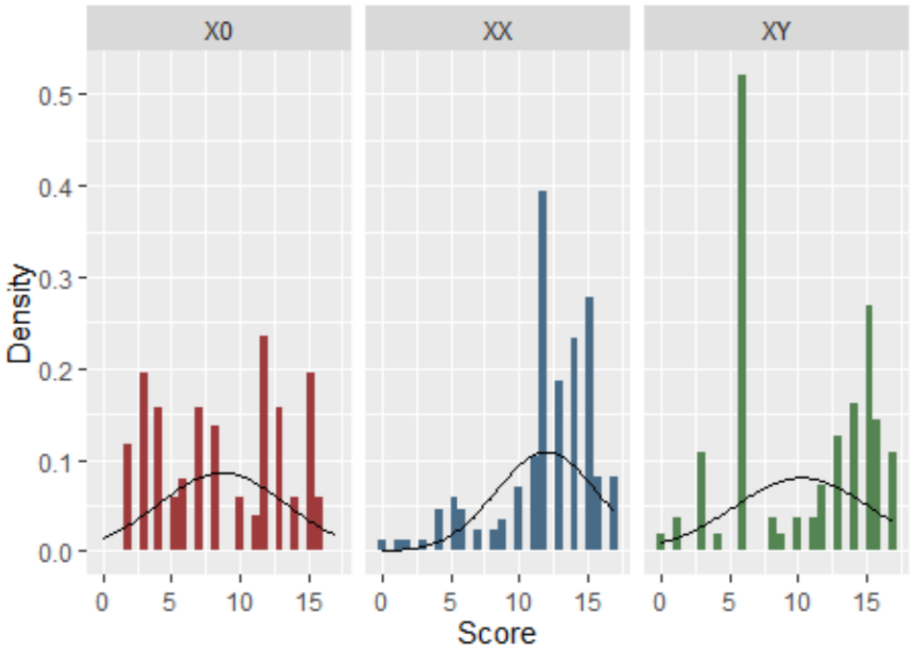

Figure C.3 Density plot of accuracy for the Mental Rotation Task between the three groups.

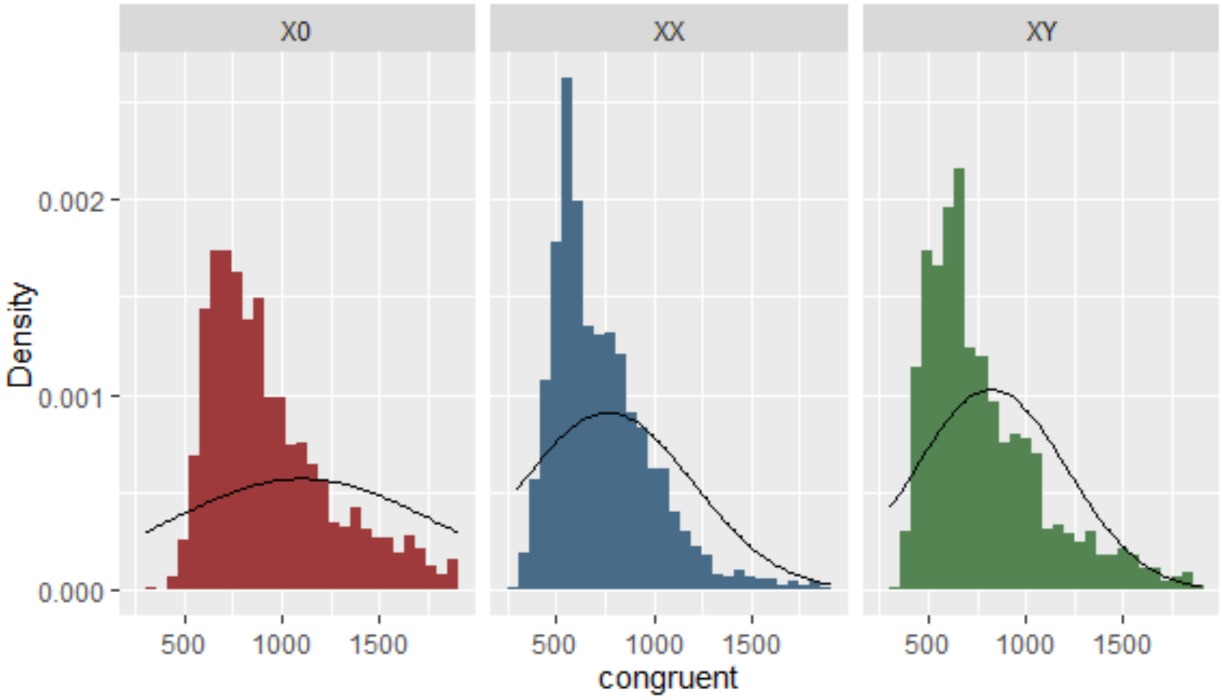

Figure C.4 Density plot of reaction time (ms) for the Flanker Task for congruent responses between the three groups.

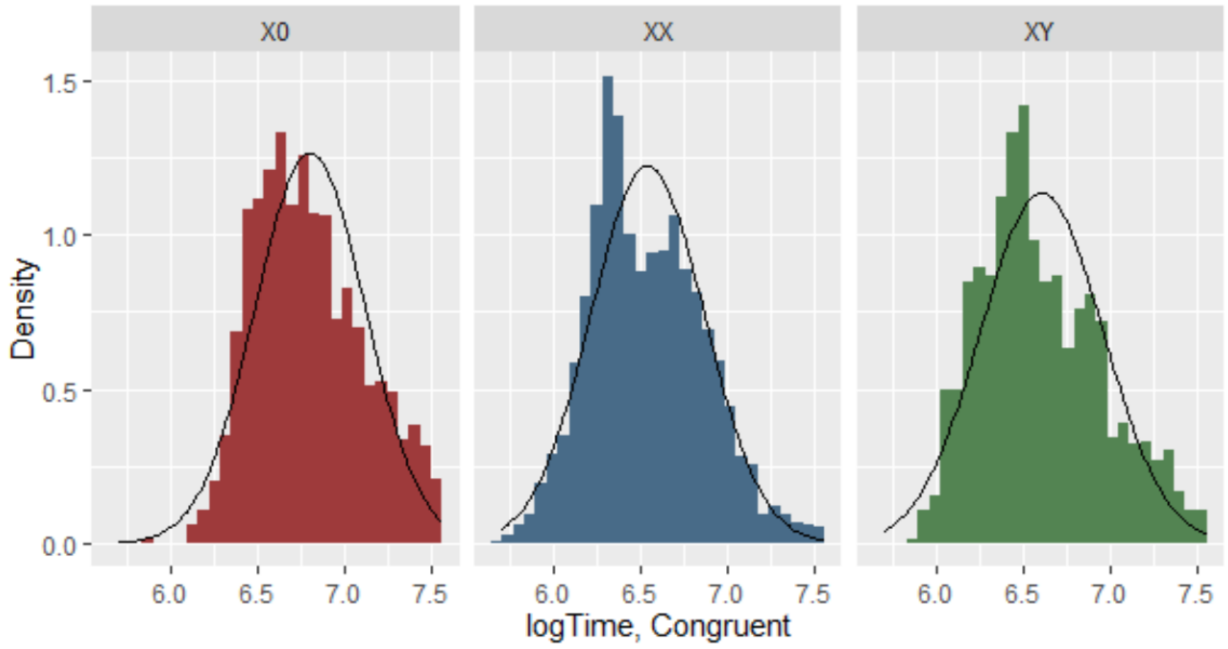

Figure C.5 Density plot of reaction time (ms) after log transformation for congruent responses for the Flanker Task between the three groups.

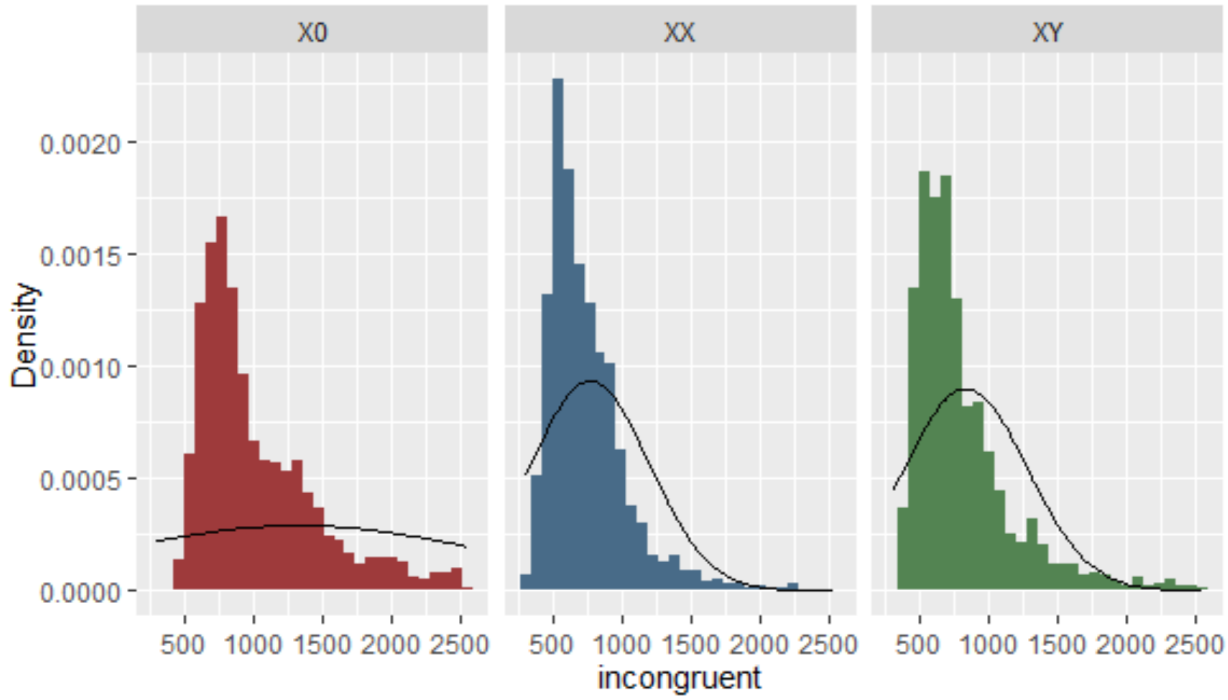

Figure C.6 Density plot of reaction time (ms) for the Flanker Task for incongruent responses between the three groups.

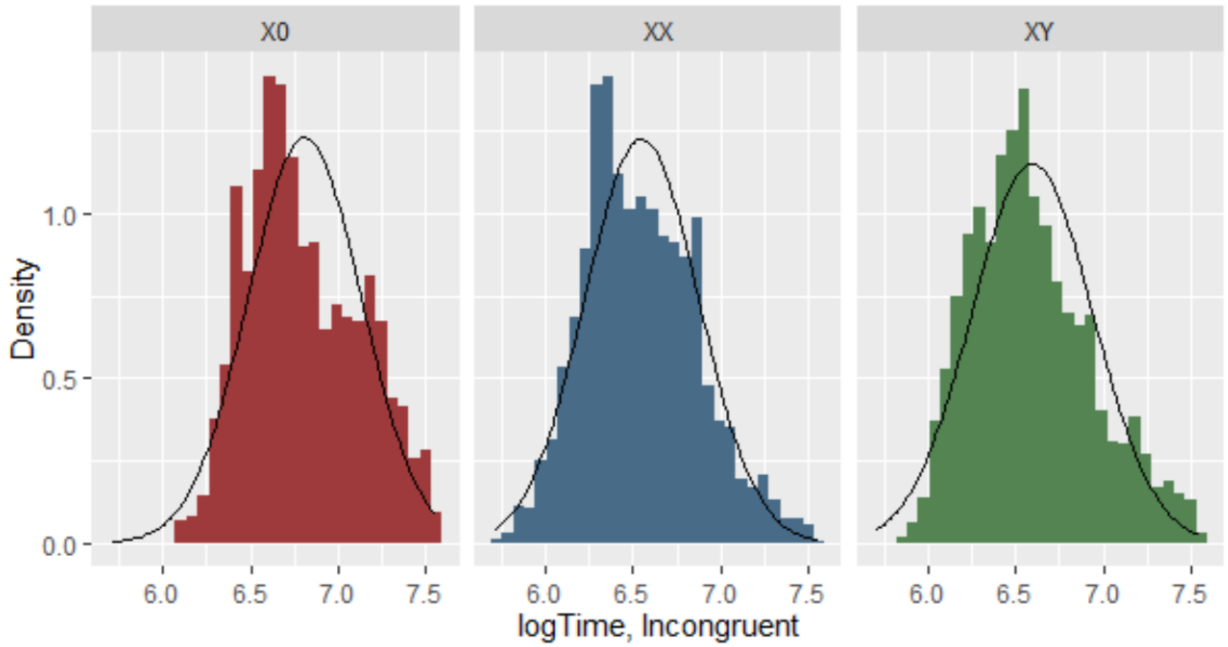

Figure C.7 Density plot of reaction time (ms) after log transformation for incongruent responses for the Flanker Task between the three groups.

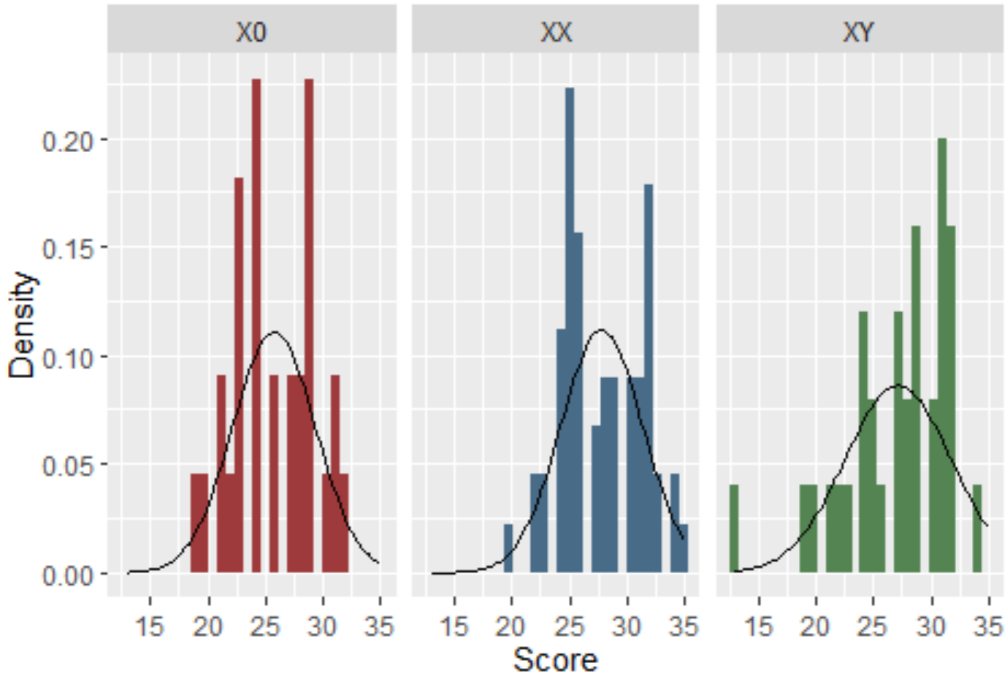

Figure C.8 Density plot of accuracy for Reading the Mind in the Eyes between the three groups.

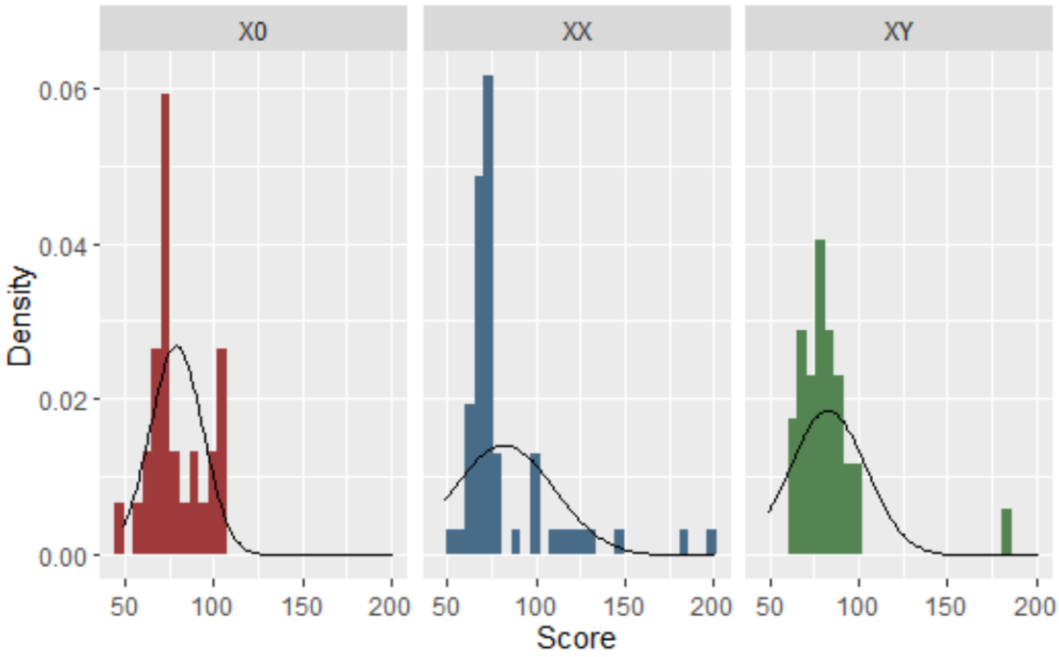

Figure C.9 Density plot of accuracy for the Continuous Performance Task between the three groups before outlier removal.

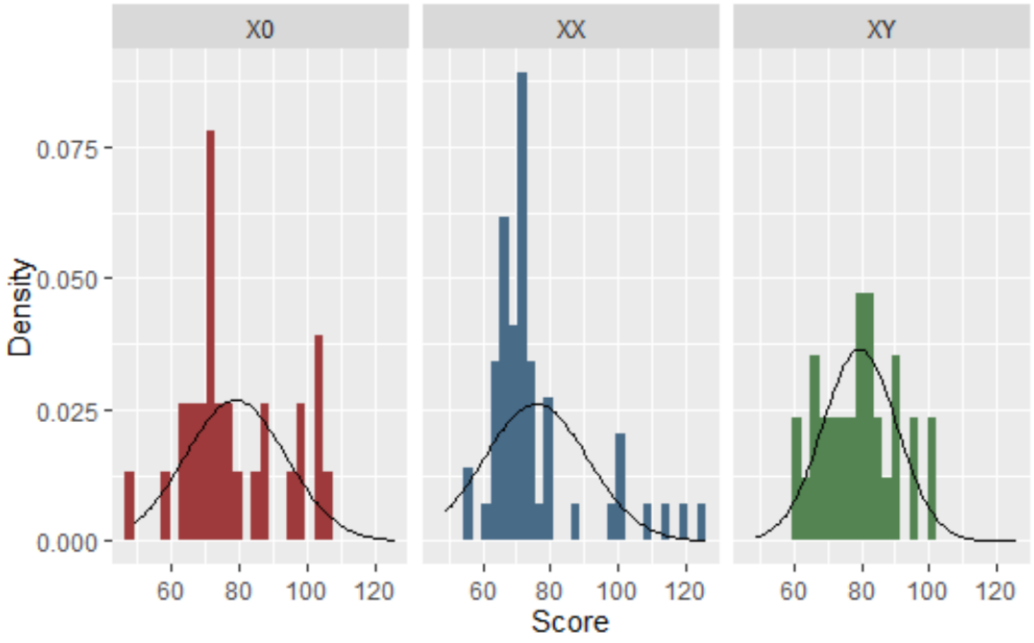

Figure C.10 Density plot of accuracy for the Continuous Performance Task between the three groups after outlier removal.

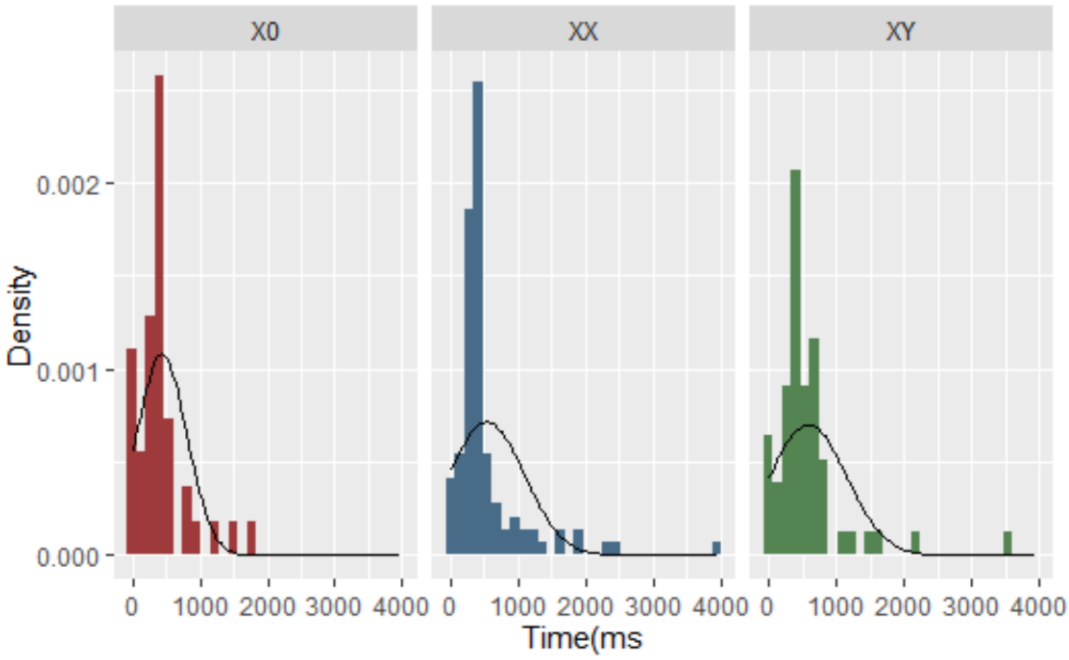

Figure C.11 Density plot of reaction time (ms) for the Continuous Performance Task between the three groups before outlier removal.

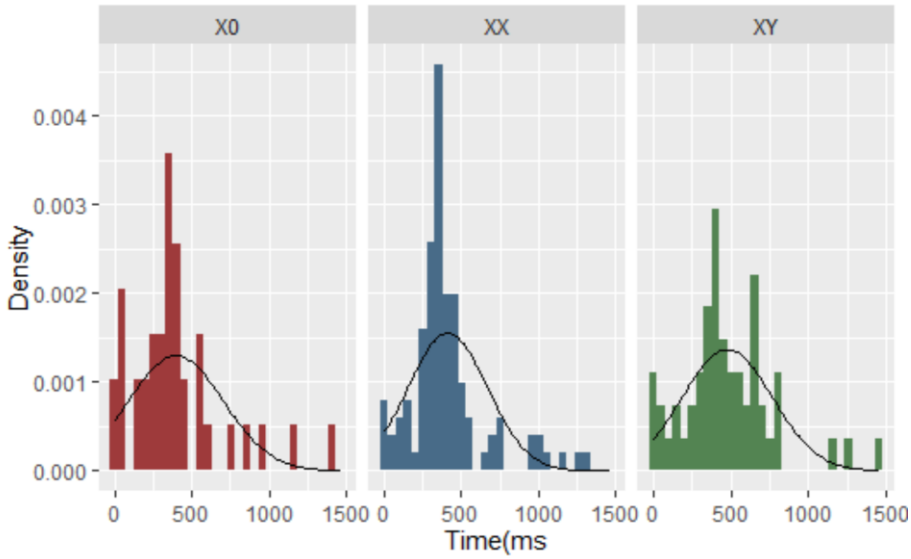

Figure C.12 Density plot of reaction time (ms) for the Continuous Performance Task between the three groups after outlier removal.

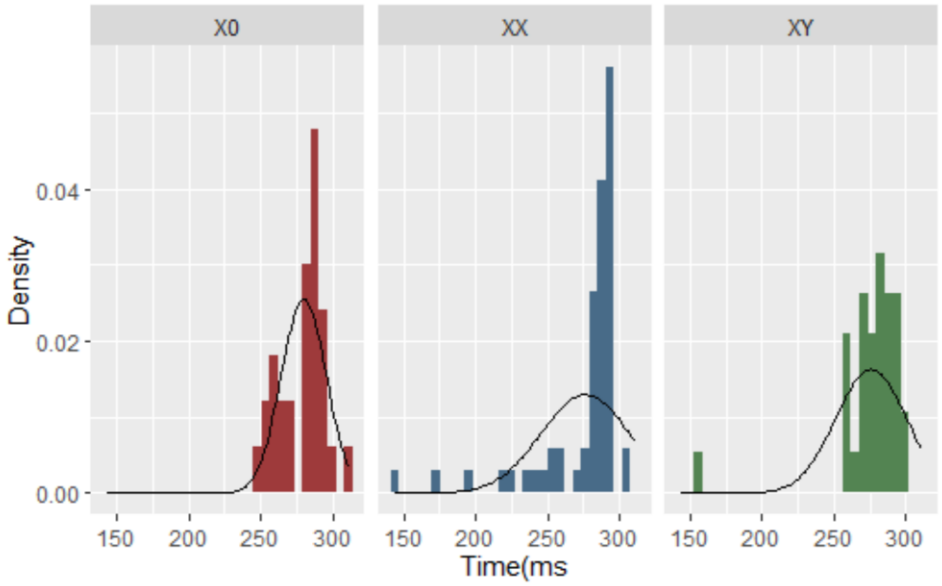

Figure C.13 Density plot of reaction time (ms) for the Continuous Performance Task for errors of commission between the three groups before outlier removal.

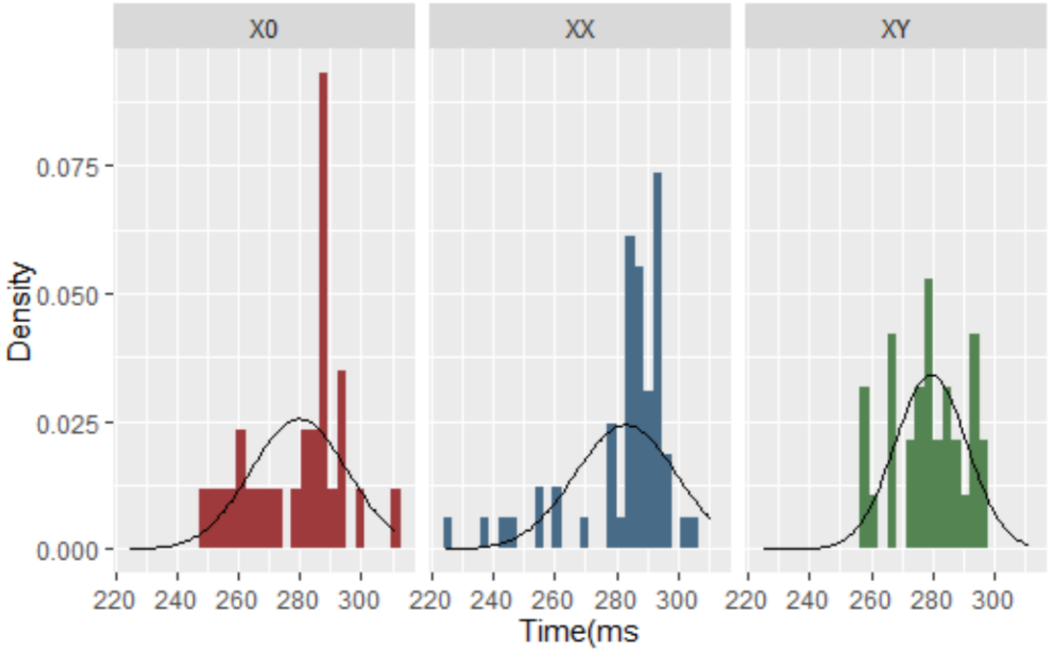

Figure C.14 Density plot of reaction time (ms) for the Continuous Performance Task for errors of commission between the three groups after outlier removal.

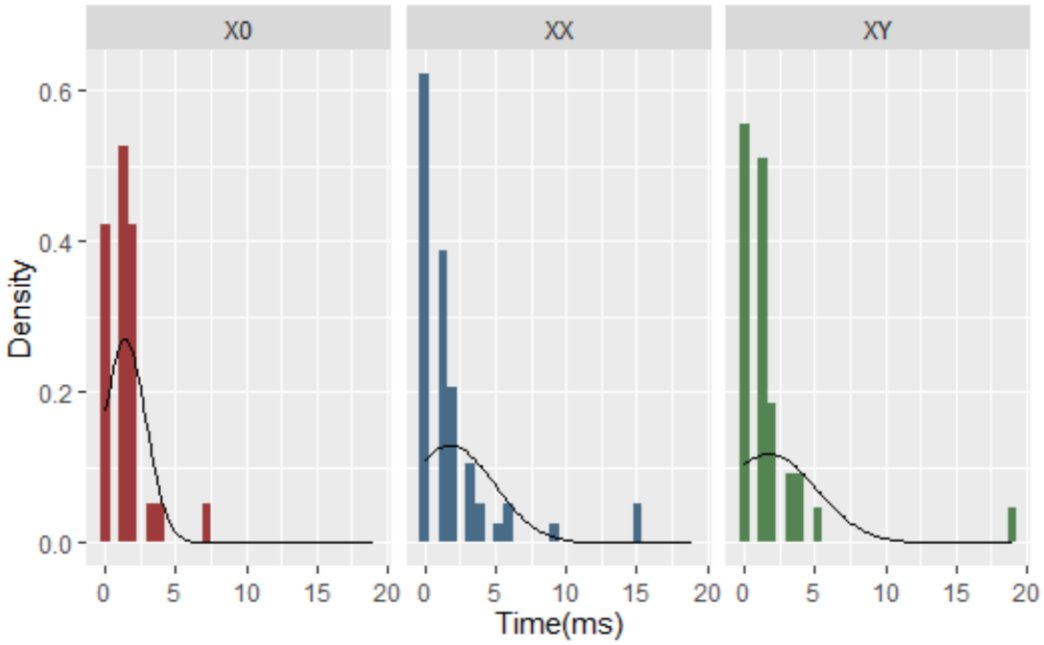

Figure C.15 Density plot of reaction time (ms) for the Continuous Performance Task for errors of omission between the three groups before outlier removal.

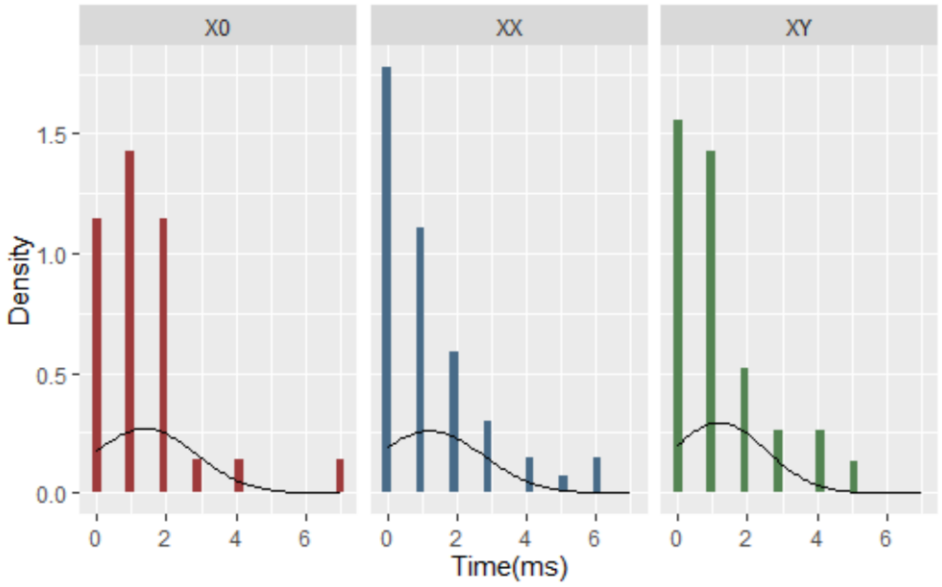

Figure C.16 Density plot of reaction time (ms) for the Continuous Performance Task for errors of omission between the three groups after outlier removal.

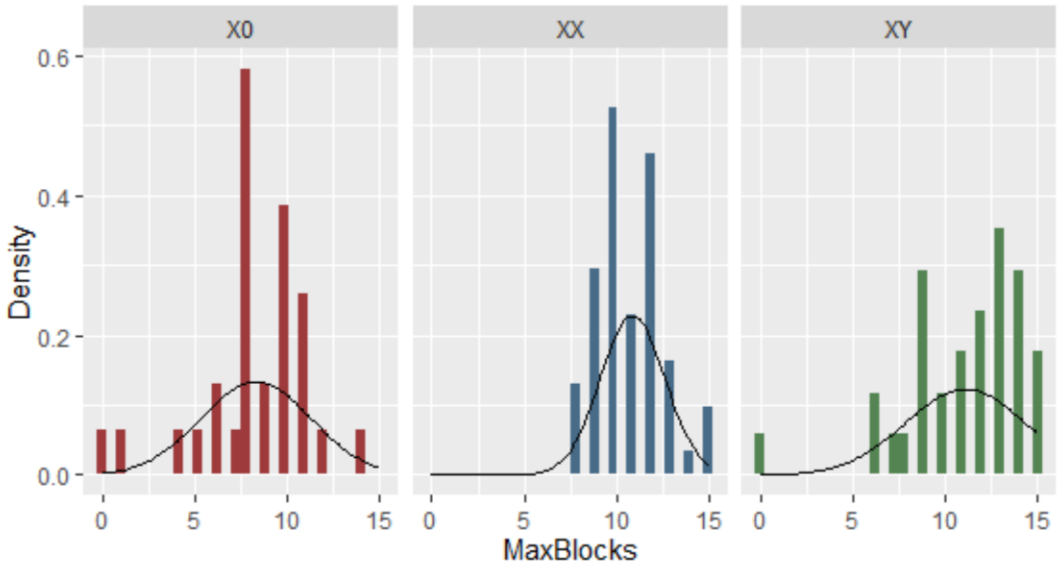

Figure C.17 Density plot of the maximum blocks repeated for the Corsi Block Task between the three groups before outlier removal.

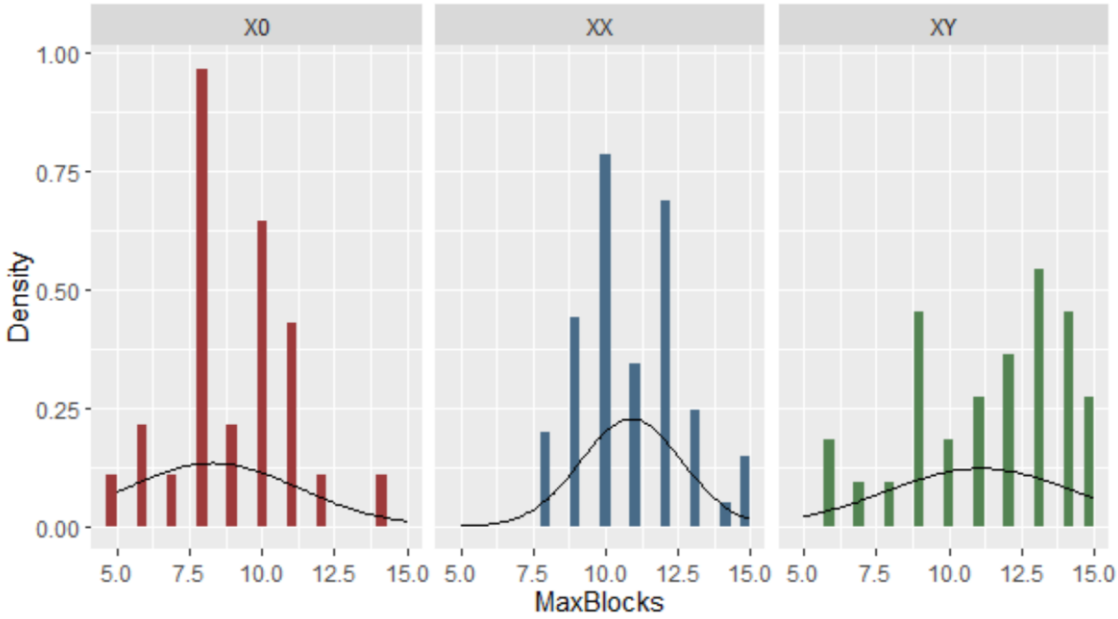

Figure C.18 Density plot of the maximum blocks repeated for the Corsi Block Task between the three groups after outlier removal.

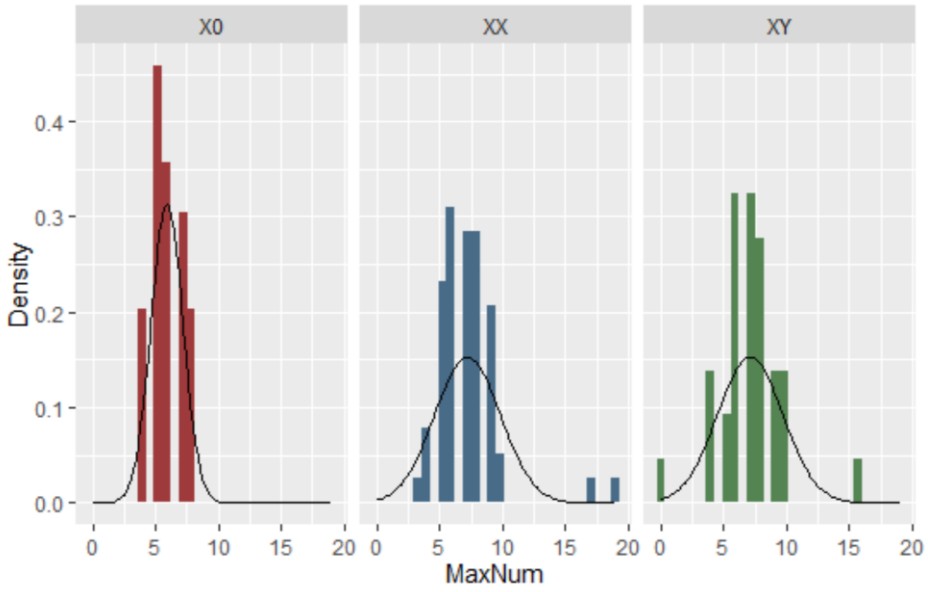

Figure C.19 Density plot of the maximum number length repeated for the Corsi Block Task between the three groups.

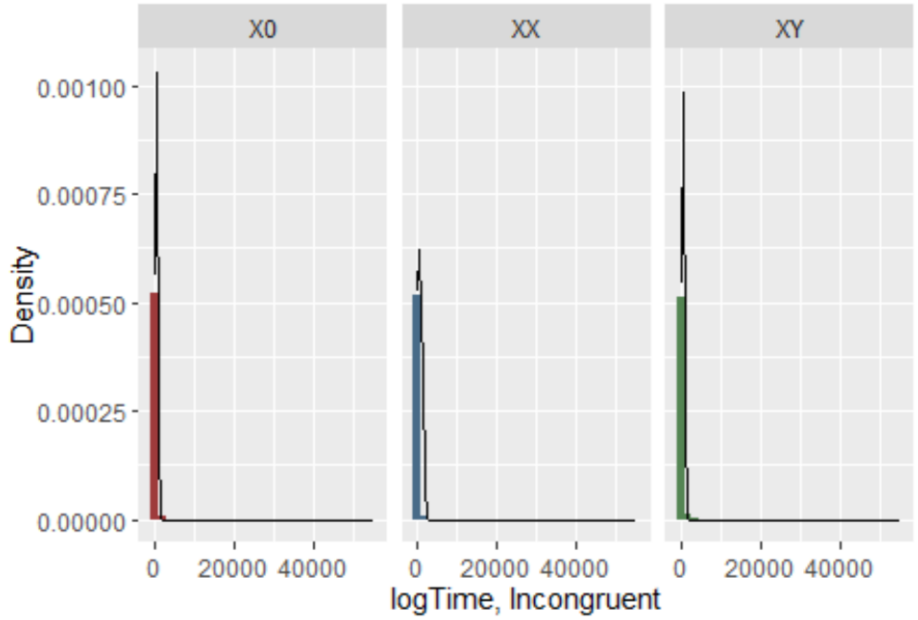

Figure C. 20 Density plot of the reaction time in milliseconds on the Simple Response Time Task between the three groups before log transformation.

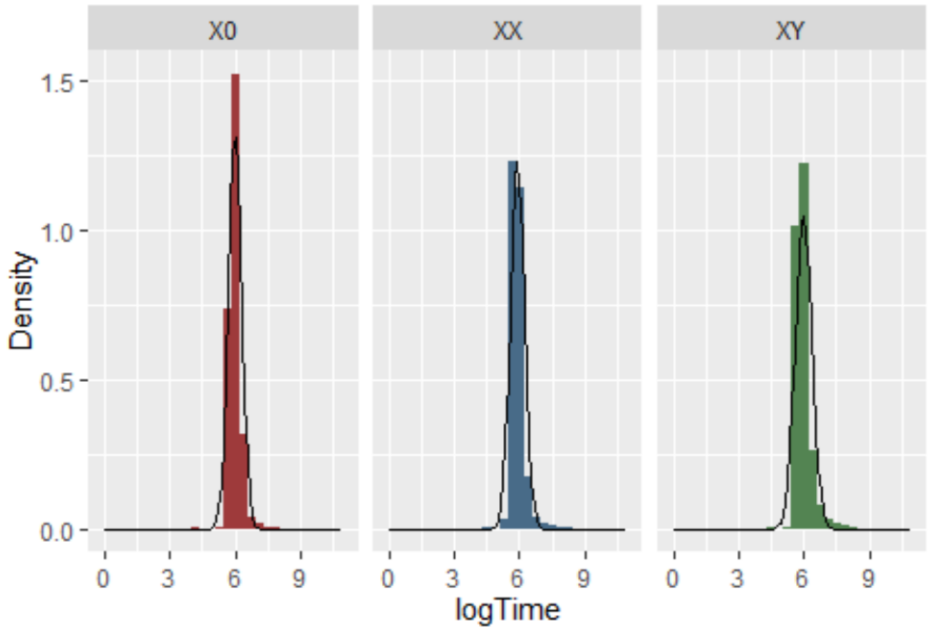

Figure C.21 Density plot of the reaction time in milliseconds on the Simple Response Time Task between the three groups after log transformation.

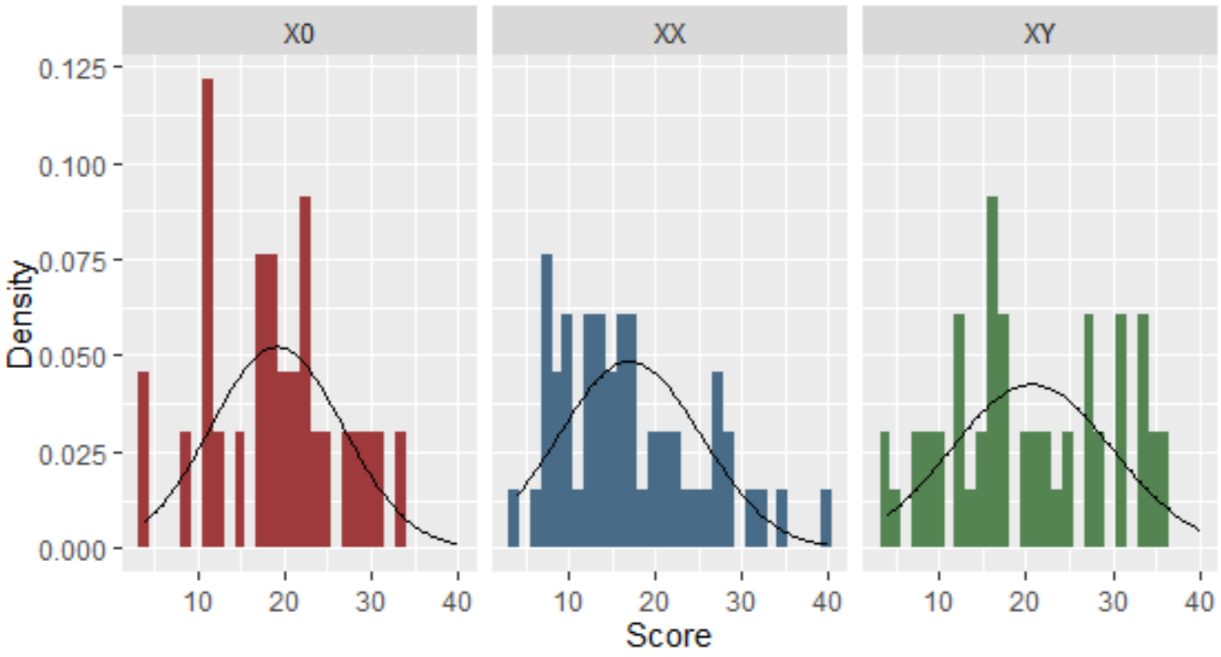

Figure C.22 Density plot of the accuracy on the Autism Spectrum Quotient between the three groups.

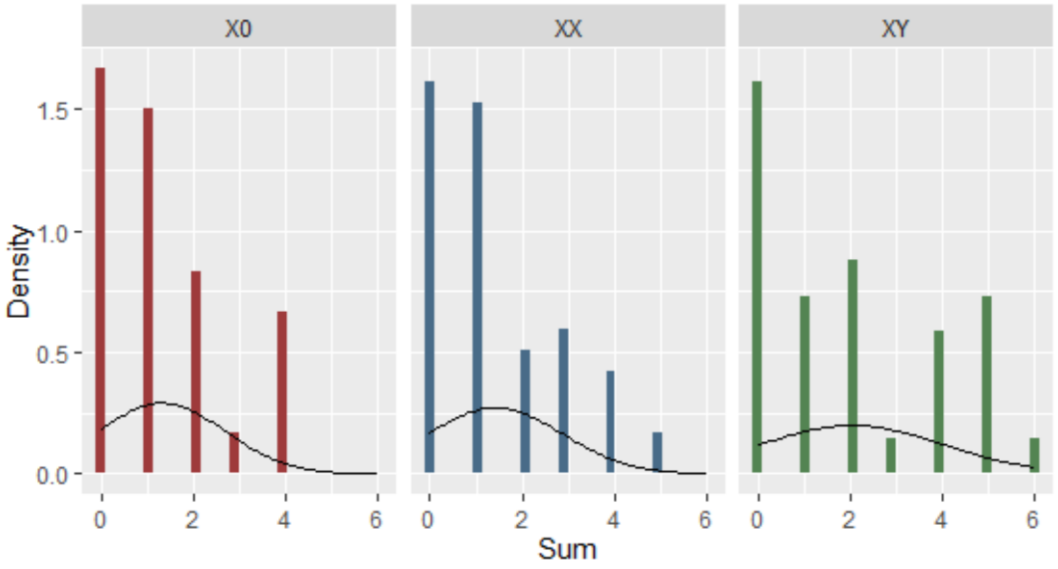

Figure C.23 Density plot of the score on the ADHD report scale between the three groups before outlier removal.

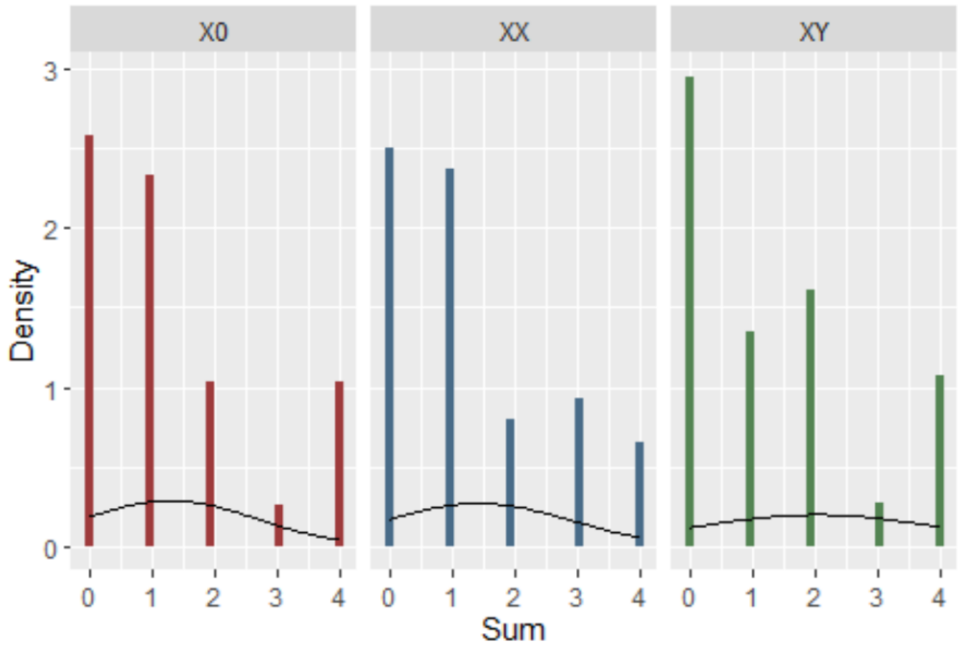

Figure C.24 Density plot of the score on the ADHD report scale between the three groups after outlier removal.

REFERENCES

REFERENCES

1. Logothetis, N. K. The neural basis of the blood-oxygen-level-dependent functional magnetic resonance imaging signal. *Philos Trans R Soc Lond B Biol Sci* **357**, 1003–1037 (2002).

2. Biswal, B., Yetkin, F. Z., Haughton, V. M. & Hyde, J. S. Functional connectivity in the motor cortex of resting human brain using echo-planar MRI. *Magn Reson Med* **34**, 537–541 (1995).

3. Biswal, B. B., Kylen, J. V. & Hyde, J. S. Simultaneous assessment of flow and BOLD signals in resting-state functional connectivity maps. *NMR in Biomedicine* **10**, 165–170 (1997).

4. Raichle, M. E. *et al.* A default mode of brain function. *Proc Natl Acad Sci U S A* **98**, 676–682 (2001).

5. Fox, M. D. *et al.* The human brain is intrinsically organized into dynamic, anticorrelated functional networks. *Proceedings of the National Academy of Sciences* **102**, 9673–9678 (2005).

6. Bzdok, D. *et al.* Characterization of the temporo-parietal junction by combining data-driven parcellation, complementary connectivity analyses, and functional decoding. *NeuroImage* **81**, 381–392 (2013).

7. Spreng, R. N., Mar, R. A. & Kim, A. S. N. The Common Neural Basis of Autobiographical Memory, Prospection, Navigation, Theory of Mind, and the Default Mode: A Quantitative Meta-analysis. *Journal of Cognitive Neuroscience* **21**, 489–510 (2009).

8. Herlin, B., Navarro, V. & Dupont, S. The temporal pole: From anatomy to function—A literature appraisal. *Journal of Chemical Neuroanatomy* **113**, 101925 (2021).

9. Kringelbach, M. L. The human orbitofrontal cortex: linking reward to hedonic experience. *Nat Rev Neurosci* **6**, 691–702 (2005).

10. Marek, S. & Dosenbach, N. U. F. The frontoparietal network: function, electrophysiology, and importance of individual precision mapping. *Dialogues Clin Neurosci* **20**, 133–140 (2018).

11. Vossel, S., Geng, J. J. & Fink, G. R. Dorsal and Ventral Attention Systems. *Neuroscientist* **20**, 150–159 (2014).

12. Le Bihan, D. *et al.* Diffusion tensor imaging: concepts and applications. *J Magn Reson Imaging* **13**, 534–546 (2001).

13. Jütten, K. *et al.* Diffusion Tensor Imaging Reveals Microstructural Heterogeneity of Normal-Appearing White Matter and Related Cognitive Dysfunction in Glioma Patients. *Front. Oncol.* **9**, (2019).

14. Winklewski, P. J. *et al.* Understanding the Physiopathology Behind Axial and Radial Diffusivity Changes—What Do We Know? *Front. Neurol.* **9**, (2018).

15. Ivanova, M. V., Zhong, A., Turken, A., Baldo, J. V. & Dronkers, N. F. Functional Contributions of the Arcuate Fasciculus to Language Processing. *Frontiers in Human Neuroscience* **15**, (2021).

16. Barbey, A. K. *et al.* An integrative architecture for general intelligence and executive function revealed by lesion mapping. *Brain* **135**, 1154–1164 (2012).

17. De Benedictis, A., Efisio Marras, C., Petit, L. & Sarubbo, S. The inferior fronto-occipital fascicle: a century of controversies from anatomy theaters to operative neurosurgery. *Journal of Neurosurgical Sciences* (2021).

18. Koshiyama, D. *et al.* Association between the superior longitudinal fasciculus and perceptual organization and working memory: A diffusion tensor imaging study. *Neuroscience Letters* **738**, 135349 (2020).

19. Urger, S. E. *et al.* The Superior Longitudinal Fasciculus in Typically Developing Children and Adolescents: Diffusion Tensor Imaging and Neuropsychological Correlates. *J Child Neurol* **30**, 9–20 (2015).

20. Herbet, G., Zemmoura, I. & Duffau, H. Functional Anatomy of the Inferior Longitudinal Fasciculus: From Historical Reports to Current Hypotheses. *Front. Neuroanat.* **0**, (2018).

21. Bubb, E. J., Metzler-Baddeley, C. & Aggleton, J. P. The cingulum bundle: Anatomy, function, and dysfunction. *Neurosci Biobehav Rev* **92**, 104–127 (2018).

22. Benear, S. L., Ngo, C. T. & Olson, I. R. Dissecting the Fornix in Basic Memory Processes and Neuropsychiatric Disease: A Review. *Brain Connect* **10**, 331–354 (2020).

23. Goldstein, A., Covington, B. P., Mahabadi, N. & Mesfin, F. B. Neuroanatomy, Corpus Callosum. in *StatPearls* (StatPearls Publishing, 2022).

24. Natali, A. L., Reddy, V. & Bordoni, B. Neuroanatomy, Corticospinal Cord Tract. in *StatPearls* (StatPearls Publishing, 2022).

25. Nuñez, A. & Malmierca, E. Corticofugal modulation of sensory information. *Adv Anat Embryol Cell Biol* **187**, 1 p following table of contents, 1–74 (2007).

26. Jang, S. H. & Lee, S. J. Corticoreticular Tract in the Human Brain: A Mini Review. *Frontiers in Neurology* **10**, (2019).

27. Diamond, A. Executive Functions. *Annu Rev Psychol* **64**, 135–168 (2013).

28. Lehto, J. E., Juujarvi, P., Kooistra, L. & Pulkkinen, L. Dimensions of executive functioning: Evidence from children. *The British Journal of Developmental Psychology* **21**, 59 (2003).

29. Eriksen, B. A. & Eriksen, C. W. Effects of noise letters upon the identification of a target letter in a nonsearch task. *Perception & Psychophysics* **16**, 143–149 (1974).

30. Stroop, J. R. Studies of interference in serial verbal reactions. *Journal of Experimental Psychology* **18**, 643–662 (1935).

31. Kessels, R. P., van Zandvoort, M. J., Postma, A., Kappelle, L. J. & de Haan, E. H. The Corsi Block-Tapping Task: standardization and normative data. *Appl Neuropsychol* **7**, 252–258 (2000).

32. Wechsler, D. *The measurement of adult intelligence*. ix, 226 (Williams & Wilkins Co, 1939). doi:10.1037/10020-000.

33. Insel, T. *et al.* Research domain criteria (RDoC): Toward a new classification framework for research on mental disorders. *The American Journal of Psychiatry* **167**, 748–751 (2010).

34. Martel, M., Nikolas, M. & Nigg, J. T. Executive Function in Adolescents With ADHD. *Journal of the American Academy of Child & Adolescent Psychiatry* **46**, 1437–1444 (2007).

35. Holmes, J. *et al.* The Diagnostic Utility of Executive Function Assessments in the Identification of ADHD in Children. *Child and Adolescent Mental Health* **15**, 37–43 (2010).

36. Johnson, J. & Reid, R. Overcoming Executive Function Deficits With Students With ADHD. *Theory Into Practice* **50**, 61–67 (2011).

37. Channon, S. & Green, P. S. S. Executive function in depression: the role of performance strategies in aiding depressed and non-depressed participants. *Journal of Neurology, Neurosurgery & Psychiatry* **66**, 162–171 (1999).

38. Cotrena, C., Branco, L. D., Ponsoni, A., Shansis, F. M. & Fonseca, R. P. Neuropsychological Clustering in Bipolar and Major Depressive Disorder. *Journal of the International Neuropsychological Society* **23**, 584–593 (2017).

39. Velligan, D. I. & Bow-Thomas, C. C. Executive function in schizophrenia. *Semin Clin Neuropsychiatry* **4**, 24–33 (1999).

40. Eisenberg, D. P. & Berman, K. F. Executive Function, Neural Circuitry, and Genetic Mechanisms in Schizophrenia. *Neuropsychopharmacol* **35**, 258–277 (2010).

41. Wobrock, T. *et al.* Cognitive impairment of executive function as a core symptom of schizophrenia. *The World Journal of Biological Psychiatry* **10**, 442–451 (2009).

42. Demetriou, E. A. *et al.* Autism spectrum disorders: a meta-analysis of executive function. *Mol Psychiatry* **23**, 1198–1204 (2018).

43. Demetriou, E. A., DeMayo, M. M. & Guastella, A. J. Executive Function in Autism Spectrum Disorder: History, Theoretical Models, Empirical Findings, and Potential as an Endophenotype. *Front. Psychiatry* **0**, (2019).

44. Johnston, K., Murray, K., Spain, D., Walker, I. & Russell, A. Executive Function: Cognition and Behaviour in Adults with Autism Spectrum Disorders (ASD). *Journal of Autism and Developmental Disorders* **49**, 4181–4192 (2019).

45. Danielson, M. L. *et al.* Prevalence of Parent-Reported ADHD Diagnosis and Associated Treatment Among U.S. Children and Adolescents, 2016. *J Clin Child Adolesc Psychol* **47**, 199–212 (2018).

46. *Diagnostic and statistical manual of mental disorders: DSM-5™, 5th ed*. xliv, 947 (American Psychiatric Publishing, Inc., 2013). doi:10.1176/appi.books.9780890425596.

47. Brown, T. E. ADD/ADHD and impaired executive function in clinical practice. *Curr Atten Disord Rep* **1**, 37–41 (2009).

48. Yuan, P. & Raz, N. Prefrontal Cortex and Executive Functions in Healthy Adults: A Meta-Analysis of Structural Neuroimaging Studies. *Neurosci Biobehav Rev* **0**, 180–192 (2014).

49. Corbetta, M. & Shulman, G. L. Spatial Neglect and Attention Networks. *Annual Review of Neuroscience* **34**, 569–599 (2011).

50. Menon, V. & D'Esposito, M. The role of PFC networks in cognitive control and executive function. *Neuropsychopharmacol.* **47**, 90–103 (2022).

51. Aron, A. R., Robbins, T. W. & Poldrack, R. A. Inhibition and the right inferior frontal cortex: one decade on. *Trends in Cognitive Sciences* **18**, 177–185 (2014).

52. Wallis, G., Stokes, M., Cousijn, H., Woolrich, M. & Nobre, A. C. Frontoparietal and Cingulo-opercular Networks Play Dissociable Roles in Control of Working Memory. *Journal of Cognitive Neuroscience* **27**, 2019–2034 (2015).

53. Todd, J. J., Fougnie, D. & Marois, R. Visual Short-Term Memory Load Suppresses Temporo-Parietal Junction Activity and Induces Inattentional Blindness. *Psychol Sci* **16**, 965–972 (2005).

54. Shulman, G. L. *et al.* Interaction of Stimulus-Driven Reorienting and Expectation in Ventral and Dorsal Frontoparietal and Basal Ganglia-Cortical Networks. *J. Neurosci.* **29**, 4392–4407 (2009).

55. Rapado-Castro, M. *et al.* Fronto-Parietal Gray Matter Volume Loss Is Associated with Decreased Working Memory Performance in Adolescents with a First Episode of Psychosis. *Journal of Clinical Medicine* **10**, 3929 (2021).

56. Haldane, M., Cunningham, G., Androutsos, C. & Frangou, S. Structural brain correlates of response inhibition in Bipolar Disorder I. *J Psychopharmacol* **22**, 138–143 (2008).

57. Collette, F. *et al.* Involvement of both prefrontal and inferior parietal cortex in dual-task performance. *Cognitive Brain Research* **24**, 237–251 (2005).

58. Barch, D. M. & Csernansky, J. G. Abnormal Parietal Cortex Activation During Working Memory in Schizophrenia: Verbal Phonological Coding Disturbances Versus Domain-General Executive Dysfunction. *AJP* **164**, 1090–1098 (2007).

59. Olesen, P. J., Westerberg, H. & Klingberg, T. Increased prefrontal and parietal activity after training of working memory. *Nat Neurosci* **7**, 75–79 (2004).

60. Jubault, T., Ody, C. & Koechlin, E. Serial Organization of Human Behavior in the Inferior Parietal Cortex. *J. Neurosci.* **27**, 11028–11036 (2007).

61. Hahn, B., Robinson, B. M., Leonard, C. J., Luck, S. J. & Gold, J. M. Posterior Parietal Cortex Dysfunction Is Central to Working Memory Storage and Broad Cognitive Deficits in Schizophrenia. *J. Neurosci.* **38**, 8378–8387 (2018).

62. Shomstein, S. Cognitive functions of the posterior parietal cortex: top-down and bottom-up attentional control. *Frontiers in Integrative Neuroscience* **6**, (2012).

63. Esterman, M., Chiu, Y.-C., Tamber-Rosenau, B. J. & Yantis, S. Decoding cognitive control in human parietal cortex. *PNAS* **106**, 17974–17979 (2009).

64. Cole, M. W., Pathak, S. & Schneider, W. Identifying the brain's most globally connected regions. *Neuroimage* **49**, 3132–3148 (2010).

65. Cole, M. W., Yarkoni, T., Repovš, G., Anticevic, A. & Braver, T. S. Global Connectivity of Prefrontal Cortex Predicts Cognitive Control and Intelligence. *J Neurosci* **32**, 8988–8999 (2012).

66. Reineberg, A. E., Andrews-Hanna, J. R., Depue, B. E., Friedman, N. P. & Banich, M. T. Resting-state networks predict individual differences in common and specific aspects of executive function. *NeuroImage* **104**, 69–78 (2015).

67. Cole, M. W. *et al.* Multi-task connectivity reveals flexible hubs for adaptive task control. *Nat. Neurosci.* **16**, 1348–1355 (2013).

68. Anticevic, A. *et al.* The Role of Default Network Deactivation in Cognition and Disease. *Trends Cogn Sci* **16**, 584–592 (2012).

69. Jia, W. *et al.* Disruptions of frontoparietal control network and default mode network linking the metacognitive deficits with clinical symptoms in schizophrenia. *Human Brain Mapping* **41**, 1445–1458 (2020).

70. Schneider, F. C. *et al.* Modulation of the default mode network is task-dependant in chronic schizophrenia patients. *Schizophr Res* **125**, 110–117 (2011).

71. Dreher, J.-C. *et al.* Common and differential pathophysiological features accompany comparable cognitive impairments in medication-free patients with schizophrenia and in healthy aging subjects. *Biol Psychiatry* **71**, 890–897 (2012).

72. Whitfield-Gabrieli, S. *et al.* Hyperactivity and hyperconnectivity of the default network in schizophrenia and in first-degree relatives of persons with schizophrenia. *Proc Natl Acad Sci U S A* **106**, 1279–1284 (2009).

73. Anticevic, A., Repovs, G. & Barch, D. M. Working memory encoding and maintenance deficits in schizophrenia: neural evidence for activation and deactivation abnormalities. *Schizophr Bull* **39**, 168–178 (2013).

74. Frye, R. E. *et al.* Superior longitudinal fasciculus and cognitive dysfunction in adolescents born preterm and at term. *Developmental Medicine & Child Neurology* **52**, 760–766 (2010).

75. Sasson, N. *et al.* Controlling for Response Biases Clarifies Sex and Age Differences in Facial Affect Recognition. *Journal of Nonverbal Behavior* **34**, 207–221 (2010).

76. Vestergaard, M. *et al.* White matter microstructure in superior longitudinal fasciculus associated with spatial working memory performance in children. *J Cogn Neurosci* **23**, 2135–2146 (2011).

77. Sasson, E., Doniger, G. M., Pasternak, O., Tarrasch, R. & Assaf, Y. White matter correlates of cognitive domains in normal aging with diffusion tensor imaging. *Front. Neurosci.* **0**, (2013).

78. Karlsgodt, K. H. *et al.* Diffusion Tensor Imaging of the Superior Longitudinal Fasciculus and Working Memory in Recent-Onset Schizophrenia. *Biological Psychiatry* **63**, 512–518 (2008).

79. Fitzgerald, J. *et al.* Abnormal fronto-parietal white matter organisation in the superior longitudinal fasciculus branches in autism spectrum disorders. *European Journal of Neuroscience* **47**, 652–661 (2018).

80. Kinoshita, M. *et al.* Chronic spatial working memory deficit associated with the superior longitudinal fasciculus: a study using voxel-based lesion-symptom

mapping and intraoperative direct stimulation in right prefrontal glioma surgery. *Journal of Neurosurgery* **125**, 1024–1032 (2016).

81. Cristofori, I. *et al.* White and gray matter contributions to executive function recovery after traumatic brain injury. *Neurology* **84**, 1394–1401 (2015).

82. Arain, M. *et al.* Maturation of the adolescent brain. *Neuropsychiatr Dis Treat* **9**, 449–461 (2013).

83. Gogtay, N. *et al.* Dynamic mapping of human cortical development during childhood through early adulthood. *PNAS* **101**, 8174–8179 (2004).

84. Hansen, P. E., Ballesteros, M. C., Soila, K., Garcia, L. & Howard, J. M. MR imaging of the developing human brain. Part 1. Prenatal development. *RadioGraphics* **13**, 21–36 (1993).

85. Cholfin, J. A. & Rubenstein, J. L. R. Patterning of frontal cortex subdivisions by Fgf17. *Proc Natl Acad Sci U S A* **104**, 7652–7657 (2007).

86. Cholfin, J. A. & Rubenstein, J. L. R. Frontal Cortex Subdivision Patterning Is Coordinately Regulated by Fgf8, Fgf17, and Emx2. *J Comp Neurol* **509**, 144–155 (2008).

87. Fuster, J. M. Frontal lobe and cognitive development. *J Neurocytol* **31**, 373–385 (2002).

88. Kostović, I. Chapter 10 Structural and histochemical reorganization of the human prefrontal cortex during perinatal and postnatal life. in *Progress in Brain Research* (eds. Uylings, H. B. M., Van Eden, C. G., De Bruin, J. P. C., Corner, M. A. & Feenstra, M. G. P.) vol. 85 223–240 (Elsevier, 1991).

89. Ruff, H. A. & Rothbart, M. K. *Attention in Early Development: Themes and Variations*. (Oxford University Press, 2001).

90. Hendry, A., Jones, E. J. H. & Charman, T. Executive function in the first three years of life: Precursors, predictors and patterns. *Developmental Review* **42**, 1–33 (2016).

91. Reznick, J. S., Morrow, J. D., Goldman, B. D. & Snyder, J. The Onset of Working Memory in Infants. *Infancy* **6**, 145–154 (2004).

92. van Houdt, C. A., Oosterlaan, J., van Wassenaer-Leemhuis, A. G., van Kaam, A. H. & Aarnoudse-Moens, C. S. H. Executive function deficits in children born preterm or at low birthweight: a meta-analysis. *Developmental Medicine & Child Neurology* **61**, 1015–1024 (2019).

93. Taylor, H. G. & Clark, C. A. C. Executive function in children born preterm: Risk factors and implications for outcome. *Seminars in perinatology* **40**, 520 (2016).

94. Power, J., van IJzendoorn, M., Lewis, A. J., Chen, W. & Galbally, M. Maternal perinatal depression and child executive function: A systematic review and meta-analysis. *Journal of Affective Disorders* **291**, 218–234 (2021).

95. DiPietro, J. A. Maternal Stress in Pregnancy: Considerations for Fetal Development. *Journal of Adolescent Health* **51**, S3–S8 (2012).

96. Teffer, K. & Semendeferi, K. Chapter 9 - Human prefrontal cortex: Evolution, development, and pathology. in *Progress in Brain Research* (eds. Hofman, M. A. & Falk, D.) vol. 195 191–218 (Elsevier, 2012).

97. Giedd, J. N. *et al.* Brain development during childhood and adolescence: a longitudinal MRI study. *Nat Neurosci* **2**, 861–863 (1999).

98. Giedd, J. N. *et al.* Puberty-related influences on brain development. *Molecular and Cellular Endocrinology* **254–255**, 154–162 (2006).

99. Fair, D. A. *et al.* Development of distinct control networks through segregation and integration. *PNAS* **104**, 13507–13512 (2007).

100. Gao, W., Alcauter, S., Smith, J. K., Gilmore, J. H. & Lin, W. Development of human brain cortical network architecture during infancy. *Brain Struct Funct* **220**, 1173–1186 (2015).

101. Gao, W. *et al.* Temporal and Spatial Evolution of Brain Network Topology during the First Two Years of Life. *PLOS ONE* **6**, e25278 (2011).

102. Huang, H. *et al.* Anatomical Characterization of Human Fetal Brain Development with Diffusion Tensor Magnetic Resonance Imaging. *J. Neurosci.* **29**, 4263–4273 (2009).

103. Horgos, B. *et al.* White Matter Dissection of the Fetal Brain. *Frontiers in Neuroanatomy* **14**, 65 (2020).

104. Hermoye, L. *et al.* Pediatric diffusion tensor imaging: Normal database and observation of the white matter maturation in early childhood. *NeuroImage* **29**, 493–504 (2006).

105. Zhang, J. *et al.* Evidence of Slow Maturation of the Superior Longitudinal Fasciculus in Early Childhood by Diffusion Tensor Imaging. *Neuroimage* **38**, 239–247 (2007).

106. Tau, G. Z. & Peterson, B. S. Normal Development of Brain Circuits. *Neuropsychopharmacology* **35**, 147–168 (2010).

107. Friedman, N. P. *et al.* Individual Differences in Executive Functions Are Almost Entirely Genetic in Origin. *J Exp Psychol Gen* **137**, 201–225 (2008).

108. Engelhardt, L. E., Briley, D. A., Mann, F. D., Harden, K. P. & Tucker-Drob, E. M. Genes Unite Executive Functions in Childhood. *Psychol Sci* **26**, 1151–1163 (2015).

109. Harden, K. P. *et al.* Genetic Associations Between Executive Functions and a General Factor of Psychopathology. *Journal of the American Academy of Child & Adolescent Psychiatry* **59**, 749–758 (2020).

110. Ando, J., Ono, Y. & Wright, M. J. Genetic structure of spatial and verbal working memory. *Behav Genet* **31**, 615–624 (2001).

111. Anokhin, A. P., Heath, A. C. & Myers, E. Genetics, prefrontal cortex, and cognitive control: a twin study of event-related brain potentials in a response inhibition task. *Neurosci Lett* **368**, 314–318 (2004).

112. Chang, S., Yang, L., Wang, Y. & Faraone, S. V. Shared polygenic risk for ADHD, executive dysfunction and other psychiatric disorders. *Transl Psychiatry* **10**, 1–9 (2020).

113. Owens, S. F. *et al.* Genetic overlap between schizophrenia and selective components of executive function. *Schizophrenia Research* **127**, 181–187 (2011).

114. Chen, L.-S., Rice, T. K., Thompson, P. A., Barch, D. M. & Csernansky, J. G. Familial aggregation of clinical and neurocognitive features in sibling pairs with and without schizophrenia. *Schizophrenia Research* **111**, 159–166 (2009).

115. Toulopoulou, T. *et al.* Substantial Genetic Overlap Between Neurocognition and Schizophrenia: Genetic Modeling in Twin Samples. *Archives of General Psychiatry* **64**, 1348–1355 (2007).

116. Berlin, L. & Bohlin, G. Response Inhibition, Hyperactivity, and Conduct Problems Among Preschool Children. *Journal of Clinical Child & Adolescent Psychology* **31**, 242–251 (2002).

117. Carlson, S. M. & Moses, L. J. Individual Differences in Inhibitory Control and Children's Theory of Mind. *Child Development* **72**, 1032–1053 (2001).

118. Vuontela, V. *et al.* Audiospatial and Visuospatial Working Memory in 6–13 Year Old School Children. *Learn. Mem.* **10**, 74–81 (2003).

119. Gaillard, A., Fehring, D. J. & Rossell, S. L. A systematic review and meta-analysis of behavioural sex differences in executive control. *European Journal of Neuroscience* **53**, 519–542 (2021).

120. Polanczyk, G., de Lima, M. S., Horta, B. L., Biederman, J. & Rohde, L. A. The Worldwide Prevalence of ADHD: A Systematic Review and Metaregression Analysis. *AJP* **164**, 942–948 (2007).

121. Rowland, A. S. *et al.* The Prevalence of ADHD in a Population-Based Sample. *J Atten Disord* **19**, 741–754 (2015).

122. Danielson, M. L. *et al.* Prevalence of Parent-Reported ADHD Diagnosis and Associated Treatment Among U.S. Children and Adolescents, 2016. *J Clin Child Adolesc Psychol* **47**, 199–212 (2018).

123. Cuffe, S. P., Moore, C. G. & McKeown, R. E. Prevalence and Correlates of ADHD Symptoms in the National Health Interview Survey. *J Atten Disord* **9**, 392–401 (2005).

124. Gaub, M. & Carlson, C. L. Gender differences in ADHD: a meta-analysis and critical review. *J Am Acad Child Adolesc Psychiatry* **36**, 1036–1045 (1997).

125. Willcutt, E. G. The Prevalence of DSM-IV Attention-Deficit/Hyperactivity Disorder: A Meta-Analytic Review. *Neurotherapeutics* **9**, 490–499 (2012).

126. Biederman, J. *et al.* Clinical Correlates of ADHD in Females: Findings From a Large Group of Girls Ascertained From Pediatric and Psychiatric Referral Sources. *Journal of the American Academy of Child & Adolescent Psychiatry* **38**, 966–975 (1999).

127. Quinn, P. O. Attention-deficit/hyperactivity disorder and its comorbidities in women and girls: An evolving picture. *Curr Psychiatry Rep* **10**, 419–423 (2008).

128. Loyer Carbonneau, M., Demers, M., Bigras, M. & Guay, M.-C. Meta-Analysis of Sex Differences in ADHD Symptoms and Associated Cognitive Deficits. *J Atten Disord* 1087054720923736 (2020) doi:10.1177/1087054720923736.

129. Martin, J. *et al.* Sex-specific manifestation of genetic risk for attention deficit hyperactivity disorder in the general population. *Journal of Child Psychology and Psychiatry* **59**, 908–916 (2018).

130. Ottosen, C. *et al.* Sex Differences in Comorbidity Patterns of Attention-Deficit/Hyperactivity Disorder. *Journal of the American Academy of Child & Adolescent Psychiatry* **58**, 412-422.e3 (2019).

131. Mowlem, F. D. *et al.* Sex differences in predicting ADHD clinical diagnosis and pharmacological treatment. *Eur Child Adolesc Psychiatry* **28**, 481–489 (2019).

132. Mowlem, F., Agnew-Blais, J., Taylor, E. & Asherson, P. Do different factors influence whether girls versus boys meet ADHD diagnostic criteria? Sex differences among children with high ADHD symptoms. *Psychiatry Research* **272**, 765–773 (2019).

133. Higgins, E. T. & Bargh, J. A. Social Cognition and Social Perception. *Annual Review of Psychology* **38**, 369–425 (1987).

134. Renfrew, C., Frith, C., Malafouris, L. & Frith, C. D. Social cognition. *Philosophical Transactions of the Royal Society B: Biological Sciences* **363**, 2033–2039 (2008).

135. Senju, A. Atypical development of spontaneous social cognition in autism spectrum disorders. *Brain and Development* **35**, 96–101 (2013).

136. Korkmaz, B. Theory of Mind and Neurodevelopmental Disorders of Childhood. *Pediatr Res* **69**, 101–108 (2011).

137. Baron-Cohen, S., Wheelwright, S., Hill, J., Raste, Y. & Plumb, I. The "Reading the Mind in the Eyes" Test Revised Version: A Study with Normal Adults, and Adults with Asperger Syndrome or High-functioning Autism. *The Journal of Child Psychology and Psychiatry and Allied Disciplines* **42**, 241–251 (2001).

138. Gur, R. C. *et al.* A method for obtaining 3-dimensional facial expressions and its standardization for use in neurocognitive studies. *J Neurosci Methods* **115**, 137–143 (2002).

139. Pinkham, A. E., Harvey, P. D. & Penn, D. L. Social Cognition Psychometric Evaluation: Results of the Final Validation Study. *Schizophr Bull* **44**, 737–748 (2018).

140. Baksh, R. A., Abrahams, S., Auyeung, B. & MacPherson, S. E. The Edinburgh Social Cognition Test (ESCoT): Examining the effects of age on a new measure of theory of mind and social norm understanding. *PLOS ONE* **13**, e0195818 (2018).

141. McDonald, S., Flanagan, S., Rollins, J. & Kinch, J. TASIT: A new clinical tool for assessing social perception after traumatic brain injury. *J Head Trauma Rehabil* **18**, 219–238 (2003).

142. Isaksson, J. *et al.* Social Cognition in Autism and Other Neurodevelopmental Disorders: A Co-twin Control Study. *J Autism Dev Disord* **49**, 2838–2848 (2019).

143. Bishop-Fitzpatrick, L., Mazefsky, C. A., Eack, S. M. & Minshew, N. J. Correlates of social functioning in autism spectrum disorder: The role of social cognition. *Research in Autism Spectrum Disorders* **35**, 25–34 (2017).

144. Shattuck, P. T. *et al.* Change in Autism Symptoms and Maladaptive Behaviors in Adolescents and Adults with an Autism Spectrum Disorder. *J Autism Dev Disord* **37**, 1735–1747 (2007).

145. Addington, J., Girard, T. A., Christensen, B. K. & Addington, D. Social cognition mediates illness-related and cognitive influences on social function in patients with schizophrenia-spectrum disorders. *J Psychiatry Neurosci* **35**, 49–54 (2010).

146. Middelboe, T. *et al.* The Nordic Study on schizophrenic patients living in the community. Subjective needs and perceived help. *European Psychiatry* **16**, 207–214 (2001).

147. Boada, L. *et al.* Social Cognition in Autism and Schizophrenia Spectrum Disorders: The Same but Different? *J Autism Dev Disord* **50**, 3046–3059 (2020).

148. Crespi, B. & Badcock, C. Psychosis and autism as diametrical disorders of the social brain. *Behavioral and Brain Sciences* **31**, 241–261 (2008).

149. Roberts, D. L. *et al.* A randomized, controlled trial of Social Cognition and Interaction Training (SCIT) for outpatients with schizophrenia spectrum disorders. *British Journal of Clinical Psychology* **53**, 281–298 (2014).

150. Coursey, R. D., Keller, A. B. & Farrell, E. W. Individual Psychotherapy and Persons With Serious Mental Illness: The Clients' Perspective. *Schizophrenia Bulletin* **21**, 283–301 (1995).

151. Bora, E. & Pantelis, C. Meta-analysis of social cognition in attention-deficit/hyperactivity disorder (ADHD): comparison with healthy controls and autistic spectrum disorder. *Psychological Medicine* **46**, 699–716 (2016).

152. Uekermann, J. *et al.* Social cognition in attention-deficit hyperactivity disorder (ADHD). *Neuroscience & Biobehavioral Reviews* **34**, 734–743 (2010).

153. Jusyte, A., Gulewitsch, M. D. & Schönenberg, M. Recognition of peer emotions in children with ADHD: Evidence from an animated facial expressions task. *Psychiatry Research* **258**, 351–357 (2017).

154. Sibley, M. H., Evans, S. W. & Serpell, Z. N. Social Cognition and Interpersonal Impairment in Young Adolescents with ADHD. *J Psychopathol Behav Assess* **32**, 193–202 (2010).

155. Parke, E. M. *et al.* Social Cognition in Children With ADHD. *J Atten Disord* **25**, 519–529 (2021).

156. Gallagher, H. L. *et al.* Reading the mind in cartoons and stories: an fMRI study of 'theory of mind' in verbal and nonverbal tasks. *Neuropsychologia* **38**, 11–21 (2000).

157. Happé, F. *et al.* 'Theory of mind' in the brain. Evidence from a PET scan study of Asperger syndrome. *NeuroReport* **8**, 197–201 (1996).

158. Fletcher, P. C. *et al.* Other minds in the brain: a functional imaging study of "theory of mind" in story comprehension. *Cognition* **57**, 109–128 (1995).

159. Birbaumer, N. *et al.* fMRI reveals amygdala activation to human faces in social phobics. *NeuroReport* **9**, 1223–1226 (1998).

160. Hart, A. J. *et al.* Differential response in the human amygdala to racial outgroup vs ingroup face stimuli. *NeuroReport* **11**, 2351–2354 (2000).

161. Baron-Cohen, S. *et al.* Social intelligence in the normal and autistic brain: an fMRI study. *European Journal of Neuroscience* **11**, 1891–1898 (1999).

162. Beer, J. S., John, O. P., Scabini, D. & Knight, R. T. Orbitofrontal cortex and social behavior: integrating self-monitoring and emotion-cognition interactions. *J Cogn Neurosci* **18**, 871–879 (2006).

163. Jonker, F. A., Jonker, C., Scheltens, P. & Scherder, E. J. A. The role of the orbitofrontal cortex in cognition and behavior. *Rev Neurosci* **26**, 1–11 (2015).

164. Cicerone, K. D. & Tanenbaum, L. N. Disturbance of social cognition after traumatic orbitofrontal brain injury. *Archives of Clinical Neuropsychology* **12**, 173–188 (1997).

165. Amodio, D. M. & Frith, C. D. Meeting of minds: the medial frontal cortex and social cognition. *Nat Rev Neurosci* **7**, 268–277 (2006).

166. Santiesteban, I., Banissy, M. J., Catmur, C. & Bird, G. Enhancing Social Ability by Stimulating Right Temporoparietal Junction. *Current Biology* **22**, 2274–2277 (2012).

167. McAlonan, G. M. *et al.* Mapping the brain in autism. A voxel-based MRI study of volumetric differences and intercorrelations in autism. *Brain* **128**, 268–276 (2005).

168. Bzdok, D. *et al.* Left inferior parietal lobe engagement in social cognition and language. *Neuroscience & Biobehavioral Reviews* **68**, 319–334 (2016).

169. Cheng, Y., Chou, K.-H., Fan, Y.-T. & Lin, C.-P. ANS: Aberrant Neurodevelopment of the Social Cognition Network in Adolescents with Autism Spectrum Disorders. *PLOS ONE* **6**, e18905 (2011).

170. Li, W., Mai, X. & Liu, C. The default mode network and social understanding of others: what do brain connectivity studies tell us. *Front Hum Neurosci* **8**, 74 (2014).

171. Wang, K. *et al.* Altered social cognition and connectivity of default mode networks in the co-occurrence of autistic spectrum disorder and attention deficit hyperactivity disorder. *Aust N Z J Psychiatry* **53**, 760–771 (2019).

172. Sutcubasi, B. *et al.* Resting-state network dysconnectivity in ADHD: A system-neuroscience-based meta-analysis. *The World Journal of Biological Psychiatry* **21**, 662–672 (2020).

173. Samson, D., Apperly, I. A., Chiavarino, C. & Humphreys, G. W. Left temporoparietal junction is necessary for representing someone else's belief. *Nat Neurosci* **7**, 499–500 (2004).

174. Jackson, P. L., Brunet, E., Meltzoff, A. N. & Decety, J. Empathy examined through the neural mechanisms involved in imagining how I feel versus how you feel pain. *Neuropsychologia* **44**, 752–761 (2006).

175. Young, L., Camprodon, J. A., Hauser, M., Pascual-Leone, A. & Saxe, R. Disruption of the right temporoparietal junction with transcranial magnetic stimulation reduces the role of beliefs in moral judgments. *Proc Natl Acad Sci U S A* **107**, 6753–6758 (2010).

176. Mars, R. B., Sallet, J., Neubert, F.-X. & Rushworth, M. F. S. Connectivity profiles reveal the relationship between brain areas for social cognition in human and monkey temporoparietal cortex. *PNAS* **110**, 10806–10811 (2013).

177. Penner, J. *et al.* Temporoparietal Junction Functional Connectivity in Early Schizophrenia and Major Depressive Disorder. *Chronic Stress* **2**, 2470547018815232 (2018).

178. Poeppl, T. B. *et al.* Imbalance in subregional connectivity of the right temporoparietal junction in major depression. *Human Brain Mapping* **37**, 2931–2942 (2016).

179. Wang, Y., Metoki, A., Alm, K. H. & Olson, I. R. White matter pathways and social cognition. *Neuroscience & Biobehavioral Reviews* **90**, 350–370 (2018).

180. Fletcher, P. T. *et al.* Microstructural connectivity of the arcuate fasciculus in adolescents with high-functioning autism. *Neuroimage* **51**, 1117–1125 (2010).

181. Barnea-Goraly, N., Lotspeich, L. J. & Reiss, A. L. Similar white matter aberrations in children with autism and their unaffected siblings: a diffusion tensor imaging study using tract-based spatial statistics. *Arch Gen Psychiatry* **67**, 1052–1060 (2010).

182. Fishman, I., Datko, M., Cabrera, Y., Carper, R. A. & Müller, R.-A. Reduced integration and differentiation of the imitation network in autism: A combined functional connectivity magnetic resonance imaging and diffusion-weighted imaging study. *Annals of Neurology* **78**, 958–969 (2015).

183. Im, W. Y. *et al.* Impaired White Matter Integrity and Social Cognition in High-Function Autism: Diffusion Tensor Imaging Study. *Psychiatry Investig* **15**, 292–299 (2018).

184. Lo, Y.-C., Chen, Y.-J., Hsu, Y.-C., Tseng, W.-Y. I. & Gau, S. S.-F. Reduced tract integrity of the model for social communication is a neural substrate of social communication deficits in autism spectrum disorder. *Journal of Child Psychology and Psychiatry* **58**, 576–585 (2017).

185. Noriuchi, M. *et al.* Altered white matter fractional anisotropy and social impairment in children with autism spectrum disorder. *Brain Research* **1362**, 141–149 (2010).

186. Miyata, J. *et al.* Reduced white matter integrity as a neural correlate of social cognition deficits in schizophrenia. *Schizophrenia Research* **119**, 232–239 (2010).

187. Kana, R. K., Libero, L. E., Hu, C. P., Deshpande, H. D. & Colburn, J. S. Functional Brain Networks and White Matter Underlying Theory-of-Mind in Autism. *Social Cognitive and Affective Neuroscience* **9**, 98–105 (2014).

188. Stiles, J. & Jernigan, T. L. The Basics of Brain Development. *Neuropsychol Rev* **20**, 327–348 (2010).

189. Prayer, D. *et al.* MRI of normal fetal brain development. *European Journal of Radiology* **57**, 199–216 (2006).

190. Grossmann, T. & Johnson, M. H. The development of the social brain in human infancy. *European Journal of Neuroscience* **25**, 909–919 (2007).

191. Li, G. *et al.* Mapping Region-Specific Longitudinal Cortical Surface Expansion from Birth to 2 Years of Age. *Cereb Cortex* **23**, 2724–2733 (2013).

192. Nelson, C. A. The Recognition of Facial Expressions in the First Two Years of Life: Mechanisms of Development. *Child Development* **58**, 889–909 (1987).

193. Liszkowski, U., Carpenter, M., Striano, T. & Tomasello, M. 12- and 18-Month-Olds Point to Provide Information for Others. *Journal of Cognition and Development* **7**, 173–187 (2006).

194. Slaughter, V. Theory of Mind in Infants and Young Children: A Review. *Australian Psychologist* **50**, 169–172 (2015).

195. Rodger, H., Vizioli, L., Ouyang, X. & Caldara, R. Mapping the development of facial expression recognition. *Developmental Science* **18**, 926–939 (2015).

196. Wellman, H. M., Cross, D. & Watson, J. Meta-Analysis of Theory-of-Mind Development: The Truth about False Belief. *Child Development* **72**, 655–684 (2001).

197. Wellman, H. M. & Liu, D. Scaling of Theory-of-Mind Tasks. *Child Development* **75**, 523–541 (2004).

198. Bowman, L. C., Thorpe, S. G., Cannon, E. N. & Fox, N. A. Action mechanisms for social cognition: behavioral and neural correlates of developing Theory of Mind. *Developmental Science* **20**, e12447 (2017).

199. Mitter, C., Prayer, D., Brugger, P. C., Weber, M. & Kasprian, G. In Vivo Tractography of Fetal Association Fibers. *PLOS ONE* **10**, e0119536 (2015).

200. Huang, H. *et al.* White and gray matter development in human fetal, newborn and pediatric brains. *NeuroImage* **33**, 27–38 (2006).

201. Cohen, A. H. *et al.* Development of human white matter fiber pathways: From newborn to adult ages. *International Journal of Developmental Neuroscience* **50**, 26–38 (2016).

202. Turk, E. *et al.* Functional Connectome of the Fetal Brain. *J. Neurosci.* **39**, 9716–9724 (2019).

203. Hoff, G. E. A.-J., Van Den Heuvel, M., Benders, M. J. N. L., Kersbergen, K. J. & de Vries, L. S. On development of functional brain connectivity in the young brain. *Frontiers in Human Neuroscience* **7**, 650 (2013).

204. Collin, G. & van den Heuvel, M. P. The Ontogeny of the Human Connectome: Development and Dynamic Changes of Brain Connectivity Across the Life Span. *Neuroscientist* **19**, 616–628 (2013).

205. Thomason, M. E. *et al.* Intrinsic functional brain architecture derived from graph theoretical analysis in the human fetus. *PLoS ONE* **9**, e94423 (2014).

206. Thomason, M. E. *et al.* Age-related increases in long-range connectivity in fetal functional neural connectivity networks in utero. *Dev Cogn Neurosci* **11**, 96–104 (2015).

207. van den Heuvel, M. I. & Thomason, M. E. Functional Connectivity of the Human Brain in Utero. *Trends in Cognitive Sciences* **20**, 931–939 (2016).

208. Fransson, P. *et al.* Spontaneous Brain Activity in the Newborn Brain During Natural Sleep—An fMRI Study in Infants Born at Full Term. *Pediatric Research* **66**, 301–305 (2009).

209. Gao, W. *et al.* Evidence on the emergence of the brain's default network from 2-week-old to 2-year-old healthy pediatric subjects. *PNAS* (2009) doi:10.1073/pnas.0811221106.

210. Fair, D. A. *et al.* The maturing architecture of the brain's default network. *PNAS* **105**, 4028–4032 (2008).

211. Davis, M. C. *et al.* Associations between oxytocin receptor genotypes and social cognitive performance in individuals with schizophrenia. *Schizophrenia Research* **159**, 353–357 (2014).

212. Barlati, S. *et al.* Social Cognition in a Research Domain Criteria Perspective: A Bridge Between Schizophrenia and Autism Spectra Disorders. *Frontiers in Psychiatry* **11**, (2020).

213. Wilczyński, K. M., Siwiec, A. & Janas-Kozik, M. Systematic Review of Literature on Single-Nucleotide Polymorphisms Within the Oxytocin and Vasopressin Receptor Genes in the Development of Social Cognition Dysfunctions in Individuals Suffering From Autism Spectrum Disorder. *Front Psychiatry* **10**, 380 (2019).

214. Reuter, M. *et al.* Functional characterization of an oxytocin receptor gene variant (rs2268498) previously associated with social cognition by expression analysis in vitro and in human brain biopsy. *Social Neuroscience* **12**, 604–611 (2017).

215. Robinson, E. B. *et al.* Genetic risk for autism spectrum disorders and neuropsychiatric variation in the general population. *Nat Genet* **48**, 552–555 (2016).

216. Micalizzi, L. *et al.* Single nucleotide polymorphism heritability and differential patterns of genetic overlap between inattention and four neurocognitive factors in youth. *Dev Psychopathol* **33**, 76–86 (2021).

217. Coleman, J. R. I. *et al.* Genome-wide association study of facial emotion recognition in children and association with polygenic risk for mental health disorders. *Am J Med Genet B Neuropsychiatr Genet* **174**, 701–711 (2017).

218. St Pourcain, B. *et al.* Common variation contributes to the genetic architecture of social communication traits. *Mol Autism* **4**, 34 (2013).

219. St Pourcain, B. *et al.* Variability in the common genetic architecture of social-communication spectrum phenotypes during childhood and adolescence. *Mol Autism* **5**, 18 (2014).

220. Scourfield, J., Martin, N., Lewis, G. & McGuffin, P. Heritability of social cognitive skills in children and adolescents. *The British Journal of Psychiatry* **175**, 559–564 (1999).

221. Robinson, E. B. *et al.* The genetic architecture of pediatric cognitive abilities in the Philadelphia Neurodevelopmental Cohort. *Mol Psychiatry* **20**, 454–458 (2015).

222. Germine, L. *et al.* Association between polygenic risk for schizophrenia, neurocognition and social cognition across development. *Transl Psychiatry* **6**, e924–e924 (2016).

223. Russell, T. A., Tchanturia, K., Rahman, Q. & Schmidt, U. Sex differences in theory of mind: A male advantage on Happé's "cartoon" task. *Cognition and Emotion* **21**, 1554–1564 (2007).

224. Proverbio, A. M., Matarazzo, S., Brignone, V., Zotto, M. D. & Zani, A. Processing valence and intensity of infant expressions: The roles of expertise and gender. *Scandinavian Journal of Psychology* **48**, 477–485 (2007).

225. Proverbio, A. M. Sex differences in social cognition: The case of face processing. *Journal of Neuroscience Research* **95**, 222–234 (2017).

226. Hall, J. K., Hutton, S. B. & Morgan, M. J. Sex differences in scanning faces: Does attention to the eyes explain female superiority in facial expression recognition? *Cognition and Emotion* **24**, 629–637 (2010).

227. Hall, J. A. Gender effects in decoding nonverbal cues. *Psychological Bulletin* **85**, 845–857 (1978).

228. Thompson, A. E. & Voyer, D. Sex differences in the ability to recognise non-verbal displays of emotion: A meta-analysis. *Cognition and Emotion* **28**, 1164–1195 (2014).

229. Dimberg, U. & Lundquist, L.-O. Gender differences in facial reactions to facial expressions. *Biological Psychology* **30**, 151–159 (1990).

230. Di Tella, M., Miti, F., Ardito, R. B. & Adenzato, M. Social cognition and sex: Are men and women really different? *Personality and Individual Differences* **162**, 110045 (2020).

231. Messinger, D. S. *et al.* Early sex differences are not autism-specific: A Baby Siblings Research Consortium (BSRC) study. *Molecular Autism* **6**, 32 (2015).

232. Loomes, R., Hull, L. & Mandy, W. P. L. What Is the Male-to-Female Ratio in Autism Spectrum Disorder? A Systematic Review and Meta-Analysis. *Journal of the American Academy of Child & Adolescent Psychiatry* **56**, 466–474 (2017).

233. Özerk, K. & Cardinal, D. Prevalence of Autism/ASD Among Preschool and School-age Children in Norway. *Contemp School Psychol* **24**, 419–428 (2020).

234. Maenner, M. J. Prevalence of Autism Spectrum Disorder Among Children Aged 8 Years — Autism and Developmental Disabilities Monitoring Network, 11 Sites, United States, 2016. *MMWR Surveill Summ* **69**, (2020).

235. Baird, G. *et al.* Prevalence of disorders of the autism spectrum in a population cohort of children in South Thames: the Special Needs and Autism Project (SNAP). *The Lancet* **368**, 210–215 (2006).

236. Russell, G., Rodgers, L. R., Ukoumunne, O. C. & Ford, T. Prevalence of Parent-Reported ASD and ADHD in the UK: Findings from the Millennium Cohort Study. *J Autism Dev Disord* **44**, 31–40 (2014).

237. Petrou, A. M., Parr, J. R. & McConachie, H. Gender differences in parent-reported age at diagnosis of children with autism spectrum disorder. *Research in Autism Spectrum Disorders* **50**, 32–42 (2018).

238. Evans, S. C., Boan, A. D., Bradley, C. & Carpenter, L. A. Sex/Gender Differences in Screening for Autism Spectrum Disorder: Implications for Evidence-Based Assessment. *Journal of Clinical Child & Adolescent Psychology* **48**, 840–854 (2019).

239. Lawson, L. P., Joshi, R., Barbaro, J. & Dissanayake, C. Gender Differences During Toddlerhood in Autism Spectrum Disorder: A Prospective Community-Based Longitudinal Follow-Up Study. *J Autism Dev Disord* **48**, 2619–2628 (2018).

240. Dean, M., Harwood, R. & Kasari, C. The art of camouflage: Gender differences in the social behaviors of girls and boys with autism spectrum disorder. *Autism* **21**, 678–689 (2017).

241. Halsall, J., Clarke, C. & Crane, L. “Camouflaging” by adolescent autistic girls who attend both mainstream and specialist resource classes: Perspectives of girls, their mothers and their educators. *Autism* **25**, 2074–2086 (2021).

242. Schuck, R. K., Flores, R. E. & Fung, L. K. Brief Report: Sex/Gender Differences in Symptomology and Camouflaging in Adults with Autism Spectrum Disorder. *J Autism Dev Disord* **49**, 2597–2604 (2019).

243. Dworzynski, K., Ronald, A., Bolton, P. & Happé, F. How Different Are Girls and Boys Above and Below the Diagnostic Threshold for Autism Spectrum Disorders? *Journal of the American Academy of Child & Adolescent Psychiatry* **51**, 788–797 (2012).

244. de Giambattista, C., Ventura, P., Trerotoli, P., Margari, F. & Margari, L. Sex Differences in Autism Spectrum Disorder: Focus on High Functioning Children and Adolescents. *Frontiers in Psychiatry* **12**, (2021).

245. Rutherford, M. *et al.* Gender ratio in a clinical population sample, age of diagnosis and duration of assessment in children and adults with autism spectrum disorder. *Autism* **20**, 628–634 (2016).

246. TURNER, H. H. A SYNDROME OF INFANTILISM, CONGENITAL WEBBED NECK, AND CUBITUS VALGUS1. *Endocrinology* **23**, 566–574 (1938).

247. Nielsen, J. & Wohlert, M. Chromosome abnormalities found among 34,910 newborn children: results from a 13-year incidence study in Arhus, Denmark. *Hum. Genet.* **87**, 81–83 (1991).

248. McCarthy, K. & Bondy, C. A. Turner syndrome in childhood and adolescence. *Expert Review of Endocrinology & Metabolism* **3**, 771–775 (2008).

249. Ford, C. E., Jones, K. W., Polani, P. E., De Almeida, J. C. & Briggs, J. H. A sex-chromosome anomaly in a case of gonadal dysgenesis (Turner’s syndrome). *Lancet* **1**, 711–713 (1959).

250. Pievsky, M. A. & McGrath, R. E. The Neurocognitive Profile of Attention-Deficit/Hyperactivity Disorder: A Review of Meta-Analyses. *Arch Clin Neuropsychol* **33**, 143–157 (2018).

251. Bedford, R. *et al.* Neurocognitive and observational markers: prediction of autism spectrum disorder from infancy to mid-childhood. *Molecular Autism* **8**, 49 (2017).

252. Creswell, C. S. & Skuse, D. H. Autism in association with Turner syndrome: Genetic implications for male vulnerability to pervasive developmental disorders. *Neurocase* **5**, 511–518 (1999).

253. Avdic, H. B. *et al.* Neurodevelopmental and psychiatric disorders in females with Turner syndrome: a population-based study. *Journal of Neurodevelopmental Disorders* **13**, (2021).

254. Russell, H. F. *et al.* Increased Prevalence of ADHD in Turner Syndrome with No Evidence of Imprinting Effects. *J Pediatr Psychol* **31**, 945–955 (2006).

255. Green, T. *et al.* Elucidating X chromosome influences on Attention Deficit Hyperactivity Disorder and executive function. *Journal of Psychiatric Research* **68**, 217–225 (2015).

256. Carrel, L. & Willard, H. F. X-inactivation profile reveals extensive variability in X-linked gene expression in females. *Nature* **434**, 400–404 (2005).

257. Cutter, W. J. *et al.* Influence of X chromosome and hormones on human brain development: a magnetic resonance imaging and proton magnetic resonance spectroscopy study of Turner syndrome. *Biol. Psychiatry* **59**, 273–283 (2006).

258. Holzapfel, M., Barnea-Goraly, N., Eckert, M. A., Kesler, S. R. & Reiss, A. L. Selective Alterations of White Matter Associated with Visuospatial and Sensorimotor Dysfunction in Turner Syndrome. *J. Neurosci.* **26**, 7007–7013 (2006).

259. Molko, N. *et al.* Brain Anatomy in Turner Syndrome: Evidence for Impaired Social and Spatial–Numerical Networks. *Cereb Cortex* **14**, 840–850 (2004).

260. Brown, W. E. *et al.* Brain development in Turner syndrome: a magnetic resonance imaging study. *Psychiatry Res* **116**, 187–196 (2002).

261. Marzelli, M. J., Hoeft, F., Hong, D. S. & Reiss, A. L. Neuroanatomical spatial patterns in Turner syndrome. *Neuroimage* **55**, 439–447 (2011).

262. Kesler, S. R. *et al.* Amygdala and hippocampal volumes in Turner syndrome: a high-resolution MRI study of X-monosomy. *Neuropsychologia* **42**, 1971 (2004).

263. Knickmeyer, R. C. & Hooper, S. R. The deep biology of cognition: Moving toward a comprehensive neurodevelopmental model of Turner syndrome. *American Journal of Medical Genetics Part C: Seminars in Medical Genetics* **181**, 51–59 (2019).

264. Villalon, J. *et al.* White matter microstructural abnormalities in girls with chromosome 22q11.2 deletion syndrome, Fragile X or Turner syndrome as evidenced by diffusion tensor imaging. *Neuroimage* **81**, 441–454 (2013).

265. Yamagata, B. *et al.* White matter aberrations in prepubertal estrogen-naive girls with monosomic Turner syndrome. *Cereb. Cortex* **22**, 2761–2768 (2012).

266. van Eimeren, L. *et al.* Structure-function relationships underlying calculation: a combined diffusion tensor imaging and fMRI study. *Neuroimage* **52**, 358–363 (2010).

267. Thiebaut de Schotten, M. *et al.* A lateralized brain network for visuospatial attention. *Nat. Neurosci.* **14**, 1245–1246 (2011).

268. Green, T., Saggar, M., Ishak, A., Hong, D. S. & Reiss, A. L. X-Chromosome Effects on Attention Networks: Insights from Imaging Resting-State Networks in Turner Syndrome. *Cereb Cortex* **28**, 3176–3183 (2018).

269. Xie, S. *et al.* The Effects of the X Chromosome on Intrinsic Functional Connectivity in the Human Brain: Evidence from Turner Syndrome Patients. *Cereb. Cortex* **27**, 474–484 (2017).

270. Bray, S., Dunkin, B., Hong, D. S. & Reiss, A. L. Reduced Functional Connectivity during Working Memory in Turner Syndrome. *Cereb Cortex* **21**, 2471–2481 (2011).

271. Bray, S., Hoeft, F., Hong, D. S. & Reiss, A. L. Aberrant functional network recruitment of posterior parietal cortex in turner syndrome. *Human Brain Mapping* **34**, 3117–3128 (2013).

272. Davenport, M. L. *et al.* Altered Brain Structure in Infants with Turner Syndrome. *Cerebral Cortex* **30**, 587–596 (2020).

273. Auerbach, J. G., Atzaba-Poria, N., Berger, A. & Landau, R. Emerging developmental pathways to ADHD: possible path markers in early infancy. *Neural Plast.* **11**, 29–43 (2004).

274. Miller, M., Iosif, A.-M., Young, G. S., Hill, M. M. & Ozonoff, S. Brief Report: Early detection of ADHD: Insights from infant siblings of children with autism. *J Clin Child Adolesc Psychol* **47**, 737–744 (2018).

275. Stephens, R. L., Elsayed, H. E., Reznick, J. S., Crais, E. R. & Watson, L. R. Infant Attentional Behaviors Are Associated with ADHD Symptomatology and Executive Function in Early Childhood. *J Atten Disord* **25**, 1908–1918 (2021).

276. McKinnon, C. J. *et al.* Restricted and Repetitive Behavior and Brain Functional Connectivity in Infants at Risk for Developing Autism Spectrum Disorder. *Biol Psychiatry Cogn Neurosci Neuroimaging* **4**, 50–61 (2019).

277. Piven, J., Elison, J. T. & Zylka, M. J. Toward a conceptual framework for early brain and behavior development in autism. *Mol Psychiatry* **22**, 1385–1394 (2017).

278. Courchesne, E., Gazestani, V. H. & Lewis, N. E. Prenatal Origins of ASD: The When, What, and How of ASD Development. *Trends in Neurosciences* **43**, 326–342 (2020).

279. Birnbaum, R., Jaffe, A. E., Hyde, T. M., Kleinman, J. E. & Weinberger, D. R. Prenatal Expression Patterns of Genes Associated With Neuropsychiatric Disorders. *AJP* **171**, 758–767 (2014).

280. Hall, L. S. *et al.* Cis-effects on gene expression in the human prenatal brain associated with genetic risk for neuropsychiatric disorders. *Mol Psychiatry* **26**, 2082–2088 (2021).

281. Walton, E. *et al.* Epigenetic profiling of ADHD symptoms trajectories: a prospective, methylome-wide study. *Mol Psychiatry* **22**, 250–256 (2017).

282. St Clair, D. *et al.* Rates of adult schizophrenia following prenatal exposure to the Chinese famine of 1959-1961. *JAMA* **294**, 557–562 (2005).

283. Susser, E. *et al.* Schizophrenia after prenatal famine. Further evidence. *Arch Gen Psychiatry* **53**, 25–31 (1996).

284. Susser, E., Hoek, H. W. & Brown, A. Neurodevelopmental disorders after prenatal famine: The story of the Dutch Famine Study. *Am J Epidemiol* **147**, 213–216 (1998).

285. Pearson, R. M. *et al.* Maternal Depression During Pregnancy and the Postnatal Period: Risks and Possible Mechanisms for Offspring Depression at Age 18 Years. *JAMA Psychiatry* **70**, 1312–1319 (2013).

286. Plant, D. T., Pariante, C. M., Sharp, D. & Pawlby, S. Maternal depression during pregnancy and offspring depression in adulthood: Role of child maltreatment. *The British Journal of Psychiatry* **207**, 213–220 (2015).

287. Bergman, K., Sarkar, P., O'connor, T. G., Modi, N. & Glover, V. Maternal Stress During Pregnancy Predicts Cognitive Ability and Fearfulness in Infancy. *Journal of the American Academy of Child & Adolescent Psychiatry* **46**, 1454–1463 (2007).

288. Lyoo, I. K. *et al.* Lithium-Induced Gray Matter Volume Increase As a Neural Correlate of Treatment Response in Bipolar Disorder: A Longitudinal Brain Imaging Study. *Neuropsychopharmacology* **35**, 1743–1750 (2010).

289. Ho, B.-C., Andreasen, N. C., Ziebell, S., Pierson, R. & Magnotta, V. Long-term Antipsychotic Treatment and Brain Volumes: A Longitudinal Study of First-Episode Schizophrenia. *Arch Gen Psychiatry* **68**, 128–137 (2011).

290. Klein, K. O. *et al.* Estrogen Replacement in Turner Syndrome: Literature Review and Practical Considerations. *J. Clin. Endocrinol. Metab.* **103**, 1790–1803 (2018).

291. Bondy, C. A. Care of Girls and Women with Turner Syndrome: A Guideline of the Turner Syndrome Study Group. *J Clin Endocrinol Metab* **92**, 10–25 (2007).

292. Emerson, R. W. *et al.* Functional neuroimaging of high-risk 6-month-old infants predicts a diagnosis of autism at 24 months of age. *Science Translational Medicine* **9**, eaag2882 (2017).

293. Dawson, G. *et al.* Randomized, Controlled Trial of an Intervention for Toddlers With Autism: The Early Start Denver Model. *Pediatrics* **125**, e17–e23 (2010).

294. Biswal, B., Yetkin, F. Z., Haughton, V. M. & Hyde, J. S. Functional connectivity in the motor cortex of resting human brain using echo-planar mri. *Magnetic Resonance in Medicine* **34**, 537–541 (1995).

295. Barkhof, F., Haller, S. & Rombouts, S. A. R. B. Resting-State Functional MR Imaging: A New Window to the Brain. *Radiology* **272**, 29–49 (2014).

296. Wang, D. *et al.* Altered resting-state network connectivity in congenital blind. *Human Brain Mapping* **35**, 2573–2581 (2014).

297. Tedeschi, G. *et al.* Increased interictal visual network connectivity in patients with migraine with aura. *Cephalalgia* **36**, 139–147 (2016).

298. Maudoux, A. *et al.* Auditory Resting-State Network Connectivity in Tinnitus: A Functional MRI Study. *PLOS ONE* **7**, e36222 (2012).

299. Gavrilescu, M. *et al.* Reduced connectivity of the auditory cortex in patients with auditory hallucinations: a resting state functional magnetic resonance imaging study. *Psychol. Med.* **40**, 1149–1158 (2010).

300. Chadick, J. Z. & Gazzaley, A. Differential coupling of visual cortex with default or frontal-parietal network based on goals. *Nat. Neurosci.* **14**, 830–832 (2011).

301. Ekman, M., Derrfuss, J., Tittgemeyer, M. & Fiebach, C. J. Predicting errors from reconfiguration patterns in human brain networks. *Proc. Natl. Acad. Sci. U.S.A.* **109**, 16714–16719 (2012).

302. Multani, N. *et al.* Association Between Social Cognition Changes and Resting State Functional Connectivity in Frontotemporal Dementia, Alzheimer's Disease, Parkinson's Disease, and Healthy Controls. *Front. Neurosci.* **13**, (2019).

303. Bisecco, A. *et al.* Resting-State Functional Correlates of Social Cognition in Multiple Sclerosis: An Explorative Study. *Front. Behav. Neurosci.* **13**, (2020).

304. Jimenez, A. M., Riedel, P., Lee, J., Reavis, E. A. & Green, M. F. Linking resting-state networks and social cognition in schizophrenia and bipolar disorder. *Hum Brain Mapp* **40**, 4703–4715 (2019).

305. Reineberg, A. E., Gustavson, D. E., Benca, C., Banich, M. T. & Friedman, N. P. The Relationship Between Resting State Network Connectivity and Individual Differences in Executive Functions. *Front. Psychol.* **9**, (2018).

306. Markett, S. *et al.* Assessing the function of the fronto-parietal attention network: Insights from resting-state fMRI and the attentional network test. *Human Brain Mapping* **35**, 1700–1709 (2014).

307. Rosenberg, M. D. *et al.* A neuromarker of sustained attention from whole-brain functional connectivity. *Nature Neuroscience* **19**, 165–171 (2016).

308. Li, P. *et al.* Altered Brain Network Connectivity as a Potential Endophenotype of Schizophrenia. *Scientific Reports* **7**, 5483 (2017).

309. Tu, P.-C., Lee, Y.-C., Chen, Y.-S., Li, C.-T. & Su, T.-P. Schizophrenia and the brain's control network: Aberrant within- and between-network connectivity of the frontoparietal network in schizophrenia. *Schizophrenia Research* **147**, 339–347 (2013).

310. Repovs, G., Csernansky, J. G. & Barch, D. M. Brain Network Connectivity in Individuals with Schizophrenia and Their Siblings. *Biological Psychiatry* **69**, 967–973 (2011).

311. Fan, J. *et al.* Resting-State Default Mode Network Related Functional Connectivity Is Associated With Sustained Attention Deficits in Schizophrenia and Obsessive-Compulsive Disorder. *Front. Behav. Neurosci.* **12**, (2018).

312. Nomi, J. S. & Uddin, L. Q. Developmental changes in large-scale network connectivity in autism. *NeuroImage: Clinical* **7**, 732–741 (2015).

313. Jakab, A. *et al.* Fetal functional imaging portrays heterogeneous development of emerging human brain networks. *Front Hum Neurosci* **8**, 852 (2014).

314. Lin, W. *et al.* Functional Connectivity MR Imaging Reveals Cortical Functional Connectivity in the Developing Brain. *American Journal of Neuroradiology* **29**, 1883–1889 (2008).

315. Doria, V. *et al.* Emergence of resting state networks in the preterm human brain. *PNAS* (2010) doi:10.1073/pnas.1007921107.

316. Smyser, C. D. *et al.* Longitudinal Analysis of Neural Network Development in Preterm Infants. *Cereb Cortex* **20**, 2852–2862 (2010).

317. Smyser, C. D. *et al.* Effects of White Matter Injury on Resting State fMRI Measures in Prematurely Born Infants. *PLOS ONE* **8**, e68098 (2013).

318. Gao, W. *et al.* Functional Network Development During the First Year: Relative Sequence and Socioeconomic Correlations. *Cereb. Cortex* **25**, 2919–2928 (2015).

319. Satterthwaite, T. D. & Baker, J. T. How Can Studies of Resting-state Functional Connectivity Help Us Understand Psychosis as a Disorder of Brain Development? *Curr Opin Neurobiol* **0**, 85–91 (2015).

320. Glahn, D. C. *et al.* Genetic control over the resting brain. *PNAS* **107**, 1223–1228 (2010).

321. Colclough, G. L. *et al.* The heritability of multi-modal connectivity in human brain activity. *eLife* **6**, e20178 (2017).

322. Reineberg, A. E., Hatoum, A. S., Hewitt, J. K., Banich, M. T. & Friedman, N. P. Genetic and Environmental Influence on the Human Functional Connectome. *Cereb Cortex* **30**, 2099–2113 (2020).

323. Teeuw, J. *et al.* Genetic and environmental influences on functional connectivity within and between canonical cortical resting-state networks throughout adolescent development in boys and girls. *Neuroimage* **202**, 116073 (2019).

324. Gao, W. *et al.* Intersubject Variability of and Genetic Effects on the Brain's Functional Connectivity during Infancy. *J. Neurosci.* **34**, 11288–11296 (2014).

325. Qiu, A. *et al.* Prenatal maternal depression alters amygdala functional connectivity in 6-month-old infants. *Translational Psychiatry* **5**, e508–e508 (2015).

326. Malykhin, N. V., Carter, R., Hegadoren, K. M., Seres, P. & Coupland, N. J. Fronto-limbic volumetric changes in major depressive disorder. *Journal of Affective Disorders* **136**, 1104–1113 (2012).

327. Holmes, A. J. *et al.* Individual Differences in Amygdala-Medial Prefrontal Anatomy Link Negative Affect, Impaired Social Functioning, and Polygenic Depression Risk. *J. Neurosci.* **32**, 18087–18100 (2012).

328. Eijndhoven, P. van *et al.* Amygdala Volume Marks the Acute State in the Early Course of Depression. *Biological Psychiatry* **65**, 812–818 (2009).

329. Salzwedel, A. P. *et al.* Prenatal Drug Exposure Affects Neonatal Brain Functional Connectivity. *J Neurosci* **35**, 5860–5869 (2015).

330. Salzwedel, A., Chen, G., Chen, Y., Grewen, K. & Gao, W. Functional dissection of prenatal drug effects on baby brain and behavioral development. *Hum Brain Mapp* **41**, 4789–4803 (2020).

331. Li, Z., Lei, K., Coles, C. D., Lynch, M. E. & Hu, X. Longitudinal changes of amygdala functional connectivity in adolescents prenatally exposed to cocaine. *Drug and Alcohol Dependence* **200**, 50–58 (2019).

332. Radhakrishnan, R. *et al.* Resting state functional MRI in infants with prenatal opioid exposure—a pilot study. *Neuroradiology* (2020) doi:10.1007/s00234-020-02552-3.

333. Salzwedel, A. P., Grewen, K. M., Goldman, B. D. & Gao, W. Thalamocortical functional connectivity and behavioral disruptions in neonates with prenatal cocaine exposure. *Neurotoxicology and Teratology* **56**, 16–25 (2016).

334. Jha, S. C. *et al.* Environmental Influences on Infant Cortical Thickness and Surface Area. *Cereb Cortex* **29**, 1139–1149 (2019).

335. He, L. *et al.* Early prediction of cognitive deficits in very preterm infants using functional connectome data in an artificial neural network framework. *NeuroImage: Clinical* **18**, 290–297 (2018).

336. Chen, M. *et al.* Early Prediction of Cognitive Deficit in Very Preterm Infants Using Brain Structural Connectome With Transfer Learning Enhanced Deep Convolutional Neural Networks. *Front. Neurosci.* **14**, (2020).

337. Knickmeyer, R. C. *et al.* Impact of Demographic and Obstetric Factors on Infant Brain Volumes: A Population Neuroscience Study. *Cereb. Cortex* **27**, 5616–5625 (2017).

338. Gilmore, J. H. *et al.* Genetic and environmental contributions to neonatal brain structure: A twin study. *Hum Brain Mapp* **31**, 1174–1182 (2010).

339. Knickmeyer, R. C. *et al.* A structural MRI study of human brain development from birth to 2 years. *J. Neurosci.* **28**, 12176–12182 (2008).

340. Chen, Y. *et al.* The Subgrouping Structure of Newborns with Heterogenous Brain–Behavior Relationships. *Cerebral Cortex* **31**, 301–311 (2021).

341. Smith, S. M. *et al.* Advances in functional and structural MR image analysis and implementation as FSL. *Neuroimage* **23 Suppl 1**, S208-219 (2004).

342. Cox, R. W. AFNI: software for analysis and visualization of functional magnetic resonance neuroimages. *Comput. Biomed. Res.* **29**, 162–173 (1996).

343. Power, J. D. *et al.* Functional network organization of the human brain. *Neuron* **72**, 665–678 (2011).

344. Satterthwaite, T. D. *et al.* Impact of in-scanner head motion on multiple measures of functional connectivity: relevance for studies of neurodevelopment in youth. *Neuroimage* **60**, 623–632 (2012).

345. Satterthwaite, T. D. *et al.* An improved framework for confound regression and filtering for control of motion artifact in the preprocessing of resting-state functional connectivity data. *Neuroimage* **64**, 240–256 (2013).

346. Gao, W., Lin, W., Grewen, K. & Gilmore, J. H. Functional Connectivity of the Infant Human Brain: Plastic and Modifiable. *Neuroscientist* **23**, 169–184 (2017).

347. Gao, W. *et al.* The synchronization within and interaction between the default and dorsal attention networks in early infancy. *Cerebral Cortex* **23**, 594–603 (2013).

348. Alcauter, S. *et al.* Development of Thalamocortical Connectivity during Infancy and Its Cognitive Correlations. *J. Neurosci.* **34**, 9067–9075 (2014).

349. Braun, U. *et al.* Test–retest reliability of resting-state connectivity network characteristics using fMRI and graph theoretical measures. *NeuroImage* **59**, 1404–1412 (2012).

350. Li, Z., Kadivar, A., Pluta, J., Dunlop, J. & Wang, Z. Test-retest stability analysis of resting brain activity revealed by blood oxygen level-dependent functional MRI. *J Magn Reson Imaging* **36**, 344–354 (2012).

351. Birn, R. M. *et al.* The effect of scan length on the reliability of resting-state fMRI connectivity estimates. *NeuroImage* **83**, 550–558 (2013).

352. Shi, J. *et al.* Genome-wide association study of recurrent early-onset major depressive disorder. *Mol Psychiatry* **16**, 193–201 (2011).

353. Shi, F., Salzwedel, A. P., Lin, W., Gilmore, J. H. & Gao, W. Functional Brain Parcellations of the Infant Brain and the Associated Developmental Trends. *Cereb Cortex* **28**, 1358–1368 (2018).

354. Tzourio-Mazoyer, N. *et al.* Automated anatomical labeling of activations in SPM using a macroscopic anatomical parcellation of the MNI MRI single-subject brain. *Neuroimage* **15**, 273–289 (2002).

355. Yeo, B. T. T. *et al.* The organization of the human cerebral cortex estimated by intrinsic functional connectivity. *J Neurophysiol* **106**, 1125–1165 (2011).

356. R Core Team. R: A language and environment for statistical computing. *R Foundation for Statistical Computing, Vienna, Austria* (2020).

357. Gamer, M., Lemon, J., Fellows, I. & Puspendra, S. irr: Various Coefficients of Interrater Reliability and Agreement. (2019).

358. Xia, K. *et al.* Environmental and Genetic Contributors to Salivary Testosterone Levels in Infants. *Front Endocrinol (Lausanne)* **5**, (2014).

359. Achterberg, M. *et al.* Distinctive heritability patterns of subcortical-prefrontal cortex resting state connectivity in childhood: A twin study. *NEUROIMAGE* **175**, 138–149 (2018).

360. Hodel, A. S. Rapid infant prefrontal cortex development and sensitivity to early environmental experience. *Developmental Review* **48**, 113–144 (2018).

361. Saudino, K. J., Cherny, S. S. & Plomin, R. Parent ratings of temperament in twins: explaining the 'too low' DZ correlations. *Twin Res* **3**, 224–233 (2000).

362. Smyser, C. D. *et al.* Prediction of brain maturity in infants using machine-learning algorithms. *NeuroImage* **136**, 1–9 (2016).

363. Galéra, C. *et al.* Early risk factors for hyperactivity-impulsivity and inattention trajectories from age 17 months to 8 years. *Arch Gen Psychiatry* **68**, 1267–1275 (2011).

364. Rasic, D., Hajek, T., Alda, M. & Uher, R. Risk of mental illness in offspring of parents with schizophrenia, bipolar disorder, and major depressive disorder: a meta-analysis of family high-risk studies. *Schizophr Bull* **40**, 28–38 (2014).

365. Wolford, E. *et al.* Maternal depressive symptoms during and after pregnancy are associated with attention-deficit/hyperactivity disorder symptoms in their 3- to 6-year-old children. *PLoS One* **12**, e0190248 (2017).

366. Chen, M.-H. *et al.* Coaggregation of Major Psychiatric Disorders in First-Degree Relatives of Individuals With Attention-Deficit/Hyperactivity Disorder: A Nationwide Population-Based Study. *J Clin Psychiatry* **80**, (2019).

367. Vizzini, L. *et al.* Maternal anxiety, depression and sleep disorders before and during pregnancy, and preschool ADHD symptoms in the NINFEA birth cohort study. *Epidemiology and Psychiatric Sciences* **28**, 521–531 (2019).

368. Chen, L.-C. *et al.* Association of parental depression with offspring attention deficit hyperactivity disorder and autism spectrum disorder: A nationwide birth cohort study. *J Affect Disord* **277**, 109–114 (2020).

369. Eilertsen, T. *et al.* Parental socioeconomic status and child intellectual functioning in a Norwegian sample. *Scandinavian Journal of Psychology* **57**, 399–405 (2016).

370. Jeong, J., Kim, R. & Subramanian, S. V. How consistent are associations between maternal and paternal education and child growth and development outcomes across 39 low-income and middle-income countries? *J Epidemiol Community Health* **72**, 434–441 (2018).

371. González, L. *et al.* The role of parental social class, education and unemployment on child cognitive development. *Gaceta Sanitaria* **34**, 51–60 (2020).

372. Østergaard, S. D. *et al.* Polygenic risk score, psychosocial environment and the risk of attention-deficit/hyperactivity disorder. *Translational Psychiatry* **10**, 1–11 (2020).

373. Rohr, C. S. *et al.* Functional Connectivity of the Dorsal Attention Network Predicts Selective Attention in 4–7 year-old Girls. *Cerebral Cortex* **27**, 4350–4360 (2017).

374. Aboitiz, F., Ossandón, T., Zamorano, F., Palma, B. & Carrasco, X. Irrelevant stimulus processing in ADHD: catecholamine dynamics and attentional networks. *Front Psychol* **5**, 183 (2014).

375. Luke, B. & Keith, L. G. The contribution of singletons, twins and triplets to low birth weight, infant mortality and handicap in the United States. *J Reprod Med* **37**, 661–666 (1992).

376. Levy, F., McLaughlin, M., Wood, C., Hay, D. & Waldman, I. Twin-Sibling Differences in Parental Reports of ADHD, Speech, Reading and Behaviour Problems. *Journal of Child Psychology and Psychiatry* **37**, 569–578 (1996).

377. Lehn, H. *et al.* Attention Problems and Attention-Deficit/Hyperactivity Disorder in Discordant and Concordant Monozygotic Twins: Evidence of Environmental Mediators. *Journal of the American Academy of Child & Adolescent Psychiatry* **46**, 83–91 (2007).

378. Groen-Blokhuis, M. M., Middeldorp, C. M., van Beijsterveldt, C. E. M. & Boomsma, D. I. Evidence for a Causal Association of Low Birth Weight and Attention Problems. *Journal of the American Academy of Child & Adolescent Psychiatry* **50**, 1247-1254.e2 (2011).

379. Garite, T. J., Clark, R. H., Elliott, J. P., Thorp, J. A., & the Pediatrix/Obstetrix Perinatal Research Group. Twins and triplets: The effect of plurality and growth on neonatal outcome compared with singleton infants. *American Journal of Obstetrics and Gynecology* **191**, 700–707 (2004).

380. Rao, A., Sairam, S. & Shehata, H. Obstetric complications of twin pregnancies. *Best Practice & Research Clinical Obstetrics & Gynaecology* **18**, 557–576 (2004).

381. Power, J. D., Barnes, K. A., Snyder, A. Z., Schlaggar, B. L. & Petersen, S. E. Spurious but systematic correlations in functional connectivity MRI networks arise from subject motion. *Neuroimage* **59**, 2142–2154 (2012).

382. Van Dijk, K. R. A., Sabuncu, M. R. & Buckner, R. L. The influence of head motion on intrinsic functional connectivity MRI. *Neuroimage* **59**, 431–438 (2012).

383. Couvy-Duchesne, B. *et al.* Heritability of head motion during resting state functional MRI in 462 healthy twins. *Neuroimage* **102**, 424–434 (2014).

384. Engelhardt, L. E. *et al.* Children's head motion during fMRI tasks is heritable and stable over time. *Developmental Cognitive Neuroscience* **25**, 58–68 (2017).

385. Mitra, A. *et al.* Resting-state fMRI in sleeping infants more closely resembles adult sleep than adult wakefulness. *PLOS ONE* **12**, e0188122 (2017).

386. Picchioni, D. *et al.* fMRI differences between early and late stage-1 sleep. *Neuroscience Letters* **441**, 81–85 (2008).

387. Redcay, E., Kennedy, D. P. & Courchesne, E. fMRI during natural sleep as a method to study brain function during early childhood. *NeuroImage* **38**, 696–707 (2007).

388. Fransson, P., Åden, U., Blennow, M. & Lagercrantz, H. The Functional Architecture of the Infant Brain as Revealed by Resting-State fMRI. *Cereb Cortex* **21**, 145–154 (2011).

389. Liu, W.-C., Flax, J. F., Guise, K. G., Sukul, V. & Benasich, A. A. Functional connectivity of the sensorimotor area in naturally sleeping infants. *Brain Research* **1223**, 42–49 (2008).

390. Andropoulos, D. B. Effect of Anesthesia on the Developing Brain: Infant and Fetus. *FDT* **43**, 1–11 (2018).

391. York, T. P. *et al.* Fetal and maternal genes' influence on gestational age in a quantitative genetic analysis of 244,000 Swedish births. *Am J Epidemiol* **178**, 543–550 (2013).

392. Wu, W. *et al.* The heritability of gestational age in a two-million member cohort: implications for spontaneous preterm birth. *Hum Genet* **134**, 803–808 (2015).

393. Mook-Kanamori, D. O. *et al.* Heritability Estimates of Body Size in Fetal Life and Early Childhood. *PLOS ONE* **7**, e39901 (2012).

394. Turkheimer, E. & Waldron, M. Nonshared environment: A theoretical, methodological, and quantitative review. *Psychological Bulletin* **126**, 78–108 (2000).

395. Zhao, C. & Gong, G. Mapping the effect of the X chromosome on the human brain: Neuroimaging evidence from Turner syndrome. *Neuroscience & Biobehavioral Reviews* **80**, 263–275 (2017).

396. Raznahan, A. *et al.* Sex-chromosome dosage effects on gene expression in humans. *PNAS* **115**, 7398–7403 (2018).

397. Balaton, B. P., Cotton, A. M. & Brown, C. J. Derivation of consensus inactivation status for X-linked genes from genome-wide studies. *Biol Sex Differ* **6**, (2015).

398. Gravholt, C. H. *et al.* Clinical practice guidelines for the care of girls and women with Turner syndrome: proceedings from the 2016 Cincinnati International Turner Syndrome Meeting. *Eur. J. Endocrinol.* **177**, G1–G70 (2017).

399. Hong, D., Kent, J. S. & Kesler, S. COGNITIVE PROFILE OF TURNER SYNDROME. *Dev Disabil Res Rev* **15**, 270–278 (2009).

400. Hong, D. S., Dunkin, B. & Reiss, A. L. Psychosocial functioning and social cognitive processing in girls with Turner syndrome. *J Dev Behav Pediatr* **32**, 512–520 (2011).

401. Burnett, A. C., Reutens, D. C. & Wood, A. G. Social cognition in Turner's Syndrome. *Journal of Clinical Neuroscience* **17**, 283–286 (2010).

402. Kirk, J. W., Mazzocco, M. M. M. & Kover, S. T. Assessing Executive Dysfunction in Girls With Fragile X or Turner Syndrome Using the Contingency Naming Test (CNT). *Developmental Neuropsychology* **28**, 755–777 (2005).

403. Mauger, C. *et al.* Executive Functions in Children and Adolescents with Turner Syndrome: A Systematic Review and Meta-Analysis. *Neuropsychol Rev* **28**, 188–215 (2018).

404. Haberecht, M. F. *et al.* Functional neuroanatomy of visuo-spatial working memory in turner syndrome. *Human Brain Mapping* **14**, 96–107 (2001).

405. Hart, S. J., Davenport, M. L., Hooper, S. R. & Belger, A. Visuospatial executive function in Turner syndrome: functional MRI and neurocognitive findings. *Brain* **129**, 1125–1136 (2006).

406. Spiliotis, B. E. Recombinant human growth hormone in the treatment of Turner syndrome. *Ther Clin Risk Manag* **4**, 1177–1183 (2008).

407. Rubin, R. T., Reinisch, J. M. & Haskett, R. F. Postnatal Gonadal Steroid Effects on Human Behavior. *Science* **211**, 1318–1324 (1981).

408. Berman, K. F. *et al.* Modulation of cognition-specific cortical activity by gonadal steroids: A positron-emission tomography study in women. *Proceedings of the National Academy of Sciences* **94**, 8836–8841 (1997).

409. Schulz, K. M. & Sisk, C. L. The organizing actions of adolescent gonadal steroid hormones on brain and behavioral development. *Neuroscience & Biobehavioral Reviews* **70**, 148–158 (2016).

410. Girault, J. B. *et al.* White matter microstructural development and cognitive ability in the first 2 years of life. *Human Brain Mapping* **40**, 1195–1210 (2019).

411. R Core Team. R: A language and environment for statistical computing. R Foundation for Statistical Computing. (2021).

412. Verde, A. R. *et al.* UNC-Utah NA-MIC framework for DTI fiber tract analysis. *Front Neuroinform* **7**, (2014).

413. Oguz, I. *et al.* DTIPrep: quality control of diffusion-weighted images. *Front. Neuroinform.* **8**, (2014).

414. Jha, S. C. *et al.* Genetic influences on neonatal cortical thickness and surface area. *Human Brain Mapping* **39**, 4998–5013 (2018).

415. Zhu, H. *et al.* FADTTS: functional analysis of diffusion tensor tract statistics. *Neuroimage* **56**, 1412–1425 (2011).

416. Kamali, A., Flanders, A. E., Brody, J., Hunter, J. V. & Hasan, K. M. Tracing superior longitudinal fasciculus connectivity in the human brain using high resolution diffusion tensor tractography. *Brain Struct Funct* **219**, 269–281 (2014).

417. Rizio, A. A. & Diaz, M. T. Language, aging, and cognition: Frontal aslant tract and superior longitudinal fasciculus contribute to working memory performance in older adults. *Neuroreport* **27**, 689–693 (2016).

418. Koyama, T. & Domen, K. Diffusion Tensor Fractional Anisotropy in the Superior Longitudinal Fasciculus Correlates with Functional Independence Measure Cognition Scores in Patients with Cerebral Infarction. *Journal of Stroke and Cerebrovascular Diseases* **26**, 1704–1711 (2017).

419. Madhavan, K. M., McQueeny, T., Howe, S. R., Shear, P. & Szaflarski, J. Superior longitudinal fasciculus and language functioning in healthy aging. *Brain Research* **1562**, 11–22 (2014).

420. Pretzel, R. E. *et al.* Early Development of Infants with Turner Syndrome. *J Dev Behav Pediatr* **41**, 470–479 (2020).

421. Sävendahl, L. & Davenport, M. L. Delayed diagnoses of Turner's syndrome: proposed guidelines for change. *J Pediatr* **137**, 455–459 (2000).

422. Moreno-García, M., Fernández-Martínez, F. J. & Barreiro Miranda, E. Chromosomal anomalies in patients with short stature. *Pediatr Int* **47**, 546–549 (2005).

423. Bondy, C. A. Congenital Cardiovascular Disease in Turner Syndrome. *Congenital Heart Disease* **3**, 2–15 (2008).

424. Eckhauser, A., South, S. T., Meyers, L., Bleyl, S. B. & Botto, L. D. Turner Syndrome in Girls Presenting with Coarctation of the Aorta. *The Journal of Pediatrics* **167**, 1062–1066 (2015).

425. McGoey, K. E., Eckert, T. L. & Dupaul, G. J. Early Intervention for Preschool-Age Children with ADHD: A Literature Review. *Journal of Emotional and Behavioral Disorders* **10**, 14–28 (2002).

426. Jones, K., Daley, D., Hutchings, J., Bywater, T. & Eames, C. Efficacy of the Incredible Years Basic parent training programme as an early intervention for children with conduct problems and ADHD. *Child: Care, Health and Development* **33**, 749–756 (2007).

427. Re, A. M., Capodieci, A. & Cornoldi, C. Effect of training focused on executive functions (attention, inhibition, and working memory) in preschoolers exhibiting ADHD symptoms. *Front. Psychol.* **6**, (2015).

428. Eapen, V., Črnčec, R. & Walter, A. Clinical outcomes of an early intervention program for preschool children with Autism Spectrum Disorder in a community group setting. *BMC Pediatrics* **13**, 3 (2013).

429. Zwaigenbaum, L. *et al.* Early Intervention for Children With Autism Spectrum Disorder Under 3 Years of Age: Recommendations for Practice and Research. *Pediatrics* **136**, S60–S81 (2015).

430. Saaybi, S. *et al.* Pre- and Post-therapy Assessment of Clinical Outcomes and White Matter Integrity in Autism Spectrum Disorder: Pilot Study. *Front. Neurol.* **10**, (2019).

431. Swanson, M. R. & Hazlett, H. C. White matter as a monitoring biomarker for neurodevelopmental disorder intervention studies. *J Neurodevelop Disord* **11**, 33 (2019).

432. Stephens, R. L. *et al.* White Matter Development from Birth to 6 Years of Age: A Longitudinal Study. *Cereb Cortex* **30**, 6152–6168 (2020).

433. Hüppi, P. S. *et al.* Microstructural Development of Human Newborn Cerebral White Matter Assessed in Vivo by Diffusion Tensor Magnetic Resonance Imaging. *Pediatr Res* **44**, 584–590 (1998).

434. Forest, M. G., Cathiard, A. M. & Bertrand, J. A. EVIDENCE OF TESTICULAR ACTIVITY IN EARLY INFANCY. *The Journal of Clinical Endocrinology & Metabolism* **37**, 148–151 (1973).

435. REYES, F. I., BORODITSKY, R. S., WINTER, J. S. D. & FAIMAN, C. Studies on Human Sexual Development. II. Fetal and Maternal Serum Gonadotropin and Sex Steroid Concentrations1. *The Journal of Clinical Endocrinology & Metabolism* **38**, 612–617 (1974).

436. Shigeo, T. *et al.* Sex differences in fetal gonadotropins and androgens. *Journal of Steroid Biochemistry* **8**, 609–620 (1977).

437. TAPANAINEN, J., KELLOKUMPU-LEHTINEN, P., PELLINIEMI, L. & HUHTANIEMI, I. Age-Related Changes in Endogenous Steroids of Human Fetal Testis during Early and Midpregnancy*. *The Journal of Clinical Endocrinology & Metabolism* **52**, 98–102 (1981).

438. Andersson, A.-M. *et al.* Longitudinal Reproductive Hormone Profiles in Infants: Peak of Inhibin B Levels in Infant Boys Exceeds Levels in Adult Men1. *The Journal of Clinical Endocrinology & Metabolism* **83**, 675–681 (1998).

439. Kuiri-Hänninen, T. *et al.* Increased Activity of the Hypothalamic-Pituitary-Testicular Axis in Infancy Results in Increased Androgen Action in Premature Boys. *The Journal of Clinical Endocrinology & Metabolism* **96**, 98–105 (2011).

440. Gilmore, J. H., Santelli, R. K. & Gao, W. Imaging structural and functional brain development in early childhood. *Nat Rev Neurosci* **19**, 123–137 (2018).

441. Ikuta, T. *et al.* Abnormal cingulum bundle development in autism: A probabilistic tractography study. *Psychiatry Research: Neuroimaging* **221**, 63–68 (2014).

442. Bathelt, J., Johnson, A., Zhang, M. & Astle, D. E. The cingulum as a marker of individual differences in neurocognitive development. *Sci Rep* **9**, 2281 (2019).

443. Tamnes, C. K. *et al.* Brain Maturation in Adolescence and Young Adulthood: Regional Age-Related Changes in Cortical Thickness and White Matter Volume and Microstructure. *Cerebral Cortex* **20**, 534–548 (2010).

444. Lebel, C., Treit, S. & Beaulieu, C. A review of diffusion MRI of typical white matter development from early childhood to young adulthood. *NMR in Biomedicine* **32**, e3778 (2019).

445. Wu, Y., Sun, D., Wang, Y., Wang, Y. & Ou, S. Segmentation of the Cingulum Bundle in the Human Brain: A New Perspective Based on DSI Tractography and Fiber Dissection Study. *Front. Neuroanat.* **0**, (2016).

446. Metzler-Baddeley, C. *et al.* Temporal association tracts and the breakdown of episodic memory in mild cognitive impairment. *Neurology* **79**, 2233–2240 (2012).

447. Green, T. *et al.* Sex differences in amygdala shape: Insights from Turner syndrome. *Human Brain Mapping* **37**, 1593–1601 (2016).

448. Skuse, D. H., Morris, J. S. & Dolan, R. J. Functional dissociation of amygdala-modulated arousal and cognitive appraisal, in Turner syndrome. *Brain* **128**, 2084–2096 (2005).

449. Nijhuis-van der Sanden, M., Smits-Engelsman, B., Eling, P., Nijhuis, B. & Galen, G. Low Elementary Movement Speed Is Associated With Poor Motor Skill in Turner's Syndrome. *Developmental neuropsychology* **22**, 643–70 (2002).

450. Nijhuis-van der Sanden, M. W. G., Eling, P. A. T. M. & Otten, B. J. A review of neuropsychological and motor studies in Turner Syndrome. *Neuroscience & Biobehavioral Reviews* **27**, 329–338 (2003).

451. Ross, J. L., Kushner, H. & Roeltgen, D. P. Developmental changes in motor function in girls with Turner syndrome. *Pediatr Neurol* **15**, 317–322 (1996).

452. Sanden, R. W. G. N. der, Smits-Engelsman, B. C. & Eling, P. A. Motor performance in girls with Turner syndrome. *Developmental Medicine and Child Neurology* **42**, 685–690 (2000).

453. Pizzini, F. B. *et al.* Review of Corpus Callosum Topography, Analysis of Diffusion Values for the Different Callosal Fibers and Sex Differences. *Neuroradiol J* **21**, 745–754 (2008).

454. Xie, S. *et al.* The Effects of X Chromosome Loss on Neuroanatomical and Cognitive Phenotypes During Adolescence: a Multi-modal Structural MRI and Diffusion Tensor Imaging Study. *Cereb Cortex* **25**, 2842–2853 (2015).

455. Tusa, R. J. & Ungerleider, L. G. The inferior longitudinal fasciculus: A reexamination in humans and monkeys. *Annals of Neurology* **18**, 583–591 (1985).

456. Hanaie, R. *et al.* Abnormal Corpus Callosum Connectivity, Socio-communicative Deficits, and Motor Deficits in Children with Autism Spectrum Disorder: A Diffusion Tensor Imaging Study. *J Autism Dev Disord* **44**, 2209–2220 (2014).

457. Takao, H., Hayashi, N. & Ohtomo, K. Sex dimorphism in the white matter: Fractional anisotropy and brain size. *Journal of Magnetic Resonance Imaging* **39**, 917–923 (2014).

458. Shaw, P. *et al.* White Matter Microstructure and the Variable Adult Outcome of Childhood Attention Deficit Hyperactivity Disorder. *Neuropsychopharmacol* **40**, 746–754 (2015).

459. Jou, R. J. *et al.* Structural Neural Phenotype of Autism: Preliminary Evidence from a Diffusion Tensor Imaging Study Using Tract-Based Spatial Statistics. *American Journal of Neuroradiology* **32**, 1607–1613 (2011).

460. Koldewyn, K. *et al.* Differences in the right inferior longitudinal fasciculus but no general disruption of white matter tracts in children with autism spectrum disorder. *PNAS* **111**, 1981–1986 (2014).

461. Boets, B. *et al.* Alterations in the inferior longitudinal fasciculus in autism and associations with visual processing: a diffusion-weighted MRI study. *Molecular Autism* **9**, 10 (2018).

462. Krogsrud, S. *et al.* Development of white matter microstructure in relation to verbal and visuospatial working memory—A longitudinal study. *PLOS ONE* **13**, e0195540 (2018).

463. Peper, J. S., van den Heuvel, M. P., Mandl, R. C. W., Pol, H. E. H. & van Honk, J. Sex steroids and connectivity in the human brain: A review of neuroimaging studies. *Psychoneuroendocrinology* **36**, 1101–1113 (2011).

464. Green, T., Flash, S. & Reiss, A. L. Sex differences in psychiatric disorders: what we can learn from sex chromosome aneuploidies. *Neuropsychopharmacology* **44**, 9–21 (2019).

465. Ross, J. *et al.* Persistent cognitive deficits in adult women with Turner syndrome. *Neurology* **58**, 218–25 (2002).

466. Quintero, A. I., Beaton, E. A., Harvey, D. J., Ross, J. L. & Simon, T. J. Common and specific impairments in attention functioning in girls with chromosome 22q11.2 deletion, fragile X or Turner syndromes. *J Neurodevelop Disord* **6**, 1–15 (2014).

467. Attout, L., Noël, M.-P., Nassogne, M.-C. & Rousselle, L. The role of short-term memory and visuo-spatial skills in numerical magnitude processing: Evidence from Turner syndrome. *PLOS ONE* **12**, e0171454 (2017).

468. McCauley, E., Kay, T., Ito, J. & Treder, R. The Turner Syndrome: Cognitive Deficits, Affective Discrimination, and Behavior Problems. *Child Development* **58**, 464–473 (1987).

469. Downey, J. *et al.* Cognitive Ability and Everyday Functioning in Women with Turner Syndrome. *J Learn Disabil* **24**, 32–39 (1991).

470. Romans, S. M., Roeltgen, D. P., Kushner, H. & Ross, J. L. Executive function in girls with turner's syndrome. *Developmental Neuropsychology* **13**, 23–40 (1997).

471. Harris, P. A. *et al.* Research electronic data capture (REDCap)—A metadata-driven methodology and workflow process for providing translational research informatics support. *Journal of Biomedical Informatics* **42**, 377–381 (2009).

472. Harris, P. A. *et al.* The REDCap consortium: Building an international community of software platform partners. *Journal of Biomedical Informatics* **95**, 103208 (2019).

473. Ganis, G. & Kievit, R. A New Set of Three-Dimensional Shapes for Investigating Mental Rotation Processes: Validation Data and Stimulus Set. *Journal of Open Psychology Data* **3**, e3 (2015).

474. Baron-Cohen, S., Jolliffe, T., Mortimore, C. & Robertson, M. Another Advanced Test of Theory of Mind: Evidence from Very High Functioning Adults with Autism or Asperger Syndrome. *Journal of Child Psychology and Psychiatry* **38**, 813–822 (1997).

475. Klee, S. H. & Garfinkel, B. D. The computerized continuous performance task: A new measure of inattention. *J Abnorm Child Psychol* **11**, 487–495 (1983).

476. Baron-Cohen, S., Wheelwright, S., Skinner, R., Martin, J. & Clubley, E. The Autism-Spectrum Quotient (AQ): Evidence from Asperger Syndrome/High-Functioning Autism, Malesand Females, Scientists and Mathematicians. *J Autism Dev Disord* **31**, 5–17 (2001).

477. Siemann, J., Herrmann, M. & Galashan, D. The effect of feature-based attention on flanker interference processing: An fMRI-constrained source analysis. *Sci Rep* **8**, 1580 (2018).

478. van Veen, V., Cohen, J. D., Botvinick, M. M., Stenger, V. A. & Carter, C. S. Anterior cingulate cortex, conflict monitoring, and levels of processing. *Neuroimage* **14**, 1302–1308 (2001).

479. Wei, P., Szameitat, A. J., Müller, H. J., Schubert, T. & Zhou, X. The neural correlates of perceptual load induced attentional selection: an fMRI study. *Neuroscience* **250**, 372–380 (2013).

480. Hübner, R. & Töbel, L. Conflict resolution in the Eriksen flanker task: Similarities and differences to the Simon task. *PLOS ONE* **14**, e0214203 (2019).

481. Hübner, R., Steinhauser, M. & Lehle, C. A dual-stage two-phase model of selective attention. *Psychol Rev* **117**, 759–784 (2010).

482. Cyr, A.-A., Romero, K. & Galin-Corini, L. Web-Based Cognitive Testing of Older Adults in Person Versus at Home: Within-Subjects Comparison Study. *JMIR Aging* **4**, e23384 (2021).

483. Bogler, C., Vowinkel, A., Zhutovsky, P. & Haynes, J.-D. Default Network Activity Is Associated with Better Performance in a Vigilance Task. *Frontiers in Human Neuroscience* **11**, (2017).

484. Bonnelle, V. *et al.* Default Mode Network Connectivity Predicts Sustained Attention Deficits after Traumatic Brain Injury. *J. Neurosci.* **31**, 13442–13451 (2011).

485. Danckert, J. & Merrifield, C. Boredom, sustained attention and the default mode network. *Exp Brain Res* **236**, 2507–2518 (2018).

486. Tana, M. G., Montin, E., Cerutti, S. & Bianchi, A. M. Exploring Cortical Attentional System by Using fMRI during a Continuous Perfomance Test. *Comput Intell Neurosci* **2010**, 329213 (2010).

487. Woods, D. L., Wyma, J. M., Yund, E. W., Herron, T. J. & Reed, B. Factors influencing the latency of simple reaction time. *Frontiers in Human Neuroscience* **9**, (2015).

488. Turken, U. *et al.* Cognitive processing speed and the structure of white matter pathways: Convergent evidence from normal variation and lesion studies. *NeuroImage* **42**, 1032–1044 (2008).

489. Brankaer, C., Ghesquière, P., De Wel, A., Swillen, A. & De Smedt, B. Numerical magnitude processing impairments in genetic syndromes: a cross-syndrome comparison of Turner and 22q11.2 deletion syndromes. *Developmental Science* **20**, n/a-N.PAG (2017).

490. Ross, J. L., Roeltgen, D., Feuillan, P., Kushner, H. & Cutler, G. B. Use of estrogen in young girls with Turner syndrome: Effects on memory. *Neurology* **54**, 164–164 (2000).

491. Chechlacz, M., Rotshtein, P. & Humphreys, G. W. Neuronal substrates of Corsi Block span: Lesion symptom mapping analyses in relation to attentional competition and spatial bias. *Neuropsychologia* **64**, 240–251 (2014).

492. Wilson, B. A. *et al.* Egocentric Disorientation following Bilateral Parietal Lobe Damage. *Cortex* **41**, 547–554 (2005).

493. Rovet, J. & Netley, C. The mental rotation task performance of Turner syndrome subjects. *Behav Genet* **10**, 437–443 (1980).

494. Rovet, J. & Netley, C. Processing deficits in Turner's syndrome. *Developmental Psychology* **18**, 77–94 (1982).

495. Gauthier, I. *et al.* BOLD Activity during Mental Rotation and Viewpoint-Dependent Object Recognition. *Neuron* **34**, 161–171 (2002).

496. Kirkland, R., Peterson, E., Baker, C., Miller, S. & Pulos, S. Meta-analysis reveals adult female superiority in 'Reading the Mind in the Eyes Test'. *North American Journal of Psychology* **15**, 449–458 (2013).

497. Sato, W. *et al.* Structural Neural Substrates of Reading the Mind in the Eyes. *Frontiers in Human Neuroscience* **10**, (2016).

498. Sato, W. *et al.* Structural Correlates of Reading the Mind in the Eyes in Autism Spectrum Disorder. *Front Hum Neurosci* **11**, 361 (2017).

499. Holt, R. J. *et al.* 'Reading the Mind in the Eyes': an fMRI study of adolescents with autism and their siblings. *Psychol Med* **44**, 3215–3227 (2014).

500. Baker, M. 1,500 scientists lift the lid on reproducibility. *Nature* **533**, 452–454 (2016).

501. National Academies of Sciences, E. *Reproducibility and Replicability in Science*. (2019). doi:10.17226/25303.

502. Gu, Z., Jamison, K. W., Sabuncu, M. R. & Kuceyeski, A. Heritability and interindividual variability of regional structure-function coupling. *Nat Commun* **12**, 4894 (2021).

503. Baum, G. L. *et al.* Development of structure–function coupling in human brain networks during youth. *Proc Natl Acad Sci U S A* **117**, 771–778 (2020).

504. Corbitt, H. *et al.* TIMP3 and TIMP1 are risk genes for bicuspid aortic valve and aortopathy in Turner syndrome. *PLOS Genetics* **14**, e1007692 (2018).

505. Huang, A. C., Olson, S. B. & Maslen, C. L. A Review of Recent Developments in Turner Syndrome Research. *J Cardiovasc Dev Dis* **8**, 138 (2021).

506. Kruszka, P. & Silberbach, M. The state of Turner syndrome science: Are we on the threshold of discovery? *American Journal of Medical Genetics Part C: Seminars in Medical Genetics* **181**, 4–6 (2019).